Dissertation

submitted to the

Combined Faculties of the Natural Sciences and Mathematics

of the

Ruperto-Carola-University of Heidelberg, Germany

for the degree of

Doctor of Natural Sciences

Put forward by

Diplom-Physiker *Georg Jochen Ketter*

born in Mainz

Oral examination: February 4, 2015

Theoretical treatment of miscellaneous frequency-shifts in Penning traps with classical perturbation theory

Referees:

Prof. Dr. Klaus Blaum
Prof. Dr. Manfred Lindner

Zusammenfassung

Theoretische Behandlung diverser Frequenzverschiebungen in Penningfallen mittels klassischer Störungstheorie

Die ideale Penningfalle besteht aus einem homogenen Magnetfeld und einem elektrostatischen Quadrupolpotential. Aus klassischer Sicht hängen die drei charakteristischen Eigenfrequenzen eines in dieser Anordnung gespeicherten Teilchens nicht von seinen Bewegungsamplituden ab. Diese dreifache Harmonizität der Eigenbewegungen wird jedoch von höheren Beiträgen zum magnetischen Feld und elektrischen Potential sowie letztlich der speziellen Relativitätstheorie außer Kraft gesetzt. Für genaue Messungen ist es unabdingbar, den systematischen Einfluss dieser Abweichungen auf die Bewegungsfrequenzen zu verstehen.

In dieser Arbeit wird mit klassischer Störungstheorie eine Vielzahl von Frequenzverschiebungen aus der Bewegungsgleichung des Teilchens hergeleitet. Ausgehend von einer Parametrisierung zylindersymmetrischer Feldfehler in Zylinderkoordinaten wird gezeigt, wie sich die zugehörige Frequenzverschiebung konsistent in erster Ordnung berechnen lässt. Statt über einen quantenmechanischen Operatorformalismus wird die relativistische Frequenzverschiebung mittels der relativistischen Bewegungsgleichung behandelt. Weitere betrachtete Frequenzverschiebungen betreffen den Einfluss eines leicht elliptischen Quadrupolpotentials, die Wechselwirkung des Ions mit seinen Bildladungen, die es in den Fallenelektroden influenziert, und eine schwache Modulation des Quadrupolpotentials. Die so gewonnenen Frequenzverschiebungen werden in eine Verschiebung im speziellen Betriebsmodus des THe-Trap-Experiments mit stabilisierter Axialfrequenz umgerechnet.

Abstract

Theoretical treatment of miscellaneous frequency-shifts in Penning traps with classical perturbation theory

The ideal Penning trap consists of a homogeneous magnetic field and an electrostatic quadrupole potential. In this configuration, the three characteristic eigenfrequencies of a trapped particle do not depend on its motional amplitudes from a classical point of view. However, this three-fold harmonicity of the eigenmotions is compromised by higher-order terms in the magnetic field and electric potential, and ultimately by special relativity. Understanding the systematic effect of these deviations on the motional frequencies is crucial for accurate measurements.

This thesis calculates numerous frequency-shifts in the framework of classical perturbation theory working with equations of motion for the particle's trajectory. Starting from a general parametrization of cylindrically-symmetric electric and magnetic imperfections in cylindrical coordinates, it is shown how to calculate the corresponding first-order frequency-shift consistently. Relativistic frequency-shifts are handled perturbatively in the relativistic equations of motion rather than via a quantum-mechanical operator formalism. Other frequency-shifts considered include the effect of a slightly elliptic quadrupole potential, the interaction of an ion with its image charges induced in the trap electrodes, and a small modulation of the quadrupole potential. The frequency-shifts derived are translated into shifts under the operation mode of locked axial-frequency used by the THe-Trap experiment.

Contents

List of Figures

List of Tables

1. Introduction

The Penning trap—a term [28] coined by 1989 Nobel prize winner Hans Georg Dehmelt [31], who also pioneered the device, honoring Frans Michel Penning's use of an axial magnetic field in order to increase the path length of electrons in a glow discharge tube [119] that would become a vacuum gauge [120]—is more than an apparatus for storing charged particles. Owing to the storage by entirely static fields, the ion dynamics in a Penning trap are much more conducive to a theoretical treatment than in the oscillatory electric field of the Paul trap—a radio-frequency trap named after 1989 Nobel prize winner[1] Wolfgang Paul [117]. The spatial dependence of the ideal electric field in both traps is the same, each component being proportional to the corresponding coordinate, with the proportionality constants linked by the laws of electrostatics. The Penning trap features a homogeneous magnetic field in addition.

In the ideal Penning trap, the three characteristic frequencies of a stored particle are simple analytic functions of its charge and mass, and of two key parameters of the trap—the strength of the magnetic and the electric field. Because the frequencies do not depend on the particle's motional amplitudes, measurements of frequencies are likely to be reproducible, yielding precise results even when the initial conditions are not reproduced exactly before the next measurement. However, there is more to a measurement than just precision. In order to extract, say, the mass of an ion from a measurement of its eigenfrequencies, the relationship between this fundamental parameter of the ion and the eigenfrequencies has to be understood in detail, which is more complicated in a real Penning trap, of course. Nevertheless, the influence of imperfections is mostly known well from theory, which can often be checked in the experiment, and corrections—either measured or calculated—are applied. It is this strong connection between theory and experiment that allows for accurate measurements, making Penning traps such a versatile tool [10] for precision mass spectrometry [9, 50, 107].

Mass is not the only quantity that may be extracted from a measurement of the eigenfrequencies. By deliberately introducing an inhomogeneous magnetic field, the spin state of the stored particle may be detected via the axial frequency [30]. This method of continuous Stern–Gerlach effect has been demonstrated on free electrons [67, 160] and positrons [143, 161], electrons bound in hydrogenlike [71, 153] or lithiumlike [169] ionic systems, protons [36, 104, 105] and antiprotons [37], resulting in measurements of the corresponding (dimensionless) magnetic moments given by the g-factors.

Even though this use of an inhomogeneous magnetic field represents a purposeful departure from the ideal Penning trap, it has undesired consequences, to wit, the eigenfrequencies depend on the motional amplitudes. Such anharmonic frequency-shifts—whether an inadvertent, but unavoidable and somewhat necessary side-effect, spurious because of residual imperfections

[1] The year is not a misprint. Dehmelt and Paul shared half of the 1989 Nobel prize in physics "for the development of the ion trap technique." The other half was awarded to Norman Foster Ramsey [129] "for the invention of the separated oscillatory fields method and its use in the hydrogen maser and other atomic clocks."

not to be compensated for, or useful for indirectly determining one eigenfrequency while continuously measuring a different one [103]—are a major topic of this thesis. These amplitude-dependent frequency-shifts are associated with higher-order terms in the electric and magnetic fields, which also call for a coherent description based on physical constraints, and the thesis takes a closer look at imperfections with cylindrical symmetry. Moreover, special relativity leads to anharmonic frequency-shifts, thereby imposing a fundamental limitation on the harmonic nature of the ideal Penning trap.

Other deviations from the ideal Penning trap lead to frequency-shifts that do not depend on the amplitudes of the particle, or harmonic shifts. These are typically caused by modifications of the trapping fields that keep the equations of motion linear in the particle's coordinates and velocities. Examples include a break of the cylindrical symmetry in the electric field and its misalignment with respect to the magnetic field. The former is dealt with in this thesis. This thesis also considers the interaction of an ion with the image charges it induces in the trap electrodes and a modulation of the electric field.

Both types of shift—anharmonic and harmonic—have to be accounted for before making a substantiated claim about accuracy. Perturbation theory turns out to be the adequate theoretical tool of choice because the equations of motion can no longer be solved exactly for most imperfections. This thesis uses a formalism based on the classical trajectory of the particle and its equations of motions in order to extract frequency-shifts. First-order corrections to the zeroth-order trajectory are considered when frequency-shifts of second order are to be calculated, either because there is no first-order frequency-shift or in order to check its scope when computationally feasible without excessive complication.

This thesis was carried out at the Max Planck Institute for Nuclear Physics in Heidelberg (MPIK, with the letter K from the German "Kernphysik" for nuclear physics). The somewhat unpredictable evolution of an experiment had it that the primary goal emerged to be the theoretical description and understanding of systematic effects at THe-Trap. The results, however, pertain to Penning traps in general.

THe-Trap is the successor to the University of Washington Penning-trap mass spectrometer (UW-PTMS) [125, 165]. The experiment was relocated to Heidelberg in 2008 and renamed THe-Trap, short for tritium–helium trap, after briefly being referred to as the MPIK/UW-PTMS [35]. During commissioning, first mass-ratio measurements were performed [34, 148, 149].

As its name implies, the ultimate goal of THe-Trap is to measure the mass ratio of tritium (^{3}H) and helium-3 (^{3}He), in order to determine the Q-value of the beta-decay that links both isotopes. By pushing Penning-trap mass spectrometry to its limits, the uncertainty of the currently accepted value [108] might be reduced by almost two orders of magnitude. At an uncertainty down to a few tens of millielectronvolts, an independent measurement of the Q-value provides an important systematic check [114] for KATRIN, the Karlsruhe Tritium Neutrino Experiment [40], an upscaled version of its precursor in Mainz [88]. The aim is to extract—or put a model-independent upper limit on—the mass of the electron antineutrino from the kinematics of the beta-decay by measuring the spectrum of the most energetic electrons. Near this endpoint for the electrons, the neutrino carries away least kinetic energy. Its rest mass may therefore account for a significant amount of the total decay energy that is not available for the electrons.

From challenging experiments and elusive particles, let us return to something more tangible. The thesis is structured as follows:

- Chapter 2 provides the necessary background on Penning traps, with Section 2.1 discussing the ideal one as a starting point for perturbation theory. Having the real Penning trap in mind, Section 2.2 parametrizes cylindrically-symmetric imperfections of the electrostatic potential and magnetic field.
- Chapter 3 introduces the classical formulation of perturbation theory which will be used to calculate frequency-shifts. The one-dimensional anharmonic oscillator of Section 3.2 serves as a first example, before the formalism is extended to the three-dimensional Penning trap in Section 3.4. There is Section 3.3 on second-order frequency-shifts in between.
- Chapter 4 calculates anharmonic frequency-shifts with the first-order method of Section 3.4, and it comprises the major share of my publications [83, 84] as a first author. Section 4.1 deals with the frequency-shifts caused by cylindrically-symmetric imperfections of the electrostatic potential and magnetic field. Section 4.2 treats effects of special relativity. Section 4.3 includes the impact of locking the axial frequency.
- Chapter 5 deals with additional frequency-shifts—namely, by image charges in Section 5.1 and by the modulation of the trapping potential in Section 5.2. These frequency-shifts do not depend on the amplitudes of the particle.
- The summary and outlook in Chapter 6 is followed by an appendix, Chapters A–F, mostly with additional information on the mathematical background.

2. Penning-trap theory

This chapter introduces the Penning trap and highlights its intriguing properties for precision measurements: simple analytic relations between a few key parameters of the trap, the mass and charge of the stored particle, and its eigenfrequencies in the trap. Even more favorably, the three eigenfrequencies do not depend on the particle's amplitudes in the ideal Penning trap, which Section 2.1 describes. The results of this section will provide the starting point for the perturbative treatment of effects in real Penning traps, such as the cylindrically-symmetric imperfections parametrized in Section 2.2.

2.1. The ideal Penning trap

The ideal Penning trap consists of a homogeneous magnetic field

$$\vec{B}_0 = B_0 \vec{e}_z \tag{2.1}$$

that defines the z-axis and an electrostatic quadrupole potential

$$\Phi_2 = \frac{V_0 C_2}{2d^2}\left(z^2 - \frac{x^2+y^2}{2}\right) = \frac{V_0 C_2}{2d^2}\left(z^2 - \frac{\rho^2}{2}\right) \quad . \tag{2.2}$$

The prefactor will be explained shortly, whereas most of the physics is encoded in the spatial dependence. Because of the potential's azimuthal symmetry, it is convenient to introduce the cylindrical coordinate

$$\rho = \sqrt{x^2+y^2} \quad , \tag{2.3}$$

which describes the distance from the z-axis. The spatial dependence of the quadrupole potential Φ_2 is such that it fulfills the Laplace equation $\Delta\Phi_2 = 0$ with the Laplace operator

$$\Delta = \frac{\partial^2}{\partial x^2} + \frac{\partial^2}{\partial y^2} + \frac{\partial^2}{\partial z^2} \quad , \tag{2.4}$$

as any electrostatic potential in the absence of charges has to. Thus, the spatial dependence is courtesy of the laws of electrostatics. Cylindrically-symmetric contributions beyond the quadrupole potential of the ideal Penning trap will be discussed in Section 2.2.1.

As Φ_2 results from a homogenous linear differential equation, its prefactor is a matter of convention, rather than a necessity dictated by the fundamental laws of nature. Of course, Φ_2 should have the unit of voltage. The particular choice here—with three parameters for a single degree of freedom—is understood best by considering how a quadrupole potential is generated

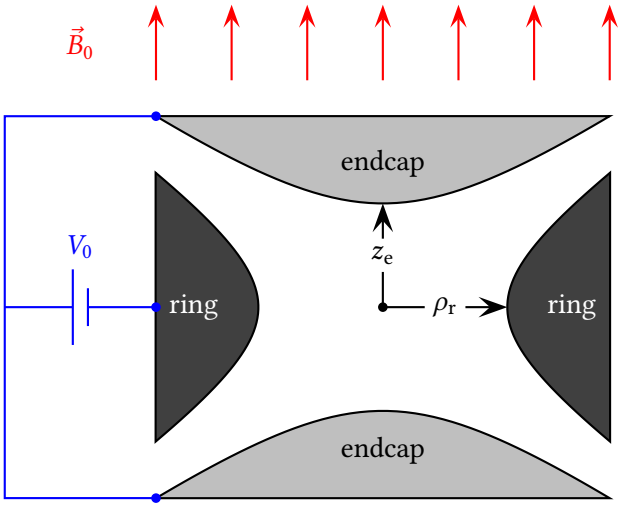

Figure 2.1.: Sectional drawing of finite hyperboloidal electrodes, formed upon rotation around the z-axis, whose direction is indicated by the magnetic field $\vec{B}_0$. Apart from truncation, other imperfections, such as holes for the injection of particles, are not shown. The shape of the electric potential inside the trap is determined by the inward-facing surfaces of the electrodes. The electrodes' bulk may therefore have a different shape for practical reasons, such as minimizing the distortion of the magnetic field. The inward-facing part of the ring electrode is a one-sheeted surface; the inward-facing part of the endcaps form a hyperboloid of two sheets. Each of the two sheets is one electrode. The distance from the geometric center of the trap to the ring and the endcaps is ρ_r and z_e, respectively. The geometric center is also the origin of the coordinate system. The voltage V_0 is applied between the endcaps, which are both at the same potential, and the ring.

in an experiment. Given that the equipotential surfaces of Φ_2 are hyperboloids of revolution, it is only natural to approximate the quadrupole potential with hyperboloidal electrodes [122], in order to provide adequate boundary conditions, with the electrodes forming the outermost of the desired equipotential surfaces. Figure 2.1 shows a sketch of such a hyperboloidal trap, where V_0 is the voltage applied between the endcaps and the ring electrode.

The geometric parameter d, also called the characteristic trap dimension, depends on the minimum distances of the endcaps and the ring from the center of the trap, given by z_e and ρ_r, respectively. The link is established by considering the boundary conditions imposed by the inward-facing surfaces of the electrodes. These surfaces set the boundary conditions that determine the potential for a charged particle inside the trap.

The equipotential surface of the endcap is given by the implicit equation

$$z^2 - \frac{\rho^2}{2} = z_e^2 \quad . \tag{2.5}$$

The inward-facing surface of the ring electrode is described by

$$z^2 - \frac{\rho^2}{2} = -\frac{\rho_\mathrm{r}^2}{2} \quad . \tag{2.6}$$

Given that the electrodes are equipotential surfaces, their potential is

$$\Phi_2(\mathrm{endcap}) = \frac{V_0 C_2}{2d^2}\left[z^2 - \frac{\rho^2}{2}\right]_\mathrm{endcap} = \frac{V_0 C_2}{2d^2} z_\mathrm{e}^2 \quad , \tag{2.7}$$

$$\Phi_2(\mathrm{ring}) = \frac{V_0 C_2}{2d^2}\left[z^2 - \frac{\rho^2}{2}\right]_\mathrm{ring} = -\frac{V_0 C_2}{2d^2}\frac{\rho_\mathrm{r}^2}{2} \quad . \tag{2.8}$$

We have plugged in Equations (2.5) and (2.6) for the two points lying on the endcap and the ring, respectively. Thus, the potential difference between any point on the endcap and a second point on the ring is

$$\Phi_2(\mathrm{endcap}) - \Phi_2(\mathrm{ring}) = \frac{V_0 C_2}{2d^2}\left(z_\mathrm{e}^2 + \frac{\rho_\mathrm{r}^2}{2}\right) = \frac{V_0 C_2}{2d^2} 2d^2 = V_0 C_2 \quad . \tag{2.9}$$

We have chosen the characteristic dimension of the trap as

$$d = \sqrt{\frac{1}{2}\left(z_\mathrm{e}^2 + \frac{\rho_\mathrm{r}^2}{2}\right)} \quad , \tag{2.10}$$

and we will justify this choice shortly based on the particular value of C_2 it produces for perfectly hyperboloidal electrodes that extend to infinity. As the potential difference should have the unit of voltage already carried by V_0, C_2 must be a dimensionless parameter. For $C_2 = 1$, the particular choice of the characteristic trap dimension d means that the potential difference between the endcaps and the ring electrode is exactly equal to the voltage V_0 applied between these electrodes.

At this point, it becomes obvious that a pure quadrupole potential is hard to produce, even with hyperboloidal electrodes. Manufacturing tolerances aside, the electrodes have to be truncated at some point, as they cannot possibly extend to infinity. For the particular choice of d in Equation (2.10), a value of C_2 different from unity indicates that the quadrupole potential Φ_2 alone does not describe the boundary conditions on the electrodes correctly. Hence, other contributions must exist, and they will be present all across the trap, not just on the electrodes where they set the boundary conditions right. A constant contribution Φ_0 will certainly not get the job done, but the difficulties with the boundary conditions explain why we have not yet introduced an offset potential that would shift the electrodes to the right absolute potential with respect to ground. Adding

$$\Phi_0 = V_\mathrm{endcap} - \frac{V_0 C_2}{2d^2} z_\mathrm{e}^2 = V_\mathrm{ring} + \frac{V_0 C_2}{2d^2}\frac{\rho_\mathrm{r}^2}{2} \tag{2.11}$$

to Equations (2.7) and (2.8) shifts the endcap and the ring to the potential V_endcap and V_ring, respectively. However, the relationship

$$V_0 = V_\mathrm{endcap} - V_\mathrm{ring} \quad , \tag{2.12}$$

which the electric connections and the voltage-source in Figure 2.1 imply, is reproduced only for $C_2 = 1$. As a constant potential does not give rise to a force on a charged particle, the absolute value of the potential in the trap with respect to the outside world is only of interest when injecting or ejecting particles. Unlike other non-quadrupole components, the constant term is of no interest for the motion of a stored particle, and we will ignore it in the following.

Fortunately, the analytic form of the potential in the whole trap all the way out to the electrodes does not need to be known for the accurate description of a charged particle's eigenmotions in the Penning trap. An accurate description of the potential near the (electrostatic) center of the trap, where the charged particle oscillates, suffices.

The dimensionless quadrupole-strength parameter C_2 has been introduced to allow for the description of the quadrupole component generated by various trap geometries, for instance cylindrical traps with flat-plate [51] or open [53] endcaps. Furthermore, cubic cells [27] feature a dominant quadrupole component [90], and the quadratic dependence with cylindrical symmetry also appears in elongated cells, if two faces are squares [76, 144]. Multitudes of trap geometries have been used [63]. The quadrupole potential is also the basis of planar Penning traps [59, 147, 166].

As hyperboloidal traps have $C_2 \approx 1$, their overall quadrupole component is sometimes defined as $1 + C_2'$, with $C_2' = 0$ describing the ideal case [47]. For maximum flexibility and the confusion caused when $C_2 \approx 1$ does not hold [54], C_2 will not be omitted from the general formulas in this thesis.

2.1.1. Equations of motion

In electromagnetic fields, a particle of charge q with velocity $\vec{v}$ is subject to the Lorentz force

$$\vec{F}_\mathrm{L} = q\left(\vec{E} + \vec{v} \times \vec{B}\right) \quad . \tag{2.13}$$

The electric field $\vec{E} = -\vec{\nabla}\Phi$ is calculated by taking the negative gradient of the electrostatic potential. For the quadrupole potential (2.2), the electric field in the ideal Penning trap is

$$\vec{E}_2 = -\vec{\nabla}\Phi_2 = \frac{V_0 C_2}{2d^2}\begin{pmatrix} x \\ y \\ -2z \end{pmatrix} \quad . \tag{2.14}$$

Combined with the uniform magnetic field (2.1) and Newton's second law

$$\vec{F} = m\vec{a} = m\dot{\vec{v}} \quad , \tag{2.15}$$

where m is the particle's rest mass and $\vec{a}$ the acceleration, the classical equations of motion in the Penning trap become

$$\begin{pmatrix} \ddot{x} \\ \ddot{y} \\ \ddot{z} \end{pmatrix} = \frac{qB_0}{m}\begin{pmatrix} \dot{y} \\ -\dot{x} \\ 0 \end{pmatrix} + \frac{qV_0 C_2}{2md^2}\begin{pmatrix} x \\ y \\ -2z \end{pmatrix} \quad . \tag{2.16}$$

Section 4.2 discusses the effect of special relativity, which is often sloppily depicted as relativistic mass-increase. However, matters are more complicated than simply inserting the relativistic

mass. In this thesis, the mass m always designates the particle's rest mass, which is a constant for the particular particle, of course.[1]

Returning to the classical equations of motion (2.16), the axial motion is a one-dimensional harmonic oscillator with the axial frequency

$$\omega_z = \sqrt{\frac{qV_0C_2}{md^2}} \quad . \tag{2.17}$$

Axial confinement requires $qV_0C_2 > 0$. In other words, the particle must sit in a potential well along the axial direction.

If there were no electrostatic potential, the particle would orbit around the magnetic field lines with the free-space cyclotron-frequency

$$\omega_c = \frac{qB_0}{m} \quad , \tag{2.18}$$

while drifting freely in the axial direction. In the light of typical experiments in persistent-mode superconducting magnets, we will assume that there is always a magnetic field, $B_0 \neq 0$, while the electrostatic quadrupole potential is adjusted at will via the applied voltage V_0. First and foremost, the magnetic field is a—if not the—characteristic feature of the PENNING trap, the use of static fields being another.

Mathematically, the radial equations of motion, the first two components of Equation (2.16), decouple without magnetic field, and the individual solutions are those of a harmonic oscillator—an inverted one for $qV_0C_2 > 0$ when there is axial confinement. In this case, the radial force is repulsive and essentially leads to exponential growth, which is not the right solution for storing a particle. Thus, the electric and the magnetic field have to cooperate for confinement in three dimensions. In the presence of both fields, the radial equations of motion are conveniently solved by introducing the complex variable [24]

$$u = x + \mathrm{i}y \quad . \tag{2.19}$$

Multiplying the second component of the equations of motion (2.16) with the imaginary unit i and then summing it with the first component yields the one-dimensional differential equation

$$\ddot{u} = -\mathrm{i}\omega_c \dot{u} + \frac{\omega_z^2}{2}u \tag{2.20}$$

for the complex variable u. Trying a solution of the kind

$$u = u_0 \mathrm{e}^{-\mathrm{i}\omega t} \tag{2.21}$$

with a constant u_0 and the frequency ω, which still has to be determined, results in the characteristic equation

$$\omega^2 - \omega_c\omega + \frac{\omega_z^2}{2} = 0 \quad . \tag{2.22}$$

[1] Even though the treatment of relativistic effects in Section 4.2 is perturbative—as almost always in this thesis for effects beyond the ideal PENNING trap—there is no expansion in the mass, which eliminates the need for the subscript 0 in the rest mass.

It is solved by the two frequencies

$$\omega_{\pm} = \frac{1}{2}\left(\omega_\mathrm{c} \pm \frac{\omega_\mathrm{c}}{|\omega_\mathrm{c}|}\sqrt{\omega_\mathrm{c}^2 - 2\omega_z^2}\right) \quad . \tag{2.23}$$

These are the frequencies of the two radial modes. Radial confinement requires that these frequencies be real and distinct. When they are equal, $\omega_+ = \omega_- = \omega_\mathrm{c}/2$ for $\omega_\mathrm{c}^2 = 2\omega_z^2$, the ansatz (2.21) produces only one fundamental solution for the second-order differential equation (2.20). The second fundamental solution is of the kind $u \propto t\exp(-\mathrm{i}\omega_\mathrm{c}t/2)$, and the amplitude of its oscillation grows with time. Thus, the argument inside the square root must be strictly positive for radial confinement: $\omega_\mathrm{c}^2 > 2\omega_z^2$.

The condition $qV_0C_2 > 0$, necessary for creating the potential well for axial confinement, implies that in turn the charged particle sees a slope in the radial direction. If there were no magnetic field, the particle would be lost by rolling down the potential hill. The condition $\omega_\mathrm{c}^2 > 2\omega_z^2$ for radial confinement tells us that the same would also happen for too low a magnetic field. In order to overcome the outward drag by the radial electric field, the magnetic field must be greater than

$$B_0 > \sqrt{2\frac{m}{q}\frac{V_0C_2}{d^2}} \quad . \tag{2.24}$$

From Equation (2.23), the three following relations can be derived between (I) the free-space cyclotron-frequency and the radial frequencies, (II) the axial frequency squared and the radial frequencies, and (III) the frequencies summed in quadrature:

$$\omega_\mathrm{c} = \omega_+ + \omega_- \quad , \tag{2.25}$$

$$\omega_z^2 = 2\omega_+\omega_- \quad , \tag{2.26}$$

$$\omega_\mathrm{c}^2 = \omega_+^2 + \omega_z^2 + \omega_-^2 \quad . \tag{2.27}$$

The first and the third relation are of practical importance in real Penning traps because they relate the measurable frequencies in the trap to the free-space cyclotron-frequency—the frequency with which the particle would orbit in a purely magnetic field without axial confinement by an electrostatic potential. Since carefully-designed superconducting magnets [163] with additional stabilization systems produce magnetic fields of extraordinary intrinsic temporal stability on the order of a few parts in 10^{12} per hour, they are the gold standard for relating a motional frequency of a particle to its charge and mass via Equation (2.18). The temporal stability of the magnetic field then enables meaningful comparisons of free-space cyclotron-frequency ratios for different species, which are trapped and measured sequentially.

Equation (2.25), sometimes called the sideband-cyclotron identity, is the basis of the time-of-flight ion cyclotron-resonance method [62, 87] and the phase-imaging ion cyclotron-resonance technique [43]. Penning traps at radioactive-beam facilities ("online traps") preferably use these methods on short-lived nuclides (with half-lives down to 10 ms [145]) produced at the facility.

Equation (2.27), baptized the Brown–Gabrielse invariance theorem by the second of its eponyms [50], requires a measurement of all three eigenfrequencies in the trap to deduce the

free-space cyclotron-frequency ω_c. However, this extra effort compared with Equation (2.25) is rewarded by the exact cancellation [19] of two imperfections in the invariance theorem: a tilt angle ("misalignment") between the z-axis of the electrostatic quadrupole potential Φ_2 and the magnetic field $\vec{B}_0$, and quadratic deviations from cylindrical symmetry in the quadrupole potential ("ellipticity," see Section 3.4.4). Since these imperfections are independent, the cancellation in the quadratic sum applies individually, too.

Having discussed relations between the three eigenfrequencies and the free-space cyclotron-frequency, we return to the shape of the radial eigenmotions. Since Equation (2.20) for the complex variable u is linear, the general solution is given by the superposition of fundamental solutions, Equation (2.21) with the two frequencies (2.23), as

$$u(t) = \hat{\rho}_+ e^{-i(\omega_+ t + \varphi_+)} + \hat{\rho}_- e^{-i(\omega_- t + \varphi_-)} \quad , \tag{2.28}$$

where the amplitudes $\hat{\rho}_k$ and phases φ_k with $k = (+, -)$ are real numbers chosen to satisfy the initial conditions. The substitution (2.19) is undone with the help of EULER's formula

$$e^{-i(\omega t + \varphi)} = \cos(\omega t + \varphi) - i \sin(\omega t + \varphi) \quad . \tag{2.29}$$

Identifying the real part of the solution (2.28) as $x(t)$ and the imaginary part as $y(t)$ yields the trajectory of a charged particle in an ideal PENNING trap:

$$x(t) = \hat{\rho}_+ \cos(\omega_+ t + \varphi_+) + \hat{\rho}_- \cos(\omega_- t + \varphi_-) \quad , \tag{2.30}$$

$$y(t) = -\hat{\rho}_+ \sin(\omega_+ t + \varphi_+) - \hat{\rho}_- \sin(\omega_- t + \varphi_-) \quad , \tag{2.31}$$

$$z(t) = \hat{z} \cos(\omega_z t + \varphi_z) \quad . \tag{2.32}$$

We have also included the general solution of the one-dimensional harmonic oscillator for the axial mode with amplitude $\hat{z}$ and initial phase φ_z. This solution is not correct in the case of $\omega_z = 0$—that is, no quadrupole potential—in which it should read $z(t) = z(0) + \dot{z}(0)t$. The initial axial position and velocity are given by $z(0)$ and $\dot{z}(0)$, respectively. In this case, there is no magnetron motion,[2] and its amplitude should be set to zero ($\hat{\rho}_- = 0$), in order to remove this motion from Equations (2.30) and (2.31). The degeneracy $\omega_+ = \omega_- = \omega_c/2$ at the limit of stability is not covered by such a simple replacement. The other cases without confinement even in the presence of the magnetic field, $qC_2V_0 < 0$ and $\omega_c^2 < 2\omega_z^2$, are described correctly by the use of an imaginary axial phase and frequency (2.17), and complex radial frequencies (2.23), respectively,[3] although there are more convenient ways to express the solutions for the trajectory with exponential functions. Since this chapter is about the PENNING *trap*, we will focus on the periodic motion brought about by three constant eigenfrequencies that are all real and different from zero.

[2] Unlike for the axial motion, the vanishing magnetron frequency $\omega_- = 0$ does not mean that there is a new solution of a different functional form. For $\omega_z^2 = 0$, Equation (2.20) reduces to a first-order differential equation, which has only one fundamental solution—the circular motion at the free-space cyclotron-frequency ω_c. A fundamental solution with a different functional form shows up for $\omega_+ = \omega_-$, however.

[3] The two cases are mutually exclusive because $\omega_c^2 > 0$ regardless, which means that $\omega_z^2 < 0$ for $qC_2V_0 < 0$ automatically ensures $\omega_c^2 > 0 > 2\omega_z^2$. From the physical point of view, there is no radial instability when the electric field (2.14) contributes to the radial restoring force. However, unlimited radial stability comes at the expense of escape in the axial direction.

The amplitudes in Equations (2.30)–(2.32) are typically taken as non-negative quantities—zero would be fine in the classical case—with a possible sign absorbed in the choice of the initial phase.[4] Because the time-dependence for the three eigenmodes has a similar structure, we introduce the abbreviation

$$\chi_k = \omega_k t + \varphi_k \tag{2.33}$$

for the total phase of all three modes, where $k = (+, -, z)$.

Figure 2.2 illustrates the eigenmotions in a Penning trap. Each of the two radial modes alone is circular. When they are combined, the faster motions represents an epicycle, whose center travels on the deferent described by the slower circular motion. For a classification of the orbits, see Reference [68]. Despite the reference to the Ptolemaic system of astronomy here, the epicycle may be larger than the deferent. The radii or amplitudes of the two circular motions are unrelated, and the two radial modes are distinguished based on their frequencies, rather than their amplitudes.

The radial frequencies are chosen such that $|\omega_+| \geq |\omega_-|$, with $\omega_+ = \omega_-$ representing the limit of radial stability. The frequency with the larger absolute value is referred to as the modified or reduced cyclotron-frequency because $|\omega_+| < |\omega_c|$ and $\omega_+ \to \omega_c$ in the limit of $V_0 \to 0$, that is, vanishing electrostatic potential. Since the frequencies of the ion of interest stored in the trap typically obey the hierarchy $|\omega_c| \gtrsim |\omega_+| \gg \omega_z \gg |\omega_-|$, its modified cyclotron-motion is dominated by the magnetic field. Note that the weaker version of the hierarchy with $\geq$-signs rather than $\gg$-signs is not generally true, because $|\omega_+| < \omega_z$ for $\omega_z > {}^2\!/_3|\omega_c|$, see Figure 3.1.

The radial frequency with the lower absolute value is called the magnetron frequency ω_-. The magnetron motion reflects a slow $\vec{E} \times \vec{B}$ drift around the center of the trap. Consequently, it vanishes in the limit of no electric field: $\omega_- \to 0$ as $V_0 \to 0$. A Taylor expansion in the limit of $\omega_z \ll |\omega_c|$ shows that the magnetron frequency is independent of the particle's charge and mass to first order:

$$\omega_- = \frac{\omega_c}{2}\left(1 - \frac{1}{|\omega_c|}\sqrt{\omega_c^2 - 2\omega_z^2}\right) = \frac{\omega_c}{2}\left(1 - \frac{|\omega_c|}{|\omega_c|}\sqrt{1 - 2\frac{\omega_z^2}{\omega_c^2}}\right) \tag{2.34a}$$

$$\approx \frac{\omega_c}{2}\left(1 - \left(1 - \frac{\omega_z^2}{\omega_c^2} + \cdots\right)\right) \approx \frac{\omega_z^2}{2\omega_c} = \frac{V_0 C_2}{2B_0 d^2} \quad . \tag{2.34b}$$

In the last step, we have used the Equations (2.17) and (2.18) for the axial frequency ω_z and the free-space cyclotron-frequency ω_c, respectively. When the magnetron frequency is proportional to the voltage V_0, the sideband identity (2.25) states that the reduced cyclotron-frequency also depends linearly on the voltage V_0. The sum of the radial frequencies in the ideal Penning trap is equal to the free-space cyclotron-frequency ω_c, which does not depend on the electrostatic potential.

In contrast to the standard definition of the radial frequencies

$$\omega'_\pm = \frac{1}{2}\left(\omega_c \pm \sqrt{\omega_c^2 - 2\omega_z^2}\right) \tag{2.35}$$

[4] To avoid negative amplitudes, send $\varphi_k \to \varphi_k + j\pi$, where j is an odd integer (which may be negative). Conventionally, the phase is chosen such that its range spans an interval of 2π, either $0 \leq \varphi_k \leq 2\pi$ or $-\pi \leq \varphi_k \leq \pi$. Never mind the overlap at the limits.

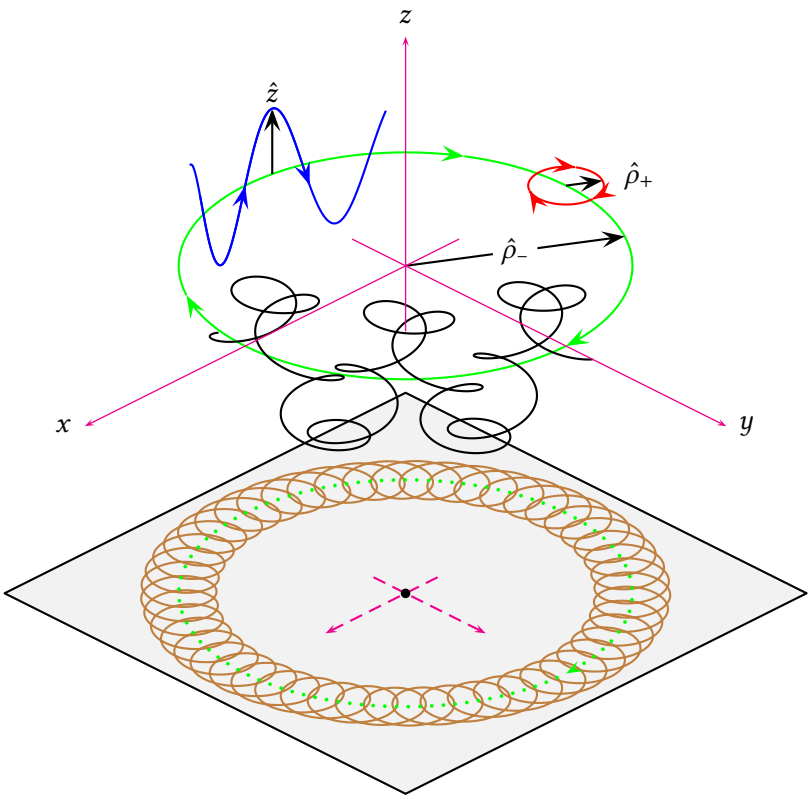

Figure 2.2.: Eigenmotions of a charged particle in a PENNING trap. The three individual eigenmotions—magnetron, cyclotron, and axial—are shown in green, red, and blue, respectively. The corresponding amplitudes are $\hat{\rho}_-$, $\hat{\rho}_+$, and $\hat{z}$. The black line shows a superposition of all the three eigenmotions. The brown line is a projection of the motion into the xy-plane (slightly offset for clarity), with the dotted green circle indicating the magnetron orbit. The frequency-ratio is chosen as $\omega_+ : \omega_z : \omega_- = 50 : 10 : 1$, satisfying Equation (2.26). The frequencies being integer multiples of one another leads to closed orbits. Such a commensurability condition will have to be ruled out later on when dealing with imperfections of the trap because such a relation between the eigenfrequencies may cause instabilities. This figure has been used multiple times. The original version is from my diploma thesis [81].

in the literature, Equation (2.23) contains essentially the sign of the free-space cyclotron-frequency ω_c as an additional prefactor in front of the square root. This prefactor makes no difference when ω_c is positive, and it flips the sign when ω_c is negative.

Figure 2.3 illustrates the problem of the standard definition for negative ω_c. When the sign of the free-space cyclotron-frequency changes, not only do the radial frequencies change their sign, which would be fine to indicate that the sense of rotation has changed, they also swap their meaning:

$$\omega'_{\pm}(-\omega_c) = \frac{1}{2}\left(-\omega_c \pm \sqrt{\omega_c^2 - 2\omega_z^2}\right) = -\frac{1}{2}\left(\omega_c \mp \sqrt{\omega_c^2 - 2\omega_z^2}\right) = -\omega'_{\mp}(\omega_c) \quad . \tag{2.36}$$

In this case, the subscript no longer identifies the two radial modes reliably, and the amplitudes $\hat{\rho}_{\pm}$ would be falsely associated with the other mode. From a mathematical point of view, the two radial modes possess an identical structure, and at least the pair of frequencies $\omega_{\pm}$ and amplitudes $\hat{\rho}_{\pm}$ is interchangeable. From the experimental point of view, the two radial modes must be distinguished. Technically, the link between frequencies and amplitudes established by the same subscript must be preserved. The problem of swapping the meaning is solved by the additional prefactor. Only the change of sign, reflecting the change in the sense of rotation, remains for the definition (2.23) chosen in this thesis:

$$\omega_{\pm}(-\omega_c) = \frac{1}{2}\left(-\omega_c \pm \frac{-\omega_c}{|\omega_c|}\sqrt{\omega_c^2 - 2\omega_z^2}\right) = -\frac{1}{2}\left(\omega_c \pm \frac{\omega_c}{|\omega_c|}\sqrt{\omega_c^2 - 2\omega_z^2}\right) = -\omega_{\pm}(\omega_c) \quad . \tag{2.37}$$

At this point, it may not be immediately obvious why the sign of ω_c or $\omega_{\pm}$ might be of any relevance. When the frequency is measured as the number of oscillations per time, the result is positive (or at least non-negative). After all, the reported quantities are frequencies $\nu = |\omega|/(2\pi)$, not angular frequencies ω. So far, we have always referred to the angular frequencies ω as frequencies without distinguishing them from the actual frequencies ν, and we will continue to do so. The symbols ω and ν should make the difference sufficiently clear.

The axial frequency ω_z was chosen positive by convention in Equation (2.17) without giving the sign any thought, because it does not represent an additional degree of freedom in the one-dimensional harmonic oscillator. A change of sign in ω_z is equivalent to changing the sign of the initial phase φ_z in the trajectory (2.32).

For the two-dimensional radial modes, the sign of $\omega_{\pm}$ encodes the sense of rotation in a natural way not covered by alternative choices of the amplitudes $\hat{\rho}_{\pm}$ and initial phases $\varphi_{\pm}$. This is also true for the cyclotron-motion with frequency ω_c in free space. Since we will work with the particle's trajectory later on—and not just the eigenfrequencies—in order to calculate frequency-shifts, not having to distinguish two cases in $x(t)$ or $y(t)$ depending on the sign of ω_c is very convenient.[5] However, the sense of rotation does not seem to have any important

[5] If the radial frequencies $\omega_{\pm}$ were defined to be positive, the sense of rotation could be incorporated by multiplying either $x(t)$ in Equation (2.30) or $y(t)$ in Equation (2.31) with the sign of qB_0. Although carrying along this additional factor is more cumbersome than allowing for a sign of the radial frequencies $\omega_{\pm}$ and the free-space cyclotron-frequency ω_c, this alternative is more general than assuming a particular sense of rotation. Such an assumption requires fixing the direction of the magnetic field as pointing along either the positive or the negative z-axis, and a restriction to either positive or negative charge.

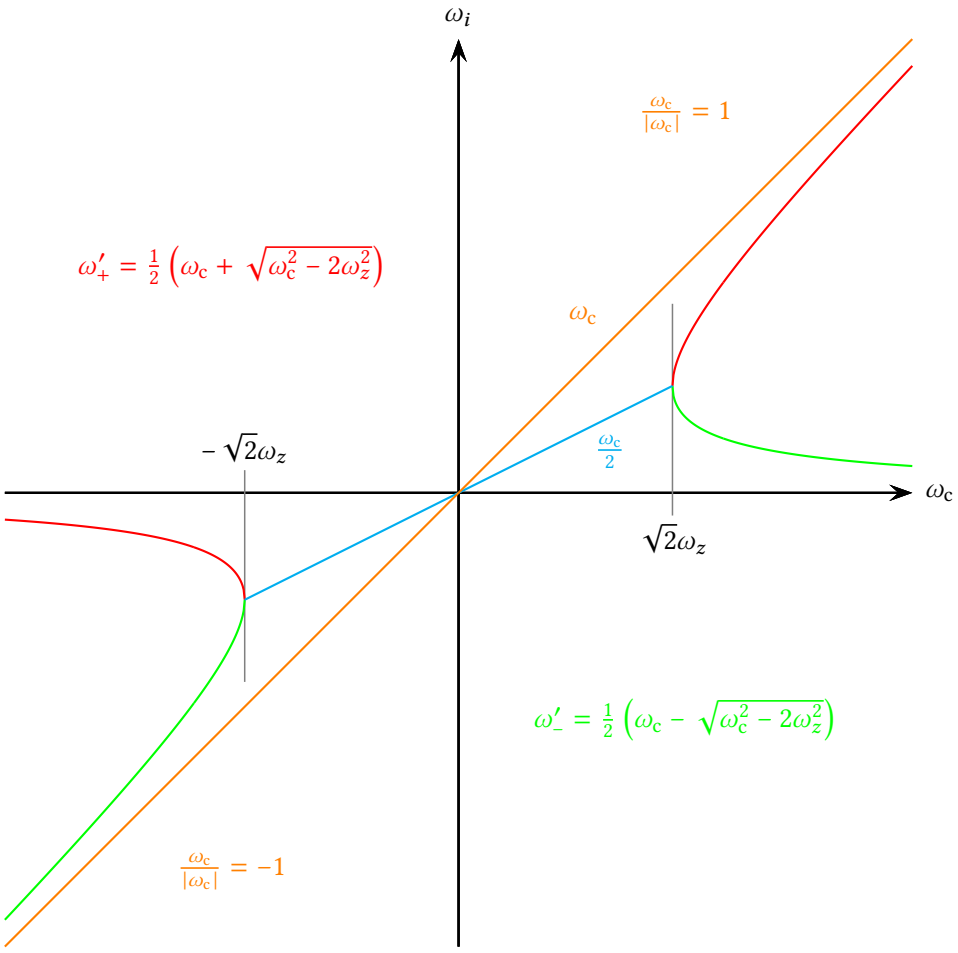

Figure 2.3.: The two radial frequencies are calculated from the standard definition (2.35) as a function of the free-space cyclotron-frequency ω_c. The orange line, representing ω_c, serves as a guide to the eye. It should be approached by the reduced cyclotron-frequency ω_+ for $|\omega_c|$ large compared with the axial frequency ω_z. The red branch has the plus sign in front of the square root; the green branch has the minus sign. For $\omega_c^2 < 2\omega_z^2$, the real part is shown in blue. Note that the red branch is always above the green one, and hence $\omega'_+ > \omega'_-$. For $\omega_c < -\sqrt{2}\omega_z$, this property means that $|\omega'_+| < |\omega'_-|$. Thus, the frequency on the red branch describes the magnetron frequency, while the green branch shows the modified cyclotron motion. This misassignment is cured by the definition (2.23). By including the sign of ω_c as a factor in front of the square root, the branches are flipped for negative ω_c. The plus sign is then always associated with the reduced cyclotron-frequency; the minus sign then belongs unambiguously to the magnetron frequency, regardless of the sign of ω_c.

physical meaning. For instance, the sign of B_0 and hence ω_c changes, when the z-axis is flipped.[6] This degree of freedom in the choice of the coordinate system cannot possible have experimental consequences, and the sign of B_0 for the particular coordinate system is never reported. Of course, the sign of ω_c also changes when the magnetic field is reversed, but this operation is more complex than playing with a definition, and it corresponds to an actual change in the experiment. The sign of ω_c changes for a particle of opposite charge, too. More precisely, the sign of ω_c reflects the sign of the product qB_0 in Equation (2.18). The same holds true for the radial frequencies $\omega_\pm$ as defined by Equation (2.23) and the standard definition (2.35), if negative free-space cyclotron-frequencies ω_c are allowed.

Since the sense of rotation for a particle with a given sign of charge is determined by the strong magnetic field of the ideal Penning trap, it is not changed by small imperfections. What would be lost if the associated frequency-shifts were calculated with the free-space cyclotron-frequency ω_c and hence the radial frequencies $\omega_\pm$ defined to be positive? For cylindrically-symmetric imperfections and the quasi-periodic motion in the Penning trap, it is hard to imagine that the sense of rotation as such could be important. However, the additional forces created by magnetic imperfections depend on the particle's velocity and, for the frequency-shifts caused, it matters whether they add to or subtract from the main forces in the ideal Penning trap. Thus, the direction of the additional magnetic field $\vec{B}_\eta$ with respect to the original magnetic field $\vec{B}_0$ has to be respected in the calculation. As described in Section 2.2.2, the relative orientation is given by the sign of the parameter B_η with respect to B_0. Concerning the calculation of frequency-shifts, the main danger of defining the free-space cyclotron-frequency ω_c to be positive is to forget the sign of B_0, when taking absolute values.[7] We shall see in Section 4.1.3 that the first-order frequency-shifts caused by cylindrically-symmetric imperfections all depend on B_η/B_0 as a global prefactor.

Devoting so much attention to the sign of the parameter B_η with respect to B_0 is largely academic. When the imperfection is caused by the magnetic susceptibility of the materials placed in the originally homogenous magnetic field, the orientation of the imperfections typically reverses when the homogenous magnetic field is flipped [20]. Consequently, the sign of B_η/B_0 is determined by the properties of the setup. However, we want to keep the final expressions for the frequency-shifts flexible, with as little assumptions or restrictions as possible. In short, the definition of the radial frequencies (2.23) ensures that the signs of the charge q and the magnetic field B_0 are handled correctly.

The particular sense of rotation in a magnetic field has an experimentally-observable consequence for the effect of the radial modes on the axial motion. It is such that the magnetic moment associated with the radial modes is always antiparallel to the magnetic field. We will prove that statement before exploring its experimental consequences.

In general, the orbital magnetic moment of a pointlike particle is defined as

$$\vec{\mu} = \frac{q}{2}\vec{r}\times\vec{v} = \frac{q}{2}\begin{pmatrix}x\\y\\z\end{pmatrix}\times\begin{pmatrix}\dot{x}\\\dot{y}\\\dot{z}\end{pmatrix} = \frac{q}{2}\begin{pmatrix}y\dot{z}-z\dot{y}\\z\dot{x}-x\dot{z}\\x\dot{y}-y\dot{x}\end{pmatrix} \quad . \tag{2.38}$$

[6] Flipping the z-axis also requires one of the other axes be flipped for the coordinate system to stay right-handed.
[7] Technically, the sign of the charge q is not important because it relates to all the (electromagnetic) forces, not just the one generated by the magnetic field of the ideal Penning trap.

With the coordinates (2.30)–(2.32) and their time-derivatives for the velocities, the components of the magnetic moment of a particle in an ideal PENNING trap become

$$\begin{aligned}\mu_x(t) = \frac{q}{2}\Big\{&\omega_z\hat{z}\sin(\chi_z)\big[\hat{\rho}_+\sin(\chi_+) + \hat{\rho}_-\sin(\chi_-)\big] \\ &+ \hat{z}\cos(\chi_z)\big[\omega_+\hat{\rho}_+\cos(\chi_+) + \omega_-\hat{\rho}_-\cos(\chi_-)\big]\Big\} \quad ,\end{aligned} \tag{2.39a}$$

$$\begin{aligned}\mu_y(t) = \frac{q}{2}\Big\{&\omega_z\hat{z}\sin(\chi_z)\big[\hat{\rho}_+\cos(\chi_+) + \hat{\rho}_-\cos(\chi_-)\big] \\ &- \hat{z}\cos(\chi_z)\big[\omega_+\hat{\rho}_+\sin(\chi_+) + \omega_-\hat{\rho}_-\sin(\chi_-)\big]\Big\} \quad ,\end{aligned} \tag{2.39b}$$

$$\mu_z(t) = -\frac{q}{2}\Big\{\omega_+\hat{\rho}_+^2 + \omega_-\hat{\rho}_-^2 + (\omega_+ + \omega_-)\hat{\rho}_+\hat{\rho}_-\cos[(\omega_+ - \omega_-)t + \varphi_+ - \varphi_+]\Big\} \quad . \tag{2.39c}$$

The radial components contain products of oscillatory terms at the axial frequency ω_z and either of the two radial frequencies $\omega_\pm$. Since $\omega_z \neq |\omega_\pm|$ apart from two exceptions,[8] there are no constant terms—see Equations (C.10)–(C.12) in the appendix for trigonometric product-to-sum identities. With the constant terms in the axial component, and the time-averaged orbital magnetic moment of the particle becomes

$$\langle\vec{\mu}\rangle_0 = -\frac{q}{2}\left(\omega_+\hat{\rho}_+^2 + \omega_-\hat{\rho}_-^2\right)\vec{e}_z \quad , \tag{2.40}$$

where $\vec{e}_z$ is a unit vector in the z-direction, the only component with a nonzero entry.[9] The angle brackets with the subscript 0 represent picking the constant component. We will introduce more of this notation in Section 3.1.

With our particular definition (2.23), the radial frequencies $\omega_\pm$ have the same sign as the product qB_0 in the free-space cyclotron-frequency ω_c. Consequently, the prefactor of the unit vector $\vec{e}_z$ in Equation (2.40) has the sign of B_0, which means that this magnetic moment is always antiparallel to the magnetic field. It is time to highlight one experimentally observed consequence of this alignment.

The energy of a magnetic moment $\vec{\mu}$ in a magnetic field $\vec{B}$ is given by $\mathcal{E}_{\text{mag}} = -\vec{\mu}\cdot\vec{B}$. For a constant magnetic moment that is always antiparallel to the magnetic field—that is, $\vec{\mu}\cdot\vec{B} < 0$—the energy is non-negative and it decreases with decreasing absolute magnetic field strength $\left|\vec{B}\right|$. Thus, the magnetic moment of the radial modes makes the ion a low-field seeker, provided this motional (or orbital rather than intrinsic) magnetic moment is a conserved quantity, rather than a function of the magnetic field itself. Indeed, the magnetic moment associated with the modified cyclotron-motion is an adiabatic invariant [23, 112]. Of course, an additional axial force caused by the radial modes will come into play only in a spatially-dependent magnetic

[8] The two exceptions are $\omega_z = \omega_- = 0$ and $\omega_z = |\omega_+| = {}^2\!/_3|\omega_c|$. In the first case, the axial motion has a different functional form than described by Equation (2.32), because, above all, there is no axial confinement. The second case is easily avoided by changing the trap voltage V_0, and it is unlikely because of the typical hierarchy $|\omega_+| \gg \omega_z$ for the ion-of-interest.

[9] For the special case of $\omega_z = |\omega_+| = {}^2\!/_3|\omega_c|$, the two radial components are $\langle\mu_x\rangle_0 = {}^1\!/_3 q\omega_c\hat{\rho}_+\hat{z}\cos(\varphi_z - \omega_c/|\omega_c|\varphi_+)$ and $\langle\mu_y\rangle_0 = {}^1\!/_3 q|\omega_c|\hat{\rho}_+\hat{z}\sin(\varphi_z - \omega_c/|\omega_c|\varphi_+)$. We will dismiss these particular relations between eigenfrequencies as accidental, in the sense that they are not fundamental or natural in any way for the ideal PENNING trap, in contrast to Equations (2.25)—(2.27), for instance.

field, not in the uniform magnetic field of the ideal Penning trap.[10] We will briefly return to the concept of modeling the interaction of the radial modes with the axial mode via their magnetic moment when Section 4.1.3 comes to axial frequency-shifts caused by magnetic imperfections. Experimentally, the additional force in the direction of lower magnetic fields is exploited by the time of flight ion cyclotron-resonance method [62] by measuring the ions' time-of-flight from the trap to a detector well outside the magnet. Because this ejection sends the ions through a region of decreasing magnetic field, their time of flight is altered by their orbital magnetic moment (2.40), which depends mainly on their cyclotron radius. In turn, radio-frequency fields allow to manipulate the cyclotron radius of the stored particles [94], thereby probing the resonance frequencies. Avowedly, the method would still work if the sense of rotation were the other way around, in which case the ions with the largest cyclotron radius would have the longest time-of-flight, because they would be slowed down most in the magnetic gradient.

2.1.2. Energies of the eigenmodes

The energy of a charged particle stored in a Penning trap follows directly from the trajectory without any analogies about magnetic moments. Because of the quadratic form of the quadrupole potential (2.2), the radial displacement squared has to be calculated. Adding Equations (2.30) and (2.31) in quadrature yields

$$\rho^2 = x^2 + y^2 = \hat{\rho}_+^2 + \hat{\rho}_-^2 + 2\hat{\rho}_+\hat{\rho}_- \cos(\chi_\mathrm{b}) \quad \text{with} \quad \chi_\mathrm{b} = \chi_+ - \chi_- \quad . \tag{2.41}$$

The time-dependence is not shown explicitly. It is hidden in the total phase χ_b from Equation (2.33) The radial displacement squared oscillates back and forth between the minimum value $\rho_\mathrm{min}^2 = (\hat{\rho}_+ - \hat{\rho}_-)^2$ and the maximum value $\rho_\mathrm{max}^2 = (\hat{\rho}_+ + \hat{\rho}_-)^2$ at the frequency

$$\omega_\mathrm{b} = \omega_+ - \omega_- \quad . \tag{2.42}$$

With the quadrupole potential (2.2) and the axial frequency (2.17), the potential energy is expressed as

$$\mathcal{E}_\mathrm{pot} = q\Phi_2 = q\frac{V_0 C_2}{2d^2}\left(z^2 - \frac{\rho^2}{2}\right) \tag{2.43}$$

$$= \frac{1}{2}m\omega_z^2\left\{\hat{z}^2\left[\cos(\chi_z)\right]^2 - \frac{\hat{\rho}_+^2 + \hat{\rho}_-^2 + 2\hat{\rho}_+\hat{\rho}_-\cos(\chi_\mathrm{b})}{2}\right\} \quad , \tag{2.44}$$

barring an offset by a constant potential Φ_0.

The velocity components are calculated by taking the time-derivatives of the trajectory (2.30)-(2.32). To obtain the kinetic energy, the velocity components are summed in quadrature. The contribution of the radial modes is

$$\dot{x}^2 + \dot{y}^2 = (\omega_+\hat{\rho}_+)^2 + (\omega_+\hat{\rho}_-)^2 + 2\omega_+\omega_-\hat{\rho}_+\hat{\rho}_-\cos(\chi_\mathrm{b}) \quad . \tag{2.45}$$

[10] Because of the scalar product in the energy $\mathcal{E}_\mathrm{mag}$, we could have ignored the radial components of the magnetic moment right away, the magnetic field of the ideal Penning trap having no entries there. However, Section 2.2.2 shows that an axial magnetic field with a spatial dependence always goes hand in hand with a radial magnetic field. This is the more interesting case for a magnetic moment, unless its the size or orientation—projection in the quantum-mechanical sense–can be changed, of course.

With the help of Equation (2.26), the product of radial frequencies is expressed as $2\omega_+\omega_- = \omega_z^2$ for the next step. Taking into account the axial oscillation, the kinetic energy becomes

$$\mathcal{E}_{\text{kin}} = \frac{1}{2}mv^2 = \frac{1}{2}m\left(\dot{x}^2 + \dot{y}^2 + \dot{z}^2\right) \tag{2.46}$$

$$= \frac{1}{2}m\left\{\omega_z^2\hat{z}^2\left[\sin(\chi_z)\right]^2 + (\omega_+\hat{\rho}_+)^2 + (\omega_+\hat{\rho}_-)^2 + \omega_z^2\hat{\rho}_+\hat{\rho}_-\cos(\chi_{\text{b}})\right\} \quad . \tag{2.47}$$

Because the axial mode is an undamped one-dimensional harmonic oscillator, the perpetual conversion of kinetic energy into potential energy and vice versa is clearly expected. For the radial modes, there is a constant contribution from each of the modes and an oscillatory term at the difference frequency ω_{b}. The oscillatory term vanishes in case one of the radial modes has zero amplitude. In this case, the particle goes around the trap center on a purely circular orbit with constant radial displacement and velocity.

In any case, the total energy of the particle

$$\mathcal{E}_{\text{tot}} = \mathcal{E}_{\text{pot}} + \mathcal{E}_{\text{kin}} = \frac{1}{2}m\omega_+(\omega_+ - \omega_-)\hat{\rho}_+^2 + \frac{1}{2}m\omega_z^2\hat{z}^2 - \frac{1}{2}m\omega_-(\omega_+ - \omega_-)\hat{\rho}_-^2 \tag{2.48}$$

is conserved. Since there are no more cross-terms of the kind $\hat{\rho}_+\hat{\rho}_-$, the individual contributions are readily attributed to the three eigenmodes as

$$\mathcal{E}_+ = \frac{1}{2}m\omega_+(\omega_+ - \omega_-)\hat{\rho}_+^2 \approx \frac{1}{2}m\omega_+^2\hat{\rho}_+^2 \quad , \tag{2.49}$$

$$\mathcal{E}_- = -\frac{1}{2}m\omega_-(\omega_+ - \omega_-)\hat{\rho}_-^2 \approx -\frac{1}{2}m\omega_+\omega_-\hat{\rho}_-^2 = -\frac{1}{4}m\omega_z^2\hat{\rho}_-^2 \quad , \tag{2.50}$$

$$\mathcal{E}_z = \frac{1}{2}m\omega_z^2\hat{z}^2 \quad . \tag{2.51}$$

The approximations use $|\omega_+| \gg |\omega_-|$. Additionally, the product of the radial frequencies is expressed as $2\omega_+\omega_- = \omega_z^2$ with Equation (2.26). The energy of the modified cyclotron-mode is dominated by kinetic energy, whereas the magnetron mode is dominated by potential energy. Because the quadrupole potential Φ_2 is repulsive in the radial direction, the energy of the magnetron mode decreases with magnetron radius $\hat{\rho}_-$. Hence, the magnetron mode is metastable. Upon dissipating energy, the amplitude of the magnetron mode increases.

In the quantum-mechanical case, the total energy of a spinless particle in a PENNING trap

$$\mathcal{E}_{\text{tot}} = \hbar|\omega_+|\left(n_+ + \frac{1}{2}\right) + \hbar\omega_z\left(n_z + \frac{1}{2}\right) - \hbar|\omega_-|\left(n_- + \frac{1}{2}\right) \tag{2.52}$$

is given by the sum of three independent harmonic oscillators [60, 146]. Here, $\hbar$ is the reduced Planck constant, and the $n_k = 0, 1, 2, 3, \ldots$ are the quantum numbers of the harmonic oscillator associated with each of the three modes. Like in the classical case, the energy of the magnetron mode is negative, because the magnetron mode actually represents an inverted harmonic oscillator. The zero-point energy $1/2\hbar|\omega_k|$ each oscillator has for $n_k = 0$ means that the classical amplitudes of the modes cannot vanish.

2.2. Cylindrically-symmetric deviations

This section discusses physical constraints on electromagnetic fields in free space, with the interior of the Penning trap in mind. These will be applied in Sections 2.2.1 and 2.2.2 to derive the permissible spatial dependence of electrostatic potentials and static magnetic fields with cylindrical symmetry, respectively. Sections 3.4.4 and 5.1 touch on effects beyond cylindrical symmetry, and Chapter A in the appendix gives a more general parametrization.

Already when discussing the potential of the ideal Penning trap in Section 2.1, it became obvious that contributions beyond the quadrupole potential are practically unavoidable. Since the electrostatic potential is produced with electrodes of cylindrical symmetry, its imperfections are expected to have the same symmetry. Moreover, the particle averages over some deviations from cylindrical symmetry, while it orbits around the center of the trap in the strong magnetic field. Recently, a peculiar segmentation of a cell used for Fourier-transform ion cyclotron-resonance (FT-ICR) has been proposed [11] and demonstrated [111] to produce an effective quadrupole potential upon averaging the actual electrostatic potential along the modified cyclotron-motion, thereby harmonizing the cell dynamically. Because of this motional averaging, many imperfections may be described as effectively cylindrically-symmetric. This is of particular importance for the magnetic field [107, 150], whose symmetry axis does not have to run through the electrostatic center of the trap, provided cylindrical symmetry is present at all. The magnetic field is typically created by currents in solenoidal coils, but the trap may not sit on their central axis. If the higher-order terms arise from the magnetic susceptibility of cylindrically-symmetric electrodes placed in an originally uniform magnetic field, the symmetry carries over, but, outside of the electrodes, rotational symmetry is typically a discrete one at best. The same breaking of the continuous symmetry pertains to segmented electrodes, which affects the electric potential, too.

Nevertheless, many dominant imperfections are expected to possess (effective) cylindrical-symmetry, which warrants a general description of such terms in the electric potential and the magnetic field. From the experimental point of view, the peculiar spatial dependence as such is of little importance. It is simply necessary to calculate the associated frequency-shifts (Section 4.1), which affect the most relevant observables—the eigenfrequencies. Since the fields of a Penning trap suspend a charged particle in free space, the fields at the position of the particle are governed by Maxwell's equations in vacuum.[11] In differential form, they read

$$\vec{\nabla} \times \vec{E} = -\dot{\vec{B}} \quad , \qquad \vec{\nabla} \cdot \vec{B} = 0 \quad , \tag{2.53}$$

$$\vec{\nabla} \cdot \vec{E} = \frac{\varrho}{\varepsilon_0} \quad , \qquad \vec{\nabla} \times \vec{B} = \mu_0 \vec{j} + \mu_0 \varepsilon_0 \dot{\vec{E}} \quad . \tag{2.54}$$

The first line contains the homogeneous equations, which do not have any source terms. The inhomogeneous equations in the second line contain the charge density ϱ and the current density $\vec{j}$ as sources. The vacuum permittivity is given by ε_0; the vacuum permeability is given by μ_0.

[11] Here, free space refers to vacuum in contrast to matter. This should not be confused with the use in the free-space cyclotron-frequency, which refers to the absence of an electric field, possibly because of the absence of trap electrodes.

The fields $\vec{B}$ and $\vec{E}$ may also be expressed in terms of the vector potential $\vec{A}$ and the scalar potential Φ as

$$\vec{B} = \vec{\nabla} \times \vec{A} \quad , \qquad \vec{E} = -\vec{\nabla}\Phi - \frac{\partial \vec{A}}{\partial t} \quad . \tag{2.55}$$

With these definitions, the homogeneous Maxwell equations (2.53) are automatically satisfied because $\vec{\nabla} \times \vec{\nabla}\Phi = 0$ and $\vec{\nabla} \cdot (\vec{\nabla} \times \vec{A}) = 0$ for a scalar function Φ and a vector function $\vec{A}$ in general, assuming differentiability.

In most cases, describing the fields of the Penning trap sufficiently well does not require the most general expression, and a number of simplifications is typically applied. Here, the static fields used for storing the particles in the Penning trap are of primary importance, since they are always present. Everything else is optional. Of course, there must be at least one charged particle in the trap for experiments, and, in addition to the charge, there is a current associated with this oscillating particle. Fortunately, these effects may be dealt with separately, because Maxwell's equations are linear, and the superposition principle holds. The equations may therefore be solved separately for fields of different origin. Furthermore, the coupling between electric and magnetic fields brought about by the time-derivatives in Equations (2.53) and (2.54) vanishes for static fields. In this case, the electric and magnetic fields are unrelated, and we will deal with them individually. Even for time-dependent fields, such as the fields caused by the oscillating particle, or oscillatory fields employed to excite or couple its eigenmotions, the problem is treated as static one, when the frequencies are low enough. The solution from the static case is used, with the fields then taking their instantaneous value for the particular conditions at that very instant. When the time-derivatives and wave effects, such as propagation delay or reflection, are negligible, oscillatory fields are not conceptually different from static ones.

So far, the discussion applies to electric and magnetic fields in free space in general. For possible solutions of Maxwell's equations in a Penning trap, we will now restrict ourselves to fields with cylindrical symmetry. In this way, we will learn about the general structure of the solutions for this particular kind of symmetry without invoking the exact boundary conditions, which differ from trap to trap. The fundamental solutions, however, are the same. Only their contributions to the specific overall solution differ.

2.2.1. Electrostatic

Combining the inhomogeneous Maxwell equation (2.54) for the electric field $\vec{E}$ with the scalar potential Φ defined by Equation (2.55) yields the Poisson equation

$$\vec{\nabla} \cdot \vec{E} = \vec{\nabla} \cdot (-\vec{\nabla}\Phi) = -\Delta\Phi = \frac{\varrho}{\varepsilon_0} \quad , \tag{2.56}$$

where $\Delta = \vec{\nabla} \cdot \vec{\nabla}$ is the Laplace operator, given for Cartesian coordinates in Equation (2.4). Even though the charge-density ϱ inside a Penning trap is given by the oscillating ion, we have neglected the time-derivative of the vector potential $\vec{A}$. The dominant component of the magnetic field is the static one. Interaction between ions is typically modeled by Coulomb interaction or space-charge via electric rather than magnetic forces.

While the limitation to a single ion eliminates ion–ion interaction and space-charge effects, the single charge still interacts with the image charges it induces in the trap electrodes. For particles heavier than electrons, the image charges mainly modify the electrostatic potential seen by the particle, which results in a frequency-shift that can be treated as a small perturbation [127, 152, 162]. Section 5.1 takes a closer look. Although the distribution of image charges for a particle displaced from the z-axis breaks cylindrical symmetry, the resulting potential at the particle's position is cylindrically-symmetric, provided the electrodes have that symmetry. However, the link between the dependence on ρ and z we will establish in this section does not have to be valid, because the ion samples the potential it generates via the image charges only at its own position, and not in terms of a general coordinate elsewhere [157]. Because the potential of the image charges is small compared with the potential generated by applying different voltages on the trap electrodes, it is usually sufficient to include only the lowest-order terms, which are quadratic in z and ρ at the position of the ion, as a modification to the quadrupole potential in the ideal trap. In this case, the frequency-shift to the three eigenfrequencies does not depend on the particle's amplitudes.[12]

From here on, we will focus on the external potential used for trapping the particle. Since the image-charge interaction is expected to be attractive when approaching the trap electrodes, axial confinement could not be guaranteed otherwise, no matter how slow the particle. Moreover, the image-charge shifts are avoidable experimentally, because they are strongly suppressed for larger traps.

In the empty trap with $\varrho = 0$, the Poisson equation (2.56) simplifies to the Laplace equation

$$\Delta\Phi = 0 \quad . \tag{2.57}$$

In the literature, cylindrically-symmetric solutions that do not diverge at the origin [170] are typically expressed as

$$\Phi_\eta(r, \theta) = C_\eta \frac{V_0}{2d^\eta} r^\eta P_\eta\big(\cos(\theta)\big) \tag{2.58}$$

in spherical coordinates,[13] where P_η is a Legendre polynomial and $\eta = 0, 1, 2, 3, \ldots$ a non-negative integer. An explicit form of the Legendre polynomials P_η is not needed in this section and is therefore relegated to Equation (A.14) in the appendix. For curiosity, Table A.1 there shows the first few P_η. Making the substitution $r^\eta \to r^{-(\eta+1)}$ also results in a valid solution to the Laplace equation (see Section A.1 in the appendix). However, the singularity for $r = 0$ would be associated with a point charge at the origin, and free charges are ruled out by selecting the charge-density $\varrho = 0$ inside the empty trap.

[12] If the potential of the image charges does not obey the form of the quadrupole potential (2.2), the shifted eigenfrequencies violate the invariance theorem (2.27), even though an entirely quadratic potential in ρ and z does not give rise to anharmonic frequency-shifts [25]. For such an electrostatic potential, which does not couple the axial and the radial modes, the cyclotron-sideband identity (2.25) remains valid, because the shifts to the radial modes are equal in magnitude, but opposite in sign.

[13] In some publications, for instance [3, 12, 99, 170], the distance from the z-axis is called r, whereas the distance from the origin is called ρ (if used at all). In this case, the meaning of r and ρ is opposite to the definition used here. See Equation (2.61) and Figure 2.4.

Other solutions with singularities exist, the natural logarithm $\ln(\rho)$ of the radial coordinate (2.3) being among the most simple functional dependencies.[14] Clearly, $\ln(\rho)$ diverges for $\rho = 0$, that is, on the z-axis,[15] Such a potential might be generated by a charged wire running along this axis,[16] and such an arrangement may also be used to trap ions [26, 121]. The concept has also been used for increasing the path length of electrons in electrostatic ion gauges [106] and vacuum pumps [39] ("orbitron"). The Kingdon trap [58, 85, 86] and the orbitrap [73, 100]—both of which operate without a magnetic field—come with a central wire and an inner electrode, respectively, around which the ions orbit. Since the Penning trap has no electrodes in its trapping volume, mathematical solutions with singularities do not have to be elaborated here, and we return to the standard solution in the literature.

Because Φ_η of Equation (2.58) satisfies a homogenous linear differential equation, the spatial dependence expressed by $r^\eta P_\eta(\cos(\theta))$ is the crucial part. Consequently, other prefactors have been used.[17] Here, the prefactor is chosen to match the definition (2.2) of the quadrupole potential Φ_2 for $\eta = 2$. In the context of the experiment, V_0 is understood as an applied voltage. The dimensionless parameter C_η describes the strength of the contribution. The characteristic trap dimension d, defined in Equation (2.10), removes the dimension of (length)$^\eta$ carried by r^η, such that the overall expression has the unit of voltage.

As the individual Φ_η are fundamental solutions of the Laplace equation, the overall potential is given by a suitable superposition, with the C_η adjusted to match the shape of the potential. In the case of the Penning trap, the overall potential is found by solving the Laplace equation for the Dirichlet boundary conditions imposed by the electrodes. Without any dependence on the azimuth angle ϕ, the Φ_η are indeed cylindrically symmetric, but they do not use the natural coordinate system of the trap. The discussion of a particle's motion in Section 2.1.1 has distinguished between the axial mode and the two radial modes, and the potential was described best with cylindrical coordinates. Therefore, we would like to find the coefficient $a_\eta(k)$ in

$$r^\eta P_\eta\big(\cos(\theta)\big) \equiv \sum_{k=0}^{\lfloor \eta/2 \rfloor} a_\eta(k)\, z^{\eta-2k}\, \rho^{2k} \quad . \tag{2.59}$$

The upper limit of the sum is given by the floor function[18]

$$\left\lfloor \frac{\eta}{2} \right\rfloor = \begin{cases} \frac{\eta}{2} & \text{if } \eta \text{ is even,} \\ \frac{\eta-1}{2} & \text{if } \eta \text{ is odd.} \end{cases} \tag{2.60}$$

[14] Rather than using the Laplace operator (2.4) in Cartesian coordinates on the radial coordinate expressed via Equation (2.3), the statement about $\ln(\rho)$ solving the Laplace equation is confirmed more conveniently with the Laplace operator (2.63) in cylindrical coordinates.

[15] Other solutions with a singularity on the z-axis are obtained by replacing the Legendre polynomial P_η by the Legendre function of the second kind, Q_η, see Section A.1 in the appendix.

[16] Inside the wire, the potential has a different form, and the singularity has no practical consequence.

[17] Most notably, the potential associated with odd η is often normalized to z_e, the distance from the trap center to the endcap (see Figure 2.1), because the limiting values approached for large $\rho_\mathrm{r}^2/(2z_\mathrm{e}^2)$ become independent of $\rho_\mathrm{r}/z_\mathrm{e}$ [48, 51, 53]. Moreover, the odd coefficients C_η are called c_η or B_η in earlier papers, the latter choice conflicting with the coefficients of higher orders in the magnetic field to be introduced in Section 2.2.2.

[18] Here, the floor function is defined only for integers, which is most convenient for our purpose. In general, the floor function $\lfloor x \rfloor$ gives the largest integer not greater than x.

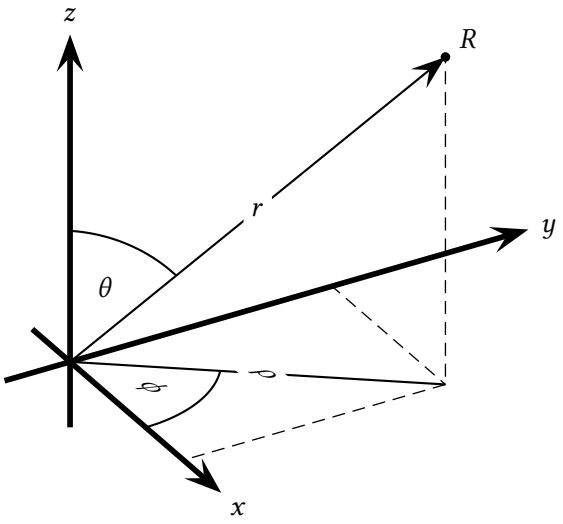

Figure 2.4.: Coordinate system used in this thesis. The distance from the z-axis is given by ρ; the distance from the origin by r. In radians rather than degrees, the azimuth angle ϕ runs from 0 to 2π; the zenith angle θ from 0 (pointing along the positive-z axis) to π (pointing along the negative z-axis).

Using the explicit expression (A.12b) for the Legendre polynomials, it is easy to verify that the right-hand side of Equation (2.59) must have this particular form (see Section A.2 in the appendix). Section B.1 in the appendix verifies the polynomial form independently via Bessel functions—a nonpolynomial solution to the Laplace equation. Here, we will simply motivate the choice and prove that it works.

Overall, the right-hand side has the dimension of (length)$^\eta$, just like the left-hand side, and the limits for the summation variable k are chosen such that there are no negative exponents, neither for ρ nor for z, because the solution must not possess a singularity, neither at the origin nor on on the z-axis.[19] There are only even powers of ρ, because neither spherical coordinate

$$r = \sqrt{\rho^2 + z^2} \quad , \tag{2.61}$$

$$\cos(\theta) = \frac{z}{r} = \frac{z}{\sqrt{\rho^2 + z^2}} \tag{2.62}$$

depends on the sign of ρ. Figure 2.4 illustrates the link between the coordinate systems, and it clarifies the use of r and ρ.

It looks like the straightforward way to determine the coefficient $a_\eta(k)$ is to express the spherical coordinates on the left-hand side of Equation (2.59) as a function of the cylindrical coordinates, knowing an explicit expression for the Legendre polynomial. However, Section A.2

[19] From the physical point of view, a singularity is associated with the presence of a pointlike charge, which we have ruled out by assuming zero charge-density inside the trap. Moreover, several pointlike charges of different sign would be necessary to create a potential that falls off more strongly than the usual $1/r$ dependence of the Coulomb potential.

in the appendix shows that this ansatz seems to require an elaborate knowledge of mathematical identities. Consequently, we will follow a second route that requires almost no knowledge about Legendre polynomials.

Only very rarely are general expressions for the cylindrically-symmetric potential in cylindrical coordinates shown in the literature [99]. References [3, 99] both express $r^\eta P_\eta(\cos(\theta))$ as a function $H_\eta(\rho, z)$, but Reference [3] gives explicit expressions for the first few η only. When it comes to finding a general expression in mathematical handbooks, it does not help that these special functions come with different names: solid harmonics [99, 187] or (zonal) spherical harmonics [3, 189]. Even with this name known, the coefficient $a_\eta(k)$ in Equation (2.59) is hard to look up, and there seems to be little inspiration from other fields (of physics), despite the multitude of applications with electric and magnetic fields.

The general solution (2.58) for the potential Φ_η for a boundary value problem with azimuthal symmetry seems to be inspired by the classical textbook [79]. A second textbook solution with cylindrical symmetry involves a product of (modified) Bessel functions with the radial coordinate ρ as the argument and (complex) exponential functions of the axial coordinate z. This factorization into functions of ρ and z is particularly helpful for the analytic calculation of the potential in a cylindrical trap—most appropriately a can-shaped trap with a cylindrical ring electrode and flat-plate endcaps [5, 13]—because on the electrodes, where the boundary conditions hold, one of the two coordinates is a constant, rather than a function of the other coordinate. In order to evaluate the multipole components of the potential, the solution is expanded about the center of the trap in a polynomial of ρ and z. Analytically, the coefficients C_η may be extracted by equating the solution on the z-axis alone [51, 53]. In this way, the dependence on ρ of the polynomial solution (2.59) to the Laplace equation is not deduced independently by a series expansion of the (modified) Bessel function in its argument ρ, even though this would avoid a conversion of coordinates. Instead, the dependence on ρ is borrowed from a known polynomial solution to the Laplace equation, which typically involves a Legendre polynomial. Section B.1 in the appendix shows that there is no need to reintroduce the dependence on ρ by hand because it carries over naturally to the polynomial solution with little mathematical effort.

As the Penning-trap literature almost exclusively relies on the standard parametrization (2.58) in spherical coordinates, converting to cylindrical coordinates manually for every η considered, the general conversion is worth being presented here.[20] We shall see that the major step is more about looking for a solution of the Laplace equation in cylindrical coordinates right from the start than an actual conversion based on the explicit form of the Legendre polynomial.[21]

The approach starts by applying the Laplace operator [180] in cylindrical coordinates

$$\Delta = \frac{1}{\rho}\frac{\partial}{\partial\rho}\left(\rho\frac{\partial}{\partial\rho}\right) + \frac{1}{\rho^2}\frac{\partial^2}{\partial\phi^2} + \frac{\partial^2}{\partial z^2} \tag{2.63}$$

[20] Of course, it speaks to the quality of a (quadrupole) trap that its potential is described by just a few low-order terms, thereby rendering the general conversion (2.59) to cylindrical coordinates unimportant from a practical point of view.

[21] The idea is similar to the description of the electrostatic potential in Reference [135], where the different coefficients in the expansion of a potential in terms of polynomials in ρ and z are calculated from an analytic expression of that very potential. However, no direct link between the expansion coefficients is given. Reference [134] does that, without establishing the link to Legendre polynomials though.

to the right-hand side of Equation (2.59). We now consider the two terms that will have to cancel after applying the Laplace operator, for the right-hand side to be a solution of the Laplace equation, just like the left-hand side already is, thanks to the special properties of the Legendre polynomial. For a given value k of the summation variable, we pick the component with $k+1$ for the radial part of the Laplace operator and obtain

$$\frac{1}{\rho}\frac{\partial}{\partial\rho}\left(\rho\frac{\partial}{\partial\rho}\right)\left[a_\eta(k+1)z^{\eta-2k-2}\rho^{2k+2}\right] = (2k+2)^2\,a_\eta(k+1)\,z^{\eta-2k-2}\rho^{2k} \quad . \tag{2.64}$$

For the axial part of the Laplace operator, picking the component with k yields

$$\frac{\partial^2}{\partial z^2}\left[a_\eta(k)z^{\eta-2k}\rho^{2k}\right] = (\eta-2k)(\eta-2k-1)\,a_\eta(k)\,z^{\eta-2k-2}\rho^{2k} \quad . \tag{2.65}$$

In both cases, the exponents of z and ρ are the same. Thus, the prefactors have to vanish upon summation, which results in the recursive relationship

$$a_\eta(k+1) = -\frac{(\eta-2k)\,(\eta-2k-1)}{2^2\,(k+1)^2}\,a_\eta(k) \quad . \tag{2.66}$$

We try to guess an explicit expression after applying the recursion multiple times:

$$a_\eta(4) = \frac{-(\eta-6)\,(\eta-7)}{2^2\,4^2}\,a_\eta(3) = \frac{-(\eta-6)\,(\eta-7)}{2^2\,4^2}\,\frac{-(\eta-4)\,(\eta-5)}{2^2\,3^2}\,a_\eta(2) \tag{2.67a}$$

$$= \frac{-(\eta-6)\,(\eta-7)}{2^2\,4^2}\,\frac{-(\eta-4)\,(\eta-5)}{2^2\,3^2}\,\frac{-(\eta-2)\,(\eta-3)}{2^2\,2^2}\,a_\eta(1) \tag{2.67b}$$

$$= \frac{-(\eta-6)\,(\eta-7)}{2^2\,4^2}\,\frac{-(\eta-4)\,(\eta-5)}{2^2\,3^2}\,\frac{-(\eta-2)\,(\eta-3)}{2^2\,2^2}\,\frac{-\eta\,(\eta-1)}{2^2\,1^2}\,a_\eta(0) \tag{2.67c}$$

$$= \frac{(-1)^4}{2^{2\cdot4}}\,\frac{\eta(\eta-1)(\eta-2)(\eta-3)(\eta-4)(\eta-5)(\eta-6)(\eta-7)}{(4\cdot3\cdot2\cdot1)^2}\,a_\eta(0) \quad . \tag{2.67d}$$

In the last step, we have rearranged the factors to underline the general structure. Spotting the pattern leads to the explicit expression

$$a_\eta(k) = \frac{(-1)^k}{2^{2k}}\,\frac{\eta(\eta-1)\cdots(\eta-2k-2)(\eta-2k-1)}{(k!)^2}\,a_\eta(0) \tag{2.68a}$$

$$= \frac{(-1)^k}{2^{2k}}\,\frac{\eta!}{(\eta-2k)!(k!)^2}\,a_\eta(0) \quad . \tag{2.68b}$$

In the last step, we have expanded the fraction with a factor of $(\eta-2k)!$, where the factorial of a non-negative integer n is as usual given by the product

$$n! = n(n-1)(n-2)\cdots3\cdot2\cdot1 \quad \text{with} \quad 0! = 1 \quad . \tag{2.69}$$

This expansion is fine because the upper limit $k \leq \lfloor\eta/2\rfloor$ of the sum (2.59) means that $\eta - 2k \geq 0$. The explicit expression (2.68b) agrees with Equation (3.20) in Reference [134].

The recursive relationship (2.66) does not determine the absolute value of the coefficient $a_\eta(k)$. The value has to adjusted to match some special value of the Legendre polynomial, the property

$P_\eta(1) = 1$, for example. In spherical coordinates, $1 = \cos(0)$ describes a point on the positive z-axis, where $\rho = 0$ and hence $r = z$ according to Equation (2.61). Consequently, the only contribution on the right-hand side of Equation (2.59) comes from $k = 0$, and the equation for the remaining coefficient reads

$$r^\eta P_\eta(1) = r^\eta \cdot 1 = z^\eta \cdot 1 = a_\eta(0) z^\eta \quad . \tag{2.70}$$

Thus, $a_\eta(0) = 1$, and the explicit expression (2.68b) for the coefficient simplifies to

$$a_\eta(k) = \frac{(-1)^k}{2^{2k}} \frac{\eta!}{(\eta - 2k)!\,(k!)^2} \quad . \tag{2.71}$$

As a cross-check, the recursive relation (2.66) is satisfied because

$$-\frac{(\eta - 2k)\,(\eta - 2k - 1)}{2^2\,(k+1)^2}\, a_\eta(k) = -\frac{(\eta - 2k)\,(\eta - 2k - 1)}{2^2\,(k+1)^2}\, \frac{(-1)^k}{2^{2k}} \frac{\eta!}{(\eta - 2k)!\,(k!)^2} \tag{2.72a}$$

$$= \frac{(-1)^{k+1}}{2^{2(k+1)}} \frac{\eta!}{[\eta - 2(k+1)]!\,[(k+1)!]^2} = a_\eta(k+1) \quad . \tag{2.72b}$$

At this point, we have found the general expression

$$\Phi_\eta(\rho, z) = C_\eta \frac{V_0}{2d^\eta} \sum_{k=0}^{\lfloor \eta/2 \rfloor} a_\eta(k)\, z^{\eta - 2k}\, \rho^{2k} \tag{2.73}$$

for cylindrically-symmetric solutions of the Laplace equation (2.57) that do not diverge at the origin, and we have done so naturally in cylindrical coordinates without invoking special functions. The result agrees with Equation (C.7) in Reference [99], which was derived from a general expression for the Legendre polynomial. Table 2.1 shows the spatial dependence of Equation (2.73) for the first few η.

As mentioned before to justify the ansatz (2.59), there are only even powers of ρ, but, as the distance from the z-axis, ρ is typically taken to be a positive quantity anyway. With this convention, the cylindrical symmetry is reflected by the absence of the azimuth angle ϕ. The fundamental solutions Φ_η are even functions with respect to z when η is even, that is, $\Phi_\eta(\rho, -z) = \Phi_\eta(\rho, z)$. They are odd functions when η is odd, that is, $\Phi_\eta(\rho, -z) = -\Phi_\eta(\rho, z)$. Therefore, the terms with η odd are typically associated with a voltage applied asymmetrically between the endcaps. Since the trap shown in Figure 2.1 has perfect reflection symmetry about the xy-plane, the coefficients C_η with η odd would vanish in the configuration shown. Fortunately, the prefactor of the sum may be changed at will, with Φ_η staying a solution of the Laplace equation as long as the spatial dependence is not altered.

We have yet to derive the electric field $\vec{E}_\eta$ associated with the electrostatic potential Φ_η by taking the negative gradient according to Equation (2.55). This will be done at the beginning of Section 4.1.2 when the electric field has to be plugged into an actual equation of motion. Traditionally, the Penning trap is characterized by its magnetic field and its electrostatic potential, rather than its electric field. The electrostatic potential parametrizes the same information in a more compact way because it is a scalar quantity.

2.2.2. Magnetostatic

Unlike the electrostatic potential, the magnetic field is not calculated as easily from first principles because its boundary conditions are more intricate. Whereas the electrodes are equipotential surfaces for the electric potential and hence free of (static) electric fields, thereby shielding the ion from the outside electrically, they are penetrated by the magnetic field. Since the coils that generate the magnetic field sit outside of the trap volume, the magnetic penetration is indispensable from the experimental point of view, but for a theoretical description, the Maxwell equations in matter with interface conditions would have to be consulted. Even if the geometry of the trap and its magnetic properties are known, an exact solution is difficult, because the geometry of the coils in the magnet is often kept secret by the manufacturer. The coils would therefore have to be modeled (or reverse engineered) based on a measurement of the magnetic field without the trap in place. In many cases, considering the distortion of the measured field by the trap apparatus is enough to estimate the influence on the trapped ion. Without going into details about boundary and interface conditions, it is possible to derive some general properties of the magnetic field inside the trap, simply from the fact the Maxwell's equations have to be satisfied there, too.

Inside the trap, Maxwell's equations in free space hold. Most notably, there are no coils carrying current. Neglecting the current by the oscillating ion, there is no current density inside the trap, that is, $\vec{j} = 0$. The fields caused by the ion aside, the problem is a static one, and all the time-derivatives in Equations (2.53) and (2.54) vanish. With these simplifications, the inhomogeneous Maxwell equation for the magnetic field reads $\vec{\nabla} \times \vec{B} = 0$. Naturally, the magnetic field has no sources: $\vec{\nabla} \cdot \vec{B} = 0$. These two equations are the same as for the electric field $\vec{E}$ in the static case with no charge density ϱ. Instead of deriving the magnetic field from a vector potential according to Equation (2.55), it is more convenient to use a scalar potential Ψ linked via $\vec{B} = -\vec{\nabla}\Psi$. Like for the electrostatic case with Φ in Equation (2.57), the scalar potential Ψ fulfills the Laplace equation $\Delta\Psi = 0$. Basically, the whole treatment carries over. Because the magnetic field is more familiar than the scalar magnetic potential, we will derive the former from the latter as soon as possible, even though the expression for the magnetic field is more space-consuming than for the scalar potential.

Cylindrically-symmetric fundamental solutions for the potential Ψ_η without a singularity at the origin or on the whole z-axis—with no free currents inside the trap, the magnetic field is finite there—are written as

$$\Psi_\eta(r,\theta) = -\frac{B_\eta}{\eta+1}\, r^{\eta+1} P_{\eta+1}\big(\cos(\theta)\big) \tag{2.74}$$

$$= -\frac{B_\eta}{\eta+1} \sum_{k=0}^{\left\lfloor \frac{\eta+1}{2} \right\rfloor} a_{\eta+1}(k)\, z^{\eta+1-2k}\, \rho^{2k} = \Psi_\eta(\rho,z) \tag{2.75}$$

in analogy to the electrostatic potential Φ_η in Equation (2.58) with spherical coordinates. Again, $\eta = 0, 1, 2, \ldots$ is a non-negative integer, and P_η is a Legendre polynomial. The transformation to cylindrical coordinates is the same as in Equation (2.59), with the coefficient $a_{\eta+1}(k)$ defined by Equation (2.71). The strength of a contribution is described by the parameter B_η, and the superposition principle holds for the Ψ_η. The choice of $\eta + 1$ will become obvious when considering the exact form of the axial magnetic field that results from the potential Ψ_η.

The additional axial and magnetic field associated with the scalar potential Ψ_η are calculated by taking the negative gradient:

$$\vec{B}_\eta(\rho,z) = -\frac{\partial\Psi_\eta(\rho,z)}{\partial z}\,\vec{e}_z - \frac{\partial\Psi_\eta(\rho,z)}{\partial\rho}\,\vec{e}_\rho \tag{2.76}$$

$$= B_\eta^{(z)}(\rho,z)\,\vec{e}_z + B_\eta^{(\rho)}(\rho,z)\,\vec{e}_\rho \quad . \tag{2.77}$$

Here, $\vec{e}_z$ and $\vec{e}_\rho$ are the unit vectors in the axial and radial direction, respectively.

The axial magnetic field takes the form

$$B_\eta^{(z)}(\rho,z) = -\frac{\partial\Psi_\eta(\rho,z)}{\partial z} = B_\eta \sum_{k=0}^{\lfloor\eta/2\rfloor} a_\eta(k)\; z^{\eta-2k}\,\rho^{2k} \quad , \tag{2.78}$$

which has the same spatial dependence as the electrostatic potential Φ_η (see Equation (2.73) for the general expression and Table 2.80 for first few η), because

$$\frac{\eta-2k+1}{\eta+1}\,a_{\eta+1}(k) = \frac{(-1)^k}{2^{2k}}\,\frac{\eta!}{(\eta-2k)!(k!)^2} = a_\eta(k) \tag{2.79}$$

according to Equation (2.71). In the literature, the axial magnetic field is therefore often expressed with Legendre polynomials in spherical coordinates (see Equation (2.82)). This explains the peculiar use of $\eta+1$ when defining the potential Ψ_η in Equation (2.75). Note that we have lowered the upper limit of the summation from $\lfloor(\eta+1)/2\rfloor$ in Equation (2.75) to $\lfloor\eta/2\rfloor$ in Equation (2.78). The factor $\eta-2k+1$, which results from taking the derivative with respect to z, ensures that there is no contribution at the original upper limit, even for η odd. If η is even, then $\lfloor(\eta+1)/2\rfloor = \lfloor\eta/2\rfloor$ anyway, see the definition (2.60) of the floor function for integer arguments. At this point, it is better not to be sloppy about the limits because $a_\eta(k)$ from Equation (2.71) is not defined for $k > \lfloor\eta/2\rfloor$, since the argument of $(\eta-2k)!$ would become negative.

Because the axial magnetic field $B_\eta^{(z)}(\rho,z)$ has the same spatial dependence as the electrostatic potential Φ_η, the symmetry carries over. Concerning the radial displacement, there are only even and no odd powers of ρ. The axial magnetic field is an even function of z for η even, and an odd function for η odd.

The radial magnetic field is

$$B_\eta^{(\rho)}(\rho,z) = -\frac{\partial\Psi_\eta(\rho,z)}{\partial\rho} = B_\eta \sum_{k=1}^{\left\lfloor\frac{\eta+1}{2}\right\rfloor} \tilde{a}_\eta(k)\; z^{\eta-2k+1}\,\rho^{2k-1} \tag{2.80}$$

with the coefficient

$$\tilde{a}_\eta(k) = \frac{(-1)^k\,k}{2^{2k-1}}\,\frac{\eta!}{(\eta-2k+1)!\,(k!)^2} \quad . \tag{2.81}$$

Note that the lower limit of the sum starts at $k=1$ rather than at $k=0$ for the scalar potential Ψ_η. Since the term in Ψ_η for $k=0$ does not depend on ρ, it is removed by taking the derivative. This is reflected in the factor of k that $\tilde{a}_\eta(k)$ contains. Because $\tilde{a}_\eta(0)=0$, not increasing the lower limit by one would not be critical here.

The radial magnetic field $B_\eta^{(\rho)}$ is an even function of z for η odd, and antisymmetric with respect to z for η even. It comes with odd powers of ρ exclusively. This means that it vanishes on the z-axis, where $\rho = 0$. It has to, because there is no direction to point to radially from the z-axis without violating cylindrical symmetry. Table 2.1 shows the spatial dependence of Equation (2.80) for the first few η.

Due to convention, the parameter B_η is not dimensionless for lack of a natural normalization length-scale. Instead, B_η bears the unit of magnetic field strength divided by (length)$^\eta$, and it should not be confused with the actual magnitude $\left|\vec{B}_\eta\right|$ of the magnetic field $\vec{B}_\eta$, which becomes a function of coordinates for $\eta \neq 0$. Apart from the homogeneous contribution, where B_0 and $\left|\vec{B}_0\right|$ differ by a sign at most, the spatial dependence of higher-order terms will have to be taken into account for the calculation of frequency-shifts. The magnitude alone is not enough, and it does not need to be designated. Consequently, the thesis uses B_η exclusively for the strength parameter of the contribution $\vec{B}_\eta$.

When normalizing the coefficient B_η with the help of B_0 and some characteristic length $\tilde{d}$ taken to the η-th power in order to arrive at a dimensionless coefficient similar to the C_η for the electrostatic potential, keep in mind that there is an extra factor of two in the denominators of Equations (2.58) and (2.73).

In the literature, cylindrically-symmetric components of the magnetic field are typically written in spherical coordinates as

$$\vec{B}_\eta(r,\theta) = B_\eta r^\eta \left[P_\eta\big(\cos(\theta)\big)\,\vec{e}_z - \frac{1}{\eta+1} P_{\eta 1}\big(\cos(\theta)\big)\,\vec{e}_\rho \right] \tag{2.82}$$

with the associated Legendre polynomial

$$P_{\eta 1}\big(\cos(\theta)\big) = \sin(\theta)\,\frac{\mathrm{d}P_\eta\big(\cos(\theta)\big)}{\mathrm{d}\cos(\theta)} \quad . \tag{2.83}$$

This definition of the associated Legendre polynomial is from Reference [20], and it is important because of different sign conventions (see Condon–Shortley phase [177]). Care should therefore be taken when evaluating Equation (2.82) for the radial field with a computer algebra system or tabulated functions. Deviating from the original layout of Reference [20], we have written the associated Legendre polynomial with two subscripts rather than the subscript η and the superscript 1 in order to distinguish the different sign conventions [172]. The general relation is $P_{\eta m} = (-1)^m P_\eta^m$, where m is an integer with $0 \leq m \leq \eta$, not to be confused with the rest mass of the particle. Table A.2 in the appendix shows explicit expressions of P_η^1 for the first few η.

Here, the sign is not a global parameter that may be adjusted at will and eventually absorbed in a different definition of B_η, because the two components of the magnetic field in Equation (2.82) are affected differently. Since they are physically related by $\vec{\nabla} \cdot \vec{B}_\eta = 0$, the sign of the radial magnetic field must not be changed independently from the axial magnetic field. The explicit expressions (2.78) and (2.80) for the two components of the magnetic field are unambiguous because they do not rely on special functions. Moreover, they express cylindrically-symmetric terms of the magnetic field naturally in cylindrical coordinates for all η.

Nevertheless, Equation (A.36a) from the appendix offers a general expression of the product $r^\eta P_\eta^m(\cos(\theta))$ in cylindrical coordinates. Using the expression for $m = 1$ on the radial magnetic field in Equation (2.82), where the minus is removed by the different sign convention for the associated Legendre polynomial, yields

$$\frac{r^\eta P_\eta^m(\cos(\theta))}{\eta+1} = \frac{(-1)}{2}\frac{(\eta+1)!}{\eta+1}\sum_{k=0}^{\left\lfloor\frac{\eta-1}{2}\right\rfloor}\frac{(-1)^k}{2^{2k}}\frac{z^{\eta-1-2k}\rho^{1+2k}}{k!\,(k+1)!\,(\eta-1-2k)!} \tag{2.84a}$$

$$= \eta!\sum_{k=0}^{\left\lfloor\frac{\eta-1}{2}\right\rfloor}\frac{(-1)^{k+1}(k+1)}{2^{2k+1}}\frac{z^{\eta-1-2k}\rho^{1+2k}}{[(k+1)!]^2\,(\eta-1-2k)!} \tag{2.84b}$$

$$= \sum_{k=1}^{\left\lfloor\frac{\eta+1}{2}\right\rfloor}\frac{(-1)^k k}{2^{2k-1}}\frac{z^{\eta-2k+1}\rho^{2k-1}}{(k!)^2\,(\eta-2k+1)!} \quad . \tag{2.84c}$$

In the last step, we have shifted the summation variable according to $k \to k-1$, which transformed the upper limit as $1+\lfloor(\eta-1)/2\rfloor = \lfloor(\eta+1)/2\rfloor$. The result is identical to the spatial component of the radial magnetic field (2.80).

Other general expressions are hard to find in the literature, most notably those with cylindrical coordinates. Reference [6] from the field of atoms traps gives tabulated expressions for cylindrically-symmetric magnetic fields in cylindrical coordinates, which may be compared with Table 2.1. Apart from what seem to be a few misprints, there is agreement.[22]

Reference [99], which offers a parametrization of the cylindrically-symmetric electrostatic potential in cylindrical coordinates, also gives such a parametrization for magnetic fields with the same symmetry for η even. However, some derivatives still need to be evaluated before a direct comparison with Equations (2.78) and (2.80) is possible. After all, the expressions agree. Since Hamiltonian perturbation theory is used to calculate the frequency-shifts caused by the imperfections there, the vector potential $\vec{A}$ rather than the magnetic field $\vec{B}$ is the relevant quantity. In this thesis, we will tackle the problem with classical equations of motion, which naturally require the use of fields, both electric and magnetic, instead of potentials, in order to calculate forces.

[22] Interestingly, the conversion of $r^\eta P_\eta(\cos(\theta))$ to cylindrical coordinates is shown twice—once in Table I for the scalar magnetic potential and once in Table II for the axial magnetic field—without mentioning the identical nature of the expressions. Upon closer inspection the prefactors of the term $z^2\rho^4$ differ: $^{45}/_{8}$ for $L = 6$ in Table I, $^{45}/_{56}$ for $n = 6$ in Table II. Table 2.1 sides with the former result. Other discrepancies [with the suggestion from this thesis shown in square brackets] include the exponent of ρ^2 [ρ^3] and the term $-33z^6$ [$-3z^5\rho$] in the radial magnetic field for $n = 3$ and $n = 6$, respectively, as well as the numerical prefactors 1675 [1575] and -67 [-63] in the scalar magnetic potential for $L = 0$.

Table 2.1.: The second column shows the spatial dependence of cylindrically-symmetric, polynomial solutions to the Laplace equation. These show up in the electrostatic potential (2.73), the scalar magnetic potential (2.75) and the axial magnetic field (2.78). The coefficient $a_\eta(k)$ is defined in Equation (2.71). All these solutions come with even powers of ρ only. The solutions are symmetric (antisymmetric) with respect to z when η is even (odd). The third column shows the spatial dependence of the radial magnetic field (2.80) with cylindrical symmetry. The coefficient $\tilde{a}_\eta(k)$ is defined in Equation (2.81). Apart from the exception for $\eta = 0$, these solutions come with odd powers of ρ only, and they are symmetric (antisymmetric) with respect to z when η is odd (even). The divergence of a vector field with the corresponding entries from the second and the third column taken as the axial and the radial component, respectively, vanishes for each η.

η	$\sum_{k=0}^{\lfloor \eta/2 \rfloor} a_\eta(k)\, z^{\eta-2k} \rho^{2k}$	$\sum_{k=1}^{\lfloor (\eta+1)/2 \rfloor} \tilde{a}_\eta(k)\, z^{\eta-2k+1} \rho^{2k-1}$
0	1	0
1	z	$-\frac{1}{2}\rho$
2	$z^2 - \frac{1}{2}\rho^2$	$-z\rho$
3	$z^3 - \frac{3}{2}z\rho^2$	$-\frac{3}{2}z^2\rho + \frac{3}{8}\rho^3$
4	$z^4 - 3z^2\rho^2 + \frac{3}{8}\rho^4$	$-2z^3\rho + \frac{3}{2}z\rho^3$
5	$z^5 - 5z^3\rho^2 + \frac{15}{8}z\rho^4$	$-\frac{5}{2}z^4\rho + \frac{15}{4}z^2\rho^3 - \frac{5}{16}\rho^5$
6	$z^6 - \frac{15}{2}z^4\rho^2 + \frac{45}{8}z^2\rho^4 - \frac{5}{16}\rho^6$	$-3z^5\rho + \frac{15}{2}z^3\rho^3 - \frac{15}{8}z\rho^5$
7	$z^7 - \frac{21}{2}z^5\rho^2 + \frac{105}{8}z^3\rho^4 - \frac{35}{16}z\rho^6$	$-\frac{7}{2}z^6\rho + \frac{105}{8}z^4\rho^3 - \frac{105}{16}z^2\rho^5 + \frac{35}{128}\rho^7$
8	$z^8 - 14z^6\rho^2 + \frac{105}{4}z^4\rho^4 - \frac{35}{4}z^2\rho^6 + \frac{35}{128}\rho^8$	$-4z^7\rho + 21z^5\rho^3 - \frac{35}{2}z^3\rho^5 + \frac{35}{16}z\rho^7$

3. Perturbation theory

This chapter[1] introduces the theoretical tool to calculate frequency-shifts caused by imperfections of the PENNING trap.[2] Since a general analytic solution for many effects beyond the ideal PENNING trap is somewhere between impracticable and impossible [72, 95], the theoretical treatment has to rely on approximative methods. Perturbation theory is one such method, and it has been employed multiple times on issues regarding real PENNING traps. The situation for frequency-shifts caused by cylindrically-symmetric imperfections of the electric and magnetic field is summarized at the beginning of Section 4.1; the past treatment of relativistic effects is reviewed in Section 4.2. In general, the focus has always been on the frequency-shifts associated with the imperfections, because frequencies are the major observables in a PENNING trap, and this thesis is no exception. However, modeling a particle stored in a PENNING trap is not all about frequencies. In order to describe the electronic signal by the image charges the orbiting particle induces on the electrodes, knowing the effect of imperfections on the particle's trajectory would be worthwhile, though difficult [93]. The trajectory also plays a key role upon excitation or coupling of the eigenmodes. Nevertheless, static frequency-shifts as in the case of constant motional amplitudes are important in their own right.

Perturbation theory builds the solution bottom up iteratively, starting from the ideal case, which still has an exact solution. Additions beyond this foundation are then treated as small imperfections, which slightly alter and add to the original solution. For the validity of the perturbative approach, it helps that the real PENNING traps used for precision measurements of motional frequencies are typically very good approximations of the ideal one. Even if the PENNING trap is just used as a storage device, possibly for cooling and preparing a pure sample of ions, a reproducible manipulation of the ion motion does not tolerate too large a deviation from the ideal case. Meticulous care is taken designing, manufacturing and assembling the trap electrodes, in order to produce as harmonic a potential as possible. Additionally, correction electrodes [158] allow to tune contributions beyond the quadrupole potential. The homogeneity of the magnetic field is optimized by shimming [133], and correction coils [1, 159]. In many cases, alignment of the trap with respect to the magnetic field is possible.

Concerning our implementation of perturbation theory, we will try to work with as little theoretical background as necessary, in order to demystify the calculation. The solution should follow smoothly from simple assumptions, rather than from a sophisticated, but arcane theo-

[1] The chapter is partly based on my earlier report [82] on cylindrically-symmetric imperfections of the electric and magnetic field. A much-compressed version focusing on the actual method that is subsequently applied to calculate first-order frequency-shifts in Chapter 4 is found in the paper [84]. Section 3.3 about second order is, well, a first (at least for me).

[2] For lack of a less cumbersome and more appropriate expression, and in the spirit of perturbation theory, we will sloppily refer to everything that is not present in the nonrelativistic treatment of the ideal PENNING trap with its uniform magnetic field $\vec{B}_0$ and the quadrupole potential Φ_2 as an imperfection, even though these imperfections may be an integral part of the detection system by design [30, 103].

retical framework. This pragmatic approach should make the calculation easy to comprehend, even though the framework has to be established first. With no pre-built framework to invoke, the basics make for a lengthy chapter. The imperfections will be treated classically based on trajectories rather than quantum-mechanical states, as was the ideal PENNING trap in Section 2.1. This result will provide the starting point. The rest of the treatment calls for perturbation theory, which we will motivate in the following.

Suppose there is a hard problem with no obvious solution in a closed form.[3] Generally speaking, a perturbative solution takes the following steps[4]:

1. Find or introduce a small parameter ϵ in the hard problem, such that the problem reduces to an exactly solvable—and hopefully solved—one for $\epsilon = 0$.

2. Try to solve the problem with a power series

$$f(\epsilon) = k_0 + \epsilon k_1 + \epsilon^2 k_2 + \dots \tag{3.1}$$

   in the perturbation parameter ϵ. The k_i are coefficients or functions that need to be determined from the fact that $f(\epsilon)$ must solve the problem in each order individually.

3. Sum the series (3.1).

The last step is optional, and it requires several orders to be known. If all the terms were known, the summation might not be trivial, and the radius of convergence must be checked. In the case of the PENNING trap, calculating the first nonvanishing term is typically sufficient for a valuable estimate at the experimental level of precision. Thus, the first two steps need to be applied to the imperfections in the PENNING trap, hoping to read off a frequency-shift in the process.

Before we proceed, a clarification about orders is, well, in order, because we use the term both for perturbation theory and the imperfections. In perturbation theory, the order of a term counts the power of the perturbation parameter ϵ in the prefactor. Hence, going from left to right on the right-hand side of the expansion (3.1), the three terms are of zeroth, first and second order, respectively. The dots indicate that terms of at least third order are not shown. When we speak of a first-order frequency-shift, we mean that the perturbation parameter is present once in the expression.

For the imperfections, order often refers to the index η in the components of the magnetic field $\vec{B}_\eta$ and the electrostatic potential Φ_η, without giving actual numbers for the order. For instance, Φ_6—represented by the parameter C_6—is considered an imperfection of higher order than Φ_4, because the effect of the former is typically less important.[5] Accordingly for the magnetic

[3] Of course, we are free to try perturbation theory on exactly solvable problems as a benchmark.

[4] These "axioms" of perturbation theory are inspired by a three-day lecture series given by Carl M. BENDER in October 2010. He is a proponent of multiple-scale perturbation theory (MSPT), a theory so general that he calls it the mother of all perturbation theories, because all the incarnations can be derived from it. Not surprisingly, MSPT [4] handles the secular term encountered in Section 3.2.1, but we will not use its general form here, because we opt for a dedicated formalism geared towards first-order frequency-shifts more than anything.

[5] In that sense, order may also refer to how strongly the frequency-shift depends on the particle's amplitude or energy, typically counting the exponent of the latter. However, the actual magnitude of the frequency-shift depends on more than just the scaling with amplitude, which is also only revealed towards the end of the calculation. Check the discussion at the beginning of Section 3.3.3 how the introduction of an order parameter as an addition to the perturbation parameter might help.

field, the component $\vec{B}_2$—represented by its strength parameter B_2—is deemed an imperfection of lower order than $\vec{B}_4$, because the effect of the former is typically more pronounced. Terms beyond the ideal PENNING trap are generally referred to as higher order with respect to its uniform magnetic field $\vec{B}_0$ and its quadrupole potential Φ_2.

This chapter relates the power series (3.1) for the trajectory to the frequency-shift in the PENNING trap, and it is organized as follows: In Section 3.2, we introduce the one-dimensional anharmonic oscillator as a test bench for the perturbative approach. For the oscillatory problem, a single power series in Section 3.2.1 will spell trouble. Section 3.2.2 offers a mathematical remedy, which Section 3.4 puts on more physical grounds. Section 3.4.2 generalizes this implementation of first-order perturbation theory to the radial modes in the PENNING trap.

Perturbation theory uses the oscillatory solutions (2.30)–(2.32) from the ideal PENNING trap as the zeroth-order input. These solutions contain trigonometric functions. From the functional dependence of the higher-order electrostatic potential (2.73) as well as the magnetic field (2.78) and (2.80), powers of trigonometric functions arise. The next section will therefore first provide the mathematical tools to handle these powers adequately in the perturbative calculation.

3.1. Powers of cosine

Expressing powers of cosine as a sum of oscillatory terms at different individual frequencies—possibly including a constant term at zero frequency—starts by writing cosine as a sum of exponential functions according to $2\cos(\chi) = \mathrm{e}^{\mathrm{i}\chi} + \mathrm{e}^{-\mathrm{i}\chi}$ based on EULER's formula. Powers of cosine then follow as a sum of single-frequency terms from the right-hand side, rearranged after binomial expansion to produce simple trigonometric functions. Section C.1 in the appendix shows the details of the calculation.

For even powers of cosine, the result (C.3e) with ωt as the argument[6] is

$$[\cos(\omega t)]^{2n} = \frac{1}{2^{2n}} \left[\binom{2n}{n} + 2 \sum_{j=1}^{n} \binom{2n}{n-j} \cos(2j\omega t) \right] \tag{3.2}$$

with the binomial coefficient defined as

$$\binom{n}{k} = \begin{cases} \dfrac{n!}{k!\,(n-k)!} & \text{if } 0 \le k \le n, \\ 0 & \text{otherwise.} \end{cases} \tag{3.3}$$

Here, n and k are non-negative integers, for which the factorial is defined in Equation (2.69). We will frequently use the identity

$$\binom{n}{k} = \binom{n}{n-k} \quad . \tag{3.4}$$

[6] For the sake of space and clarity, we use ωt rather than $\omega t + \varphi$ as the argument of the trigonometric function in this section, because a constant phase φ does not change the amplitudes or the frequencies of the individual terms. Including the additional phase φ is straightforward by making the above substitution, something we will do when returning to the oscillatory motion of the particle.

So far, the limits of the sum over j in Equation (3.2) ensure that the binomial coefficient is always given by its explicit expression (3.3) with factorials. However, this will no longer be the case in Chapter 4. Particularly when evaluating the general expressions for frequency-shifts, it is important to note that some binomial coefficients vanish. This is the case when n or k are negative, and when $k > n$. We will mention these special cases in due time when they occur, and we will still take care that the arguments n and k are integers in any case. Not using the explicit expression (3.3) with its two cases for the binomial coefficient will allow for more compact formulas, since the two cases do not have to be addressed individually—at least not until evaluating the general expressions. Fortunately, computer algebra systems often come with built-in functions for the binomial coefficient that are in line with the definition (3.3).

For odd powers of cosine, Equation (C.6e) from the appendix, with ωt as the argument here, reads

$$[\cos(\omega t)]^{2n+1} = \frac{1}{2^{2n}} \sum_{j=0}^{n} \binom{2n+1}{n-j} \cos\left[(2j+1)\omega t\right] \quad . \tag{3.5}$$

At this point, we perform a general frequency-analysis, in order to identify the fundamental differences between even and odd powers of cosine. Because the calculation of frequency-shifts essentially requires the identification of terms at particular frequencies, these properties will be very helpful for understanding where such terms may potentially originate from.

Even powers of $\cos(\omega t)$ come with a constant term and oscillatory terms at even higher harmonics of the fundamental frequency ω. There is no term at the fundamental frequency. According to Equation (3.2), $[\cos(\omega t)]^{2n}$ has frequency-components at $0, 2\omega, 4\omega, \ldots, 2(n-1)\omega, 2n\omega$.

Odd powers of $\cos(\omega t)$ do not come with a constant term. Instead, there is a term at the fundamental frequency ω, and there are higher harmonics at its odd multiples. According to Equation (3.5), $[\cos(\omega t)]^{2n+1}$ oscillates at the frequencies $\omega, 3\omega, \ldots, (2n-1)\omega, (2n+1)\omega$.

Fortunately, we do not have to consider all the frequency-components to calculate first-order frequency-shifts. As it turns out, the two most important components are the constant one (because it does not change the frequency of other terms in the product) and the one at the fundamental frequency ω (because such a term may be proportional to the original solution).

In order to facilitate the handling of terms at a particular frequency, we introduce the piece of notation $\langle\cdot\rangle_\omega$. It retrieves the term at the frequency ω from the argument in angle brackets. From Equation (3.2), we have

$$\left\langle [\cos(\omega t)]^{2n} \right\rangle_0 = \frac{1}{2^{2n}} \binom{2n}{n} = \frac{(2n)!}{2^{2n}(n!)^2} \tag{3.6}$$

for the constant component and from Equation (3.5)

$$\left\langle [\cos(\omega t)]^{2n+1} \right\rangle_\omega = \binom{2n+1}{n} \frac{\cos(\omega t)}{2^{2n}} = \frac{(2n+2)!\cos(\omega t)}{2^{2n+1}\left[(n+1)!\right]^2} \tag{3.7}$$

for the oscillatory term at the fundamental frequency ω. In addition to the amplitude, the whole oscillatory term is recovered, too. This includes a possible phase φ to go along with the argument ωt.

By approximating the factorials in Equations (3.6) and (3.7) for large n with STIRLING's formula

$$n! \approx \sqrt{2\pi n}\, n^n \mathrm{e}^{-n} \quad , \tag{3.8}$$

the asymptotic behavior[7] is identified as

$$\left\langle [\cos(\omega t)]^{2n} \right\rangle_0 \simeq \frac{1}{\sqrt{\pi n}} \quad , \qquad \left\langle [\cos(\omega t)]^{2n+1} \right\rangle_\omega \simeq \frac{2\cos(\omega t)}{\sqrt{\pi(n+1)}} \quad . \tag{3.9}$$

With the dependence on the inverse of the square root, these contributions fall off rather weakly with n, and this scaling alone does not explain why higher-order imperfections are of lesser importance. The suppression has to be mediated by a different mechanism, and we will examine the functional dependence of the higher-order imperfections. We have not yet considered the (constant) amplitude of the trigonometric functions, which has to be taken to the same power, too, and will then remain as a prefactor of the selected frequency-component, without being subject to any selection itself.

3.2. The one-dimensional anharmonic oscillator

In this section, we formulate the problem to which we apply perturbation theory based on the steps outlined before, as a first test case. As the axial equation of motion (2.16) for a charged particle in an ideal PENNING trap describes the one-dimensional harmonic oscillator, it is natural to consider this equation with an anharmonic term. Such a term would arise for instance from the cylindrically-symmetric imperfections of the electrostatic potential discussed in Section 2.2. The additional electrostatic potential on the z-axis

$$\Phi_\eta = C_\eta \frac{V_0}{2d^\eta} z^\eta \tag{3.10}$$

is obtained from Equation (2.73) by setting the radial displacement $\rho = 0$, which corresponds to a particle in a PENNING trap with vanishing amplitudes of the radial motions. In the classical case, this is possible, and the treatment is indeed classical here. At this point, we are still trying to model the problem with the extension to the PENNING trap in mind, for which the one-dimensional case is already useful. The influence of the radial modes will be discussed in Section 4.1.2.

As a reminder, η is a non-negative integer. For η even, the potential Φ_η is symmetric with respect to z, that is, $\Phi_\eta(-z) = \Phi_\eta(z)$. For η odd, the potential Φ_η is antisymmetric with respect to z, that is, $\Phi_\eta(-z) = -\Phi_\eta(z)$. Depending on the parity of η, we will refer to the potential Φ_η or its dimensionless coefficient C_η as odd or even for briefness. Of course, the statement relates to the index η and its role in the exponent of the potential, rather than the actual value of the potential Φ_η or the coefficient C_η, which are most likely no integers anyway.

From the electrostatic potential (3.10), the axial electric field follows as

$$E_\eta^{(z)} = -\frac{\partial}{\partial z}\Phi_\eta = -\eta C_\eta \frac{V_0}{2d^\eta} z^{\eta-1} \quad , \tag{3.11}$$

[7] The approximation is quite good, even for small n.

and its symmetry with respect to z is opposite[8] to the potential Φ_η. Including the contribution from the harmonic oscillator with $\eta = 2$, the equation of motion reads

$$\ddot{z} = \frac{q}{m} E^{(z)} = \frac{q}{m} \left(E_2^{(z)} + E_\eta^{(z)} \right) = -\frac{qC_2V_0}{md^2} \left(z + \frac{C_\eta}{C_2} \frac{\eta}{2d^{\eta-2}} z^{\eta-1} \right) \quad . \tag{3.12}$$

So far, we have included only one additional term. Of course, we could sum over η. However, we shall see that the first-order frequency-shifts caused by terms with different η add linearly. This is why we will work with only one higher-order term to yield the first-order frequency-shift for η in general. Before we get to the perturbative calculation, two remarks concerning nonperturbative treatments are in order.

First, the term associated with C_1 is not a source of anharmonicity, because it is eliminated from the equations of motion by shifting the z-coordinate as

$$z = z' - \frac{C_1}{C_2} \frac{d}{2} \quad . \tag{3.13}$$

In the z'-coordinate, the equation of motion (3.12) looks like the ordinary harmonic oscillator. In other words, the C_1-term shifts the equilibrium position without affecting the frequency. A linear potential alone, such as $\Phi_1 \propto z$, has no influence on the effective curvature of the potential, and hence leaves the frequency unchanged. For the remainder of this chapter, we shall assume that the origin of the z-coordinate, where $z = 0$, coincides with the equilibrium position, where $C_1 = 0$.

Second, there is an analytic expression for the period of oscillation T in this one-dimensional case. The conservation of energy for the particle's total energy $\mathcal{E}_{\text{tot}}$ reads

$$\mathcal{E}_{\text{tot}} = \mathcal{E}_{\text{kin}} + \mathcal{E}_{\text{pot}} = \frac{1}{2} m\dot{z}^2 + q \sum_{\eta=0} \Phi_\eta(z) \quad . \tag{3.14}$$

The first term on the right-hand side is the kinetic energy; the second one the potential energy. Because the analytic expression will turn out to be nonlinear, we have included a sum over all Φ_η in the potential energy. Solving for the velocity yields

$$\dot{z} = \frac{\mathrm{d}z}{\mathrm{d}t} = \pm \sqrt{\frac{2(\mathcal{E}_{\text{tot}} - \mathcal{E}_{\text{pot}})}{m}} \quad . \tag{3.15}$$

The sign in front of the square root is due to the fact that the direction of the particle is lost when calculating its kinetic energy $\mathcal{E}_{\text{kin}}$, because of the quadratic dependence on the velocity $\dot{z}$. Consequently, the direction of the velocity—a vector quantity—cannot be recovered from the kinetic energy—a scalar quantity. The insensitivity to directions also explains why this approach possibly fails when more than one spatial dimension is involved. Thus, it will be of no help for the three-dimensional case of the Penning trap. Here, we will pick the correct sign depending on whether the particle goes in the direction of the positive or negative z-axis.

[8] To avoid confusion while actually talking about the same η, convention disfavors speaking of even or odd electric fields, and we will refrain from doing so.

Integrating the inverse of the velocity $\dot{z}$ over the coordinate z from one classical turning point to the other one gives in the period of oscillation

$$\frac{T}{2} = \int_{z_-}^{z_+} \sqrt{\frac{m}{2[\mathcal{E}_{\mathrm{tot}} - \mathcal{E}_{\mathrm{pot}}(z)]}}\,\mathrm{d}z \quad . \tag{3.16}$$

At the classical turning points $z_\pm$, the particle is at rest ($\mathcal{E}_{\mathrm{kin}} = 0$), and hence their coordinates are found by solving[9] the equation $\mathcal{E}_{\mathrm{tot}} = \mathcal{E}_{\mathrm{pot}}(z_\pm)$. For the choice $z_- < z_+$, the velocity is positive when traveling from z_- to z_+, and the plus sign in Equation (3.15) was chosen.

Since there is the analytic expression (3.16) for the period of oscillation T, the benefit of perturbation theory in the one-dimensional case might be in doubt. However, the analytic expression (3.16) may require some approximations of its own to be useful, because analytic antiderivatives for the integral may not exist for all potentials Φ_η, and the situation is even worse for a sum of Φ_η. Even if they existed, there may be no explicit expression for the classical turning points $z_\pm$. Numerical integration is likely to be delicate, owing to the singularity of the integrand for $z_\pm$, where the velocity vanishes and its inverse diverges. The situation in these critical areas is furthermore complicated by the use of numerical values for $z_\pm$. Moreover, the dependence of the frequency on parameters such as C_η and the particle's total energy is harder to extract from a numerical calculation than from an analytic approximation. Of course, such an approximation may be obtained from Equation (3.16), but approximations in integrals are tricky, and a second step is required for the limits $z_\pm$. Here, perturbation theory shows its merits by building the solution from bottom up order by order natively, rather than top down with adequate expansions of the most general result to be introduced afterwards, if the general result is too complicated and unpractical.

With the unperturbed axial frequency ω_z from Equation (2.17), the equation of motion (3.12) becomes

$$\ddot{z} + \omega_z^2 z = -\epsilon\kappa_\eta z^{\eta-1}\,, \quad \text{where} \quad \kappa_\eta = \frac{\eta\omega_z^2}{2C_2 d^{\eta-2}} \quad . \tag{3.17}$$

We have chosen $\epsilon = C_\eta$ as the perturbation parameter. By speaking of the unperturbed axial frequency, we have implicitly made the assumption that $qV_0C_2 > 0$, which was necessary for axial confinement in the ideal Penning trap. Since the additional potential Φ_η is considered a small perturbation, it does create enough of a potential well in the region dominated by Φ_2 to store the particle, even for $qV_0C_\eta > 0$ and η even. Do not think Mexican-hat potential here. For typical parameters, the calculated minimum would lie outside the trap volume, which makes it pointless, because the potential there is very different from the situation described here. Conversely, the potential well created by Φ_2 is deep enough to prevent the particle from reaching the slope created by Φ_η for $qV_0C_\eta < 0$ and η even. For η odd, there is always a slope on one side, no matter the sign of qV_0C_η, which precludes particle storage in such a potential alone. The statement about the confinement by Φ_2 holds nonetheless.

[9] The turning points are not symmetric with respect to the origin ($|z_-| \neq |z_+|$), if terms with odd η are involved. In this asymmetric case, the amplitude of the particle is hard to define, and the particle is better described by its total energy.

The exact choice of the perturbation parameter is uncritical. Its main purpose is to indicate the order of a term in the perturbative expansion. In the end, the whole prefactor of the additional term matters for the frequency-shift. For a perturbative ansatz to have some credibility, we demand that the acceleration[10] created by the (gradient of the) additional potential Φ_η is always much smaller than the acceleration resulting from the harmonic potential Φ_2. Expressed as a formula, the requirement is $|\epsilon\kappa_\eta z^{\eta-1}| \ll |\omega_z^2 z|$ for all z. Having excluded[11] the case of $\eta = 1$, the condition is easier to satisfy for small z. If it is satisfied at the classical turning points, where z is maximum, the condition will be satisfied everywhere on the particle's trajectory, apart from at $z = 0$, where both accelerations vanish. Therefore, the special case at the origin is of no concern from the physical point of view. We can avoid this peculiarity mathematically and be somewhat more consistent for all z, by demanding that the ratio of accelerations be small:

$$\left|\frac{\epsilon\kappa_\eta z^{\eta-1}}{\omega_z^2 z}\right| = \left|\frac{\epsilon\eta}{2C_2}\frac{z^{\eta-2}}{d^{\eta-2}}\right| \ll 1 \quad . \tag{3.18}$$

With the prerequisites for perturbation theory laid out, we will try to determine frequency-shifts from a simple power series ansatz in the perturbation parameter ϵ.

3.2.1. Simplistic series solution

Inspired by the generic power series (3.1), we attempt to satisfy Equation (3.17) for the one-dimensional anharmonic oscillator order by order with the power series ansatz

$$z(t) = z_0(t) + \epsilon z_1(t) + \epsilon^2 z_2(t) + \ldots \quad , \tag{3.19}$$

where the $z_i(t)$ are unknown functions that need to be determined. Plugging the ansatz $z(t)$ into Equation (3.17) yields

$$\ddot{z}_0(t) + \omega_z^2 z_0(t) + \epsilon\left[\ddot{z}_1(t) + \omega_z^2 z_1(t)\right] + \ldots = -\epsilon\kappa_\eta [z_0(t)]^{\eta-1} + \ldots \tag{3.20}$$

up to first order in the perturbation parameter ϵ. The dots indicate that terms of at least second order have been neglected. Since the additional contribution on the right-hand side is of first order right away and

$$[z(t)]^{\eta-1} = [z_0(t)]^{\eta-1} + \epsilon(\eta-1)[z_0(t)]^{\eta-2} z_1(t) + \ldots \quad , \tag{3.21}$$

only the zeroth-order solution $z_0(t)$ gives a first-order contribution in the equation of motion. All other terms from the binomial expansion (3.21) are of higher order.

We will now solve the equations of motion (3.20) for the series solution order by order. For the zeroth order, the differential equation

$$\ddot{z}_0(t) + \omega_z^2 z_0(t) = 0 \tag{3.22}$$

[10] Since there is only a factor of mass m between force and acceleration in the classical case, the same statement applies to forces, too. We will use the two terms interchangeably.

[11] It looks like there might be a singularity at the origin for $\eta = 0$, but $\kappa_0 = 0$. As expected, there is no force from the constant potential Φ_0.

is satisfied by

$$z_0(t) = \hat{z}_0 \cos(\omega_z t + \varphi_z) \quad . \tag{3.23}$$

The amplitude $\hat{z}_0$ and the phase φ_z are determined by the initial conditions.

For the first order solution $z_1(t)$, the differential equation reads

$$\ddot{z}_1(t) + \omega_z^2 z_1(t) = -\kappa_\eta [z_0(t)]^{\eta-1} \quad , \tag{3.24}$$

with the zeroth-order solution $z_0(t)$ as an inhomogeneous term. Other than that, $z_1(t)$ has the same homogeneous solutions as $z_0(t)$, because the homogeneous differential equation is the harmonic oscillator with frequency ω_z again.

At this point, we need to illustrate a problem that arises when the right-hand side of, for instance, Equation (3.24) drives this harmonic oscillator on resonance. To this end, we choose η to be even and write $\eta = 2n$. The same problem would also occur for odd η, albeit in second order (see Section 3.3). Since the problem is a conceptual one that necessitates an addition to the simplistic series ansatz, we would like to uncover the limitations as quickly as possible—in first order, that is.

As Equations (3.2) and (3.5) show, taking the cosine in $z_0(t)$ to the power of $\eta - 1$, results in a sum of oscillatory terms (for $\eta > 2$, which is the case for all anharmonic terms, $\eta = 2$ being the harmonic one), and a constant term if η is odd. For $\eta = 2n$, the exponent $\eta - 1$ is odd, and the right-hand side of Equation (3.24) contains an oscillatory term at the fundamental frequency ω_z, as well as oscillatory terms at its odd multiples. The term at the fundamental frequency ω_z drives the left-hand side on resonance; the higher harmonics are nonresonant drives.

For the sinusoidally driven harmonic oscillator

$$\ddot{z}_1 + \omega_z^2 z_1 = \hat{a}_\mathrm{d} \cos(\omega_\mathrm{d} t + \varphi_\mathrm{d}) \quad , \tag{3.25}$$

the response differs, depending on whether the frequency ω_d is equal to the fundamental frequency ω_z or not. Here, $\hat{a}_\mathrm{d}$ is the amplitude of acceleration by the drive and φ_d is a phase.

In the nonresonant case (subscript "nr")—that is, $\omega_\mathrm{d} \neq \omega_z$—the general solution is

$$\begin{aligned} z_{1,\mathrm{nr}}(t) = &\left[z_1(0) + \frac{\hat{a}_\mathrm{d} \cos(\varphi_\mathrm{d})}{\omega_\mathrm{d}^2 - \omega_z^2} \right] \cos(\omega_z t) + \left[\frac{\dot{z}_1(0)}{\omega_z} - \frac{\omega_\mathrm{d}}{\omega_z} \frac{\hat{a}_\mathrm{d} \sin(\varphi_\mathrm{d})}{\omega_\mathrm{d}^2 - \omega_z^2} \right] \sin(\omega_z t) \\ &- \frac{\hat{a}_\mathrm{d}}{\omega_\mathrm{d}^2 - \omega_z^2} \cos(\omega_\mathrm{d} t + \varphi_\mathrm{d}) \quad , \end{aligned} \tag{3.26}$$

where the first line describes the homogeneous solution—an oscillation at the fundamental frequency ω_z—and the second line is the inhomogeneous solution—an oscillation at the frequency ω_d of the drive. The initial amplitude and velocity at time $t = 0$ are given by $z_1(0)$ and $\dot{z}_1(0)$, respectively. Unless for very specific initial conditions, a nonresonant drive also triggers some response at the fundamental frequency ω_z. If there is damping, this undriven component fades. Without damping, it is here to stay. In the nonresonant case, the solution $z_{1,\mathrm{nr}}(t)$ stays bounded; the amplitudes of the individual terms do not change with time. The only

time-dependence is in the arguments of the trigonometric functions, which are periodic taken on their own.[12]

For a resonant drive (subscript "res")—that is, $\omega_\mathrm{d} = \omega_z$—the general solution is

$$z_{1,\mathrm{res}}(t) = z_1(0)\cos(\omega_z t) + \left[\frac{\dot{z}_1(0)}{\omega_z} - \frac{\hat{a}_\mathrm{d}\sin(\varphi_\mathrm{d})}{2\omega_z^2}\right]\sin(\omega_z t) + \frac{\hat{a}_\mathrm{d} t}{2\omega_z}\sin(\omega_z t + \varphi_\mathrm{d}) \quad . \tag{3.27}$$

The first two oscillatory terms are the homogeneous solution, which sets the initial conditions right. The last term on the right-hand side is the inhomogeneous solution, and its amplitude grows with time.[13] Such a term is called secular. See Chapter D in the appendix for two definitions of secularity. For our purpose of dealing with oscillatory problems, Poincaré's notion is sufficient. A secular term means that time is on the loose, having left the friendly confines of the trigonometric function. However, unlimited growth does not seem to be the right solution—certainly not for this problem, and maybe neither for others. Although $z_1(t)$ is suppressed by a factor of the perturbation parameter ϵ in the series solution (3.19), the secular term will dominate for large times. This growth violates the conservation of energy in the static potential, where we expect a periodic solution, as the particle goes back and forth between the classical turning points. If damping were present, the dissipation of energy could be explained. However, the equation of motion (3.17) of the one-dimensional anharmonic oscillator does not include damping at all, which means that even negative damping is not an option. Moreover, there is no external drive, which could excite the particle. Consequently, the secular term is unphysical. In fact, it is related to the perturbative method, rather than being a fundamental problem from the physical perspective. Poincaré's definition of secularity also comments on its origin (see Chapter D in the appendix), and his explanation has to do with the frequency-shift in the oscillatory system.

Looking back at the zeroth-order solution $z_0(t)$ in Equation (3.23), we now note that it oscillates at the unperturbed frequency ω_z. Since we expect $z_0(t)$ to be the major contribution in the series solution for the trajectory $z(t)$ in Equation (3.19), we should have questioned the ansatz, even before the secular term occurred. The first order alone cannot set right the shortcoming of having fixed the frequency to the unperturbed value, and it diverges. Reference [4] recovers the first-order frequency-shift from the most secular terms in all orders. However, going through all orders to set the first order right is not particularly appealing, and it partly goes against the bottom-up approach of perturbation theory. Fortunately, there are alternatives, which prevent the secular term from arising, directly when the corresponding resonant term appears.

3.2.2. A Lindstedt–Poincaré method

To remove the unphysical effect of resonant coupling between different orders of the perturbative expansion, multiple time-scales or strained variables of time are often introduced. Inspired by

[12] Strictly speaking, the overall solution does not have to be periodic, because the fraction of ω_d and ω_z is not necessarily a rational number. However, we may still consider the solution to be quasi-periodic.

[13] To emphasize that $\omega_\mathrm{d} = \omega_z$, we have written ω_z rather than ω_d in the argument of the trigonometric function, even though the combination of ω_z and φ_d may look like a misprint. The phase φ_d of the external drive, however, is unrelated to the initial phase of the axial motion.

Reference [8], we expand the fundamental frequency (squared)[14] as

$$\Omega_z^2 = \omega_z^2 + \epsilon\omega_1^2 + \epsilon^2\omega_2^2 + \dots \quad . \tag{3.28}$$

The coefficients ω_i^2 are determined from the fact that we cannot have secularity. They will thus absorb resonant terms in the different orders to prevent a secular term from arising. We have written ω_i^2 rather than ω_i for the coefficients in the expansion, in order to indicate that they represent a change of the frequency squared. The use of the square is not meant to exclude negative values for the ω_i^2. The perturbed fundamental frequency is given by Ω_z. For $\epsilon = 0$, it is equal to the unperturbed frequency ω_z of the harmonic oscillator.

After substituting the ansatz (3.28) for the unperturbed fundamental frequency squared ω_z^2, the original equation of motion (3.17) reads

$$\ddot{z} + (\Omega_z^2 - \epsilon\omega_1^2 - \epsilon^2\omega_2^2 - \dots)z = -\epsilon\kappa_\eta z^{\eta-1} \quad . \tag{3.29}$$

The factor κ_η also contains ω_z^2. Whether the expansion (3.28) is necessary there essentially depends on whether the unperturbed frequency ω_z is known. If it is, we are free to work with it, since ω_z^2 is more convenient than its series representation with Ω_z^2 and the ω_i^2. In fact, if ω_z is known, we would most probably like to express the actual frequency Ω_z of the anharmonic oscillator as a function of the particle's amplitude, and Ω_z is unknown. However, if ω_z is to be inferred from the perturbed frequency Ω_z, which has been determined for instance from a measurement, expressing the frequency-shift in terms of the known quantity Ω_z is favorable. Substituting the expansion (3.28) for ω_z^2 in κ_η then eliminates the unknown frequency ω_z from the determination of the ω_i^2. This statement is true either way. We solve for the unknown quantity as a function of known ones, and we do not want the unknown frequency to be hidden deep in the problem—eventually in the ω_i^2, that is.

Plugging in the power series (3.19) for $z(t)$ into the equation of motion (3.29) yields

$$\ddot{z}_0 + \Omega_z^2 z_0 + \epsilon\left[\ddot{z}_1 + \Omega_z^2 z_1 - \omega_1^2 z_0\right] + \dots = -\epsilon\kappa_\eta z_0^{\eta-1} - \dots \tag{3.30}$$

up to first order in the perturbation parameter ϵ. The dots indicate that terms of second order and higher are not shown. For clarity, the time-dependence of the $z_i(t)$ has been suppressed.

The zeroth-order solution

$$z_0(t) = \hat{z}_0 \cos(\Omega_z t + \varphi_z) \tag{3.31}$$

is almost identical to Equation (3.23), but there is one very important difference. The oscillation is at the perturbed frequency Ω_z, rather than the unperturbed one. Thus, the frequency-shift to all orders shows up in the zeroth-order trajectory $z_0(t)$.

The differential equation for the first-order trajectory

$$\ddot{z}_1 + \Omega_z^2 z_1 - \omega_1^2 z_0 = -\kappa_\eta z_0^{\eta-1} \tag{3.32}$$

contains one additional term compared with Equation (3.24). We will choose ω_1^2 such that the resonant term from the right-hand side is canceled, which prevents a secular term in the

[14] Since the term Lindstedt–Poincaré method encompasses various expansions of the frequency or the time, we have not used the definite article in the title of this section.

inhomogeneous solution for $z_1(t)$. From Equations (3.2) and (3.5), and Section 3.2.1, we know that a term at the fundamental frequency Ω_z is present in $z_0^{\eta-1}$ only if the exponent $\eta - 1$ is odd. Thus, η must be even, and we write $\eta = 2n$. The cancellation of the resonant drive-term requires

$$\omega_1^2 z_0 = \kappa_{2n} \left\langle z_0^{2n-1} \right\rangle_{\Omega_z} = \frac{n\omega_z^2}{C_2 d^{2n-2}} \frac{(2n)!\, \hat{z}_0^{2n-1}}{2^{2n-1}(n!)^2} \cos(\Omega_z t + \varphi_z) = \frac{\omega_z^2}{C_2} \frac{n\,(2n)!}{2^{2n-1}(n!)^2} \frac{\hat{z}_0^{2n-2}}{d^{2n-2}} z_0 \quad , \tag{3.33}$$

and hence ω_1^2 is fixed. The oscillatory term at Ω_z is given by Equation (3.7); the parameter κ_{2n} is defined in Equation (3.17), where $\eta = 2n$. In the last step, we have used one factor of $\hat{z}_0$ to write the oscillatory term as proportional to $z_0(t)$ from Equation (3.31). The overall phase was right to do so, and ω_1^2 turns out to be time-independent, just like we would wish for a quantity that describes a static frequency-shift. With static we mean that the frequency is constant, as long as no changes are made to the system. In the anharmonic oscillator (3.17) treated so far, all the parameters were constant.

With the knowledge of ω_1^2 from Equation (3.33), the first-order frequency-shift follows from the series expansion (3.28) of the frequency squared. Since we expect the frequency-shift to be small, we expand the square root for $|\epsilon\omega_1^2/\omega_z^2| \ll 1$ and obtain

$$\Omega_z \approx \omega_z + \frac{\epsilon}{2}\frac{\omega_1^2}{\omega_z} + \ldots = \omega_z + \omega_z \frac{C_{2n}}{C_2} \frac{n\,(2n)!}{2^{2n}(n!)^2} \frac{\hat{z}_0^{2n-2}}{d^{2n-2}} + \ldots \quad . \tag{3.34}$$

In the last step, we have undone the substitution $\epsilon = C_{2n}$. The dots indicate terms of second order and higher. As implied by the name anharmonic oscillator, the frequency-shift depends on the amplitude of the particle. The sign is as expected. For $C_{2n}/C_2 > 0$, the additional potential (3.10) hardens the original quadratic potential, and the additional restoring force leads to a faster oscillation with increased frequency. The opposite happens for $C_{2n}/C_2 < 0$, where the softening of the potential and the reduced restoring force slow down the oscillation and decrease the frequency.[15]

The perturbative approach is backed by the fact that the relative frequency-shift is small, provided the additional force by the anharmonic term is small. In this sense, there are no surprises, which would enhance the effect of the anharmonic term, such as resonances. In fact, the relative frequency-shift is smaller than the maximum ratio of the additional force and the harmonic restoring force, mentioned in Equation (3.18) as a prerequisite for the application of perturbation theory. From a physical point of view, it is understandable why the additional force has a smaller impact on the frequency than the harmonic restoring force: only a part of the former is actually resonant with the original motion fueled by the latter.[16] We will return to this aspect in Section 3.4.

In order to justify the above statements mathematically for all n, we have to show that $\frac{(2n)!}{2^{2n}(n!)^2} < 1$, which is the additional factor in the relative frequency-shift (3.34) compared with

[15] Storing the particle in the quadratic potential required $qV_0C_2 > 0$. Therefore, C_2 may have both sign (even though the effective voltage V_0 is often defined such that C_2 turns out positive), and the sign of C_{2n} with respect to C_2 matters for the interplay between the two potentials concerning hardening and softening, and hence the frequency-shift.

[16] Indeed, if the additional force were harmonic ($\eta = 2$ and $n = 1$), the relative frequency-shift would exactly reflect the relative strength (3.18), up to a factor of 1/2 resulting from the suppression of small changes by the square root, when going from the force-gradient to the frequency of the harmonic oscillator.

the ratio of forces (3.18). To this end, we consider the binomial expansion

$$2^{2n} = (1+1)^{2n} = \sum_{k=0}^{2n} \binom{2n}{k} 1^k 1^{2n-k} = \sum_{k=0}^{2n} \binom{2n}{k} \quad . \tag{3.35}$$

According to their explicit definition (3.3), binomial coefficients are non-negative, which means that a sum of them is not less than the largest binomial coefficient present. As the binomial coefficients in the sum above are all nonzero (for $n \geq 1$), each of them has to be smaller than the sum as a whole. Therefore, we conclude

$$2^{2n} > \binom{2n}{k} \quad \text{for all } k, \text{ and in particular} \quad 2^{2n} > \binom{2n}{n} = \frac{(2n)!}{(n!)^2} \quad \text{for } k = 2n \quad . \tag{3.36}$$

The second inequality for the factorials had to be proven.[17]

Upon closer inspection of the ratio of forces (3.18) and the relative first-order frequency-shift (3.34), there is the difference between the maximum displacement of the particle and the amplitude $\hat{z}_0$ of the zeroth-order trajectory (3.31). As the power series (3.19) for the trajectory shows, the difference is at least of first order in the perturbation parameter. As long as there are no secular terms in higher orders, the difference is fine to ignore in the first-order frequency-shift, just like higher-order contributions to the trajectory. This also explains why we have been sloppy about initial conditions without negative consequences so far, leaving the amplitude $\hat{z}_0$ and the initial phase φ_z in the zeroth-order solution (3.31) as free parameters.

3.3. Second-order effects

This section outlines the calculation of frequency-shifts beyond first order as an extended demonstration of the Lindstedt–Poincaré method from the previous section. It will become clear why higher orders in the frequency-shift require much more computational effort, and they are only considered in detail, when they are really of experimental relevance. A general treatment, such as for first-order frequency-shifts in Chapter 4, is therefore hardly ever attempted.

This section is meant to be self-contained. When skipping it, in order to continue with Section 3.4 right away, understanding the calculation of first-order frequency-shifts should be possible, because this section has nothing new to say about them. Since the perturbative formalism is such that any given order does not require results from higher orders, the calculation may be stopped at any order, at least from the mathematical point of view. Meanwhile, it remains to be checked how well the experiment is described. It is our firm belief that higher orders in perturbation theory play a lesser role in reality—at best no role at all at the experimental level of precision.

[17] This factor is also present in the constant contribution (3.6) of $[\cos(\omega t)]^{2n}$. Since $|\cos(\omega t)| \leq 1$, and the oscillatory terms $\cos(2j\omega t)$ with $1 \leq j \leq n$ from the decomposition (3.2) do not shift the baseline, the constant contribution cannot be larger than unity. Equality would hold only in the absence of oscillations, that is, for $\omega = 0$. In Equation (3.9), we have used Stirling's formula (3.8) to identify the asymptotic behavior of the factor for large n as a decay with the inverse of the square root, thereby already confirming the second inequality (3.36) for large enough n. Here, we needed it to be valid for all n.

By considering second order, thereby highlighting higher-order features, this section demonstrates what our single-minded obsession with first-order frequency-shifts misses out on. Moreover, second order is not only required to constrain the validity of the first-order result (3.34), but also to produce the first nonvanishing term for the frequency-shift caused by a potential Φ_η with η odd.[18] Consequently, we will at least provide some guidelines for going beyond first order here.

In the light of frequency-shifts, the title of this section promises a little too much. Just like we stopped the first-order calculation right after discovering the associated frequency-shift, we will do the same here, without specifying the second-order trajectory $z_2(t)$. However, getting to the second-order frequency-shift means that we will actually have to complete the first-order calculation by finding the corresponding trajectory $z_1(t)$.

First, we will check what is required to determine the second-order frequency-shift. Using Equation (3.21), the differential equation for the second-order term $z_2(t)$ in the power series (3.19) for the trajectory becomes

$$\ddot{z}_2 + \Omega_z^2 z_2 - \omega_1^2 z_1 - \omega_2^2 z_0 = -\kappa_\eta(\eta - 1) z_0^{\eta-2} z_1 \quad . \tag{3.37}$$

Like for the first order z_1 in Equation (3.32), the differential equation describes a harmonic oscillator for z_2 with the natural frequency Ω_z and some inhomogeneous terms given by solutions from lower orders. In analogy to ω_1^2 in the first order, the parameter ω_2^2 from the power series (3.28) for the perturbed frequency Ω_z (squared) will be chosen to eliminate resonant terms at the natural frequency Ω_z, because these would otherwise cause $z_2(t)$ to pick up secular term and grow with time.

Before calculating the second-order frequency-shift parameter ω_2^2, the first-order trajectory $z_1(t)$ has to be determined from Equation (3.32), taking into account the initial conditions. Although these do not affect the frequency-shift for the periodic motion in the potential, certain choices are more convenient for the calculation. We select $z(0) = \hat{z}$ and $\dot{z}(0) = 0$ for the position and the velocity at time $t = 0$, respectively. In other words, the particle starts at rest from one classical turning-point.[19] The zeroth-order solution (3.31) for the trajectory then simplifies to

$$z_0(t) = \hat{z} \cos(\Omega_z t) \quad , \tag{3.38}$$

where we have suppressed any subscript about the order in the amplitude to indicate that $\hat{z}$ is a global property of the power series (3.19). Since $z(0) = z_0(0) = \hat{z}$, the initial positions of all other orders vanish: $z_i(0) = 0$ for all $i > 0$. No order of the power series (3.19) has any initial velocity: $\dot{z}(0) = \dot{z}_i(0) = 0$.

In the zeroth-order solution, the global starting position $\hat{z}$ clearly is an amplitude. However, it is not necessarily equal to the maximum displacement of the particle in a potential with an

[18] Of course, this could be considered checking the scope of zero as the first approximation.

[19] Using the conservation of energy in this potential, Equation (3.14) yields the velocity for any position of the particle. Conversely, it assigns (at least implicitly) two classical turning-points $\hat{z}_\pm$ to any combination of initial position $z(0)$ and velocity $\dot{z}(0)$. If the potential is not symmetric with respect to the reflection $z \to -z$, the absolute values of the two classical turning-points differ: $|\hat{z}_-| \neq |\hat{z}_+|$. It would be interesting to confirm that the power series (3.28) indeed gives the same frequency for both starting positions. However, since the frequency-shifts associated with odd terms in the potential are at least of second order, the calculation of higher orders would be required to account for the difference between $\hat{z}_-$ and $\hat{z}_+$.

antisymmetric contribution. Moreover, we shall see that $\hat{z}$ is not equal to the amplitude of the particle motion at the fundamental frequency. Nevertheless, we will also refer to $\hat{z}$ as an amplitude for the sake of simplicity, which is fine to zeroth order.

3.3.1. Antisymmetric anharmonic potential add-on

When we demonstrated the problem of secularity as an unhandled consequence of resonant terms for the simplistic series solution in Section 3.2.1, we chose $\eta = 2n$ even, in order to encounter the problem in first order. Although the potential associated with odd η does not produce any resonant terms in first order, we claimed the same problem would occur in the next order—second order, that is. We will now confirm the claim. Writing $\eta = 2n + 1$, the differential equation (3.32) for the first-order trajectory $z_1(t)$ has the inhomogeneous term z_0^{2n} on the right-hand side. Taking the cosine in the zeroth-order solution (3.38) to the power of $2n$ results in a constant term and oscillatory terms at even higher-harmonics of the fundamental frequency Ω_z according to Equation (3.2). Since there is no resonant term at the fundamental frequency Ω_z itself, there is no first-order frequency-shift ($\omega_1^2 = 0$), and the solution for the first-order trajectory

$$z_1(t) = -\frac{\kappa_{2n+1}\,\hat{z}^{2n}}{2^{2n}\Omega_z^2}\left\{\binom{2n}{n}[1-\cos(\Omega_z t)] - 2\sum_{j=1}^{n}\binom{2n}{n-j}\frac{\cos(2j\Omega_z t)-\cos(\Omega_z t)}{(2j)^2-1}\right\} \tag{3.39}$$

is constructed from superpositions of Equation (3.26), which even has the constant term covered with the choice $\omega_\mathrm{d} = 0$. Note the replacement $\omega_z \to \Omega_z$. Apart from higher harmonics, there are oscillatory terms at the fundamental frequency, which means that the amplitude $\hat{z}$ of the zeroth-order solution (3.38) is not equal to the amplitude of this frequency-component in the series solution (3.19) for the trajectory $z(t)$.

With the first-order solution completed, we turn the differential equation (3.37) for the second order. For a second-order frequency-shift to exist, there must be resonant terms from the inhomogeneous contributions. With no first-order frequency-shift ($\omega_1^2 = 0$), the resonant terms to be absorbed by the second-order frequency-shift parameter ω_2^2 must originate from the right-hand side. In the notation from Section 3.1 with angle brackets for selecting terms at a particular frequency given as a subscript, the resonant terms at the fundamental frequency Ω_z of the harmonic oscillator for z_2 are written as

$$\omega_2^2 z_0(t) = \kappa_{2n+1}\,2n\left\langle z_1\, z_0^{2n-1}\right\rangle_{\Omega_z} \quad . \tag{3.40}$$

Both terms in angle brackets are explicitly time-dependent—a dependence we have suppressed for conciseness here, hoping that $z_0(t)$ (on the left-hand side) and z_0 (on the right-hand side) are not mistaken for two different quantities. The second-order frequency-shift does not depend on the second-order trajectory z_2, just like the first-order frequency-shift did not depend on the first-order trajectory z_1. As stated before, we will not determine z_2, settling for the second-order frequency-shift.

We will examine the frequency spectrum of the two time-dependent terms involved in Equation (3.40), in order to understand how resonant terms come about via mixing. The basic

message of Equation (C.10) for the multiplication of two cosines is that, when two oscillatory terms are multiplied, the resulting two oscillatory terms are at the sum and the difference frequency. The first-order solution $z_1(t)$ from Equation (3.39) contains oscillatory terms at the frequencies $0\Omega_z, 1\Omega_z, 2\Omega_z, 4\Omega_z, \ldots, (2n-2)\Omega_z, 2n\Omega_z$. The term at the fundamental frequency Ω_z, which bucks the trend of even multiples, is from the homogeneous solution, and it implements the initial conditions. The other terms result from the anharmonic force along the zeroth-order trajectory of the particle. According to Equation (3.5), z_0^{2n-1} oscillates at the fundamental frequency Ω_z and its odd higher-harmonics with a total frequency spectrum of $1\Omega_z, 3\Omega_z, \ldots (2n-3)\Omega_z, (2n-1)\Omega_z$. There are three sources of terms at the fundamental frequency Ω_z in the product $z_1 z_0^{2n-1}$:

1. Preserve the resonant term in z_0^{2n-1} by multiplying it with the constant term in z_1.
2. Multiply the oscillating terms at the frequency $2\Omega_z, 4\Omega_z, \ldots, (2n-4)\Omega_z, (2n-2)\Omega_z$ in z_1 with the oscillatory term at the same spot on the list $3\Omega_z, 5\Omega_z, \ldots (2n-3)\Omega_z, (2n-1)\Omega_z$ from z_0^{2n-1}. The resonant terms are at the difference frequency $\Omega_z = (3-2)\Omega_z = (5-4)\Omega_z = \cdots = ((2n-1)-(2n-2))\Omega_z$ of the first, the second, …, the last two terms.
3. Multiply the oscillating terms at the frequency $2\Omega_z, 4\Omega_z, \ldots, (2n-2)\Omega_z, 2n\Omega_z$ in z_1 with the oscillatory term at the same spot on the list $1\Omega_z, 3\Omega_z, \ldots (2n-3)\Omega_z, (2n-1)\Omega_z$ from z_0^{2n-1}. The resonant terms are again at the difference frequency $\Omega_z = (2-1)\Omega_z = (4-3)\Omega_z = \cdots = (2n-(2n-1))\Omega_z$ of the first, the second, …, the last two terms.

Mixing reduces the amplitude by a factor of 2. For two cosines, the resulting term at the difference frequency is a cosine with no additional phase, see Equation (C.10) in the appendix.

With $z_0(t)$ from Equation (3.38), and $z_1(t)$ from Equation (3.39), the resonant term in Equation (3.40) becomes

$$\begin{aligned}\omega_2^2 z_0(t) = -\frac{\kappa_{2n+1}^2\, 2n}{2^{4n-2}\Omega_z^2}\hat{z}^{4n-2}\, z_0(t)\Bigg[&\binom{2n}{n}\binom{2n-1}{n-1} \\ &- \sum_{j=1}^{n-1}\frac{1}{(2j)^2-1}\binom{2n}{n-j}\binom{2n-1}{n-1-j} - \sum_{j=1}^{n}\frac{1}{(2j)^2-1}\binom{2n}{n-j}\binom{2n-1}{n-j}\Bigg] \quad .\end{aligned} \tag{3.41}$$

There is a total factor of $\hat{z}^{4n-1}$ on the right-hand side—a factor of $\hat{z}^{2n}$ from $z_1(t)$, a factor of $\hat{z}^{2n-1}$ from z_0^{2n-1}. One of these factors has been combined with $\cos(\Omega_z t)$ to form the zeroth-order solution $z_0(t)$ according to Equation (3.38). The three terms in square brackets correspond to the three prescription outlined above. The first binomial coefficient in each term results from z_1, the second one from z_0^{2n-1}. For the third term, the summation variable in the equivalent of Equation (3.5) for the exponent $2n-1$ (rather than $2n+1$) was shifted according to $j \to j-1$ as in

$$[\cos(\Omega_z t)]^{2n-1} = \frac{1}{2^{2n-2}}\sum_{j=0}^{n-1}\binom{2n-1}{n-1-j}\cos[(2j+1)\Omega_z t] \tag{3.42a}$$

$$= \frac{1}{2^{2n-2}}\sum_{j=1}^{n}\binom{2n-1}{n-j}\cos[(2j-1)\Omega_z t] \quad . \tag{3.42b}$$

For the same value of the summation variable j, the oscillatory terms in Equation (3.42b) then match the ones in $z_1(t)$ from Equation (3.39) for the production of resonant terms via the third mechanism. For the second term in square brackets in Equation (3.41), the summation in Equation (3.42a) (without a change of the summation variable) starts at $j = 1$, because the first odd higher-harmonic is $\cos(3\Omega_z t)$ in the second production mechanism for resonant terms.

The first product of binomial coefficients in Equation (3.41) is simplified with the identity

$$\binom{2n-1}{n-1} = \frac{(2n-1)!}{(n-1)!n!} = \frac{n}{2n}\frac{(2n)!}{(n!)^2} = \frac{1}{2}\binom{2n}{n} \quad . \tag{3.43}$$

Two other binomial are summed as

$$\binom{2n-1}{n-1-j} + \binom{2n-1}{n-j} = \binom{2n}{n-j} \quad . \tag{3.44}$$

Equation (4.46c) proves this identity when the binomial coefficients are given by the explicit expression (3.3) with factorials. Because the identity also holds when the first binomial coefficient vanishes for $j = n$, we raise the upper limit of the first sum in Equation (3.41) from $n-1 \to n$, in order to have equal limits for both sums.

With the parameter κ_η defined in Equation (3.17) and the two identities above, the second-order frequency-shift parameter becomes

$$\omega_2^2 = -\frac{1}{C_2^2}\frac{\omega_z^4}{\Omega_z^2}\frac{n(2n+1)^2}{2^{4n}}\left\{\left[\binom{2n}{n}\right]^2 - \sum_{j=1}^{n}\left[\binom{2n}{n-j}\right]^2 \frac{2}{(2j)^2-1}\right\}\frac{\hat{z}^{4n-2}}{d^{4n-2}} \quad . \tag{3.45}$$

As a special case of Equation (3.75), which provided a spark (well after "completing" this section), the term is curly brackets is simplified as

$$\left[\binom{2n}{n}\right]^2 - \sum_{j=1}^{n}\left[\binom{2n}{n-j}\right]^2 \frac{2}{(2j)^2-1} = \frac{1}{(2n+1)^2}\frac{(4n+1)!}{[(2n)!]^2} \quad . \tag{3.46}$$

Up to second order, the perturbed frequency expressed by the power series (3.28) is given by

$$\Omega_z = \sqrt{\omega_z^2 + \epsilon^2\omega_2^2 + \ldots} \approx \omega_z + \frac{\epsilon^2}{2}\frac{\omega_2^2}{\omega_z} + \ldots = \omega_z + \Delta\omega_z + \ldots \quad , \tag{3.47}$$

where we have expanded the square root for $|\epsilon^2\omega_2^2| \ll \omega_z^2$. The first-order term $\epsilon\omega_1^2$ in the series is absent, because there is no first-order frequency-shift for the imperfections of the electrostatic potential without reflection symmetry about the z-axis. After undoing the substitution $\epsilon = C_{2n+1}$ for the perturbation parameter, the second-order frequency-shift for an additional potential Φ_{2n+1} from Equation (3.10) is given by

$$\frac{\Delta\omega_z}{\omega_z} = -\frac{C_{2n+1}^2}{C_2^2}\frac{n}{2^{4n+1}}\frac{(4n+1)!}{[(2n)!]^2}\frac{\hat{z}^{4n-2}}{d^{4n-2}} \quad . \tag{3.48}$$

To second order in the frequency-shift, we have ignored the difference between the perturbed frequency Ω_z and the unperturbed frequency ω_z in ω_2^2 from Equation (3.45). As Equation (3.47)

shows, the difference between these two frequencies is at least of second order in the perturbation parameter ϵ, and hence of no relevance in the ratio ω_z^2/Ω_z^2 from ω_2^2. Parametrized by $\epsilon^2\omega_2^2$, the frequency-shift shown here is at least of second-order by design, because ω_2^2 does not contain any term that is inversely proportional to (some power of) the perturbation parameter ϵ. The perturbation parameter ϵ in the power series (3.28) for Ω_z^2 in the denominator of ω_2^2 will not exactly cancel with ϵ^2 in $\epsilon^2\omega_2^2$. Instead, there will be a modified power series, of which we have picked the second-order contribution to the frequency-shift, by making the substitution $\Omega_z^2 \to \omega_z^2$, before using ω_2^2 of Equation (3.45) in Equation (3.48)

With the choice $\eta_{\text{odd}} = 2n + 1$ for the odd coefficients, the exponent of the particle's starting position $\hat{z}$ is $4n-2 = 2\eta_{\text{odd}}-4$. Compared with the exponent $\eta_{\text{even}}-2$ in the first-order frequency shift (3.34) by an even coefficient $C_{\eta_{\text{even}}}$, the two exponents are the same for $\eta_{\text{even}} = 2\eta_{\text{odd}} - 2$. With the exception of C_3, the first nonvanishing term in the frequency-shifts associated with η_{odd} scales more strongly with $\hat{z}$ than for the neighboring η_{even}. This is a consequence of second versus first order.

Table 3.1 shows explicit expressions for the second-order frequency-shift (3.48) by the first few perturbation parameters C_η with odd η. It is always negative. We do not expect the sign of C_η to matter, because the associated potential (3.10) is always hardening on one side of the z-axis, leading to an additional restoring force, and softening on the other, weakening the restoring force there. The sign merely determines on which side of the z-axis hardening or softening occurs.[20] Since the particle spends more time in the softened region due to the reduced restoring force, and it also travels further out there, before reaching the classical turning point, the reduced frequency appears logical. Keep in mind the convex nature of the function $1/v$ (for $v > 0$), where v stands for velocity, like $\dot{z}$ does in Equation (3.16). Speeding up by an amount Δv reduces the infinitesimal journey time less than slowing down by the same amount increases it. Hence, the net effect of the antisymmetric potential with softening on one side and hardening on the other is to increase the period of the oscillation, which is equivalent to a reduction of the frequency.

Reference [59] gives the frequency-shift up to $\hat{z}^7$, and the applicable results shown for C_3^2 and C_5^2 agree. The agreement is comforting, since Reference [59] expands the perturbed frequency rather than its square.

3.3.2. Symmetric anharmonic potential add-on

In this paragraph, we calculate the second-order frequency-shift for an additional potential Φ_η with η even. Unlike an antisymmetric potential with η odd, such a symmetric potential already gives rise to a first-order frequency-shift (3.33). Hence, second-order perturbation theory is not necessary to calculate the first nonvanishing term in the expansion (3.28) of the perturbed frequency (squared). However, the second-order result gives an impression of how accurate

[20] The question of sign is more complex than it may seem at first. In higher orders, there are terms with odd powers of C_η, which are of course sensitive to the sign [59]. For an antisymmetric potential associated with odd η, the overall oscillation does not seem to change when the sign of C_η is flipped, and the existence of such a term seems strange. However, the initial conditions strike. Because the particle starts at an initial displacement $\hat{z}$, its total energy depends on the sign of C_η. Indeed, these seemingly questionable terms are also sensitive to the sign of $\hat{z}$. Table 3.3 shows such second-order cross-terms, too.

Table 3.1.: Second-order frequency-shift (3.48) caused by a potential Φ_η with odd η. The parameter η_{even} shows which coefficient $C_{\eta_{\text{even}}}$ would result in a first-order frequency-shift (3.34) with the same power of $\hat{z}$.

η	3	5	7	9	11
$\dfrac{\Delta\omega_z}{\omega_z}$	$-\dfrac{15}{16}\dfrac{C_3^2}{C_2^2}\dfrac{\hat{z}^2}{d^2}$	$-\dfrac{315}{128}\dfrac{C_5^2}{C_2^2}\dfrac{\hat{z}^6}{d^6}$	$-\dfrac{9009}{2048}\dfrac{C_7^2}{C_2^2}\dfrac{\hat{z}^{10}}{d^{10}}$	$-\dfrac{109\,395}{16\,384}\dfrac{C_9^2}{C_2^2}\dfrac{\hat{z}^{14}}{d^{14}}$	$-\dfrac{4\,849\,845}{524\,288}\dfrac{C_{11}^2}{C_2^2}\dfrac{\hat{z}^{18}}{d^{18}}$
η_{even}	4	8	12	16	20

the first-order approximation is for a given perturbation. This benchmark goes beyond the finding at the end of Section 3.2.2 that small anharmonic forces (3.18) result in an even smaller first-order frequency-shift, and it is quantitative. Of course, knowing the second-order result still requires confidence that there are no surprises in third order or higher.[21] As long as the energy is conserved in the potential, wild excursions are not expected, and the experiment tests the theoretical predictions.

The result (3.38) for the zeroth-order trajectory $z_0(t)$ is identical to the case of odd η in Section 3.3.1. We write $\eta = 2n$ and solve the differential equation (3.29) for the first-order trajectory $z_1(t)$ by decomposing z_0^{2n-1} into single oscillatory terms with the help of Equation (3.42a), a descendant of Equation (3.5). So far, we have stopped the calculation in Section 3.2.2 after absorbing the resonant term $\cos(\Omega_z t)$ as

$$\omega_1^2 = \binom{2n-1}{n-1}\frac{\kappa_{2n}\hat{z}^{2n-2}}{2^{2n-2}} \tag{3.49}$$

in the expansion of the perturbed frequency (3.28). Apart from having fixed the amplitude $\hat{z}_0$ of the zeroth-order trajectory as $\hat{z}$, the result is the same as in Equation (3.33). We will retain the binomial coefficient here, because it will be contracted with similar terms more easily.

Having prevented secular terms from arising with the particular choice of ω_1^2, we turn to the nonresonant terms in z_0^{2n-1}. With the help of Equations (3.26) (replacing $\omega_z \to \Omega_z$) and (3.42a), the first-order trajectory for the initial conditions $z_1(t) = 0$ and $\dot{z}_1(t) = 0$ becomes

$$z_1(t) = \frac{\kappa_{2n}\hat{z}^{2n-1}}{2^{2n}\Omega_z^2}\sum_{j=1}^{n-1}\binom{2n-1}{n-1-j}\frac{\cos[(2j+1)\Omega_z t] - \cos(\Omega_z t)}{j(j+1)} \quad , \tag{3.50}$$

where we have written

$$(2j+1)^2 - 1 = 4j(j+1) \tag{3.51}$$

in the denominator. Like for $z_1(t)$ from Equation (3.39) for an odd anharmonic potential, there are terms at the perturbed fundamental frequency Ω_z. The higher harmonics, or sidebands, are at its odd rather than even multiples here, however; and there is no constant term.

[21] Paraphrasing the justification of perturbation theory in the words of Carl M. Bender: Mathematicians are pathological people, always looking for a pathological example to fool you. Nature is kind.

With the entire first-order solution for both the frequency-shift and the trajectory known, we turn to the differential equation (3.37) for second order. For the second-order frequency-shift, we have to absorb resonant terms at the perturbed frequency Ω_z in the parameter ω_2^2, which is written as

$$\omega_2^2 z_0 = \kappa_{2n}(2n-1)\left\langle z_1\, z_0^{2n-2}\right\rangle_{\Omega_z} - \omega_1^2\left\langle z_1\right\rangle_{\Omega_z} \tag{3.52}$$

in our notation. The first-order solution $z_1(t)$ from Equation (3.50) has oscillatory terms at $1\Omega_z, 3\Omega_z, \ldots, (2n-1)\Omega_z$. According to Equations (3.2) and (3.38), z_0^{2n-2} comes with a constant term and even higher harmonics of the fundamental frequency Ω_z. Its frequency spectrum is $0\Omega_z, 2\Omega_z, \ldots, (2n-2)\Omega_z$. Thus, there are the following possibilities to produce resonant terms:

1. The second term on the right-hand side of Equation (3.52) naturally possesses a resonant contribution—the oscillatory term at Ω_z in $z_1(t)$.

2. In the first term on the right-hand side of Equation (3.52), the oscillatory term at Ω_z in $z_1(t)$ is preserved by multiplying it with the constant contribution from z_0^{2n-2}.

3. Multiplying the oscillatory term at Ω_z in $z_1(t)$ with the term at frequency $2\Omega_z$ in z_0^{2n-2} results in an oscillatory term at frequency Ω_z.

4. Multiplying the oscillatory term from z_1 at frequency $3\Omega_z, 5\Omega_z, \ldots, (2n-1)\Omega_z$ with the corresponding term on the list $2\Omega_z, 4\Omega_z, \ldots, (2n-2)\Omega_z$ from z_0^{2n-2} results in the resonant term $\Omega_z = (3-2)\Omega_z = (5-4)\Omega_z = \cdots = ((2n-1)-(2n-2))\Omega_z$.

5. Multiplying the oscillatory term from z_1 at frequency $3\Omega_z, 5\Omega_z, \ldots, (2n-3)\Omega_z$ with the corresponding term on the list $4\Omega_z, 6\Omega_z, \ldots, (2n-2)\Omega_z$ from z_0^{2n-2} results in the resonant term $\Omega_z = (4-3)\Omega_z = (6-5)\Omega_z = \cdots = ((2n-2)-(2n-3))\Omega_z$.

With ω_1^2 from Equation (3.49) and $z_1(t)$ from Equation (3.50), the first mechanism on the list is written as

$$\omega_1^2\left\langle z_1\right\rangle_{\Omega_z} = -z_0(t)\,\frac{\kappa_{2n}^2\hat{z}^{4n-4}}{2^{4n-2}\Omega_z^2}\binom{2n-1}{n-1}\sum_{j=1}^{n-1}\binom{2n-1}{n-j-1}\frac{1}{j(j+1)} \quad , \tag{3.53}$$

where we have absorbed a factor of $\hat{z}$ and the oscillatory term $\cos(\Omega_z t)$ in the zeroth-order solution $z_0(t)$ from Equation (3.38). This particular step will be repeated for all other contributions, too.

The four remaining mechanisms for the production of resonant terms are summarized as follows:

$$\begin{aligned}\left\langle z_1\, z_0^{2n-2}\right\rangle_{\Omega_z} = z_0(t)\,\frac{\kappa_{2n}\hat{z}^{4n-4}}{2^{4n-2}\Omega_z^2}\Bigg\{&-\left[\binom{2n-2}{n-1}+\binom{2n-2}{n-2}\right]\sum_{j=1}^{n-1}\binom{2n-1}{n-j-1}\frac{1}{j(j+1)}\\ &+\sum_{j=1}^{n-1}\binom{2n-2}{n-j-1}\binom{2n-1}{n-j-1}\frac{1}{j(j+1)}+\sum_{j=1}^{n-2}\binom{2n-2}{n-j-2}\binom{2n-1}{n-j-1}\frac{1}{j(j+1)}\Bigg\} \quad .\end{aligned} \tag{3.54}$$

The origin of the individual terms becomes more obvious after writing Equation (3.2) for the even powers of cosine more appropriately for z_0^{2n-2} as

$$[\cos(\Omega_z t)]^{2n-2} = \frac{1}{2^{2n-2}}\left[\binom{2n-2}{n-1} + 2\sum_{j=1}^{n-1}\binom{2n-2}{n-1-j}\cos(2j\Omega_z t)\right] \tag{3.55a}$$

$$= \frac{1}{2^{2n-2}}\left[\binom{2n-2}{n-1} + 2\sum_{j=0}^{n-2}\binom{2n-2}{n-2-j}\cos[2(j+1)\Omega_z t]\right] \quad . \tag{3.55b}$$

In the last step, we have shifted the summation variable as $j \longrightarrow j+1$, because the fifth mechanism on the list starts with $\cos(4\Omega_z t)$, which is then produced for $j = 1$, just like the corresponding term $\cos(3\Omega_z t)$ in $z_1(t)$.

In Equation (3.54), the common binomial coefficient and the denominator $j(j+1)$ result from $z_1(t)$. The other binomial coefficients are from z_0^{2n-2}, and the factor of 2 that is still present in front of the sum in Equations (3.55a) and (3.55b) is lost by mixing according to Equation (C.10) from the appendix. The four different binomial coefficients in Equation (3.54) belong to the production mechanisms 2–5 on the list. Similar to Equation (3.44), some binomial coefficients are summed as

$$\binom{2n-2}{n-1} + \binom{2n-2}{n-2} = \binom{2n-1}{n-1} \quad \text{and} \quad \binom{2n-2}{n-j-1} + \binom{2n-2}{n-j-2} = \binom{2n-1}{n-1-j} \quad . \tag{3.56}$$

The particular definition (3.3) of the binomial coefficients allows to increase the upper limit of the last sum in Equation (3.54) from $n-2$ to $n-1$, such that it becomes the same as for the other two sums. Equation (3.54) is then summarized as

$$\left\langle z_1\, z_0^{2n-2}\right\rangle_{\Omega_z} = z_0(t)\,\frac{\kappa_{2n}\hat{z}^{4n-4}}{2^{4n-2}\Omega_z^2}\sum_{j=1}^{n-1}\frac{1}{j(j+1)}\binom{2n-1}{n-j-1}\left[\binom{2n-1}{n-j-1} - \binom{2n-1}{n-1}\right] \quad . \tag{3.57}$$

With the definition (3.17) of κ_{2n} and the result from Equation (3.53), the second-order frequency-shift parameter ω_2^2 is extracted from Equation (3.52) as

$$\omega_2^2 = \frac{\omega_z^4}{\Omega_z^2}\frac{n^2(2n-1)}{2^{4n-2}C_2^2}\frac{\hat{z}^{4n-4}}{d^{4n-4}}\sum_{j=1}^{n-1}\frac{\binom{2n-1}{n-j-1}}{j(j+1)}\left[\binom{2n-1}{n-j-1} - \left[1-\frac{1}{2n-1}\right]\binom{2n-1}{n-1}\right] \tag{3.58a}$$

$$= \frac{\omega_z^4}{\Omega_z^2}\frac{n^2(2n-1)}{2^{4n-2}C_2^2}\frac{\hat{z}^{4n-4}}{d^{4n-4}}\sum_{j=1}^{n-1}\frac{1}{j(j+1)}\binom{2n-1}{n-j-1}\left[\binom{2n-1}{n-j-1} - 2\binom{2n-2}{n}\right] \quad . \tag{3.58b}$$

In the last step, we have used

$$\left[1-\frac{1}{2n-1}\right]\binom{2n-1}{n-1} = 2\binom{2n-2}{n} \quad , \tag{3.59}$$

where the fraction results from the absence of the factor $2n-1$ in Equation (3.53). Other than that, the two terms on the right-hand side of Equation (3.52) share the same prefactor. The difference

between the perturbed frequency Ω_z and the unperturbed frequency ω_z in the prefactor results in additional terms of higher order. These will be ignored here for the frequency-shift up to second order, because ω_2^2 with the zeroth-order substitution $\Omega_z \to \omega_z$ alone results in a contribution of second order in the frequency-shift already.

Before turning to the actual second-order frequency-shift, we take a close look at the sign of the coefficient ω_2^2, which is determined by the sum over the two binomial coefficients in square brackets in Equation (3.58b). We shall show that all contributions are negative. Since the second of the binomial coefficients in question does not depend on the summation variable j, we try to estimate the sign by comparing the negative part with the positive contribution from the largest of the first binomial coefficients. To this end, we need to figure out for which value of j the first binomial coefficient reaches its maximum. If even the largest positive term cannot compensate for the negative contribution, which is independent of j, the terms in the sum do not have to be inspected individually, in order to know that the sum will turn out negative.

Generally, two subsequent binomial coefficients are related recursively via

$$\binom{n}{k} = \frac{n!}{k!\,(n-k)!} = \frac{n!}{(k-1)!\,(n-k+1)!}\,\frac{n-k+1}{k} = \binom{n}{k-1}\left[\frac{n+1}{k} - 1\right] \quad , \tag{3.60}$$

which means that the binomial coefficient does not decrease, while the term in square brackets is at least unity. This condition requires $k \leq (n+1)/2$, and hence a maximum[22] is reached for $k = \lfloor (n+1)/2 \rfloor$, with the floor function defined in Equation (2.60). For the first binomial coefficient in square brackets in Equation (3.58b), this condition $k = n = n - j - 1$ for the maximum is not to be fulfilled. For the values of j permitted by the range of the summation, the local maximum is reached for $j = 1$. The corresponding binomial coefficient is related to the second one in square brackets via

$$\binom{2n-1}{n-2} = \frac{(2n-1)!}{(n-2)!\,(n+1)!} = \frac{(2n-2)!}{(n-2)!\,n!}\,\frac{2n-1}{n+1} = \binom{2n-2}{n}\underbrace{\left[2 - \frac{3}{n+1}\right]}_{<2} \quad . \tag{3.61}$$

Since the term in square brackets here is always smaller than 2, the terms of the sum over j in Equation (3.58b) are all negative, and so is ω_2^2.

With ω_1^2 and ω_2^2 from Equations (3.49) and (3.58b), respectively, the first two amplitude-dependent terms in the expansion (3.28) of the perturbed frequency (squared) have now been calculated. To obtain a power series for the frequency rather than its square, we expand the square root for $|\epsilon| \ll 1$ as

$$\sqrt{1+\epsilon} \approx 1 + \frac{\epsilon}{2} - \frac{\epsilon^2}{8} + \dots \tag{3.62}$$

up to second order this time. The perturbed frequency is then given by

$$\Omega_z = \sqrt{\omega_z^2 + \epsilon\omega_1^2 + \epsilon^2\omega_2^2 + \dots} \approx \omega_z \left[1 + \epsilon\frac{\omega_1^2}{2\omega_z^2} + \epsilon^2\left(\frac{\omega_2^2}{2\omega_z^2} - \frac{\omega_1^4}{8\omega_z^4}\right) + \dots\right] \quad , \tag{3.63}$$

[22] For n odd, the maximum is not unique. Identity (3.4) shows that the same value is also obtained for $k = (n-1)/2$.

Table 3.2.: Explicit expressions for frequency-shift up to second order according to Equation (3.63) with the parametrization $\Omega_z = \omega_z(1+\epsilon k_1+\epsilon^2 k_2+\dots)$ and the perturbation parameter $\epsilon = C_\eta$.

η	4	6	8	10	12
ϵk_1	$\frac{3}{4}\frac{C_4}{C_2}\frac{\hat{z}^2}{d^2}$	$\frac{15}{16}\frac{C_6}{C_2}\frac{\hat{z}^4}{d^4}$	$\frac{35}{32}\frac{C_8}{C_2}\frac{\hat{z}^6}{d^6}$	$\frac{315}{216}\frac{C_{10}}{C_2}\frac{\hat{z}^8}{d^8}$	$\frac{693}{512}\frac{C_{12}}{C_2}\frac{\hat{z}^{10}}{d^{10}}$
$\epsilon^2 k_2$	$-\frac{21}{64}\frac{C_4^2}{C_2^2}\frac{\hat{z}^4}{d^4}$	$-\frac{645}{1024}\frac{C_6^2}{C_2^2}\frac{\hat{z}^8}{d^8}$	$-\frac{8365}{8192}\frac{C_8^2}{C_2^2}\frac{\hat{z}^{12}}{d^{12}}$	$-\frac{391\,365}{262\,144}\frac{C_{10}^2}{C_2^2}\frac{\hat{z}^{16}}{d^{16}}$	$-\frac{4\,274\,655}{2\,097\,152}\frac{C_{12}^2}{C_2^2}\frac{\hat{z}^{20}}{d^{20}}$

where the first-order contribution $\epsilon\omega_1^2$ in the frequency squared results in an additional second-order contribution for the frequency as such because of the nonlinear transformation by the square root. Unlike ω_2^2 in Equation (3.58b), ω_1^2 from Equation (3.49) does not contain the perturbed frequency Ω_z, which has spared as from making the substitution $\Omega_z \to \omega_z$ to first order in the frequency-shift. The absence of Ω_z in ω_1^2 also means that there are no hidden higher-order terms in it, and we are in particular not forgetting a secret second-order contribution from ω_1^2 here.

Plugging the explicit expression for ω_1^2 and ω_2^2 into Equation (3.63) would lead to a lengthy expression, probably without any notable insights. Nevertheless, one general statement is possible without evaluating the expression explicitly. Since $\omega_2^2 < 0$ (and $\omega_1^4 = (\omega_1^2)^2 > 0$, with $\omega_1^2 > 0$ for Equation (3.49), anyway), the second-order contribution to the frequency-shift is always negative, regardless of the sign of the perturbation parameter C_η. Unlike for the case of the antisymmetric anharmonic potential associated with η odd, there is no intuitive physical explanation here.

Table 3.2 evaluates the expression for the first few even η. Since Reference [59] shows frequency-shifts up to $\hat{z}^7$, the comparison of second-order terms is limited to C_4^2, for which there is agreement.

3.3.3. Cross-terms

In this paragraph, we consider how two anharmonic imperfections of the potential produce an additional frequency-shift in concert. For judging the validity of the first-order approximation, these cross-terms are as important as the previous second-order results for one imperfection alone, because the electrostatic potential of Penning traps is typically characterized by multiple anharmonic coefficients C_η. In this case, there may be an additional frequency-shift proportional to $C_{\eta_a}C_{\eta_b}$ with weaker dependence on the axial amplitude—a smaller exponent of $\hat{z}$, that is—than the second-order result proportional to $C_{\eta_a}^2$ or $C_{\eta_b}^2$ for one anharmonic term alone. Moreover, the subsequent calculation gives a good impression of the rich phenomena (and difficulties) in perturbation theory beyond first order, where multiple effects would still add linearly. In higher orders, the effects compound more intricately.

Unfortunately, our approach is not designed to go beyond first order with multiple imperfections, but we have gained enough experience in the course of this chapter to understand the

second-order frequency-shift by cross-terms without reformulating the whole ansatz. Because we have been so instructive about perturbation theory by introducing the strength parameter C_η as the perturbation parameter ϵ, we have given up the possibility to distinguish between different imperfections. The proper way would be to introduce ϵ in the series expansions (3.19) and (3.28), as well as the equation of motion (3.17) as an order parameter, while retaining the coefficient C_η in the prefactor κ_η of the anharmonic term. As its name suggests, the order parameter keeps track of the order during the calculation, and it is set to unity at the end, thereby disappearing from the final result. The strength of the perturbation is then described by the actual perturbation parameter C_η. However, we will not introduce an order parameter here just for this section, appealing to the reader's recognition of patterns instead, in order to understand where cross-terms in the frequency-shift originate from. The key insights are as follows:

- The additional anharmonic forces add linearly, and the show up on the right-hand side of the differential equations for the z_i in the expansion (3.19) of the trajectory.
- The functional structure of the zeroth-order solution (3.38) does not depend on the imperfections.[23] Therefore, the same function for z_0 shows up in the inhomogeneous term of the differential equations for higher-order z_i.
- The differential equation (3.32) for the first-order trajectory z_1 is linear in z_1. Therefore, each imperfection C_{η_a} and C_{η_b} independently creates its own first-order solution $z_{1,a}$ and $z_{1,b}$, respectively.
- The differential equation (3.37) for the second-order trajectory z_2 is linear in z_2 and z_1. Consequently, the effect of two first-order solutions $z_{1,a}$ and $z_{1,b}$ adds linearly.

Thus, a second-order frequency-shift by cross-terms $C_{\eta_a} C_{\eta_b}$ arises from the resonant terms in

$$\begin{aligned} \omega_{2,ab}^2 z_0 = \kappa_{\eta_a}(\eta_a - 1)\left\langle z_{1,b}\, z_0^{\eta_a - 2}\right\rangle_{\Omega_z} + \kappa_{\eta_b}(\eta_b - 1)\left\langle z_{1,a}\, z_0^{\eta_b - 2}\right\rangle_{\Omega_z} \\ - \omega_{1,a}^2 \left\langle z_{1,b}\right\rangle_{\Omega_z} - \omega_{1,b}^2 \left\langle z_{1,a}\right\rangle_{\Omega_z} \quad . \end{aligned} \tag{3.64}$$

Essentially, the first-order trajectory $z_{1,a}$ of the imperfection C_{η_a} creates an additional force in the potential of the other imperfection C_{η_b}, and vice versa. From the series expansion of the frequency, there is also the combination of the frequency-shift coefficient $\omega_{1,a}^2$ from C_{η_a} with the resonant terms of the first-order trajectory $z_{1,b}$ of the other imperfection C_{η_b}, and vice versa. In order to accommodate these cross-term, the expansion (3.28) of the frequency squared then has to be amended as

$$\Omega_z^2 = \omega_z^2 + \epsilon_a \omega_{1,a}^2 + \epsilon_b \omega_{1,b}^2 + \epsilon_a^2 \omega_{2,a}^2 + \epsilon_b^2 \omega_{2,b}^2 + \epsilon_a \epsilon_b \omega_{2,ab}^2 + \dots \quad , \tag{3.65}$$

where $\epsilon_a = C_{\eta_a}$ and accordingly for η_b. The dots indicate that terms beyond second order have been neglected. The term $\omega_{2,ab}^2$ is the actual cross-term; the terms with single indices a and b are also present for one imperfection alone. This situation is recreated by setting either ϵ_a or

[23] Of course, the frequency Ω_z does, which is the main point of emphasis here.

ϵ_b to zero. With more than two imperfections, we would have to sum over the index a for the effect of the C_{η_a} alone, and the combinations of a and b for the cross-terms $C_{\eta_a}C_{\eta_b}$. We omit the sums here and pick any combination at will, resting assured that the second-order effects add linearly, provided we keep track of the cross-terms.

By using the series expansion (3.62) of the square root on Equation (3.65), the perturbed frequency Ω_z is expressed as

$$\Omega_z \approx \omega_z \left(1 + w_a + w_b + w_{ab} + \dots\right) \quad , \tag{3.66}$$

with the two abbreviations

$$w_a = \epsilon_a \frac{\omega_{1,a}^2}{2\omega_z^2} + \epsilon_a^2 \left(\frac{\omega_{2,a}^2}{2\omega_z^2} - \frac{\omega_{1,a}^4}{8\omega_z^4} \right) \qquad \text{and} \qquad w_{ab} = \epsilon_a \epsilon_b \left(\frac{\omega_{2,ab}^2}{2\omega_z^2} - \frac{\omega_{1,a}^2 \omega_{1,b}^2}{4\omega_z^4} \right) \tag{3.67}$$

for the relative frequency-shift.[24] The ω_1^2 and ω_2^2 have already been calculated for their use in w_a. For even $\eta_a = 2n_a$ or $\eta_b = 2n_b$, they are given by Equations (3.49) and (3.58b), respectively (with the proper replacement of $n \to n_a$ or $n \to n_b$). For odd $\eta_a = 2n_a + 1$, Equation (3.45) shows $\omega_{2,a}^2$. Since $\omega_{1,a}^2 = 0$ for odd coefficients, the product $\omega_{1,a}^2 \omega_{1,b}^2$ in the cross-term w_{ab} contributes only for two even coefficients. We will now calculate the unknown $\omega_{2,ab}^2$ for the three different combinations of parities the two parameters η_a and η_b may have: even–odd, odd–odd and even–even.[25]

Even–odd

We choose even $\eta_a = 2n_a$ and odd $\eta_b = 2n_b + 1$. There is no first-order frequency-shift associated with odd coefficients: $\omega_{1,b}^2 = 0$. The other contributions to Equation (3.64) in search of resonant terms need more scrutiny, because the first two represent a combination that we have not encountered so far—a first-order trajectory resulting from an antisymmetric potential Φ_{2n_b+1} with the zeroth-order solution z_0 taken to the even power $2n_a - 2$ and vice versa. We will first examine the other combination, $z_{1,a} z_0^{2n_b-1}$—the first-order trajectory $z_{1,a}$ resulting from the symmetric potential Φ_{2n_a} multiplied with the zeroth-order solution z_0 taken to the odd power $2n_b - 1$. With z_0 from Equation (3.38) and the odd powers of cosine shown in Equation (3.42a), it becomes clear that $z_0^{2n_b-1}$ features the frequencies $1\Omega_z, 3\Omega_z, \dots, (2n_b - 1)\Omega_z$. In other words, there is a term at the fundamental frequency, as well as its odd higher harmonics. The first-order trajectory $z_{1,a}$ from Equation (3.50) (with the substitution $n \to n_a$) for a symmetric potential features very similar frequencies: $1\Omega_z, 3\Omega_z, \dots, (2n_a - 1)\Omega_z$. Only the upper limit may be different. According to Equation (C.10) from the appendix, there is no chance to produce a resonant term at the frequency Ω_z by mixing, because both the sum and the difference frequencies in this case are even multiples of the fundamental frequency (or zero), and we

[24] The different factor in the last denominator of Equation (3.67) is not a misprint. When calculating the frequency squared from Ω_z in the expansion (3.66), there are two possibilities to produce the term $\omega_{1,a}^2 \omega_{1,b}^2$ with the product $w_a w_b$, whereas there is only one chance to obtain $\omega_{1,a}^4$ from w_a^2.

[25] We count even–odd as one possibility, because the cross-term w_{ab} is symmetric in the two parameters. It does not matter which of the two is even and which one is odd.

conclude

$$\left\langle z_{1,a}\, z_0^{2n_b-1} \right\rangle_{\Omega_z} = 0 \quad . \tag{3.68}$$

The other cross-term of trajectories in Equation (3.64) is more involved. The first-order trajectory $z_{1,b}$ from Equation (3.39) (with the replacement $n \to n_b$) for an antisymmetric potential has the frequency spectrum $0\Omega_z, \Omega_z, 2\Omega_z, 4\Omega_z, \ldots, 2n_b\Omega_z$. According to Equation (3.55a), the frequency spectrum of $z_0^{2n_a-2}$ is $0\Omega_z, 2\Omega_z, \ldots, (2n_a-2)\Omega_z$. There are two mechanisms for producing resonant terms at the fundamental frequency Ω_z here:

1. Preserve the resonant term in $z_{1,b}$ by multiplying it with the constant term in $z_0^{2n_a-2}$.
2. Create a resonant term according to Equation (C.10) by multiplying $\cos(\Omega_z t)$ in $z_{1,b}$ with $\cos(2\Omega_z t)$ from $z_0^{2n_a-2}$.

Other than that, the sum and difference frequencies of multiplying two terms at even harmonics of the fundamental frequency will stay even harmonics (or zero). The two relevant mechanisms listed above result in

$$\begin{aligned}\left\langle z_{1,b}\, z_0^{2n_a-2} \right\rangle_{\Omega_z} &= -\frac{\kappa_{2n_b+1}\,\hat{z}^{2n_b}}{2^{2n_b}\,\Omega_z^2}\,\frac{\hat{z}^{2n_a-3}}{2^{2n_a-2}}\,z_0 \\ &\quad\cdot\left\{\left[-\binom{2n_b}{n_b} + 2\sum_{j=1}^{n_b}\binom{2n_b}{n_b-j}\frac{1}{(2j)^2-1}\right]\left[\binom{2n_a-2}{n_a-1}+\binom{2n_a-2}{n_a-2}\right]\right\} \qquad (3.69a)\\ &= \frac{\kappa_{2n_b+1}\,\hat{z}^{2(n_a+n_b)-3}}{2^{2(n_a+n_b)-2}\,\Omega_z^2}\,z_0\binom{2n_a-1}{n_a-1}\left[\binom{2n_b}{n_b} - 2\sum_{j=1}^{n_b}\binom{2n_b}{n_b-j}\frac{1}{(2j)^2-1}\right] \quad . \qquad (3.69b)\end{aligned}$$

As usual, we have absorbed the oscillatory term $\cos(\Omega_z t)$ and one factor of the amplitude $\hat{z}$ in the zeroth-order solution z_0 from Equation (3.38). In the last step, the two binomial coefficients are added with the help of Equation (3.56).

The remaining term in Equation (3.64) is

$$\left\langle z_{1,b} \right\rangle_{\Omega_z} = -\frac{\kappa_{2n_b+1}\,\hat{z}^{2n_b-1}}{2^{2n_b}\,\Omega_z^2}\,z_0\left[-\binom{2n_b}{n_b} + 2\sum_{j=1}^{n_b}\binom{2n_b}{n_b-j}\frac{1}{(2j)^2-1}\right] \quad , \tag{3.70}$$

which needs to be combined with the first-order coefficient $\omega_{1,a}^2$ from Equation (3.49) (with the replacement $n \to n_a$). Fortunately, the two terms contributing to Equation (3.64) have a very similar structure then, and even the sum is executed by hand with the identity

$$\binom{2n_b}{n_b} - 2\sum_{j=1}^{n_b}\binom{2n_b}{n_b-j}\frac{1}{(2j)^2-1} = \frac{2^{2n_b}}{2n_b+1} \quad . \tag{3.71}$$

Because proving the identity is probably beyond the scope of this chapter (and I have no proof in mind), we accept it as an unsolicited gift,[26] which Wolfram *Mathematica*® 9 confirms on a general basis with the command `FullSimplify`.

[26] The conjecture (3.71) was inspired by observing that the numerical prefactor of the explicit terms in Table 3.3 does not depend on n_b. Thus, a cancellation of the n_b from the term in square brackets in Equations (3.69b) and (3.70) with the n_b from $\kappa_{2n_b+1}/2^{2n_b}$ was expected.

Overall, the second-order coefficient for cross-terms in the expansion of the frequency (squared) then becomes

$$\omega_{2,ab}^2 = \frac{\kappa_{2n_a}\kappa_{2n_b+1}}{2^{2n_a-2}\Omega_z^2}\frac{2n_a-2}{2n_b+1}\binom{2n_a-1}{n_a-1}\hat{z}^{2(n_a+n_b)-3} = \frac{1}{C_2^2}\frac{\omega_z^4}{\Omega_z^2}\frac{n_a(n_a-1)}{2^{2n_a-1}}\frac{(2n_a)!}{(n_a!)^2}\frac{\hat{z}^{2(n_a+n_b)-3}}{d^{2(n_a+n_b)-3}} \quad . \tag{3.72}$$

The last step uses the definition (3.17) of the prefactor κ_η, and Equation (3.43) for the binomial coefficient. The relative-frequency shift (3.66) due to the even–odd cross-terms is given by

$$w_{ab} = C_{2n_a}C_{2n_b+1}\frac{\omega_{2,ab}^2}{2\omega_z^2} = \frac{C_{2n_a}C_{2n_b+1}}{C_2^2}\frac{n_a(n_a-1)}{2^{2n_a}}\frac{(2n_a)!}{(n_a!)^2}\frac{\hat{z}^{2(n_a+n_b)-3}}{d^{2(n_a+n_b)-3}} \quad . \tag{3.73}$$

To second order in the frequency-shift, we have ignored the difference between the perturbed frequency Ω_z and the harmonic frequency ω_z, by sending $\Omega_z \to \omega_z$. The prefactor of $w_{a,b}$ does not depend on n_b; the exponent of $\hat{z}/d$ does.

The exponent for the second-order frequency-shift (3.48) by C_{2n_b+1} is $4n_b - 2$. Thus, the exponent of $\hat{z}$ in this second-order cross-term is smaller than in the second-order term by the odd coefficient itself for $2n_a < 2n_b + 1$, or equivalently $\eta_a < \eta_b$. For the second-order frequency-shift (3.63) of the even coefficient C_{2n_a}, the exponent of $\hat{z}$ is $4n_a - 4$. The condition for a lower exponent of the cross-term than for the second-order term itself is exactly opposite: $2n_a > 2n_a + 1$, or equivalently $\eta_a > \eta_b$. In either case, there will be a second-order term by one coefficient with a lower exponent and one with a higher exponent of $\hat{z}$ than the second-order cross-term.

Table 3.3 evaluates the relative frequency-shift (3.73) first few even–odd cross-terms. There is agreement with Reference [59], which shows the same for the six combinations C_4C_3, C_4C_5, C_4C_7, C_6C_3, C_6C_5 and C_8C_3, which are all the even–odd cross-terms with a dependence of at most $\hat{z}^7$.

Odd–odd

We choose odd $\eta_a = 2n_a + 1$ and odd $\eta_b = 2n_b + 1$. Because there is no first-order frequency-shift ($\omega_{1,a}^2 = \omega_{1,b}^2 = 0$) for odd terms, only the products of coordinates in Equation (3.64) remain. We will infer a lot from the calculation for one odd contribution to the overall potential in Section 3.3.1, and we will work with analogies as much a possible. In fact, the only difference between $z_{1,a}$ and $z_{1,b}$ is the adequate replacement $n \to n_a$ or $n \to n_b$, respectively, in Equation (3.39). Similarly, the switch from $z_0^{2n_a-1}$ to $z_0^{2n_b-1}$ is made by selecting the adequate n in Equation (3.42a). Therefore, resonant terms are produced in close analogy with Equation (3.41). We simply have to recall where which term is from: the first binomial coefficient of each product is from z_1; the second one from z_0^{2n-1}. Taking into account the two different solutions with n_a and n_b, the corresponding expression (barring the prefactor $\kappa_{2n_a+1}2n_a$, and the term with the

Table 3.3.: Relative frequency-shift $w_{a,b}$ from Equation (3.73) for even–odd cross-terms in the expansion (3.66) of the frequency. For a given even coefficient C_{2n}, the numerical prefactor does not depend on the index of the odd coefficients; the exponent of z/d does.

	C_3	C_5	C_7	C_9
C_4	$\frac{3}{4}\frac{C_3C_4}{C_2^2}\frac{\hat{z}^3}{d^3}$	$\frac{3}{4}\frac{C_5C_4}{C_2^2}\frac{\hat{z}^5}{d^5}$	$\frac{3}{4}\frac{C_7C_4}{C_2^2}\frac{\hat{z}^7}{d^7}$	$\frac{3}{4}\frac{C_9C_4}{C_2^2}\frac{\hat{z}^9}{d^9}$
C_6	$\frac{15}{8}\frac{C_3C_6}{C_2^2}\frac{\hat{z}^5}{d^5}$	$\frac{15}{8}\frac{C_5C_6}{C_2^2}\frac{\hat{z}^7}{d^7}$	$\frac{15}{8}\frac{C_7C_6}{C_2^2}\frac{\hat{z}^9}{d^9}$	$\frac{15}{8}\frac{C_9C_6}{C_2^2}\frac{\hat{z}^{11}}{d^{11}}$
C_8	$\frac{105}{32}\frac{C_3C_8}{C_2^2}\frac{\hat{z}^7}{d^7}$	$\frac{105}{32}\frac{C_5C_6}{C_2^2}\frac{\hat{z}^9}{d^9}$	$\frac{105}{32}\frac{C_7C_8}{C_2^2}\frac{\hat{z}^{11}}{d^{11}}$	$\frac{105}{32}\frac{C_9C_8}{C_2^2}\frac{\hat{z}^{13}}{d^{13}}$
C_{10}	$\frac{315}{64}\frac{C_3C_{10}}{C_2^2}\frac{\hat{z}^9}{d^9}$	$\frac{315}{64}\frac{C_5C_{10}}{C_2^2}\frac{\hat{z}^{11}}{d^{11}}$	$\frac{315}{64}\frac{C_7C_{10}}{C_2^2}\frac{\hat{z}^{13}}{d^{13}}$	$\frac{315}{64}\frac{C_9C_{10}}{C_2^2}\frac{\hat{z}^{15}}{d^{15}}$

indices a and b swapped) becomes

$$\left\langle z_{1,a}\, z_0^{2n_b-1}\right\rangle_{\Omega_z} = -\frac{\kappa_{2n_a+1}}{2^{2n_a}\Omega_z^2}\frac{\hat{z}^{2n_a}}{2^{2n_b-2}}\frac{\hat{z}^{2n_b-2}}{}\, z_0 \left\{\binom{2n_a}{n_a}\binom{2n_b-1}{n_b-1} - \sum_{j=1}^{n_{\min}}\frac{1}{(2j)^2-1}\binom{2n_a}{n_a-j}\left[\binom{2n_b-1}{n_b-1-j}+\binom{2n_b-1}{n_b-j}\right]\right\} \tag{3.74a}$$

$$= -\frac{\kappa_{2n_a+1}}{2^{2(n_a+n_b)-1}\,\Omega_z^2}\,\hat{z}^{2(n_a+n_b)-2}\, z_0\left[\binom{2n_a}{n_a}\binom{2n_b}{n_b} - 2\sum_{j=1}^{n_{\min}}\frac{\binom{2n_a}{n_a-j}\binom{2n_b}{n_b-j}}{(2j)^2-1}\right] . \tag{3.74b}$$

The oscillatory term $\cos(\Omega_z t)$ and one factor of $\hat{z}$ are absorbed in the zeroth-order solution z_0 from Equation (3.38). The last step simplifies the binomials with the help of Equations (3.43) and (3.44). Although the summation over j should stop at the minimum of n_a and n_b, no harm is done by exceeding this upper limit, because the explicit definition (3.3) nulls the unwanted terms.[27] Fortunately for the use of analogies, the lower limit is the same in both cases.

The term in angle brackets with the binomial coefficients is simplified by executing the sum with a more general version of Equation (3.46) as

$$\binom{2n_a}{n_a}\binom{2n_b}{n_b} - 2\sum_{j=1}^{n_{\min}}\frac{\binom{2n_a}{n_a-j}\binom{2n_b}{n_b-j}}{(2j)^2-1} = \frac{1}{(2n_a+1)(2n_b+1)}\frac{[2(n_a+n_b)+1]!}{[(n_a+n_b)!]^2} . \tag{3.75}$$

[27] That is also why have not bothered about using two different limits for the sum over j, which we still did in Equation (3.41).

We have no proof to offer here.[28] As a test with the command `FullSimplify` in Wolfram *Mathematica*® 10 shows, an advanced knowledge of generalized hypergeometric functions might help. The conjecture (3.75) has been tested numerically for combinations of n_a and n_b well beyond experimental relevance.

With the prefactor $\kappa_{2n_a} 2n_a$ and the term with a and b swapped, the coefficient $\omega^2_{2,ab}$ in Equation (3.64) becomes

$$\omega^2_{2,ab} = -2(n_a+n_b)\frac{\kappa_{2n_a+1}\,\kappa_{2n_b+1}}{2^{2(n_a+n_b)-1}\,\Omega_z^2}\,\hat{z}^{2(n_a+n_b)-2}\,\frac{1}{(2n_a+1)(2n_b+1)}\,\frac{[2(n_a+n_b)+1]!}{[(n_a+n_b)!]^2} \tag{3.76a}$$

$$= -\frac{\omega_z^4}{\Omega_z^2}\,\frac{1}{C_2^2}\,\frac{n_a+n_b}{[(n_a+n_b)!]^2}\,\frac{[2(n_a+n_b)+1]!}{2^{2(n_a+n_b)}}\,\frac{\hat{z}^{2(n_a+n_b)-2}}{d^{2(n_a+n_b)-2}} \quad . \tag{3.76b}$$

The last step plugs in the κ_η from Equation (3.17). As expected for the cross-term caused by two odd η, the final expression is symmetric in n_a and n_b. For $n_a = n_b$ the corresponding expression (3.45) for the second-order effect of one odd coefficient C_{2n+1} is not quite reproduced. Because of the double counting in Equation (3.64) for $n_a = n_b$, the result (3.76b) has an additional factor of 2.

With $\omega^2_{2,ab}$ from Equation (3.76b), the relative frequency-shift (3.66) by the odd–odd cross-term follows from Equation (3.67) with $\epsilon_a = C_{2n_a+1}$ (and accordingly for ϵ_b) as

$$w_{ab} = -\frac{C_{2n_a+1}C_{2n_b+1}}{C_2^2}\,\frac{n_a+n_b}{[(n_a+n_b)!]^2}\,\frac{[2(n_a+n_b)+1]!}{2^{2(n_a+n_b)+1}}\,\frac{\hat{z}^{2(n_a+n_b)-2}}{d^{2(n_a+n_b)-2}} \quad , \tag{3.77}$$

where the replacement $\Omega_z \to \omega_z$ in $\omega^2_{2,ab}$ is fine to second order in the frequency-shift. The result is always negative, and it depends on the sum of n_a and n_b, rather than are more complicated combination of the two. Thus, the cross-term is actually a function of the single variable $n_a + n_b$. Table 3.4 evaluates the first few terms. There is agreement with the two odd–odd terms C_3C_5 and C_3C_7 shown in Reference [59].

The exponent of $\hat{z}$ for the second-order frequency-shift (3.48) by C_{2n_a+1} is $4n_a - 2$ (and accordingly for n_b), which is also the result for $n_a = n_b$ in Equation (3.77). Consequently, the second-order cross-term has a smaller exponent than the second-order term for C_{2n_a+1} for $n_b < n_a$, or equivalently $\eta_b < \eta_a$. Without even coefficients, the second-order frequency-shift with the lowest exponent of $\hat{z}$ results from the odd C_η with the smallest η rather than the cross-term.

Even–even

We choose $\eta_a = 2n_a$ and $\eta_b = 2n_b$ both even. Similar to the odd–odd terms, we will feast on analogies with the second-order calculation for one even term C_{2n} in Section 3.3.2, in order to identify resonant terms in Equation (3.64). The four original mechanisms for producing

[28] I thank the *On-Line Encyclopedia of Integer Sequences*® (`https://oeis.org`) for helping me spot a pattern, after having the hunch (from the explicit expressions partly shown in Table 3.4) that the frequency-shift (3.77) depends only on the sum of n_a and n_b. Their sequence A002457 (formerly M4198 N1752), with the explicit representation $(2n+1)!/(n!)^2$, is produced by the left-hand side of Equation (3.75) multiplied with $(2n_a+1)(2n_b+1)$, while keeping $n = n_a + n_b$ constant.

Table 3.4.: Relative frequency-shift $w_{a,b}$ from Equation (3.77) for odd–odd cross-terms of in the expansion (3.66) of the frequency. Since the result is symmetric in the two odd coefficients, it is printed only once, and hence the empty entries. Moreover, the expressions are identical for two odd coefficients C_η whose indices sum to the same value. Refer to Table 3.1 and Equation (3.48) for the second-order shift by C_{2n+1}^2 alone. The cross (×) indicates that Equation (3.76b) is not applicable (without an additional factor of ½).

	C_5	C_7	C_9	C_{11}
C_3	$-\frac{105}{32}\frac{C_3C_5}{C_2^2}\frac{\hat{z}^4}{d^4}$	$-\frac{315}{64}\frac{C_3C_7}{C_2^2}\frac{\hat{z}^6}{d^6}$	$-\frac{3465}{512}\frac{C_3C_9}{C_2^2}\frac{\hat{z}^8}{d^8}$	$-\frac{9009}{1024}\frac{C_3C_{11}}{C_2^2}\frac{\hat{z}^{10}}{d^{10}}$
C_5	×	$-\frac{3465}{512}\frac{C_5C_7}{C_2^2}\frac{\hat{z}^8}{d^8}$	$-\frac{9009}{1024}\frac{C_5C_9}{C_2^2}\frac{\hat{z}^{10}}{d^{10}}$	$-\frac{45\,045}{4096}\frac{C_5C_{11}}{C_2^2}\frac{\hat{z}^{12}}{d^{12}}$
C_7		×	$-\frac{45\,045}{4096}\frac{C_7C_9}{C_2^2}\frac{\hat{z}^{12}}{d^{12}}$	$-\frac{109\,395}{8192}\frac{C_7C_{11}}{C_2^2}\frac{\hat{z}^{14}}{d^{14}}$
C_9			×	$-\frac{2\,078\,505}{131\,072}\frac{C_9C_{11}}{C_2^2}\frac{\hat{z}^{16}}{d^{16}}$

resonant terms resulted in Equation (3.54), where the first binomial in each product is from z_0^{2n-2}, while the second one stems from z_1. Here, the n is not the same. In $z_{1,a}$, the replacement is $n \to n_a$ in Equation (3.50); in $z_0^{2n_b-2}$ (with z_0 from Equation (3.38)), the replacement is $n \to n_b$ in Equation (3.55a). The extended version of Equation (3.54) then takes the form

$$\begin{aligned}\left\langle z_{1,a}\, z_0^{2n_b-2}\right\rangle_{\Omega_z} = z_0\,\frac{\kappa_{2n_a}\hat{z}^{2n_a-1}}{2^{2n_a}\,\Omega_z^2}\frac{\hat{z}^{2n_b-3}}{2^{2n_b-2}}\Bigg\{&-\left[\binom{2n_b-2}{n_b-1}+\binom{2n_b-2}{n_b-2}\right]\sum_{j=1}^{n_a-1}\frac{\binom{2n_a-1}{n_a-j-1}}{j(j+1)}\\ &+\sum_{j=1}^{n_{\min}-1}\left[\binom{2n_b-2}{n_b-j-1}+\binom{2n_b-2}{n_b-j-2}\right]\frac{\binom{2n_a-1}{n_a-j-1}}{j(j+1)}\Bigg\}\end{aligned} \tag{3.78a}$$

$$= z_0\,\frac{\kappa_{2n_a}\hat{z}^{2(n_a+n_b)-4}}{2^{2(n_a+n_b)-2}\Omega_z^2}\sum_{j=1}^{n_a-1}\frac{\binom{2n_a-1}{n_a-j-1}}{j(j+1)}\left[\binom{2n_b-1}{n_b-j-1}-\binom{2n_b-1}{n_b-1}\right]\quad. \tag{3.78b}$$

The zeroth-order solution z_0 contains a factor of $\hat{z}$ and the oscillatory term $\cos(\Omega_z t)$. With the help of Equation (3.56), the binomial coefficients are summed in the last step. Because the explicit definition (3.3) of the binomial coefficient produces vanishing terms when the summation variable j exceeds the nominal upper limit, we extend it at will.[29] This allows

[29] In fact, we have not bothered about the two different upper limits of the sums in Equation (3.54) anymore.

us to use the upper limit $n_a - 1$ for both sums in Equation (3.78a), with the second sum not contributing once j has reached (or exceeded) the minimum of n_a and n_b.

With $\omega_{1,b}^2$ from Equation (3.49), where $n \to n_b$, and $z_{1,a}$ from Equation (3.50), where $n \to n_a$, the equivalent of Equation (3.53) becomes

$$\omega_{1,b}^2 \left\langle z_{1,a} \right\rangle_{\Omega_z} = -\binom{2n_b - 1}{n_b - 1} \frac{\kappa_{2n_b}\, \hat{z}^{2n_b-2}}{2^{2n_b-2}} z_0 \frac{\kappa_{2n_a} \hat{z}^{2n_a-2}}{2^{2n_a} \Omega_z^2} \sum_{j=1}^{n_a-1} \frac{\binom{2n_a-1}{n_a-1-j}}{j(j+1)} \quad . \tag{3.79}$$

Similar two Equation (3.58b), Equations (3.78b) and (3.79) are summed (with the prefactors mandated by Equation (3.64)) as

$$\kappa_{2n_b}(2n_b - 1) \left\langle z_{1,a}\, z_0^{2n_b-2} \right\rangle_{\Omega_z} + \omega_{1,b}^2 \left\langle z_{1,a} \right\rangle_{\Omega_z} = z_0 \frac{\kappa_{2n_a} \kappa_{2n_b}\, (2n_b - 1)}{2^{2(n_a+n_b)-2}\, \Omega_z^2} \hat{z}^{2(n_a+n_b)-4} \sum_{j=1}^{n_a-1} \frac{\binom{2n_a - 1}{n_a - j - 1}}{j(j+1)} \left[\binom{2n_b - 1}{n_b - j - 1} - 2\binom{2n_b - 2}{n_b} \right] \tag{3.80}$$

with the help of Equation (3.59). The resulting expression is not symmetric in n_a and n_b, and we define the abbreviation

$$s(n_a, n_b) = (2n_b - 1) \sum_{j=1}^{n_a-1} \frac{1}{j(j+1)} \binom{2n_a - 1}{n_a - j - 1} \left[\binom{2n_b - 1}{n_b - j - 1} - 2\binom{2n_b - 2}{n_b} \right] \tag{3.81}$$

for the asymmetric part. To complete the right-hand side of Equation (3.64), Equation (3.80) has to be added with n_a and n_b swapped. With the abbreviation (3.81) and the definition (3.17) of the κ_η, the parameter $\omega_{2,ab}^2$ is given by

$$\omega_{2,ab}^2 = \frac{\omega_z^4}{\Omega_z^2} \frac{1}{C_2^2} \frac{n_a n_b}{2^{2(n_a+n_b)-2}} \frac{\hat{z}^{2(n_a+n_b)-4}}{d^{2(n_a+n_b)-4}} \left[s(n_a, n_b) + s(n_b, n_a) \right] \quad . \tag{3.82}$$

For the second-order frequency-shift, the replacement $\Omega_z \to \omega_z$ is fine. Because there is a first-order frequency-shift associated with each even coefficient C_{2n}, the relative frequency-shift

$$w_{ab} = C_{2n_a} C_{2n_b} \left(\frac{\omega_{2,ab}^2}{2\omega_z^2} - \frac{\omega_{1,a}^2 \omega_{1,b}^2}{4\omega_z^4} \right) \tag{3.83}$$

in the expansion (3.66) also contains two ω_1^2 from Equation (3.49) (with the adequate replacement $n \to n_a$ and $n \to n_b$). Like for the odd–odd cross-term, the expression is not quite correct for $n_a = n_b$ because of the double counting in Equation (3.64). Consequently, there is an additional factor of 2 compared with Equation (3.63) for the second-order frequency-shift by one even coefficient C_{2n}. However, the exponent of $\hat{z}$ is correctly reproduced for $n_a = n_b$. Consequently, the exponent of $\hat{z}$ in the second-order cross-term is lower than in the second-order term for C_{2n_a} itself for $\eta_b < \eta_a$, or equivalently $\eta_b < \eta_a$. The dominant second-order frequency-shift—apart from $C_{2n_a}^2$ for the smallest n_a—may well be the cross-terms with this C_{2n_a}, rather than the actual second-order contributions of the individual C_{2n_b} themselves.

Table 3.5.: Relative frequency-shift $w_{a,b}$ from Equation (3.83) for even–even cross-terms in the expansion (3.66) of the frequency. Since the frequency-shift is symmetric in the coefficients, results from the upper corner of the table are not repeated in the lower corner. The cross (×) indicates that Equation (3.83) (without a factor of 1/2) does not apply to terms of the kind C_{2n}^2. Refer to Table 3.2 and Equation (3.63) instead.

	C_6	C_8	C_{10}	C_{12}
C_4	$-\frac{57}{64}\frac{C_4C_6}{C_2^2}\frac{\hat{z}^6}{d^6}$	$-\frac{561}{512}\frac{C_4C_8}{C_2^2}\frac{\hat{z}^8}{d^8}$	$-\frac{1311}{1024}\frac{C_4C_{10}}{C_2^2}\frac{\hat{z}^{10}}{d^{10}}$	$-\frac{5937}{4096}\frac{C_4C_{12}}{C_2^2}\frac{\hat{z}^{12}}{d^{12}}$
C_6	×	$-\frac{1629}{1024}\frac{C_6C_8}{C_2^2}\frac{\hat{z}^{10}}{d^{10}}$	$-\frac{7755}{4096}\frac{C_6C_{10}}{C_2^2}\frac{\hat{z}^{12}}{d^{12}}$	$-\frac{17\,805}{8192}\frac{C_6C_{12}}{C_2^2}\frac{\hat{z}^{14}}{d^{14}}$
C_8		×	$-\frac{20\,145}{8192}\frac{C_8C_{10}}{C_2^2}\frac{\hat{z}^{14}}{d^{14}}$	$-\frac{373\,305}{131\,072}\frac{C_8C_{12}}{C_2^2}\frac{\hat{z}^{16}}{d^{16}}$
C_{10}			×	$-\frac{912\,345}{262\,144}\frac{C_{10}C_{12}}{C_2^2}\frac{\hat{z}^{18}}{d^{18}}$

For fear of wasting a lot of space while finding little to simplify in the meantime, we do not plug in the full expressions here. Table 3.5 evaluates the relative frequency-shift (3.83) for the first few terms. Reference [59] offers an expression for the frequency-shift by C_4C_6, and it agrees. In short, no discrepancy has been found. However, Reference [59] does not give a general expression for the frequency-shift of first and second order, while showing many more terms of higher order explicitly.

3.4. First-order perturbative method

The Lindstedt–Poincaré method presented in Section 3.2.2 relies on expressing the fundamental frequency as a power series. The method works nicely, when then fundamental frequency of the unperturbed system is easily spotted, which was the case for the one-dimensional anharmonic oscillator. For the radial modes in the Penning trap, however, neither of the corresponding frequencies $\omega_\pm$ from Equation (2.23) shows up directly in the equations of motion (2.16). Therefore, an expansion of a single frequency will not suffice, and a more sophisticated approach is required. It might consist in expanding the effective free-space cyclotron-frequency ω_c and the effective axial frequency ω_z, which are both present in the equations of motion (2.16) and the expression (2.23) for the radial frequencies $\omega_\pm$. Section 5.2.2 gives an example. Fortunately, there is a simpler formalism, if we are willing to settle for first-order frequency-shifts. The formalism draws heavily from References [128, 155], and the concept of searching for resonant terms is very similar, although the notation is somewhat different. We will demonstrate the approach for the axial mode first, because we have a result to compare with.

3.4.1. The one-dimensional anharmonic oscillator revisited

For the Lindstedt–Poincaré method of Section 3.2.2, the first-order frequency-shift was determined by the zeroth-order solution alone, because the acceleration caused by the additional term was of first order right from the start. Therefore, the first-order correction to the trajectory $z(t)$ did not have to be calculated, and we are free to drop its series expansion (3.19). The first-order frequency-shift followed from absorbing a resonant term, which resulted entirely from the zeroth-order solution being inserted into the additional term, as a frequency-shift. Therefore, we will use the solution

$$\tilde{z}(t) = \hat{z}\cos(\tilde{\omega}_z t + \tilde{\varphi}_z) \tag{3.84}$$

from the unperturbed case with a little twist. The tilde on $\tilde{\omega}_z$ indicates that the frequency has yet to be determined. In the perturbed case, it is not fixed by Equation (2.17).

From the physical perspective, the resonant term is interpreted as follows: while the particle travels along the trajectory, the additional term gives rise to new forces, most of which are nonresonant, and only lead to small oscillations at their nonresonant frequency. Since these forces are essentially generated by the motion of the particle—they would not be present if the particle were at rest[30]—the particle's response is like a motional sideband. The particle also experiences resonant forces that look like the main force, which gave rise to the original motion. If these resonant forces are always in phase with the main force, they do not act like a resonant drive. Instead, they add coherently to the main force. When discussing the sinusoidally driven harmonic oscillator (3.25), the phase φ_d of the drive was not related to the phase of the motion. Since the phase of the motion with respect to the drive changes upon excitation, the drive term could not be absorbed as a frequency-shift. Instead, the resonant drive resulted in a secular term, which caused Equation (3.27) to diverge with time. For the motional drives generated by the anharmonic terms, the situation is different, because the force is produced from the motion itself. Therefore, the frequency and the phase-relationship are fixed—something not accomplished with an external drive. Of course, Equation (3.27) suggests that a phase relative to the drive is imprinted on the ion by exciting it long enough on resonance. However, the anharmonic terms generate resonant terms with a phase relative to the motion, and not the other way around, as the external drive would do.

In short, the resonant drive terms that are always in phase with the original (zeroth-order) trajectory $\tilde{z}(t)$ are absorbed by the dimensionless parameter ε_z in the effective equation of motion[31]

$$\ddot{\tilde{z}}(t) + \omega_z^2(1+\varepsilon_z)\,\tilde{z}(t) = 0 \quad . \tag{3.85}$$

The nonresonant terms are ignored because the do not cause a first-order frequency-shift. If they were not present, $\tilde{\omega}_z = \omega_z\sqrt{1+\varepsilon_z}$ would be the exact frequency. For $|\varepsilon_z| \ll 1$, as in the

[30] To be more precise, we should say that the particle would not be subject to additional forces, if it sat at the (unstable) equilibrium position of the electrostatic potential, which entails staying at rest in the Penning trap.

[31] Originally, when only cylindrically-symmetric imperfections were considered [82, 84], the parameter ε_z was called γ_z, in order to avoid confusion with the perturbation parameter ϵ. When the calculation was extended to relativistic effects, the Lorentz factor γ posed the bigger threat. A similar parameter in Equation (3.105) was renamed accordingly.

case of small anharmonic perturbations, the relative first-order frequency shift is given by

$$\frac{\Delta\omega_z}{\omega_z} = \frac{\varepsilon_z}{2} \tag{3.86}$$

after expanding the square root. Generally speaking, we define the frequency-shift as the difference between the perturbed frequency $\tilde{\omega}_i$ and the unperturbed frequency ω_i:

$$\Delta\omega_i = \tilde{\omega}_i - \omega_i \quad . \tag{3.87}$$

When we use this formalism that is specially geared towards first-order frequency-shifts, we will not explicitly stress that $\Delta\omega_i$ is good to first order only.

With the technicalities laid out, we apply the formalism to the anharmonic oscillator (3.17). Resonant terms to be absorbed in the effective axial equation of motion (3.85) are expressed as

$$\varepsilon_z \tilde{z}(t) = \frac{\epsilon\kappa_\eta}{\omega_z^2} \left\langle \left[\tilde{z}(t)\right]^{\eta-1} \right\rangle_{\tilde{\omega}_z} \tag{3.88}$$

in our notation. Like in several sections before, Equations (3.2) and (3.5) show that an oscillatory term at the perturbed axial frequency $\tilde{\omega}_z$ is present only if the exponent $\eta-1$ is odd. Consequently, η has to be even, and we write $\eta = 2n$. With the help of Equation (3.7), the resonant contribution is found as

$$\left\langle \left[\tilde{z}(t)\right]^{2n-1} \right\rangle_{\tilde{\omega}_z} = \frac{\hat{z}^{2n-1}}{2^{2n-1}} \frac{(2n)!}{(n!)^2} \cos(\tilde{\omega}_z t + \tilde{\varphi}_z) = \frac{\hat{z}^{2n-2}}{2^{2n-1}} \frac{(2n)!}{(n!)^2} \tilde{z}(t) \quad . \tag{3.89}$$

In the last step, one factor of $\hat{z}$ is used to write the result as proportional to $\tilde{z}(t)$, such that it fits into the effective equation of motion (3.85) for the first-order frequency-shift. With κ_{2n} from Equation (3.17) and the substitution $\epsilon = C_{2n}$, the result is related to the first-order frequency-shift

$$\frac{\Delta\omega_z}{\omega_z} = \frac{C_{2n}}{C_2} \frac{n}{2^{2n}} \frac{(2n)!}{(n!)^2} \frac{\hat{z}^{2n-2}}{d^{2n-2}} \tag{3.90}$$

with the help of Equation (3.86). This expression agrees with the result (3.34) from the Lindstedt–Poincaré method.

Quantum-mechanical analogy

The treatment of terms that are in phase with the zeroth-order solution as a frequency-shift is similar to the calculation of the first-order energy-shift in quantum-mechanical perturbation theory. Suppose there is no closed-form solution of the Schrödinger equation for the Hamiltonian $\hat{H} = \hat{H}_0 + \epsilon\hat{H}_\mathrm{p}$, where $\hat{H}_\mathrm{p}$ describes the time-independent perturbation, while the eigenvalue problem $\hat{H}_0 |\Psi_0\rangle = \mathcal{E}_0 |\Psi_0\rangle$ for the unperturbed operator $\hat{H}_0$ has an analytic solution. The dimensionless perturbation[32] parameter ϵ has already been introduced in the

[32] We could also consider it an order parameter, which will be set to unity at the end of the calculation. However, we want to stress the similarity with our formalism of classical perturbation theory here.

Hamiltonian $\hat{H}$ to do the bookkeeping of the individual orders in the perturbative expansion of the state[33]

$$|\Psi\rangle = |\Psi_0\rangle + \epsilon\,|\Psi_1\rangle + \epsilon^2\,|\Psi_2\rangle + \dots \tag{3.91}$$

and its corresponding energy

$$\mathcal{E} = \mathcal{E}_0 + \epsilon\mathcal{E}_1 + \epsilon^2\mathcal{E}_2 + \dots \quad . \tag{3.92}$$

Setting $\epsilon = 0$ recovers the unperturbed case. For convenience, quantum-numbers are not shown; the subscripts refer to the order of the expansion. Such an expansion is possible for all the eigenstates. Of course, the wave functions Ψ_i and the coefficients $\mathcal{E}_i$ will differ for different quantum-numbers.

Since the Schrödinger equation has to be solved for eigenvalues and eigenstates, it is only natural to expand both quantities in the perturbation parameter right away. When the original state is affected by a perturbation, so is the corresponding energy. The expansions are not independent, because the energy $\mathcal{E}$ is related to the state by the Hamiltonian $\hat{H}$. Equation (3.92) results by applying $\langle\Psi|\hat{H}$ from the left to Equation (3.91). On the right-hand side, the expansion of $\langle\Psi|$ in the perturbation parameter ϵ is to be used.[34] Despite this relation, the additional expansion (3.92) for the energy $\mathcal{E}$ as an actual observable is convenient.

The situation was not quite so obvious in the classical case of the anharmonic oscillator, and the need for two powers series expansion did not became clear at first sight. Because the frequency-shift was supposed to be contained in the trajectory, Section 3.2.1 featured only the power series (3.19) for the trajectory—the classical equivalent of expanding the quantum-mechanical eigenstate (3.91). This ansatz was soon found to be too restrictive to account for frequency-shifts. The Lindstedt–Poincaré method of Section 3.2.2 added the expansion (3.28) of the fundamental frequency—the equivalent of expanding the energy (3.92) here. Section 3.4.1 simplified the formalism by restricting it to the first-order frequency-shift.

Quantum-mechanical perturbation theory has a similar prescription for the first-order energy-shift. Assuming that the energy $\mathcal{E}_0$ is a nondegenerate eigenvalue[35] of the unperturbed Hamiltonian $\hat{H}_0$, the first-order coefficient $\mathcal{E}_1$ in the series expansion (3.92) of the energy is

$$\mathcal{E}_1 = \left\langle \Psi_0 \left| \hat{H}_\mathrm{p} \right| \Psi_0 \right\rangle \tag{3.93}$$

in the usual bra–ket notation for the inner product. Like the first-order frequency-shift in the classical case, the quantum-mechanical first-order energy-shift $\epsilon\mathcal{E}_1$ is determined entirely by the zeroth-order solution (and the perturbation, of course).[36] Here, these are the eigenstate $|\Psi_0\rangle$

[33] Unlike in the classical case, there are no initial conditions the pure state $|\Psi\rangle$ has to satisfy, provided the ion is not in a superposition of states. However, the interpretation of the absolute value of the wave function squared $|\Psi|^2$ as a probability density demands the normalization $\langle\Psi|\Psi\rangle = 1$, because the total probability of the particle being in this state has to be unity.

[34] The perturbation parameter ϵ has to be a real number. With ϵ complex, the Hamiltonian $\hat{H}$ would not be Hermitian, even if $\hat{H}_0$ and $\hat{H}_\mathrm{p}$ were.

[35] If several unperturbed eigenstates had the same energy, the first-order energy-shift $\mathcal{E}_1$ would have to be calculated for superpositions of these degenerate states.

[36] In second order, the situation is no longer that simple. Calculating $\mathcal{E}_2$ requires the whole orthogonal set of eigenstates and their eigenvalues for the unperturbed Hamiltonian $\hat{H}_0$.

and the Hamiltonian $\hat{H}_\mathrm{p}$. In the classical case, the corresponding quantities are the zeroth-order trajectory and the acceleration by the additional term in the equation of motion. Speaking in orders of perturbation theory, the perturbation $\hat{H}_\mathrm{p}$ may alter the energy of the state $|\Psi\rangle$ even before it affects the wave function of the state as such. In the classical case, the additional acceleration may shift the frequency before it adds new terms to the trajectory. The cautionary "may" in both statements signals that not every perturbation causes a first-order energy-shift or frequency-shift, respectively. However, a first-order change of the state or the trajectory is not optional. If there is none, there is typically no need for perturbation theory.

Here, Equation (3.93) projects the perturbation $\hat{H}_\mathrm{p}$ onto the original state $|\Psi_0\rangle$. What remains from the projection—the component that is not orthogonal to the original state—results in the first-order energy-shift. The orthogonal components first manifest themselves in $|\Psi_1\rangle$, as a correction to the unperturbed state $|\Psi_0\rangle$, which eventually results in higher-order energy-shifts. Similarly, the first-order frequency-shift is determined by the component of the acceleration that is in phase (and in resonance) with the original motion. In that sense, the nonresonant contributions are orthogonal when averaged over one period of the original motion. They add small oscillations to the trajectory without causing a first-order frequency-shift. Although the functional form of the trajectory contains the frequencies of the motion, there is no general recipe like Equation (3.93) to extract the frequency-shift. Instead, the additional acceleration has to be translated into a frequency-shift based on the equation of motion.

3.4.2. Generalization to the radial modes

The implementation of first-order perturbation theory for the first-order frequency-shift to the radial modes is very similar to the formalism from Section 3.4.1 for the axial mode. In fact, it was developed with the radial modes in mind. We tested it on the simpler axial mode first, which is one-dimensional and has only one characteristic frequency, in order to gain some familiarity, before turning to the more complex radial modes here.

As the zeroth-order solution for the particle's coordinates, we will use

$$\tilde{x}(t) = \hat{\rho}_+ \cos(\tilde{\omega}_+ t + \tilde{\varphi}_+) + \hat{\rho}_- \cos(\tilde{\omega}_- t + \tilde{\varphi}_-) \quad , \tag{3.94}$$

$$\tilde{y}(t) = -\hat{\rho}_+ \sin(\tilde{\omega}_+ t + \tilde{\varphi}_+) - \hat{\rho}_- \sin(\tilde{\omega}_- t + \tilde{\varphi}_-) \quad , \tag{3.95}$$

$$\tilde{z}(t) = \hat{z} \cos(\tilde{\omega}_z t + \tilde{\varphi}_z) \quad . \tag{3.96}$$

To first order in the frequency-shift, the amplitudes $\hat{\rho}_\pm$ and $\hat{z}$ of the zeroth-order solutions may be thought of as the amplitudes of the eigenmotions. The zeroth-order solutions, indicated with a tilde, almost look like the solutions (2.30)–(2.32) from the ideal Penning trap, where the frequencies ω_z and $\omega_\pm$ were given by Equations (2.17) and (2.23), respectively. However, the tilde on top of the frequencies indicates that they need to be determined. To this end, resonant terms at the radial frequencies have to be identified. Before we get to the details, we will introduce some more pieces of notation.

The zeroth-order velocity follows from the time-derivative of the coordinate as

$$\dot{\tilde{x}}(t) = -\tilde{\omega}_+\hat{\rho}_+ \sin(\tilde{\omega}_+ t + \tilde{\varphi}_+) - \tilde{\omega}_-\hat{\rho}_- \sin(\tilde{\omega}_- t + \tilde{\varphi}_-) \quad , \tag{3.97}$$

$$\dot{\tilde{y}}(t) = -\tilde{\omega}_+\hat{\rho}_+ \cos(\tilde{\omega}_+ t + \tilde{\varphi}_+) - \tilde{\omega}_-\hat{\rho}_- \cos(\tilde{\omega}_- t + \tilde{\varphi}_-) \quad , \tag{3.98}$$

$$\dot{\tilde{z}}(t) = -\tilde{\omega}_z\hat{z} \sin(\tilde{\omega}_z t + \tilde{\varphi}_z) \quad . \tag{3.99}$$

Because resonant terms occur at both radial frequencies, the abbreviations

$$\tilde{x}_\pm = \langle \tilde{x} \rangle_{\tilde{\omega}_\pm} = \hat{\rho}_\pm \cos(\tilde{\omega}_\pm t + \tilde{\varphi}_\pm) \quad , \tag{3.100}$$

$$\tilde{y}_\pm = \langle \tilde{y} \rangle_{\tilde{\omega}_\pm} = -\hat{\rho}_\pm \sin(\tilde{\omega}_\pm t + \tilde{\varphi}_\pm) \tag{3.101}$$

for the coordinates of the two radial eigenmotions are convenient. The same holds for the associated velocities

$$\dot{\tilde{x}}_\pm = \left\langle \dot{\tilde{x}} \right\rangle_{\tilde{\omega}_\pm} = -\tilde{\omega}_\pm\hat{\rho}_\pm \sin(\tilde{\omega}_\pm t + \tilde{\varphi}_\pm) \quad , \tag{3.102}$$

$$\dot{\tilde{y}}_\pm = \left\langle \dot{\tilde{y}} \right\rangle_{\tilde{\omega}_\pm} = -\tilde{\omega}_\pm\hat{\rho}_\pm \cos(\tilde{\omega}_\pm t + \tilde{\varphi}_\pm) \quad . \tag{3.103}$$

The zeroth-order solutions $\tilde{x}$, $\tilde{y}$ and $\tilde{z}$, as well as the corresponding velocities $\dot{\tilde{x}}$, $\dot{\tilde{y}}$ and $\dot{\tilde{z}}$ are time-dependent—with and without the plus–minus sign in the subscript—although we will often suppress the time-dependence for the sake of space and the visual obstruction by the extra brackets. The amplitudes $\hat{\rho}_\pm$ and $\hat{z}$ are constant.

Since the structure of the argument inside the trigonometric functions is very similar for all three eigenmodes, the short-hand notation

$$\tilde{\chi}_i = \tilde{\omega}_i t + \tilde{\varphi}_i \tag{3.104}$$

similar to Equation (2.33) saves space.

After inserting the zeroth-order coordinates and velocities into the equation of motion beyond the ideal Penning trap, all the terms that are proportional to a component of the zeroth-order solutions are to be collected in the effective radial equations of motion[37]

$$\begin{pmatrix} \ddot{\tilde{x}}_\pm \\ \ddot{\tilde{y}}_\pm \end{pmatrix} = \omega_c(1+\beta_\pm) \begin{pmatrix} \dot{\tilde{y}}_\pm \\ -\dot{\tilde{x}}_\pm \end{pmatrix} + \frac{\omega_z^2(1+\varepsilon_\pm)}{2} \begin{pmatrix} \tilde{x}_\pm \\ \tilde{y}_\pm \end{pmatrix} \quad . \tag{3.105}$$

The change in frequency is expressed by the dimensionless parameters $\beta_\pm$ and $\varepsilon_\pm$. The subscript indicates that they may be different for the two radial modes.[38]

Nonresonant terms are ignored by the effective equation of motion (3.105), because they do not give rise to a first-order frequency-shift. If they were absent, the complete equation of motion would have been solved by the zeroth-order ansatz, and the radial frequencies $\tilde{\omega}_\pm$

[37] The parameter $\varepsilon_\pm$ was originally called $\gamma_\pm$ for cylindrically-symmetric imperfections [82, 84]. It was renamed, when the relativistic Lorentz factor γ came into play. A similar parameter in Equation (3.85) was also renamed. Since the parameter $\beta_\pm$ stayed, we will not use $\beta = v/c$ for the velocity v normalized to the speed of light c.

[38] Even though it also parametrizes frequency-shifts caused by higher orders in the magnetic field, the parameter $\beta_\pm$ is not to be confused with the β_η used in some publication as the dimensionless equivalent of the B_η, which characterize components of the magnetic field.

would be calculated exactly by making the replacements $\omega_\mathrm{c} \to \omega_\mathrm{c}(1+\beta_\pm)$ and $\omega_z^2 \to \omega_z^2(1+\varepsilon_\pm)$ in Equation (2.23). Note that the parameter $\beta_\pm$ describes a relative change of the effective free-space cyclotron-frequency, whereas the parameter $\varepsilon_\pm$ describes a change of the effective axial frequency squared. Typically, neither $\omega_\mathrm{c}(1+\beta_\pm)$ nor $\omega_z\sqrt{1+\varepsilon_\pm}$ represent actual motional frequencies in the problem. According to Equation (3.85), the actual axial frequency is given by $\omega_z\sqrt{1+\varepsilon_z}$.

To warrant a perturbative treatment, we expect the anharmonic frequency-shifts to be small. For $|\beta_\pm| \ll 1$ and $|\varepsilon_\pm| \ll 1$, a Taylor expansion of Equation (2.23) about the unperturbed frequencies ω_c and ω_z^2 yields the first-order frequency-shift.[39] Before taking the corresponding derivatives of Equation (2.23), we use this equation to establish the link

$$\omega_+ - \omega_- = \frac{\omega_\mathrm{c}}{|\omega_\mathrm{c}|}\sqrt{\omega_\mathrm{c}^2 - 2\omega_z^2} \tag{3.106}$$

between the difference of the radial frequencies and the term with the square root. The prefactor $\omega_\mathrm{c}/|\omega_\mathrm{c}|$, which gives the sign of the free-space cyclotron-frequency ω_c, is of no concern for the derivatives, because it is constant where the radial frequencies are real, that is, for $|\omega_\mathrm{c}| \geq \sqrt{2}\omega_z$. At $\omega_\mathrm{c} = 0$, where the prefactor is discontinuous, the storage of a particle is not possible, and this point is of no practical interest.

The derivative of the radial frequencies $\omega_\pm$ from Equation (2.23) with respect to the free-space cyclotron-frequency ω_c is

$$\frac{\partial\omega_\pm}{\partial\omega_\mathrm{c}} = \frac{1}{2}\left(1 \pm \frac{\omega_\mathrm{c}}{|\omega_\mathrm{c}|}\frac{\omega_\mathrm{c}}{\sqrt{\omega_\mathrm{c}^2 - 2\omega_z^2}}\right) = \frac{1}{2}\frac{\omega_+ - \omega_- \pm (\omega_+ + \omega_-)}{\omega_+ - \omega_-} = \frac{\pm\omega_\pm}{\omega_+ - \omega_-} \quad . \tag{3.107}$$

The second step uses the sideband identity (2.25) and the property $\omega_\mathrm{c}/|\omega_\mathrm{c}| = |\omega_\mathrm{c}|/\omega_\mathrm{c}$ for the prefactor of the square root in Equation (3.106). Similarly, the derivative of the radial frequencies $\omega_\pm$ with respect to the axial frequency squared ω_z^2 becomes

$$\frac{\partial\omega_\pm}{\partial\omega_z^2} = \pm\frac{1}{2}\frac{\omega_\mathrm{c}}{|\omega_\mathrm{c}|}\frac{-1}{\sqrt{\omega_\mathrm{c}^2 - 2\omega_z^2}} = \frac{\mp 1}{2(\omega_+ - \omega_-)} \quad . \tag{3.108}$$

Figure 3.1 shows the dependence of the radial frequencies on ω_c and ω_z^2, and it visualizes some properties of the derivatives.

Finally, the first-order frequency-shift associated with the parameters $\beta_\pm$ and $\varepsilon_\pm$ is given by

$$\tilde{\omega}_\pm = \omega_\pm + \frac{\partial\omega_\pm}{\partial\omega_\mathrm{c}}\omega_\mathrm{c}\beta_\pm + \frac{\partial\omega_\pm}{\partial\omega_z^2}\omega_z^2\varepsilon_\pm + \ldots \tag{3.109a}$$

$$= \omega_\pm \underbrace{\pm\frac{\omega_\pm\omega_\mathrm{c}}{\omega_+ - \omega_-}\beta_\pm \mp \frac{\omega_+\omega_-}{\omega_+ - \omega_-}\varepsilon_\pm}_{\Delta\omega_\pm} + \ldots \quad . \tag{3.109b}$$

In the last step, the axial frequency squared is written as a product of the radial frequencies according to Equation (2.26), in order to express shifts to the radial frequencies as a function

[39] Since the radial frequencies $\omega_\pm$ are a function of ω_z^2, and the parameter $\varepsilon_\pm$ in the effective equations of motion (3.105) describes a change of the effective ω_z^2, it is easier to work with the axial frequency squared here.

of these frequencies. The singularity for $\omega_+ = \omega_-$ reminds us that we have to be careful at the limit of stability.

As usual, the upper symbol has to be used for the shift $\Delta\omega_+$ to the reduced cyclotron-frequency ω_+ (indicated with a plus in the index), whereas the lower symbol has to used for the shift $\Delta\omega_-$ to the magnetron frequency ω_- (indicated with a minus in the index). However, one of the two expression suffices. The other one is then generated with the substitution $\pm \to \mp$ in the indices alone, while the denominator takes the role of swapping the plus–minus signs in front of the fractions. We will use this technical symmetry later on for checking basic properties of the frequency-shifts.

Although it may look like in the effective equations of motion (3.105) that the parameter $\beta_\pm$ is associated with frequency-shifts caused by the magnetic field, while the parameter $\varepsilon_\pm$ contains frequency-shifts caused by the electrostatic potential, the parameters are interchangeable. There are no strictly $\beta_\pm$-like or $\varepsilon_\pm$-like shifts. Since the zeroth-order coordinates and velocities may be interchanged as $\dot{\tilde{x}}_\pm = \tilde{\omega}_\pm \tilde{y}_\pm$ and $\dot{\tilde{y}}_\pm = -\tilde{\omega}_\pm \tilde{x}_\pm$ according to Equations (3.100)–(3.103), a term associated with $\beta_\pm$ in the effective equations of motion (3.105) is rewritten as

$$\omega_\mathrm{c}\beta_\pm \begin{pmatrix} \dot{\tilde{y}}_\pm \\ -\dot{\tilde{x}}_\pm \end{pmatrix} = -\omega_\mathrm{c}\beta_\pm\tilde{\omega}_\pm \begin{pmatrix} \tilde{x}_\pm \\ \tilde{y}_\pm \end{pmatrix} \tag{3.110}$$

to take the form of a term associated with the parameter $\varepsilon_\pm$, given by

$$\varepsilon_\pm = -\frac{2\omega_\mathrm{c}\tilde{\omega}_\pm}{\omega_z^2}\beta_\pm = -\frac{\omega_\mathrm{c}\tilde{\omega}_\pm}{\omega_+\omega_-}\beta_\pm \quad . \tag{3.111}$$

We have used Equation (2.26) to remove the axial frequency, which is present in the effective equations of motion (3.105), but absent in Equation (3.109b) for the frequency-shift. To first order in this frequency-shift, the difference between $\tilde{\omega}_\pm$ and $\omega_\pm$ in the prefactor is safely ignored, because the frequency-shift (3.109b) is already of first-order due to the presence of $\beta_\pm$ and $\varepsilon_\pm$. Consequently, the replacement $\tilde{\omega}_\pm \to \omega_\pm$ is fine in the condition (3.111), and two parameters $\beta_\pm$ and $\varepsilon_\pm$ with this relation give the same first-order frequency shift. For the actual calculation, it is thus a matter of taste whether the resonant terms are written as proportional to velocities and absorbed in $\beta_\pm$, or written as proportional to coordinates and absorbed in $\varepsilon_\pm$. Typically, the origin of an additional term and its prefactors will favor one alternative.

3.4.3. Spurious motional resonances

The major part of calculating first-order frequency-shifts is to insert the zeroth-order solutions from the ideal Penning trap (with the perturbed eigenfrequencies left to be determined) into the additional contributions beyond the ideal configuration. The resulting powers of oscillatory terms are decomposed such that the frequency of the individual terms is readily analyzed. So far, we have classified them as nonresonant and resonant terms. The former are ignored in the effective equations of motion (3.85) and (3.105), because they do not give rise to a first-order frequency-shift, whereas the resonant terms do. In order to incorporate these as a first-order frequency-shift in the effective equations of motion, the resonant terms have to be proportional to some component of the zeroth-order trajectory or velocity. For the one-dimensional anharmonic

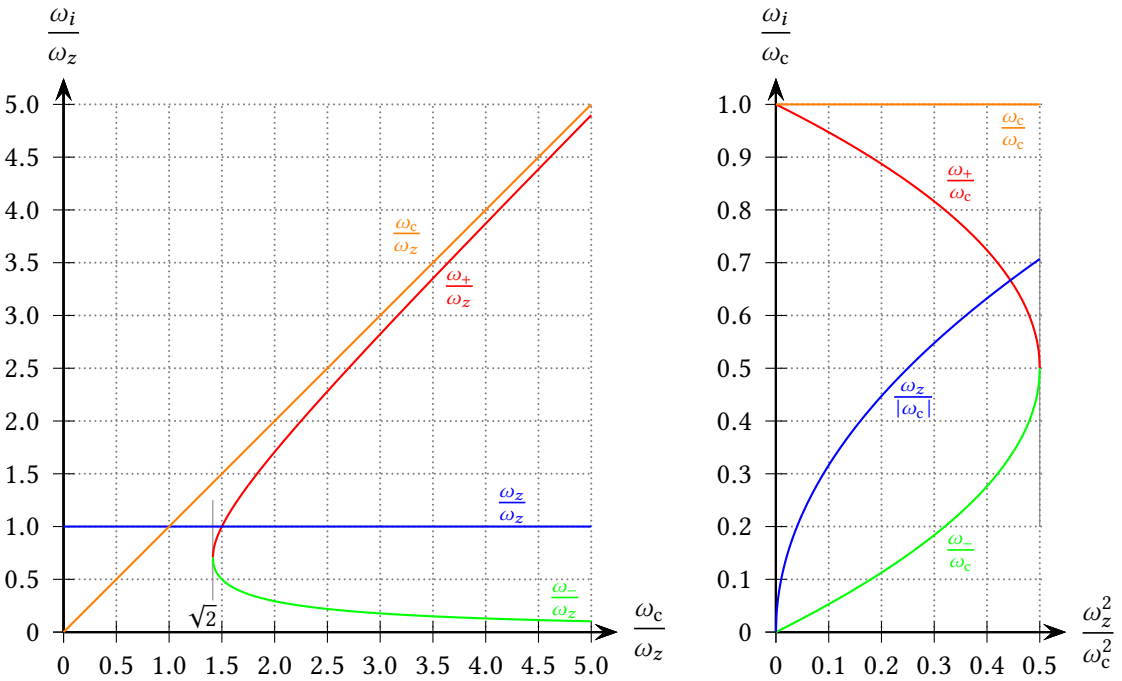

Figure 3.1.: Dependence of the radial frequencies $\omega_\pm$ from Equation (2.23) on the free-space cyclotron-frequency ω_c (left) and the axial frequency squared ω_z^2 (right). For space, negative radial frequencies (as a consequence of $\omega_c < 0$) are not shown. The left graph (apart from ω_z/ω_z) would be obtained by point reflection at the origin, see Figure 2.3. The right graph would not change because of its normalization, which cancels the overall sign. The frequencies are normalized to ω_z (left) and ω_c (right). In both cases, there is a vertical derivative at the limit of stability—the singularity in Equations (3.107) and (3.108) for $\omega_+ = \omega_-$. The reduced cyclotron-frequency grows more strongly with ω_c than the free-space cyclotron-frequency itself, and hence the corresponding derivative (3.107) is larger than unity. The dependence of the radial frequencies $\omega_\pm$ on ω_z^2 is equal in magnitude but opposite in sign. Consequently, the derivatives (3.108) sum to zero, as expected from the sideband identity (2.25), because, as its name suggest, the free-space cyclotron-frequency does not depend on the electrostatic potential.

oscillator considered in Section 3.2, this was always the case—almost miraculously, to the extent that it may seem natural for resonant terms come with the right phase no matter what. We shall see that the preservation of the original phase is related to the conservation of energy.

For the one-dimensional anharmonic oscillator, conservation of energy implies that the amplitude of the motion remains constant. In the PENNING trap, the exchange of energy between the three eigenmodes is conceivable, while the total energy is still conserved in the absence of damping. Additionally, the electrostatic quadrupole potential (2.2)—the dominant electrostatic potential even in the non-ideal PENNING trap—falls off quadratically in the radial direction, which results in a negative potential energy of the radial modes. As the total energy (2.49) of the modified cyclotron mode is dominated by the kinetic energy, no energy is released when the radius of this mode increases, and the reduced potential energy even further below the saddle point remains inaccessible. For the magnetron mode, however, the negative potential energy outweighs the kinetic energy, and the particle would happily roll down the hill in the radial direction, if the excess energy could be transferred into a different mode.

Since the three modes and the shape of the quadrupole potential in the PENNING trap allow for time-dependent phenomena beyond the oscillations with constant amplitudes at the eigenfrequencies, we will investigate how higher-order terms may couple different eigenmodes. This kind of coupling goes beyond the anharmonic effect that the frequency of one mode depends on the amplitudes of other modes. In that sense, the frequencies rather than the modes as a whole are coupled. The coupling meant here influences the amplitudes. Its discussion in this section is not mathematically rigorous, because we will not be able to offer a treatment of motionally-induced coupling via higher-order terms and the associated anharmonic frequency-shifts. We will have to stick with the standard mode of operation with constant amplitudes, in which the excitation or coupling of eigenmodes is accomplished by time-dependent fields. In this mode, frequency-shifts are calculated for constant amplitudes—before and after, but not during excitation or coupling.[40] Nevertheless, we need to understand when higher-order terms possibly result in more than just static frequency-shifts, in order to rule out these conditions. Typically, choosing a particular working point of the PENNING trap to realize the stable normal mode of operation is not problematic.

Suppose a term like $\cos(\tilde{\omega}t)$ in the zeroth-order solution had incurred a phase-shift φ along its way through the equation of motion, whereas the frequency has not changed. The resulting term $\cos(\tilde{\omega}t + \varphi)$ is not proportional to the zeroth-order solution $\cos(\tilde{\omega}t)$ (unless for $\varphi = 0$ or $\varphi = \pi$), and the method from Sections 3.4 and 3.4.2 fails to absorb the resonant term as a first-order frequency-shift. With the trigonometric identity

$$\cos(\tilde{\omega}t + \varphi) = \cos(\tilde{\omega}t)\cos(\varphi) - \sin(\tilde{\omega}t)\sin(\varphi) \quad , \tag{3.112}$$

at least part of $\cos(\tilde{\omega}t + \varphi)$, namely the first term on the right-hand side, has the correct form to be dealt with in the usual way as a frequency-shift. However, the second term on the right-hand side is still unaccounted for, and we need to understand what its consequences are. To this end,

[40] Damping is typically so slow that the time-dependence of the anharmonic frequency-shift directly reflects the time-dependence of the amplitudes (raised to the appropriate power).

we consider the work[41]

$$\mathrm{d}W = -F\,\mathrm{d}z = -F\dot{z}\,\mathrm{d}t \tag{3.113}$$

performed by a force F in the z-direction when moving along the way $\mathrm{d}z$.

Basically, the additional terms in the equation of motion describe accelerations or forces. Thus, the second-term on the right-hand side of Equation (3.112) corresponds to a force $F \propto \sin(\tilde{\omega}t)$, when the zeroth-order trajectory put into the problem was $\tilde{z} \propto \cos(\tilde{\omega}t)$. As we are mainly interested in the time-dependence, we will drop the prefactors and the signs, when it comes to proportionality. With the zeroth-order velocity $\dot{\tilde{z}} \propto \sin(\tilde{\omega}t)$, the work becomes $\mathrm{d}W \propto [\sin(\tilde{\omega}t)]^2\mathrm{d}t$. Clearly, the work performed by this additional force does not vanish when integrated over one cycle of the main oscillation, and hence the energy of the particle changes. Consequently, the amplitude of the zeroth-order trajectory becomes a dynamical quantity.[42] For the force $F \propto \cos(\tilde{\omega}t)$, which was incorporated as a frequency-shift, the work $\mathrm{d}W \propto \cos(\tilde{\omega}t)\sin(\tilde{\omega}t)\mathrm{d}t = 1/2\sin(2\tilde{\omega}t)\mathrm{d}t$ averages to zero over one cycle (even a half-cycle)—in the same way as it does for the harmonic oscillator with its restoring force being proportional to the displacement. As we have seen in Section 3.2.1, the secular term in Equation (3.27) with its unbounded increase of the amplitude was an artifact of too simplistic a series solution. The resonant terms that are in phase with the original motion shift the frequency rather than blowing up amplitudes. The last statement is not to imply that a term that changes the amplitude has no influence on the frequency. When the frequency depends on the amplitude, the influence is obvious. However, even for the harmonic oscillator (setting $\epsilon = 0$ in Equation (3.17), for instance), adding a damping term $2\gamma\dot{z}$ on the left-hand side, shifts the frequency $\omega_z \to (\omega_z^2 - \gamma^2)^{1/2}$, in addition to the exponential decay $\mathrm{e}^{-\gamma t}$ of the amplitude.

A force proportional to the velocity is the prototypical example of a phase-changing term. Since the work $\mathrm{d}W$ then depends quadratically on the velocity, the energy of the system always changes in the same direction. However, damping will not be considered here. Resonant terms with a phase different from the components of the zeroth-order solution would have to result from mixing terms at the different eigenfrequencies, see Section C.2 in the appendix. The resulting terms would then have to be resonant at the eigenfrequency of the eigenmode whose equation of motion is considered. Of course, we could calculate the whole frequency spectrum for the specific imperfections rather than just searching for naturally-resonant terms, in order to prohibit artificial resonance conditions.[43] Unfortunately, we would not see the full spectrum of spurious resonance conditions because of our self-imposed restriction to first-order terms. Higher orders in perturbation theory add to the frequency spectrum and offer new possibilities for mixing. Thus, no general rule for avoiding spurious coupling between the modes is to be expected from our implementation of first-order perturbation theory.

[41] The sign is chosen such that $\mathrm{d}W$ describes the change in potential energy, if the force originates from a potential. For nonconservative or external forces, the other sign should be chosen, in order to describe the change of energy in the system. Fortunately, the global sign is of no relevance for the argument here, which is all about zero or nonzero net work performed by a force.

[42] We have assumed this change to be so slow over one cycle that this additional time-dependence does not have to be considered for the integration of $\mathrm{d}W$. The reasoning is hand-waving at best anyhow.

[43] The report [82] does so for cylindrically-symmetric magnetic and electrostatic imperfections, hoping to identify all the conditions for spurious resonances. It was only afterwards that I realized how the sentence should go on.

A Fourier expansion of the electrostatic potential predicts instabilities when the commensurability condition

$$j_+\tilde{\omega}_+ + j_-\tilde{\omega}_- + j_z\tilde{\omega}_z = 0 \quad \text{, where} \quad |j_+| + |j_-| + |j_z| \leq \eta \quad , \tag{3.114}$$

is fulfilled [89]. The j_i are integers—positive, negative or zero—and the parameter η is the same as in the electrostatic potential Φ_η from Equation (2.73). Instabilities [142, 195] in Penning traps have been observed on trapped ions [75] and electrons [115] as a rapid loss of particles. Even if a spurious resonance condition is fulfilled, it is hard to judge from the equations whether the particle will be lost altogether or whether there will be periodic beating between several modes. In the anharmonic Penning trap, a change of the amplitudes also results in a frequency-shift, which means that the resonance condition may no longer be satisfied. However, with no damping present, even near-resonant excitation is likely to have a major impact, too. From the experimental point of view, we may take the stance: motional instability—hard to predict, but you know it when you see it. For meaningful ion work with the trap living up to its name by serving as a storage device, an operating point far away from the instabilities has to be chosen anyway. Pathological cases would have to be dealt with separately.

Our quest for first-order frequency-shift will thus focus on naturally-resonant terms. With naturally resonant we mean that no assumptions about the frequencies are necessary for the term to have the frequency of an eigenmode. These are also the terms that have the right phase to be written as proportional to a component of the zeroth-order solution.

3.4.4. Conflicting-sign would-be resonant terms in two dimensions

This section deals with an additional effect of the two-dimensional radial modes: terms that do not quite fit into the pattern for a first-order frequency-shift, even though they oscillate naturally at the frequency of an eigenmode. Such a term may fit into the first component and the second component of the effective equations of motion (3.105) individually, but globally it may not be described by the same parameter $\beta_\pm$ or $\varepsilon_\pm$. Such a term is related to a break of the cylindrical symmetry and does not give rise to a first-order frequency-shift. It is tempting to dismiss the effect as of higher order, and thus small. However, certain imperfections produce a harmonic frequency-shift, which will not disappear in the limit of vanishing motional amplitudes, of course. A misalignment of the electrostatic potential with respect to the magnetic field is one example [14, 15]. Since harmonic shifts are hard to determine experimentally, unless they depend on an easily adjustable parameter, a theoretical model is particularly valuable. We will discuss the less cumbersome example of an elliptic electrostatic potential in the following.[44]

Suppose the potential[45]

$$\Phi_{2,\epsilon} = \epsilon\frac{C_2V_0}{2d^2}\left(x^2 - y^2\right) = \epsilon\frac{m}{q}\frac{\omega_z^2}{2}\left(x^2 - y^2\right) \tag{3.115}$$

[44] The difficulty of treating misalignment for arbitrary angles is also evidenced by the need for a recursive solution in order to obtain the perturbed frequencies from implicit relations [99]. For the problem we will discuss perturbatively here, an exact algebraic solution exists [92].

[45] In case you are enamored with spherical coordinates and associated Legendre polynomials P_η^m, the spatial dependence is $x^2 - y^2 = \frac{1}{3}r^2P_2^2(\cos(\theta))\cos(2\phi)$, see Chapter A in the appendix. Clearly, cylindrical symmetry is violated here.

is added to the electrostatic quadrupole potential (2.2) of the ideal trap. Most of the prefactors carry over from there; the axial frequency ω_z is from Equation (2.17). As a new feature, the strength of the additional term $\Phi_{2,\epsilon}$ is given by the dimensionless ellipticity parameter ϵ ("ellipticity"). The ellipticity is not associated with a particular ellipse.

For $0 < |\epsilon| < 1$ and a given z, the equipotential lines of the overall potential, $\Phi_2 + \Phi_{2,\epsilon}$, are ellipses in the radial plane, rather than circles.[46] For $|\epsilon| > 1$, the equipotential lines are hyperbolas, which leads to a hyperbolic magnetron orbit and precludes[47] trapping [92].

Including the acceleration by the additional electric field

$$\vec{E}_{2,\epsilon} = -\vec{\nabla}\Phi_{2,\epsilon} = \epsilon\frac{\omega_z^2}{2}\begin{pmatrix}-x\\ y\\ 0\end{pmatrix} \quad , \tag{3.116}$$

the radial equations of motion (2.16) of the ideal Penning trap become

$$\begin{pmatrix}\ddot{x}\\ \ddot{y}\end{pmatrix} = \omega_c\begin{pmatrix}\dot{y}\\ -\dot{x}\end{pmatrix} + \frac{\omega_z^2}{2}\begin{pmatrix}x\\ y\end{pmatrix} + \epsilon\frac{\omega_z^2}{2}\begin{pmatrix}-x\\ y\end{pmatrix} \tag{3.117}$$

for the ideal elliptical Penning-trap. The axial mode is not affected because the electric field $\vec{E}_{2,\epsilon}$ has a zero z-component.

We will attempt a perturbative solution for $|\epsilon| \ll 1$ here. Working with the zeroth-order solutions $\tilde{x}$ and $\tilde{y}$ from Equations (3.94) and (3.95), respectively, would lead to the conflicting choice $\varepsilon_\pm = -\epsilon$ for the first component and $\varepsilon_\pm = \epsilon$ for the second component in the effective equations of motion (3.105). The additional term, which violates cylindrical symmetry, does not give rise to a first-order force that is resonant with the original radial modes. For the first nonvanishing term in the frequency-shift we will have to go to second order with the ansatz

$$x_\pm(t) = \hat{\rho}_\pm\left(1 + k_{1,\pm}\epsilon + k_{2,\pm}\epsilon^2 + \dots\right)\cos[(\omega_\pm + \omega_{2,\pm}\epsilon^2 + \dots)t + \varphi_\pm] \tag{3.118}$$

$$y_\pm(t) = -\hat{\rho}_\pm\left(1 - k_{1,\pm}\epsilon + k_{2,\pm}\epsilon^2 + \dots\right)\sin[(\omega_\pm + \omega_{2,\pm}\epsilon^2 + \dots)t + \varphi_\pm] \quad . \tag{3.119}$$

The dots indicate that terms higher than second-order are not shown explicitly. The coefficients $k_{1,\pm}$ and $k_{2,\pm}$ for the relative change of the amplitude and $\omega_{2,\pm}$ for the frequency-shift[48] need to be determined by satisfying the equations of motion (3.117) order by order. The ansatz is not the most general one; it capitalizes on the general structure of the problem for some simplifications:

1. The problem is still linear. Therefore, mixing between the two eigenmodes will not occur, and they may be treated separately. However, we have made provisions—indicated by the ±-sign in the index of the coefficients—for different changes to the amplitudes and frequencies of the two radial modes.

[46] The equipotential lines of the additional potential $\Phi_{2,\epsilon}$ alone are hyperbolas. That is why we refrain from calling it an elliptic potential, even though it carries the ellipticity parameter ϵ.

[47] See Reference [126]—never mind the misplaced factor of ½ in Equation (1)—for the motion in the limit of $|\epsilon| \gg 1$, that is, in the potential $\Phi_{2,\epsilon}$ without the quadrupole component Φ_2.

[48] Since we are expanding the frequency rather than its square as in Equation (3.28), the frequency-shift parameter is called $\omega_{2,\pm}$ rather than $\omega_{2,\pm}^2$ accordingly.

2. For $\epsilon > 0$, there is an additional restoring force in the x-direction and an additional repulsive force in the y-direction. When ϵ changes sign, the roles of x and y reverse, but the magnitude of the effect remains the same. Consequently, the frequency should not depend on the sign of ϵ, and a term $\omega_{1,\pm}\epsilon$ is absent from the expansion of the frequency inside the trigonometric functions.

3. When the roles of x and y reverse upon flipping the sign of ϵ, the amplitudes should exchange their roles, too. That is why the coefficient $k_{1,\pm}$, which is multiplied with the sign-sensitive ϵ, comes with different signs in Equations (3.118) and (3.119), while the coefficient $k_{2,\pm}$, which is multiplied with the sign-invariant ϵ^2, comes with the same sign.

Having justified the ansatz from Equations (3.118) and (3.119), we plug it into the equations of motion (3.117). Defining $\sigma = +1$ for the first component and $\sigma = -1$ for the second one, the constraints from both components are shown in one equation:

$$\begin{aligned} -\sigma\left(\omega_\pm + \omega_{2,\pm}\epsilon^2 + \dots\right)^2 \left(1 + \sigma k_{1,\pm}\epsilon + k_{2,\pm}\epsilon^2 + \dots\right) \\ = -\sigma\omega_\mathrm{c}\left(\omega_\pm + \omega_{2,\pm}\epsilon^2 + \dots\right)\left(1 - \sigma k_{1,\pm}\epsilon + k_{2,\pm}\epsilon^2 + \dots\right) \\ + \sigma\frac{\omega_z^2}{2}\left(1 + \sigma k_{1,\pm}\epsilon + k_{2,\pm}\epsilon^2 + \dots\right)(1 - \sigma\epsilon) \quad , \end{aligned} \tag{3.120}$$

where we have already removed the common factors of $\hat{\rho}_\pm$ and the trigonometric functions. The power series expansion of the frequency is present because of the time-derivatives in the velocity and the acceleration. After expanding the square of the series as

$$\left(\omega_\pm + \omega_{2,\pm}\epsilon^2 + \dots\right)^2 \approx \omega_\pm^2 + 2\omega_\pm\omega_{2,\pm}\epsilon^2 + \dots \quad , \tag{3.121}$$

correct to second order, we are ready to look at the orders individually.

Zeroth-order essentially yields the characteristic equation (2.22) of the radial frequencies in the ideal trap and is satisfied by design.[49] Regardless of σ, the terms of first-order in the ellipticity parameter ϵ impose the condition

$$-k_{1,\pm}\omega_\pm^2 = k_{1,\pm}\omega_\mathrm{c}\omega_\pm + k_{1,\pm}\frac{\omega_z^2}{2} - \frac{\omega_z^2}{2} \tag{3.122}$$

on the coefficient $k_{1,\pm}$. This condition simplifies to

$$\frac{\omega_z^2}{2} = k_{1,\pm}\left(\omega_\pm^2 + \omega_\mathrm{c}\omega_\pm + \frac{\omega_z^2}{2}\right) = k_{1,\pm}\Bigg(\underbrace{\omega_\pm^2 - \omega_\mathrm{c}\omega_\pm + \frac{\omega_z^2}{2}}_{0} + 2\omega_\mathrm{c}\omega_\pm\Bigg) = 2k_{1,\pm}\omega_\mathrm{c}\omega_\pm \tag{3.123}$$

with the definition (2.22) of the radial frequencies. Via Equation (2.26) for the axial frequency squared, the coefficient becomes

$$k_{1,\pm} = \frac{\omega_z^2}{4\omega_\mathrm{c}\omega_\pm} = \frac{\omega_\mp}{2\omega_\mathrm{c}} \quad . \tag{3.124}$$

[49] That is good news. If the zeroth-order problem were not easy to solve, there would be no point in choosing this particular form of the perturbative expansion. Fortunately, we have not been challenged concerning the choice—or even introduction—of a small perturbation parameter, which has always suggested itself quite naturally.

Expanding the exact solutions (59)–(63) of Reference [92], which are too bulky to reprint here, about $\epsilon = 0$ yields the same first-order correction.[50]

The shape of the magnetron mode is affected more strongly than the shape of the modified cyclotron-motion. Given that the former motion is similar to an $\vec{E} \times \vec{B}$ drift, whereas the latter motion is dominated by the magnetic field, it comes as no surprise that the influence of the electrostatic field is more pronounced in the magnetron mode. This tendency also impairs motional averaging of imperfections by the magnetron motion [160]. As discussed in Section 2.2, averaging imperfections along a circular path leads to effective cylindrical symmetry, which justified the corresponding parametrization. Violating cylindrical symmetry for an imperfection of the lowest order already, the slow magnetron mode is the gateway for the effects of other imperfections.

As usual with Penning traps, we are more interested in the frequency-shift than in the actual shape of the trajectory, and we will have to go to second order to extract the relevant coefficient $\omega_{2,\pm}$. It is related to the other coefficients by

$$-\sigma\left(2\omega_\pm\omega_{2,\pm} + \omega_\pm^2 k_{2,\pm}\right) = -\sigma\left(\omega_\mathrm{c}\omega_\pm k_{2,\pm} + \omega_\mathrm{c}\omega_{2,\pm} - \frac{\omega_z^2}{2}k_{2,\pm} + \frac{\omega_z^2}{2}k_{1,\pm}\right) \quad . \tag{3.125}$$

Like in first-order, there is only one condition, regardless of σ, which sounds like bad news, because the coefficient $k_{2,\pm}$ is unknown, too. Before questioning and overhauling the ansatz, a recurrent theme in this thesis saves us: the second-order frequency-shift does not depend on the second-order change to the trajectory. The statement also holds for first order, of course. In its incarnation here, this fundamental principle has it that the prefactors of the coefficient $k_{2,\pm}$ fulfill the characteristic equation (2.22) of the radial frequencies. With $k_{2,\pm}$ gone,[51] the condition (3.125) for the second-order frequency-shift parameter $\omega_{2,\pm}$ reads

$$\omega_{2,\pm}\left(2\omega_\pm - \omega_\mathrm{c}\right) = \pm\omega_{2,\pm}\left(\omega_+ - \omega_-\right) = \frac{\omega_z^2}{2}k_{1,\pm} \quad . \tag{3.126}$$

With the first-order coefficient $k_{1,\pm}$ from Equation (3.124), the result becomes

$$\omega_{2,\pm} = \pm\frac{\omega_z^2}{2(\omega_+ - \omega_-)}\frac{\omega_-}{2\omega_\mathrm{c}} = \pm\frac{\omega_+\omega_-\omega_\mp}{2(\omega_+ - \omega_-)(\omega_+ + \omega_-)} = \pm\frac{\omega_\pm}{2}\frac{\omega_\mp^2}{\omega_+^2 - \omega_-^2} \quad , \tag{3.127}$$

while using Equations (2.25) and (2.26) along the way.

Finally, the second-order frequency-shift due to the additional potential (3.115) is given by

$$\Delta\omega_\pm = \omega_{2,\pm}\epsilon^2 = \pm\frac{\omega_\pm}{2}\frac{\omega_\mp^2}{\omega_+^2 - \omega_-^2}\epsilon^2 \quad . \tag{3.128}$$

[50] With respect to the quadrupole potential (2.2) of the ideal Penning trap, we have defined the additional potential (3.115) with the same sign as in Reference [92]. In References [12, 19, 50] for instance, $\Phi_{2,\epsilon}$ comes with a global minus, probably to match the negative sign of $x^2 + y^2$ in the quadrupole potential Φ_2. The results should be identical after flipping the sign of ϵ, but one has to pay attention to the convention.

[51] Not being able to determine the coefficient here does not imply $k_{2,\pm} = 0$. Expanding the exact solutions (59)–(63) of Reference [92] shows that such a term should be present. Of course, only the calculation of more terms would show whether the perturbative expansion here converges to the exact solution, even as $|\epsilon| \to 1$.

The magnitude of the modified cyclotron-frequency increases; the absolute value of the magnetron frequency decreases. Like for the trajectory, the magnetron mode is also affected more strongly concerning its frequency, both in the relative and the absolute sense. The explanation carries over.

The result (3.128) agrees with the perturbative treatment in Reference [72], which leaves the actual method unspecified. In the limit of $|\omega_-| \ll |\omega_+|$, which Reference [19] also used when calculating the shifts via the characteristic equation for the three frequencies in a Penning trap perturbed by misalignment and ellipticity, there is agreement, too. The exact expression —Equations (25) and (26) of Reference [92] (with angular frequencies defined to be positive)— rewritten here as[52]

$$\omega_\pm(\epsilon) = \sqrt{\frac{1}{2}\left(\omega_+^2 + \omega_-^2\right) \pm \frac{1}{2}\sqrt{\left(\omega_+^2 - \omega_-^2\right)^2 + 4\epsilon^2\omega_+\omega_-}} \quad , \tag{3.129}$$

using Equations (2.25)–(2.27), produces the same second-order[53] term (in ϵ) when expanded about $\epsilon = 0$.

When determining the free-space cyclotron-frequency via the sideband-cyclotron identity (2.25) from a measurement of both radial frequencies, the calculated frequency is shifted from the true value ω_c by

$$\Delta\omega_c = \Delta\omega_+ + \Delta\omega_- = -\frac{\omega_+\omega_-}{\omega_c}\frac{\epsilon^2}{2} \approx -\omega_-\frac{\epsilon^2}{2} \quad . \tag{3.130}$$

The last step is valid for $\omega_+ \approx \omega_c$, or equivalently $|\omega_-| \ll |\omega_+|$, which is the case in typical experiments. In this limit, the result of Reference [50] is reproduced. In any case, the shift due to an elliptic potential does not vanish in the sideband-cyclotron identity (2.25).

Through the invariance theorem (2.27), the second-order shift vanishes:

$$(\omega_+ + \Delta\omega_+)^2 - \omega_+^2 + (\omega_- + \Delta\omega_-)^2 - \omega_-^2 \approx 2\omega_+\Delta\omega_+ + 2\omega_-\Delta\omega_- + \ldots = 0 + \ldots \quad . \tag{3.131}$$

The dots indicate the absence of terms higher than second order. This cancellation is more general and should occur in all orders because the invariance theorem holds[54] for all values of ϵ for which trapping is possible [19, 92].

Given these general results, the use of perturbation theory in this context—other than for a pedagogical benchmark—may be second-guessed, asking whether it is not second best. However, the nonperturbative inclusion of ellipticity via the exact result [92] necessitates more complicated zeroth-order solutions of the Penning trap as the starting point for the perturbative treatment of other imperfections. Therefore, we wanted to check whether ellipticity lends itself to a

[52] These radial frequencies are also obtained by solving the characteristic equation (13) of Reference [46] in the absence of damping. Comparing their radial equations of motion (4)–(5) with our Equation (3.117) shows that our ellipticity parameter ϵ fits their notation with the replacements $2w_x^2 \to \omega_z^2(1-\epsilon)$ and $2w_y^2 \to \omega_z^2(1+\epsilon)$.

[53] As we argued when justifying our ansatz, the frequency does not depend on the sign of ϵ. Concerning the frequency, but not the trajectory, an expansion in ϵ^2, with ϵ^2 counting as the first order, is practicable.

[54] For ellipticity alone, this is obvious from the exact expression (3.129) for the radial frequencies in an elliptical trap. Summed in quadrature, the remaining square roots cancel because of their different signs—their argument being the same. The unperturbed radial frequencies squared remain.

perturbative treatment—for $|\epsilon| \ll 1$, of course. It does, and, more importantly, it does so in conjunction with the imperfections which this thesis considers in detail. To zeroth order in the amplitude, the ansatz of Equations (3.118) and (3.119) is still identical to Equations (3.94) and (3.95), which were inspired by solution in the ideal PENNING trap.

With the new ansatz, cross-terms of ϵ with the perturbation parameter of other imperfections will arise, while the pure terms remain. These cross-terms are of higher order, and, for most of the imperfections considered in this thesis, they will depend on the particle's amplitudes. Like for other anharmonic frequency-shifts, their effect—if not small enough already—is removed by extrapolating the measured frequencies to zero motional amplitudes, while the harmonic shift by the ellipticity remains. If the ellipticity were large, the trap would most likely exhibit higher-order imperfections beyond cylindrical symmetry, which would require a dedicated treatment[55] anyway [92, 123]. Therefore, we will proceed with the original ansatz, retaining only the harmonic frequency-shift by ellipticity as its major consequence.

Of the two low-order imperfections ellipticity and misalignment of the electrostatic potential with respect to the magnetic field, ellipticity is probably much harder to tune in an experiment, and hence deserved a closer look. Whereas appliances for in-situ alignment are often installed, traps typically do not feature dedicated electrodes for tuning ellipticity, even though the parameter ϵ may incidentally be adjusted via segmented electrodes [16]. However, their original purpose—manipulating the ion's motion or picking up its signal—is different, and a reduction in $|\epsilon|$ may entail anharmonic terms in exchange. From the experimental side, the tuning of ellipticity is paid little attention to, other than striving to eliminate it by manufacturing traps with perfect cylindrical symmetry. Either one inevitably has to live with a certain amount of ellipticity as in the case of the time-of-flight ion cyclotron-resonance method, or its effect—and the effect of misalignment—cancels in the invariance theorem (2.27) when all three eigenfrequencies are measured.

[55] The same point must be made about misalignment, insofar as the electrostatic potential and the magnetic field do share the same principle axes.

4. Calculating first-order frequency-shifts

In this chapter, the perturbative method outlined in Chapter 3 is used to calculate the first-order frequency-shifts caused by cylindrically-symmetric imperfections (Section 4.1) and relativistic effects (Section 4.2). This succession reflects the chronological order of the original calculation. These two sections are largely based on the two papers [84] and [83], respectively, of which I am the first author.[1] There is also my earlier report [82] on the frequency-shifts caused by cylindrically-symmetric imperfections, which still uses a different notation. The notation has been improved over the course of some revisions. Apart from renaming a parameter γ in the paper [84] to ε in Section 4.1 to avoid confusion with the relativistic LORENTZ factor in Section 4.2 (see footnotes 31 and 37 in Chapter 3), the notation should be consistent with the papers. At times, the description is more detailed here in an attempt to be more pedagogical. Owing to the synergy of presenting the calculation in a single chapter rather than as two separate papers, some of the basics from Section 4.1 will not be repeated in Section 4.2. A comparison shows that, while the method is the same, the equations of motion are so different that cylindrically-symmetric imperfections and relativistic effects are not processed in one fell swoop. In other words, it is not possible to design a cylindrically-symmetric potential such that the equations of motion look like the relativistic ones. This being said, it is impossible to reduce the relativistic equations of motion to the classical ones by adding a cylindrically-symmetric potential. We shall also see that the relativistic frequency-shifts cannot be entirely compensated for with the shifts caused by cylindrically-symmetric imperfections. As even the structure of the frequency-shifts is quite different, two separate sections (and papers) are justified.

In Section 4.3, the results are then used to calculate the shifts for a specific mode of operation, predominantly used by THe-Trap and its precursor, the UW-PTMS. The content of this section has not been published because of its limited scope. Moreover, the results are readily obtained without a new concept from the more general expressions of the prior sections.

The calculation is classical rather than quantum-mechanical because I was more intimidated by a quantum-mechanical calculation than by the authoritative statement concerning frequency-shifts from the classic review paper [20] on PENNING traps:

> "This is a purely classical result, but, as we have just seen, its derivation is easy using quantum mechanics. Indeed, the frequency shifts could, of course, be computed in an entirely classical fashion, but they are most easily derived from the classical limit of the more familiar energy shift formula, which is the path that we are following."

Apart from being less general, a classical treatment is not conceptually inferior to a quantum-mechanical one, as long as quantization remains unobservable. Since any quantum theory should in general reproduce the classical limit, knowing this limit from a classical calculation

[1] The corresponding preprints 1305.4861 and 1310.4463 are on arXiv.

is essential for comparison. Moreover, an exact solution that goes beyond the ideal PENNING trap is impossible in either case, and all methods rely on perturbative techniques in order to incorporate the effects of cylindrically-symmetric imperfections and special relativity.

From a practical perspective, giving the classical limit even after a quantum-mechanical calculation [12, 20] underlines its usefulness, as many experiments are described well classically. In this case, amplitudes and frequencies are more appropriate than quantum numbers and energy levels. Because of the particular interest in the electron's magnetic moment [160], the theoretical description started from a quantum-mechanical perspective, in order to include spin. Additionally, the quantization of the electron's energy becomes important because the emission of synchrotron radiation cools the modified cyclotron-motion into its quantum-mechanical ground state. The electron will stay in this state provided thermal excitation by black-body photons is suppressed. To reach a sufficiently low ambient temperature, a dilution refrigerator is required [118].

For particles heavier than electrons, radiative cooling is inefficient [20]. Thus, the ground-state is only accessible with laser cooling [192], and merely reaching the quantum-mechanical regime with this method is hard enough. Even if the ion itself has a suitable cooling transition, its energy levels will most likely be subject to large ZEEMAN shifts in the magnetic field of the PENNING trap. Furthermore, the metastability of the magnetron mode poses an additional challenge [77]. Despite the ground-state predicted to be in reach [193], laser cooling has not been universally applied in PENNING traps. Instead, most PENNING-trap experiments for mass measurements or the determination of g-factors in heavy systems rely on more universal cooling methods [78]. Online traps use buffer-gas cooling [137] for ions of low charge. The effective resistance of the LC tank circuit for nondestructive detection via image currents acts like a thermal bath, thereby cooling the motion in resonance resistively [32]. Additionally, sideband coupling [29] mediated by a radio-frequency pulse is used to transfer energy from an uncooled mode into a cooled one, from which the energy can be removed. However, all these methods typically leave the particle in the classical domain, technical improvements such as electronic feedback [65] notwithstanding. Moreover, detecting the particle and measuring its frequencies is not always possible in the thermal limit. Moving closer to the quantum-mechanical domain with the help of advanced cooling methods would tremendously reduce systematic limitations arising from anharmonic effects [151]. Because the anharmonic frequency-shifts given in this chapter depend at least quadratically on the motional amplitudes, any reduction of the amplitudes is rewarded disproportionately in the frequency-shifts. At the current level of precision, the anharmonic shifts would probably become irrelevant in the quantum-mechanical domain, which fits nicely because the classical calculation does not account for quantization.

For resistively-cooled protons, quantum jumps in the modified cyclotron-motion have recently been on the verge of observation as a shift to the axial frequency in a huge magnetic inhomogeneity. These ill-controlled jumps driven by noise are a spurious side-effect of the extreme magnetic inhomogeneity, in which actually the frequency-shift caused by a spin flip is to be observed [36, 104]. These fluctuations need to be suppressed in order to achieve the experiment's goal [105].

Unless for these very special circumstances, quantum jumps in the frequencies related to changes of the motional quantum numbers are not seen when the experiment otherwise looks classical. In most cases of large quantum numbers, a classical treatment still yields a relevant result.

Since this chapter is entirely theoretical, we are free to make assumptions at our own will, as long as the mathematical treatment is sound. Of course, we must stay in touch with the experimental reality for the results to have any significance. It is for the reader to decide how well the assumptions are satisfied in a particular experiment, but it is for us to spell out the assumptions explicitly. As far as I can say, they are quite generic and no different from previous treatments of first-order frequency-shifts.

For the calculation, we assume a pointlike particle devoid of internal degrees of freedom that could couple to electric and magnetic fields. Clearly, this restriction excludes spin and dipole moments. Since strictly speaking among stable charged particles only electrons are pointlike, the requirement should be relaxed in order to encompass the usual ions found in Penning traps. For a particle to be considered pointlike here, the extent of the charge distribution must be small compared with the typical scales on which the fields change in a Penning trap, thereby ensuring that the whole charge distribution experiences the same field strength. For atomic ions and small molecules, these length-scales are vastly different, and it helps that the main component of the magnetic field is homogeneous. Although the electric field in the ideal Penning trap is spatially-dependent, its maximum gradient is limited, because eventually the radial modes become unstable. At first sight, it seems like the fields of the Penning trap have little dynamics to add to the charge distribution, because the harmonicity in the ideal case ensures that the charges orbit with identical frequencies regardless of their relative position, as long the interaction in the charge distribution can be neglected. However, the fields of the Penning trap may rearrange the charge distribution as the charges interact with each other. That is why polarizability may play the role of an effective mass [156]. The effect is small enough to be treated perturbatively.

We will describe the "pointlike" particle entirely by its charge q and its rest mass m. We consider only motional degrees of freedom, which are translational, not rotational for a pointlike particle. Despite the mass m, we may safely neglect gravity for a charged particle, even more so since the Penning trap consists of more than just stray fields. Additionally, the mass of a trappable particle is limited by the stability condition (2.24). As we assume the particle oscillates with constant amplitudes, damping or external excitations are ignored. The restriction to a single particle rules out ion–ion interactions.

4.1. Shifts caused by cylindrically-symmetric imperfections

Given the prevalence of cylindrically-symmetric imperfections in Penning traps, at least the frequency-shifts caused by the lowest-order imperfections have been calculated multiple times, as they are of particular experimental relevance. Since the axial mode is often used for detecting the trapped particle, shifts to the axial frequency by electrostatic imperfections were considered in the design of traps [47, 158]. The axial line-broadening caused by fluctuations of the motional amplitudes in combination with anharmonic terms presented a major obstacle to the detection. With this limitation removed by tunable electrostatic anharmonicity courtesy of correction electrodes, shifts to the radial frequencies were not dealt with on a general basis. Many results of these day appeared as abstracts in the Bulletins of the American Physical Society, which are hard to procure nowadays. However, the limited space means that there was probably not enough room for an extensive calculation.

At least, it seems safe to say that there was no general publication dedicated to frequency-shifts until the review article [20] offered a first comprehensive list for all three eigenmodes in the Penning trap (and the Larmor frequency for the precession of the spin). Concerning the paucity of references given, there was not too much prior work to rely on, and the expressions seem to come out of nowhere. The energy-shift caused by the lowest-order electrostatic and magnetic imperfections, C_4 and B_2, respectively, were calculated with a quantum-mechanical formalism and expressed as a function of the particle's quantum numbers. For the classical limit of large quantum numbers, this energy-shift was translated into a frequency-shift, expressed as a function of the particle's energy. In this step, the approximation $|\omega_+| \gg |\omega_-|$ was used.[2] The resulting expressions in the form of matrices are used in many theses and articles, for instance Reference [168].

Reference [44] derived the frequency-shifts from the quantum-mechanical energy-shift [20] without making any assumptions about the frequencies. Again, the result was expressed as a function of the particle's energies. Evaluating formulas using energies instead of amplitudes requires some extra care, because the magnetron energy (2.50) is negative. Working with equations of motions, as will be done in this chapter, naturally yields frequency-shifts as a function of amplitudes.[3]

Reference [12] used the quantum-mechanical techniques [20] to calculate the frequency-shifts caused by the electrostatic imperfections C_4 and C_6, and gave the result in the classical limit as a function of amplitudes. Moreover, the effect of the magnetic imperfection B_2 on the sideband cyclotron-frequency (2.25) was calculated.

Without showing any details, Reference [57] used classical techniques to calculate the shifts caused by (the equivalent of) C_4 and B_2 to the frequencies of the radial modes and the sideband cyclotron-frequency. As often, amplitude-dependent terms multiplied with the magnetron frequency ω_- were neglected against a corresponding term multiplied with the reduced cyclotron-frequency ω_+ in the frequency-shifts, provided the latter term exists.

Reference [22] gives the shifts caused by C_4, C_6, C_8 as well as B_2 and B_4 to the sideband cyclotron-frequency without making any assumptions about the hierarchy of the radial frequencies. The calculation is not shown.

In the aforementioned papers, the frequency-shifts are embedded in a larger context, and the focus is more on their impact than on their origin. Thus, details of the calculation are not mentioned, and the results are hard to verify without the intermediate steps. References [89, 90] outline the application of Hamiltonian perturbation theory, based on classical canonical action and angle variables, to Penning traps. Among other results, the shift caused by (the equivalent of) C_4 and C_6 is given for all three eigenfrequencies. The former is expressed in terms of amplitudes; the latter still uses canonical action variables, a result acknowledged to have "rather

[2] This is not to imply that the shift $\Delta\omega_-$ to the magnetron frequency is neglected against the shift $\Delta\omega_+$ to the reduced cyclotron-frequency, but it relates to approximations in the shifts themselves, where ω_- is neglected against ω_+, provided the corresponding term exists.

[3] We shall see that the frequency-shifts depend on even powers of the amplitudes. Consequently, a sign is not an issue, unless the amplitudes are mistakenly considered complex quantities. As a reminder, the particle's initial phases are encoded as φ_i inside the trigonometric functions, and the frequency-shifts do not depend on this component of the initial conditions. If they did, chaos is likely to ensue, and the usefulness of a Penning trap for precision measurements (characterized by repeatability and reproducibility) would be severely compromised. Of course, corrections to obtain accurate measurements would be equally hard to apply.

abstract appearance" [89]. The result for the frequency-shift caused by the very particular inhomogeneous magnetic field is hard to generalize. Rather than treating higher orders in the magnetic field independently, its total distortion is assumed to originate from the permeability of the electrodes placed in an otherwise homogeneous magnetic field. Although this model may describe the overall inhomogeneity sufficiently well in the absence of other magnetic material nearby, provided the magnetic field originally has no higher-order terms itself, the resulting magnetic field is calculated analytically only for one special set of electrodes. The spatial dependence of the magnetic distortions caused by other trap geometries may be very different, and the same holds true for the resulting frequency-shift. Moreover, apart from a change of the uniform contribution, only a B_2-like term in the particular magnetic field (or magnetic vector potential, to be more precise) is finally considered, and B_2 is determined by the choice of the geometry and the magnetic permeability of the electrodes. Of course, this quantity in the prefactor may be adjusted to match any given B_2, but higher-order terms beyond B_2 have yet to be included. For maximum flexibility and an increased scope, the frequency-shift should be calculated for a more general parametrization of the magnetic field.

Imperfections of the magnetic field have also been considered in Fourier-transform ion cyclotron-resonance (FT-ICR) mass-spectrometry [96, 102, 138]. Employing the Hamiltonian formalism [89, 90], Reference [102] calculated the frequency-shift caused by (the equivalent of) B_2 and B_4 to all the eigenfrequencies. The final result contains the approximation $\omega_+ - \omega_- \approx \omega_c$. When calculated in the context of FT-ICR, frequency-shifts caused by imperfections of the electric field [69, 101] may involve more than cylindrically-symmetric imperfections, because this symmetry is not present in cubic trapping cells. In some cases, the theoretical framework in the FT-ICR community is different from the one for Penning traps with single particles. For instance, the early papers [69, 138] use a Schrödinger wave-packet approach, and clouds of ions are considered.

Because individual expressions for frequency-shifts are scattered throughout various publications without any general result or one comprehensive reference, it is not surprising for Reference [155] to state:

> "Because the two-ion technique requires exploring a larger fraction of the trap, we need to know the frequency shifts associated with higher order terms in the expansions of the fields. In previous theses, only expressions for frequency shifts up to B_2 and C_4 were presented. These shifts also do not exist in the literature."

In the light of References [12, 89, 102], the last sentence must be argued with. At least, the results for higher-order terms in the literature do not seem to be highly visible. Following the shortage of such expressions, References [128, 155] calculate the frequency-shifts caused by the electrostatic imperfections C_4, C_6 and C_8, as well as the magnetic imperfections B_2 and B_4, the latter using the approximation $|\omega_+| \gg |\omega_-|$. In many experiments including theirs, these are even more than the most relevant terms, and that is why the calculation stopped there. Using two slightly different approaches, their results agree, thereby adding credibility.

If the results are to be trusted, why are they to be reproduced with a similar method? Maybe, the approximation $|\omega_+| \gg |\omega_-|$ could be dropped as it is not justified for all trappable ion. There seems to be no immediate interest though.

What could possibly be gained from calculating the frequency-shifts caused by imperfections of higher order still? It is probably not out of pure curiosity without any motivation from the experimental side that C_{10} and B_6 would be looked at, because as things stand, the specific calculation would yield an even longer expression than for C_8 and B_4. With the actual prefactors of the amplitude-dependent terms looking more or less random, the calculation looms as a dull exercise in number crunching. It was not with any specific cylindrically-symmetric imperfection in mind that I looked at the problem of calculating the associated frequency-shifts again. Reproducing a known result step by step may be learning experience, but whom do you trust in case of a discrepancy? It does not help that most of the results follow from an undisclosed calculation. Why have the shifts caused by the lowest-order cylindrically imperfections been calculated multiple times when these imperfections are essentially the same because their spatial dependence is constrained by nature? Of course, a consistent parametrization of imperfections is desirable for easier comparisons, but one reliable result should do. The problem of discrepancies in the literature is more frequent than expressed by the statement from Reference [128]:

> "The expressions for the effect of C_4, C_6, and B_2 have been given in previous ICR theses …but they are not always consistent with each other. The fact is that in the past nobody in this lab ever worried about the effect of any term beyond C_4 and B_2 quantitatively and there has never been a need for getting the right expression within a factor of two (and the correct sign)."

In terms of replications by means of citations (not necessarily experimental consequences), the most prominent case afflicts the shift caused by (the equivalent of) B_2 to the sideband cyclotron-frequency. In Reference [12], which is cited in most publications on the time-of-flight ion cyclotron-resonance method, a global factor of ½ is missing compared to other sources.[4] Moreover, there is a sign error in the shift caused by C_4 to the sideband cyclotron-frequency, which may me recognized more easily because of the individual results for the shift $\Delta\omega_\pm$ to both radial frequencies alone.[5]

I do not intend to bash the seminal paper [12] or start a crusade lobbying for or against any particular result; I merely find it surprising that the discrepancies have not caught anybody's attention despite the multitude of papers on the subject. Instead, doubtful results keep being reprinted [136] or even strangely reshuffled[6] [18] as if for a lack of alternatives. This might suggest that the exact result is either irrelevant or far from trivial. I believe that the problem runs deeper than the usual propensity to cite what others have cited.

Unless the calculation is made explicit, its result is hard to verify. Even though everyone should be given the chance to understand the frequency-shifts when they are important, the results are not open to the public, partly because the calculation is never shown in a hands-on

[4] As most other sources use the approximation $|\omega_+| \gg |\omega_-|$, their result may not look as exact.

[5] The shift $\Delta\omega_z$ caused by the C_6 to the axial frequency has a functional dependence on the radial modes that is very different from other results, with a partial cancellation for equal radial amplitudes and without a cross-term $\hat{\rho}_+^2\hat{\rho}_-^2$. However, Reference [12] is hardly quoted for this particular result.

[6] The frequency-shift [12] caused by the magnetic imperfection B_2 to the sideband cyclotron-frequency ω_c depends more strongly on the amplitude squared of the magnetron motion than on the amplitude squared of the modified cyclotron-motion by a factor of ω_+/ω_-. In Reference [18], the situation is approximately opposite, and the dependence has the same sign.

manner, and partly because of the sophisticated mathematical methods involved. Particularly in the latter case, the final expressions look like a time-honored result, inherited from the ancestors and passed on for generations. Of course, there is no need to verify what has been proven correct. Truth does not age, but in science it comes with an explanation. Scientific results should not be a matter of trust or faith, the controversies being reserved for their interpretation.

The perturbative approach [128, 155] based on classical equations of motion is understood intuitively on physical grounds, but even then there seems to be something so cumbersome about the calculation that the results look arcane. Talking about the n as in C_n and B_n, Reference [128] states:

> "The algebra becomes quickly overwhelming for $n > 6$ and so *Mathematica* was used to generate all the expressions below."

Because of this perception, the calculation had not realized its full potential, stopping at C_8 and B_4. Sections 4.1.2 and 4.1.3 show how to calculate the first-order frequency-shifts associated with C_η and B_η consistently. In this way, generating expressions are created from which the explicit expressions for a specific η follow. Rather than calculating and showing the frequency-shifts for different η individually, the generating expressions shown in the following sections have all η covered. For explicit expression regarding the lowest-order imperfections, see Chapter E in the appendix.

Such general expressions for the frequency-shifts caused by cylindrically-symmetric imperfections require a general parametrization of these very imperfections in cylindrical coordinates. The typical parametrization with Legendre polynomials and spherical coordinates in the literature, not just for Penning or Paul traps, but also for atom traps [6], has at least reduced the appeal of a general treatment. It may have looked like there is no general expression for the coefficients (2.71) and (2.81) that describe the imperfections as a polynomial in cylindrical coordinates. As the exact value of these coefficients does not have to be known beforehand to identify the resonant terms that drive the frequency-shifts, a general treatment would still be useful, even though evaluating the generating expressions would then involve inserting specific values of the coefficients from a different source. Here, Section 2.2 with its general expressions for the coefficients $a_\eta(k)$ and $\tilde{a}_\eta(k)$ comes to the rescue, and its importance should not be overlooked.

As a little known fact even in the Penning-trap community, a general treatment has been attempted before without resulting in a peer-reviewed publication so far. Reference [99] uses a Hamiltonian formalism to calculate the first-order frequency-shifts caused by all cylindrically-symmetric imperfections of the electric and magnetic field. These equally general results would make for a great comparison with the expressions presented in the following section. In fact, the first version of this calculation had been finished when I discovered the result [99], while looking for a benchmark beyond C_8 and B_4. Unfortunately, the general expressions for the frequency-shifts caused by magnetic imperfections do not depend on the perturbation parameter, the equivalent of B_η in our case. However, the explicit expressions shown have a different prefactor which depends on the perturbation parameter. What might therefore look like a minor misprint of the prefactor in the general expression, is in fact much harder to mend.

The general expressions for the frequency-shifts [99] have not been reprinted in the literature, and they have not been commented on. A recent review article [107] on the most precise mass

measurements in PENNING traps still cites Reference [128] as the source for the expressions for frequency-shifts up to C_8 and B_4. Of course, the absence of evidence for a different general treatment is not the same as evidence for its absence.[7] However, there is no point in having a general treatment that goes unnoticed, and a possible cross-check with other general expressions would not take away from this section, which does not have to be the first of its kind to be useful.

4.1.1. Powers of radial displacement squared

Before getting to the actual calculation of the first-order frequency-shifts caused by static electric and magnetic imperfections in Sections 4.1.2 and 4.1.3, respectively, it is helpful to derive two identities for particular frequency-components contained in powers of the radial displacement squared. For cylindrically-symmetric imperfections, powers of the radial ion displacement play a crucial role, as they are ubiquitous in the electrostatic potential (2.73), as well as in the axial magnetic field (2.78) and the radial magnetic field (2.80). The identities derived here are not necessary to spot the pattern behind the terms that cause a first-order frequency-shift, but they make the final result much more compact and easy to evaluate. That is why the calculation is shown in this section in detail.

Summing the ansatz from Equations (3.94) and (3.95) for the zeroth-order trajectory in the radial place in quadrature yields

$$\tilde{\rho}^2 = \hat{\rho}_+^2 + \hat{\rho}_-^2 + 2\hat{\rho}_+\hat{\rho}_- \cos(\tilde{\chi}_\mathrm{b}) \quad \text{with} \quad \tilde{\chi}_\mathrm{b} = \tilde{\chi}_+ - \tilde{\chi}_- \quad . \tag{4.1}$$

The result is virtually the same as Equation (2.41) for the ideal PENNING trap, apart from not having the difference frequency

$$\tilde{\omega}_\mathrm{b} = \tilde{\omega}_+ - \tilde{\omega}_- \tag{4.2}$$

fixed as in Equation (2.42). The tilde on top of the frequency indicates a possible deviation from the radial frequencies (2.23) in the ideal trap.

During the calculation, it will become clear that only even powers of radial displacement need to be dealt with. In other words, the calculation comes down to analyzing frequency-components of powers of the radial displacement squared. This is quite fortunate since the square root in radial displacement $\tilde{\rho}$ alone would greatly complicate a frequency analysis.

The radial displacement squared $\tilde{\rho}^2$ comes with a constant component and an oscillatory component at the frequency $\tilde{\omega}_\mathrm{b}$. Therefore, the frequency-spectrum of $\tilde{\rho}^{2n}$ possesses components at $0\tilde{\omega}_\mathrm{b}, 1\tilde{\omega}_\mathrm{b}, 2\tilde{\omega}_\mathrm{b}, 3\tilde{\omega}_\mathrm{b}, \ldots, n\tilde{\omega}_\mathrm{b}$, with a constant component, the fundamental frequency $\tilde{\omega}_\mathrm{b}$, and its even and odd harmonics. The individual contributions are analyzed best after converting powers of cosine into a sum of cosines.

[7] I am indebted to Robin GOLSER for using this pun in one of his talks. It could also come from Nassim Nicholas TALEB's book "The Black Swan: The Impact of the Highly Improbable."

Taking Equation (4.1) to the power of n results in

$$\tilde{\rho}^{2n} = \left[\hat{\rho}_+^2 + \hat{\rho}_-^2 + 2\hat{\rho}_+\hat{\rho}_- \cos(\tilde{\chi}_\mathrm{b})\right]^n \tag{4.3a}$$

$$= \sum_{j=0}^{n} \left[2\hat{\rho}_+\hat{\rho}_- \cos(\tilde{\chi}_\mathrm{b})\right]^j \left(\hat{\rho}_+^2 + \hat{\rho}_-^2\right)^{n-j} \tag{4.3b}$$

$$= \sum_{j=0}^{n} \sum_{k=0}^{n-j} \binom{n}{j}\binom{n-j}{k} \hat{\rho}_+^{j+2k} \hat{\rho}_-^{2(n-k)-j} \left[2\cos(\tilde{\chi}_\mathrm{b})\right]^j \tag{4.3c}$$

after applying binomial expansion twice. The truly resonant terms, which drive the first-order frequency-shifts, are generated by two specific frequency-components of $\tilde{\rho}^{2n}$: the constant (or time-independent) contribution and the oscillatory component at the difference frequency $\tilde{\omega}_\mathrm{b}$ of the two radial modes. Both components are calculated starting from Equation (4.3c).

Constant contribution

Because Equations (3.2) and (3.5) show that only even powers of cosine come with a constant term, the summation variable in Equation (4.3c) is transformed according to $j \to 2j$. The constant contribution by powers of cosine is given by Equation (3.6), which yields

$$\left\langle \tilde{\rho}^{2n} \right\rangle_0 = \sum_{j=0}^{\left\lfloor \frac{n}{2} \right\rfloor} \sum_{k=0}^{n-2j} \binom{2j}{j}\binom{n}{2j}\binom{n-2j}{k} \hat{\rho}_+^{2(j+k)} \hat{\rho}_-^{2(n-j-k)} \quad . \tag{4.4}$$

The upper limit is given by the floor function as defined in Equation (2.60). Equation (4.4) describes a polynomial of the radial amplitudes $\hat{\rho}_\pm$. In order to find the coefficient of a term like $\hat{\rho}_+^{2p}\hat{\rho}_-^{2(n-p)}$, the summation variables should be transformed such that there is one sum over constant $p = j + k$. This sum over p would then create all the terms of the polynomial, whereas the other sum would determine the coefficients. Figure 4.1 illustrates a suitable transformation given by

$$\sum_{j=0}^{\left\lfloor \frac{n}{2} \right\rfloor} \sum_{k=0}^{n-2j} f_n(j,k) = \sum_{p=0}^{n} \sum_{q=0}^{\frac{n}{2}-\left|\frac{n}{2}-p\right|} f_n(j=q, k=p-q) \tag{4.5}$$

in formal terms. Here, $f_n(j,k)$ is a generic function of the two summation variables j and k, whose transformation to p and q is indicated in the argument on the right-hand side. The transformation of the limits is equally important. Even though $j = q$, it is not straightforward since the order of the summation is changed with j aka q moving from the outer to the inner sum. Applying the full transformation (4.5) to Equation (4.4) results in

$$\left\langle \tilde{\rho}^{2n} \right\rangle_0 = \sum_{p=0}^{n} \sum_{q=0}^{\frac{n}{2}-\left|\frac{n}{2}-p\right|} \binom{2q}{q}\binom{n}{2q}\binom{n-2q}{p-q} \hat{\rho}_+^{2p} \hat{\rho}_-^{2(n-p)} \quad . \tag{4.6}$$

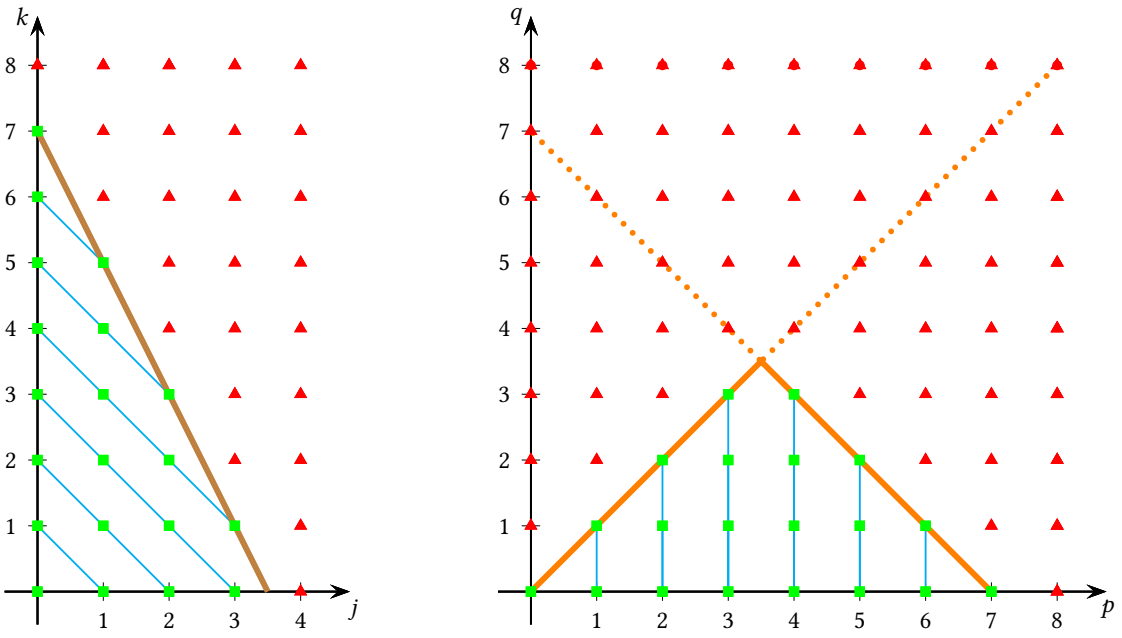

Figure 4.1.: Transformation of the summation variables and limits according to Equation (4.5) for $n = 7$. The green squares are combinations of (j, k) and (p, q) that are part of the summation; the red triangles are not, because they lie outside the range of the summation. Since all summation variables are non-negative, only the first quadrant of the coordinate system is shown. The thick brown line in jk-parameter space indicates the upper summation limit $k_{\max} = n-2j$. The thin blue lines connect points of constant $j + k = p$. Because these lines do not intersect and are not perpendicular to the j-axis, a point on this line is uniquely identified by j and p. Following the deliberate choice $p = j + k$, the other transformation of summation variables is now fixed, as j retains its meaning and its limits. To minimize confusion, j is renamed q in what is then to become the pq-parameter space. The constraints $0 \leq k \leq n - 2j$ for k read $j \leq p$ and $j \leq n - p$ after making the substitution $k = p - j$. After switching from j to q, the constraints are combined to give the upper limit $q \leq n/2 - |n/2 - p|$ indicated by the thick orange line here. The dotted orange lines are continuations of $q = p$ and $q = n - p$ outside the range of the summation.

Transforming the triple product of binomials as

$$\binom{2q}{q}\binom{n}{2q}\binom{n-2q}{p-q} = \frac{(2q)!}{(q!)^2}\frac{n!}{(2q)!(n-2q)!}\frac{(n-2q)!}{(p-q)!(n-p-q)!} \tag{4.7a}$$

$$= \frac{n!}{p!(n-p)!}\frac{p!}{q!(p-q)!}\frac{(n-p)!}{q!(n-p-q)!} \tag{4.7b}$$

$$= \binom{n}{p}\binom{p}{q}\binom{n-p}{q} \tag{4.7c}$$

removes the summation variable q from one binomial coefficient,[8] reducing the sums to

$$\left\langle \tilde{\rho}^{2n} \right\rangle_0 = \sum_{p=0}^{n} \binom{n}{p} \sum_{q=0}^{\frac{n}{2}-\left|\frac{n}{2}-p\right|} \binom{p}{q}\binom{n-p}{q} \hat{\rho}_+^{2p}\,\hat{\rho}_-^{2(n-p)} \quad . \tag{4.8}$$

As intended by the original substitution $p = j + k$, the sum over p creates the polynomial, and the sum over q determines the coefficient of the term $\hat{\rho}_+^{2p}\,\hat{\rho}_-^{2(n-p)}$. Even more pleasantly, the sum over q is executed by hand[9] with the help of Vandermonde's identity [178]

$$\sum_{q=0}^{r} \binom{n_1}{q}\binom{n_2}{r-q} = \binom{n_1+n_2}{r} \quad , \tag{4.9}$$

where the variables r, n_1 and n_2 are integers in this context.

Without giving a rigorous proof here, Vandermonde's identity is also understood from a combinatorics perspective. The first binomial coefficient on the left-hand side describes the number of possibilities to select q elements out of a total of n_1 elements, when the order of the selection does not matter. Likewise, the second binomial coefficient on the left-hand side gives the number of possibilities to pick $r - q$ elements out of n_2. Summing over the possibilities to select q elements with $0 \leq q \leq r$ out of n_1 and the remaining $r - q$ elements with $r \geq r - q \geq 0$ out of n_2 is equivalent to choosing r elements from a total pool of $n_1 + n_2$.

Before applying Vandermonde's identity (4.9) to the sum over q, the two cases

$$\frac{n}{2} - \left|\frac{n}{2} - p\right| = \begin{cases} p & \text{for } p \leq \frac{n}{2}\,, \\ n-p & \text{for } p \geq \frac{n}{2} \end{cases} \tag{4.10}$$

[8] Because of the switch from binomial coefficients to the explicit expression (3.3) and back, some attention has to be paid to whether the range of the explicit definition is preserved. For the first triple product of binomial coefficients, these conditions are $n \geq 2q \geq 0$, $p \geq q$ and $n - 2q \geq p - q$ or, equivalently, $n \geq p + q$. If these conditions are not fulfilled, the first triple product is given by zero rather than the explicit expression (4.7a). For the second triple product (4.7c), the conditions for using the explicit expression (4.7b) are $0 \leq q \leq p \leq n$ and $n \geq p + q$. When combined, these two conditions also result in $n \geq p + q \geq q + q \geq 2q$. Consequently, the identity (4.7c) holds for binomial coefficients, not just for the explicit expression with factorials. In retrospect, the constraints also justify expanding with $(n - p)!$, which we have defined in Equation (2.69) only for non-negative integer arguments.

[9] I am indebted to Martin Höcker for simplifying this sum with *Mathematica* first. It was after seeing the sum being executed with a computer algebra system that I started searching for a suitable identity to justify the *Mathematica* result.

in the upper limit have to be distinguished. The first case yields

$$\sum_{q=0}^{p} \binom{p}{q}\binom{n-p}{q} = \sum_{q=0}^{p} \binom{p}{p-q}\binom{n-p}{q} = \binom{p+n-p}{p} = \binom{n}{p} \tag{4.11}$$

with $r = p$, $n_1 = n - p$, $n_2 = p$ and the identity (3.4) for binomial coefficients. In the second case, identifying $r = n - p$, $n_1 = p$ and $n_2 = n - p$ gives

$$\sum_{q=0}^{n-p} \binom{p}{q}\binom{n-p}{q} = \sum_{q=0}^{n-p} \binom{p}{q}\binom{n-p}{n-p-q} = \binom{p+n-p}{n-p} = \binom{n}{n-p} = \binom{n}{p} \quad . \tag{4.12}$$

The result does not depend on the two case (4.10) for the upper limit of the sum. With the sum over q executed by means of Equations (4.11) and (4.12), Equation (4.8) becomes

$$\left\langle \tilde{\rho}^{2n} \right\rangle_0 = \sum_{p=0}^{n} \left[\binom{n}{p}\right]^2 \hat{\rho}_+^{2p} \hat{\rho}_-^{2(n-p)} = \sum_{p=0}^{n} \left[\binom{n}{n-p}\right]^2 \hat{\rho}_+^{2(n-p)} \hat{\rho}_-^{2p} = \sum_{p=0}^{n} \left[\binom{n}{p}\right]^2 \hat{\rho}_-^{2p} \hat{\rho}_+^{2(n-p)} \quad . \tag{4.13}$$

In the last steps, we have transformed the summation variable as $p \to n - p$, and we have used the identity (3.4) for binomial coefficients, in order to show that the final result is symmetric with respect to the amplitudes $\hat{\rho}_\pm$. This symmetry is expected because the radial displacement squared $\tilde{\rho}^2$ in Equation (4.1) is itself symmetric with respect to $\hat{\rho}_\pm$. Preserving the symmetry merely serves as a small check of the result.

The symmetry with respect to the amplitudes $\hat{\rho}_\pm$ allows to write the constant contribution from powers of the radial displacement squared as

$$\left\langle \tilde{\rho}^{2n} \right\rangle_0 = \sum_{p=0}^{n} \left[\binom{n}{p}\right]^2 \hat{\rho}_\pm^{2p} \hat{\rho}_\mp^{2(n-p)} \quad . \tag{4.14}$$

We shall see that this result is particularly useful for expressing frequency-shifts to both radial frequencies in a single formula.

Oscillatory component

As for the constant contribution, the starting point is Equation (4.3c). This time, Equations (3.2) and (3.5) show that a component at the fundamental frequency $\tilde{\omega}_\mathrm{b}$ is present only for odd powers of cosine. Therefore, the summation variable is transformed according to $j \to 2j + 1$. The contribution at the fundamental frequency is given by Equation (3.7). The oscillatory term at the fundamental frequency becomes

$$\left\langle \tilde{\rho}^{2n} \right\rangle_{\tilde{\omega}_\mathrm{b}} = 2\frac{\hat{\rho}_+}{\hat{\rho}_-} \cos(\tilde{\chi}_\mathrm{b}) \sum_{j=0}^{\lfloor \frac{n-1}{2} \rfloor} \sum_{k=0}^{n-2j-1} c_n(j,k)\, \hat{\rho}_+^{2(j+k)} \hat{\rho}_-^{2(n-j-k)} \tag{4.15}$$

with the coefficient

$$c_n(j,k) = \binom{n}{2j+1}\binom{n-2j-1}{k}\binom{2j+1}{j} \quad . \tag{4.16}$$

As for the constant contribution, Equation (4.15) describes a polynomial of the amplitudes $\hat{\rho}_\pm$. The prefactor $\hat{\rho}_+/\hat{\rho}_-$ has been factored out in order to make the terms inside the sums look like $\hat{\rho}_+^{2p}\hat{\rho}_-^{2(n-p)}$, with a similar transformation of summation variables as for the constant contribution yielding their coefficients. However, the transformation (4.5) cannot be applied directly at this point, because the upper limits are different here. They will have to be shifted up in order to match the original transformation used for the constant component. For the sum over k, there is no problem to go from $n-2j-1$ to $n-2j$ since the second binomial coefficient in Equation (4.16) vanishes for $k > n-2j-1$ anyway. For the moving the upper limit of sum over j from $\lfloor (n-1)/2 \rfloor$ to $\lfloor n/2 \rfloor$, two cases have to be considered. If n is odd, then $\lfloor (n-1)/2 \rfloor = \lfloor n/2 \rfloor$, and there is no problem. If n is even, then the first binomial coefficient in Equation (4.16) vanishes for $j_{\max} = \lfloor n/2 \rfloor = n/2$ because $2j_{\max}+1 = n+1 > n$. Consequently, the upper limits in Equation (4.15) may rightfully be extended to be compatible with those mandated by the transformation (4.5), which results in

$$\left\langle \tilde{\rho}^{2n} \right\rangle_{\tilde{\omega}_\mathrm{b}} = 2\frac{\hat{\rho}_+}{\hat{\rho}_-}\cos(\tilde{\chi}_\mathrm{b}) \sum_{j=0}^{\lfloor \frac{n}{2} \rfloor} \sum_{k=0}^{n-2j} c_n(j,k)\, \hat{\rho}_+^{2(j+k)} \hat{\rho}_-^{2(n-j-k)} \tag{4.17a}$$

$$= 2\frac{\hat{\rho}_+}{\hat{\rho}_-}\cos(\tilde{\chi}_\mathrm{b}) \sum_{p=0}^{n} \sum_{q=0}^{\frac{n}{2}-\left|\frac{n}{2}-p\right|} c_n(q,p-q)\, \hat{\rho}_+^{2p} \hat{\rho}_-^{2(n-p)} \quad . \tag{4.17b}$$

In terms of the new summation variables, the coefficient (4.16) becomes[10]

$$c_n(q,p-q) = \binom{n}{2q+1}\binom{n-2q-1}{p-q}\binom{2q+1}{q} \tag{4.18a}$$

$$= \frac{n!}{(2q+1)!(n-2q-1)!}\frac{(n-2q-1)!}{(p-q)!(n-p-q-1)!}\frac{(2q+1)!}{q!(q+1)!} \tag{4.18b}$$

$$= \frac{n!}{p!(n-p)!}\frac{p!}{q!(p-q)!}\frac{(n-p)!}{(n-p-q-1)!(q+1)!} \tag{4.18c}$$

$$= \binom{n}{p}\binom{p}{q}\binom{n-p}{q+1} \quad . \tag{4.18d}$$

Like for the constant contribution, the summation variable q has been removed from one of the three binomial coefficients, and the remaining sum over q in

$$\left\langle \tilde{\rho}^{2n} \right\rangle_{\tilde{\omega}_\mathrm{b}} = 2\frac{\hat{\rho}_+}{\hat{\rho}_-}\cos(\tilde{\chi}_\mathrm{b}) \sum_{p=0}^{n} \binom{n}{p} \sum_{q=0}^{\frac{n}{2}-\left|\frac{n}{2}-p\right|} \binom{p}{q}\binom{n-p}{q+1} \hat{\rho}_+^{2p} \hat{\rho}_-^{2(n-p)} \tag{4.19}$$

[10] Once again, we check the conditions for using the explicit expressions (4.18b) with factorial for the triple product of binomial coefficients (4.18a). These conditions are $n \geq 2q+1$, $p \geq q \geq 0$, and $n-2q-1 \geq p-q$ or, equivalently, $n \geq p+q+1$. Otherwise, the first triple product is defined to give zero. For the second triple product of binomial coefficients (4.18d), the use of the explicit expression (4.18c) requires $n \geq p \geq q \geq 0$ and $n-p \geq q+1$. These conditions can be combined as $n \geq p+q+1 \geq p+1 \geq p$ and $n \geq p+q+1 \geq q+q+1 \geq 2q+1$ in order to show that they are equivalent to those imposed by the first triple product. Hence, the overall identity (4.18d) is valid for the whole range of input values covered by the definition of the binomial coefficient (3.3). Expanding with $(n-p)!$ was fine because $n \geq p$.

determines the coefficients of the terms $\hat{\rho}_+^{2p}\hat{\rho}_-^{2(n-p)}$ in the polynomial. Vandermonde's identity (4.9) is still the key to execute the sum over q, with the two cases (4.10) for the upper limit as before.

For the first case, we find

$$\sum_{q=0}^{p}\binom{p}{q}\binom{n-p}{q+1} = \sum_{q=0}^{p}\binom{p}{p-q}\binom{n-p}{q+1} = \sum_{q=0}^{p}\binom{p}{p+1-(q+1)}\binom{n-p}{q+1} \tag{4.20a}$$

$$= \sum_{q'=1}^{p+1}\binom{p}{p+1-q'}\binom{n-p}{q'} = \sum_{q'=0}^{p+1}\binom{p}{p+1-q'}\binom{n-p}{q'} \tag{4.20b}$$

$$= \binom{p+n-p}{p+1} = \binom{n}{p+1} \quad . \tag{4.20c}$$

We have used the identity (3.4) for binomial coefficients in the first step. After transforming the summation variable as $q+1 \to q'$, the lower limit was shifted from 1 to 0, in order to match Equation (4.9) with $r = p+1$. This shift is fine because the first binomial coefficient vanishes for $q' = 0$.

For the second case, the final result is identical:

$$\sum_{q=0}^{n-p}\binom{p}{q}\binom{n-p}{q+1} = \sum_{q=0}^{n-p-1}\binom{p}{q}\binom{n-p}{q+1} = \sum_{q=0}^{n-p-1}\binom{p}{q}\binom{n-p}{n-p-1-q} \tag{4.21a}$$

$$= \binom{p+n-p}{n-p-1} = \binom{n}{n-p-1} = \binom{n}{p+1} \quad . \tag{4.21b}$$

Apart from using the identity (3.4) twice, we have shifted the upper limit of the sum to take the form on Vandermonde's identity (4.9) with $r = n-p-1$. No contribution is forgotten by this step because the second binomial coefficient vanishes for $q = n-p$. With Equations (4.20c) and (4.21b) for the sum over q, Equation (4.19) becomes

$$\left\langle\tilde{\rho}^{2n}\right\rangle_{\tilde{\omega}_\mathrm{b}} = \frac{2\hat{\rho}_+}{\hat{\rho}_-}\cos(\tilde{\chi}_\mathrm{b})\sum_{p=0}^{n}\binom{n}{p}\binom{n}{p+1}\hat{\rho}_+^{2p}\hat{\rho}_-^{2(n-p)} \quad . \tag{4.22}$$

Sending the summation variable $p \to n-1-p$ in the amplitude-dependent part

$$\sum_{p=0}^{n-1}\binom{n}{p}\binom{n}{p+1}\hat{\rho}_+^{2p+1}\hat{\rho}_-^{2(n-p)-1} = \sum_{p=0}^{n-1}\binom{n}{n-1-p}\binom{n}{n-p}\hat{\rho}_+^{2(n-p)-1}\hat{\rho}_-^{2p+1} \tag{4.23a}$$

$$= \sum_{p=0}^{n-1}\binom{n}{p+1}\binom{n}{p}\hat{\rho}_-^{2p+1}\hat{\rho}_+^{2(n-p)-1} \tag{4.23b}$$

shows that the result is indeed symmetric with respect to the amplitudes $\hat{\rho}_\pm$. Again, the symmetry serves as a check because it is expected from the same symmetry of the radial displacement squared (4.1). We have also used the identity (3.4) for binomial coefficients. The upper limit of the sum over p in Equation (4.22) could be lowered from n to $n-1$ because the

second binomial coefficient vanishes for $p = n$. However, we will find it comfortable to have the same limits as for the constant contribution (4.14), and we will therefore include a vanishing contribution here.

Taking into account the symmetry with respect to the amplitudes $\hat{\rho}_\pm$, the oscillatory term at the fundamental frequency $\tilde{\omega}_\mathrm{b}$ is written as

$$\left\langle \tilde{\rho}^{2n} \right\rangle_{\tilde{\omega}_\mathrm{b}} = \frac{2\hat{\rho}_\pm}{\hat{\rho}_\mp} \cos(\tilde{\chi}_\mathrm{b}) \sum_{p=0}^{n} \binom{n}{p} \binom{n}{p+1} \hat{\rho}_\pm^{2p} \hat{\rho}_\mp^{2(n-p)} \quad . \tag{4.24}$$

We have factored out $\hat{\rho}_\pm/\hat{\rho}_\mp$ because this term will cancel nicely when calculating the first-order frequency-shifts. The remaining amplitude-dependent parts in the sum have the same structure as for the constant contribution (4.14).

4.1.2. Electrostatic imperfections

The permissible spatial dependence of cylindrically-symmetric electrostatic imperfections was discussed in Section 2.2. As the perturbative formalism here uses classical equations of motion instead of operators, the electric field rather than the potential is required. For a given potential Φ_η from Equation (2.73), the corresponding electric field is calculated by taking the negative gradient as

$$\vec{E}_\eta(\rho, z) = -\frac{\partial \Phi_\eta(\rho, z)}{\partial z} \vec{e}_z - \frac{\partial \Phi_\eta(\rho, z)}{\partial \rho} \vec{e}_\rho \tag{4.25}$$

$$= E_\eta^{(z)}(\rho, z) \vec{e}_z + E_\eta^{(\rho)}(\rho, z) \vec{e}_\rho \tag{4.26}$$

with the axial component

$$E_\eta^{(z)} = -C_\eta \frac{V_0}{2d^\eta} \sum_{k=0}^{\lfloor \eta/2 \rfloor} a_\eta(k) \, (\eta - 2k) \, z^{\eta-2k-1} \rho^{2k} \tag{4.27}$$

and the radial component

$$E_\eta^{(\rho)} = -C_\eta \frac{V_0}{d^\eta} \sum_{k=1}^{\lfloor \eta/2 \rfloor} a_\eta(k) \, k \, z^{\eta-2k} \rho^{2k-1} \quad . \tag{4.28}$$

As the radial electric field has no contribution for $k = 0$, we have raised the lower limit of the sum from 0 to 1 straight away.

Clearly, the axial electric field comes with even powers of radial displacement ρ only. For the radial axial field, the odd exponent associated with ρ is misleading. Since the equations of motion use Cartesian coordinates, the radial unit vector is expressed as

$$\vec{e}_\rho = \frac{1}{\rho} \begin{pmatrix} x \\ y \end{pmatrix} \tag{4.29}$$

partly in these coordinates, and the two radial electric field components become

$$\begin{pmatrix} E_\eta^{(x)} \\ E_\eta^{(y)} \end{pmatrix} = \frac{E_\eta^{(\rho)}}{\rho} \begin{pmatrix} x \\ y \end{pmatrix} = -C_\eta \frac{V_0}{d^\eta} \sum_{k=1}^{\lfloor \eta/2 \rfloor} a_\eta(k)\, k\, z^{\eta-2k}\, \rho^{2k-2} \begin{pmatrix} x \\ y \end{pmatrix} \quad . \tag{4.30}$$

At this point, it is obvious that there are only even powers of radial displacement, and the identities from Section 4.1.1 for powers of radial displacement squared apply.

With the additional electric field, the equations of motion (2.16) from the ideal Penning trap pick up an additional term, and they read

$$\begin{pmatrix} \ddot{x} \\ \ddot{y} \\ \ddot{z} \end{pmatrix} = \omega_\mathrm{c} \begin{pmatrix} \dot{y} \\ -\dot{x} \\ 0 \end{pmatrix} + \frac{qV_0C_2}{2md^2} \begin{pmatrix} x \\ y \\ -2z \end{pmatrix} + \frac{q}{m} \begin{pmatrix} E_\eta^{(x)} \\ E_\eta^{(y)} \\ E_\eta^{(z)} \end{pmatrix} \quad . \tag{4.31}$$

The additional term does not contain velocities; it is only a function of coordinates. Since the velocity-dependent term will not be affected, we have already written its prefactor as the free-space cyclotron-frequency ω_c from Equation (2.18).

We will now search for resonant terms that change the axial and the radial frequencies separately, because the first-order frequency-shifts result entirely from the zeroth-order trajectories. Conceptually, the frequency-shift to the one-dimensional axial mode is the easiest to calculate, and it provides a good starting point before turning to the more intricate shifts to the radial modes.

Shifts to the axial mode

After plugging the additional axial electric field (4.27) into Equation (4.31), the axial equation of motion reads

$$\ddot{z} + \omega_z^2 z + \frac{C_\eta}{C_2} \frac{\omega_z^2}{2d^{\eta-2}} \sum_{k=0}^{\lfloor \eta/2 \rfloor} a_\eta(k)\, (\eta - 2k)\, z^{\eta-2k-1} \rho^{2k} = 0 \quad . \tag{4.32}$$

The unperturbed axial frequency ω_z in the ideal Penning trap is given by Equation (2.17). To determine the first-order frequency-shifts, we will now plug in the zeroth-order trajectories $\tilde{z}$ from Equation (3.96) and $\tilde{\rho}^2$ from Equation (4.1) into the axial equation of motion (4.32), while searching for terms that are proportional to the original ansatz $\tilde{z}$. These terms will be absorbed in the effective equation of motion (3.85) and translated into a first-order frequency-shift according to Equation (3.86). Clearly, we expect naturally-resonant terms at the axial frequency to result from the axial motion at that very frequency. Powers of the radial displacement squared possess the constant component (4.14), which means that a potentially resonant term resulting from $\tilde{z}^{\eta-2k-1}$ is preserved when multiplied with this constant contribution from $\tilde{\rho}^{2k}$. Additionally, $\tilde{\rho}^{2k}$ contains oscillatory terms at the frequencies $1\tilde{\omega}_\mathrm{b}, 2\tilde{\omega}_\mathrm{b}, 3\tilde{\omega}_\mathrm{b}, \ldots, k\tilde{\omega}_\mathrm{b}$. However, this difference frequency $\tilde{\omega}_\mathrm{b} = \tilde{\omega}_+ - \tilde{\omega}_-$ from Equation (4.2) is generally not an integer of the axial frequency $\tilde{\omega}_z$. Therefore, mixing this frequency and its higher harmonics with the axial frequency and its higher harmonics will not result in resonant terms at the axial frequency unless for a very specific choice of the three eigenfrequencies in the trap. Such a fine-tuning will be excluded

here, and we stick with the naturally-resonant terms, which arise, well naturally, with any specific assumptions about the three eigenfrequencies.

In our notation, the naturally-resonant terms are expressed as

$$\left\langle \tilde{z}^{\eta-2k-1}\tilde{\rho}^{2k}\right\rangle_{\tilde{\omega}_z} = \left\langle \tilde{z}^{\eta-2k-1}\right\rangle_{\tilde{\omega}_z}\left\langle \tilde{\rho}^{2k}\right\rangle_{0} \quad . \tag{4.33}$$

For the sake of space and clarity, the time-dependence of the zeroth-order solutions is not shown, but the oscillatory terms remain crucial for the analysis of the frequency-components. Equations (3.2) and (3.5) show that only odd powers of $\tilde{z}$ come with an oscillatory term at the fundamental axial frequency $\tilde{\omega}_z$. Therefore, η must be even, which is incorporated by writing $\eta = 2n$, where $n = 2, 3, 4, \ldots$. The additional resonant terms, caused by the anharmonic electrostatic potential, then take the form

$$\varepsilon_z \tilde{z} = \frac{C_{2n}}{C_2}\frac{1}{d^{2n-2}}\sum_{k=0}^{n-1} a_{2n}(k)\,(n-k)\left\langle \tilde{z}^{2n-2k-1}\right\rangle_{\tilde{\omega}_z}\left\langle \tilde{\rho}^{2k}\right\rangle_{0} \tag{4.34}$$

in the effective equation of motion (3.85). The upper limit of the sum has been lowered to $n-1$, because the factor $n-k$ vanishes at the previous upper limit $k = n$. The terms in angle brackets are evaluated with Equations (3.7) and (4.14); the coefficient $a_n(k)$ is defined in Equation (2.71). The parameter ε_z that describes the strength of the additional resonant terms then becomes

$$\varepsilon_z = \frac{C_{2n}}{C_2}\frac{(2n)!}{2^{2n-1}d^{2n-2}}\sum_{k=0}^{n-1}\frac{(-1)^k\,(n-k)}{[k!(n-k)!]^2}\sum_{p=0}^{k}\left[\binom{k}{p}\right]^2 \hat{\rho}_{\pm}^{2p}\,\hat{\rho}_{\mp}^{2(k-p)}\,\hat{z}^{2(n-k-1)} \quad . \tag{4.35}$$

It is related to the first-order frequency-shift

$$\frac{\Delta\omega_z}{\omega_z} = \frac{\varepsilon_z}{2} = \frac{C_{2n}}{C_2}\frac{(2n)!}{2^{2n}}\sum_{k=0}^{n-1}\sum_{p=0}^{k}\frac{(-1)^k\,(n-k)\,\hat{\rho}_{\pm}^{2p}\,\hat{\rho}_{\mp}^{2(k-p)}\,\hat{z}^{2(n-k-1)}}{[(n-k)!\,p!\,(k-p)!]^2\,d^{2n-2}} \tag{4.36}$$

via Equation (3.86). Because the limits of the sum over p are such that no cases in the definition (3.3) of the binomial coefficient have to be distinguished, we have switched to the explicit expression with factorials. Even though there is only a single frequency-shift to be expressed here, we show the two alternatives offered by Equation (4.14) for the choice of the amplitudes $\hat{\rho}_{\pm}$, in order to underline that the frequency-shift is symmetric with respect to the amplitudes of radial modes. Moreover, the two alternatives will show their benefit later in Section 4.3.1, when calculating frequency-shifts in axial lock. Even with a particular choice of either alternative here, the symmetry with respect to the amplitudes of radial modes is confirmed by sending $p \to k - p$ in Equation (4.36). It means that the first-order axial frequency-shift caused by electrostatic imperfections does not change when the amplitudes of the two radial modes are swapped. Essentially, this is due to the coupling being mediated nonresonantly through powers of the average radial displacement squared. This degeneracy of the axial frequency-shift with respect to the radial modes is lifted as soon as velocities play a role.

If the amplitudes of both radial modes vanish $\hat{\rho}_+ = \hat{\rho}_- = 0$, the only contributions to the shift come from $p = 0$ and $k = 0$. As a small cross-check, the result (3.90) for the one-dimensional

case is reproduced. As a more comprehensive benchmark, the frequency-shift (4.36) agrees with Equation (3.57) from Reference [99] assuming $c_2 = 1$ in their notation.[11]

The linear gradient C_1 Even though the resonant terms that drive the first-order frequency-shift of the axial mode have been identified and treated completely, one particular nonresonant term deserves a special mention. The contribution by C_1 is a constant one, whereas the effect of all other odd terms on the fundamental mode essentially averages to zero in first order. As in the one-dimensional case of Section 3.2, C_1 alone is not a source of anharmonicity, and it could be dealt with exactly, if there were no higher-order terms, even when the radial modes are included. As the corresponding potential $\Phi_1 \propto z$ without any dependence on the radial coordinate ρ, the radial modes are not affected directly. Since Φ_1 does not change the curvature of the potential along the axial direction, the axial frequency is no affected either. In the otherwise ideal PENNING trap, only the center of the oscillations will be shifted, which does not matter in a uniform magnetic field. In reality, the particle will experience a different magnetic field strength, which will change the radial frequencies (2.23) via the change of the free-space cyclotron-frequency (2.18), even before considering anharmonic terms. Therefore, the effect of C_1 must be examined more carefully than the impact of other odd terms. However, C_1 typically does not come separately from other odd terms, because PENNING traps do not resemble plate capacitors (for which the C_1 alone would describe the electric potential entirely). From first principles such as the geometry of the trap, it is hard to argue that C_1 must be much larger than other odd coefficients, whereas the dominance of C_2 over other even coefficients could be ensured by the hyperboloidal shape of the electrodes. Moreover, a general comparison of even and odd terms is difficult because the latter are created by applying an additional offset voltage on top of the usual trap voltage V_0. Hence, there is no general estimate for their influence.

The first strategy is to treat C_1 perturbatively by working with the modified zeroth-order solution

$$\tilde{z}'(t) = \tilde{z}(t) - \frac{C_1}{2C_2} d \quad , \tag{4.37}$$

which includes the shift of the equilibrium position in the absence of anharmonic terms.[12] Although calculating powers of $\tilde{z}'(t)$ becomes more tedious, the first-order result is unchanged. There is no direct effect of C_1 because the additional term has to propagate through the spatial

[11] Owing to their definition (3.38) of the electrostatic potential without the global prefactor of ½ present in Equation (2.58) here, the perturbation parameters c_η in Reference [99] do not have the same value as the C_η here, when they describe an identical imperfection. In this case, their relation is $c_\eta = 2^{(\eta-2)/2} C_\eta$, which means that at least the parameter for the quadrupole contribution has the same value for both definitions: $c_2 = C_2$. The characteristic trap dimension d from Equation (2.10) here is related to d_r from Reference [99] as $d_\mathrm{r} = \sqrt{2}d$ (with the subscript added because the characteristic trap dimension uses the same symbol in both cases). The effect of the different definitions cancels in the expression for the frequency-shift because of the prefactor $c_\eta / d_\mathrm{r}^{\eta-2} = C_\eta / d^{\eta-2}$. In fact, the prefactors $c_\eta / d_\mathrm{r}^{\eta}$ and $C_\eta / (2d^\eta)$ of the electrostatic potential represent only a single degree of freedom, and the aforementioned two relations for the perturbation parameters and the characteristic trap dimension ensure that this one factor is equal, if the same potential is described.

[12] The sign is different from a similar operation performed in Equation (3.13), because here a given solution is shifted to oscillate around the new equilibrium position, whereas the coordinate system was shifted in Equation (3.13). In both cases, the new equilibrium position is the same.

dependence of the other imperfections before showing up as a frequency-shift. Being associated with a product of other imperfections means that the frequency-shift caused by C_1 is at least of second order. In fact, it is caused in combination with an imperfection, not by C_1 alone. The other imperfections associated with an odd coefficient give rise to a second-order frequency-shift alone, which does not exclude combinations, of course. In the case of C_1, the second-order effects may partly lead to frequency-shifts independent of the motional amplitudes. When it comes to the design of PENNING traps, the frequency-shift by C_1C_3 to the axial mode is often mentioned as a means to measure the product of the two coefficients, which are of the same order of magnitude [48, 51, 53]. For such harmonic shifts caused by the electrostatic potential, the mechanism is similar to the aforementioned one for the particle being moved to a different position in the magnetic field. At the new equilibrium position, the higher-order terms in the electrostatic potential also contribute to its local curvature, thereby changing the effective C_2. While a global change of C_2 in the ideal PENNING trap shifts the eigenfrequencies individually, Equations (2.25) and (2.27) for the free-space cyclotron-frequency ω_c remain valid. Therefore, the major experimental concern is that the equilibrium position shifts over the course of a measurement. If it is always the same, a different approach to C_1 may be more convenient.

The second strategy is to develop the electric potential and the magnetic field around the new equilibrium position, where there is no local C_1 because of the saddle point in the potential. The perturbative treatment then proceeds as before. Only the values of the parameters C_η and B_η need to be adjusted accordingly. In particular, breaking the reflection symmetry of the PENNING trap about the xy-plane results in perturbation parameters with odd coefficients, and their associated frequency-shifts require second-order perturbation theory for a quantitative statement as before.

Shifts to the radial modes

Inserting the two radial components (4.30) of the additional electric field into Equation (4.31) yields the radial equations of motion

$$\begin{pmatrix}\ddot{x}\\ \ddot{y}\end{pmatrix} = \omega_\mathrm{c}\begin{pmatrix}\dot{y}\\ -\dot{x}\end{pmatrix} + \frac{\omega_z^2}{2}\begin{pmatrix}x\\ y\end{pmatrix}\left[1 - \frac{C_\eta}{C_2}\frac{2}{d^{\eta-2}}\sum_{k=1}^{\lfloor \eta/2\rfloor} a_\eta(k)\, k\, z^{\eta-2k}\rho^{2k-2}\right] \quad , \tag{4.38}$$

with the unperturbed axial frequency ω_z defined in Equation (2.17). The strategy is the same as for the axial mode: plug in the zeroth-order solutions from Equations (3.94)–(3.96) and search for additional terms that are proportional to components of these solutions. These resonant terms as given by Equations (3.100) and (3.101) for the two radial modes are collected in the effective equations of motion (3.105) and translated into the first-order frequency-shift according to Equation (3.109b). At this point, it is obvious that additional resonant terms will originate from the second term in square brackets in Equation (4.38). However, we must not simply average over the term, considering only its constant contribution, because of resonant mixing of $\tilde{\rho}^{2k-2}$ with $\tilde{x}$ and $\tilde{y}$, which contain oscillatory terms at two frequencies, namely $\tilde{\omega}_\pm$. Powers of the radial displacement squared contain, among others, an oscillatory component at the difference frequency $\tilde{\omega}_\mathrm{b}$ of the radial modes, and there is a fixed phase relationship with respect to the two radial modes. This means that mixing can produce resonant terms. Formally, the laws of

multiplying two trigonometric functions (see Equations (C.10) and (C.11) in the appendix)

$$\left\langle \cos(\tilde{\chi}_+ - \tilde{\chi}_-)\cos(\tilde{\chi}_\mp)\right\rangle_{\tilde{\omega}_\pm} = \frac{1}{2}\cos(\tilde{\chi}_\pm) \quad , \tag{4.39}$$

$$\left\langle \cos(\tilde{\chi}_+ - \tilde{\chi}_-)\sin(\tilde{\chi}_\mp)\right\rangle_{\tilde{\omega}_\pm} = \frac{1}{2}\sin(\tilde{\chi}_\pm) \tag{4.40}$$

show that multiplying an oscillatory term at one radial frequency with a term at the difference frequency $\tilde{\omega}_\mathrm{b}$ results in a resonant term at the frequency of the other radial mode. The second term at the frequency $|\tilde{\omega}_\pm - 2\tilde{\omega}_\mp|$ is dismissed as nonresonant. While there is the relation (4.2) between $\tilde{\omega}_\mathrm{b}$ and the radial frequencies $\tilde{\omega}_\pm$, the axial frequency $\tilde{\omega}_z$ is generally not an integer of the radial frequencies. Therefore, mixing oscillatory terms at the axial frequency $\tilde{\omega}_z$ and its multiples with oscillatory terms at the radial frequencies $\tilde{\omega}_\pm$ as well as the difference frequency $\tilde{\omega}_\mathrm{b}$ and its multiples will generally result in nonresonant terms. The resonances in the radial modes themselves are preserved by multiplying these naturally-resonant terms with the constant contribution from the axial mode. In our notation, this is written as

$$\left\langle \tilde{z}^{\eta-2k}\tilde{\rho}^{2k-2}\tilde{x}\right\rangle_{\tilde{\omega}_\pm} = \left\langle \tilde{z}^{\eta-2k}\right\rangle_0 \left\langle \tilde{\rho}^{2k-2}\tilde{x}\right\rangle_{\tilde{\omega}_\pm} \tag{4.41}$$

with $\tilde{x}$ as an example, which is no restriction. Equation (4.40) shows that the same mechanism also works for $\tilde{y}$ in the same way Equation (4.39) applies to $\tilde{x}$. Therefore, we will show the calculation only for one of the two radial coordinates. The additional resonant terms are described by the same parameter, $\varepsilon_\pm$ in this case, for both radial coordinates, because cylindrical symmetry does not allow a favored radial direction.

According to Equations (3.2) and (3.5), only even powers of $\tilde{z}$ come with a constant contribution. Consequently, η in the exponent $\eta - 2k$ has to be even, which is ensured by the choice $\eta = 2n$. The additional naturally-resonant terms caused by the anharmonic electric field are then included as

$$\varepsilon_\pm \tilde{x}_\pm = -\frac{C_{2n}}{C_2}\frac{2}{d^{2n-2}}\sum_{k=1}^{n} a_{2n}(k)\; k \left\langle \tilde{z}^{2(n-k)}\right\rangle_0 \left\langle \tilde{\rho}^{2k-2}\tilde{x}\right\rangle_{\tilde{\omega}_\pm} \tag{4.42}$$

in the effective equations of motion (3.105). The coefficient $a_n(k)$ is defined in Equation (2.71); the constant contribution from the axial mode is calculated with Equation (3.6). Given the two mechanisms for creating resonant terms at the radial frequencies, the second term in angle brackets needs a closer inspection. Formally, the two mechanisms read

$$\left\langle \tilde{\rho}^{2k-2}\tilde{x}\right\rangle_{\tilde{\omega}_\pm} = \left\langle \tilde{\rho}^{2k-2}\right\rangle_0 \tilde{x}_\pm + \left\langle \left\langle \tilde{\rho}^{2k-2}\right\rangle_{\tilde{\omega}_\mathrm{b}} \tilde{x}_\mp\right\rangle_{\tilde{\omega}_\pm} \quad . \tag{4.43}$$

The abbreviation $\tilde{x}_\pm$ is defined in Equation (3.100). Firstly, the zeroth-order solution $\tilde{x}$ already contains the two resonant terms $\tilde{x}_\pm$, and these terms are preserved by multiplying them with the constant contribution in $\tilde{\rho}^{2k-2}$. Secondly, multiplying an oscillatory term at the frequency $\tilde{\omega}_\mathrm{b}$ with a term at the radial frequency $\tilde{\omega}_\mp$ results in a resonant term at the other radial frequency $\tilde{\omega}_\pm$.

With these two mechanisms for producing resonant terms, there is no double counting; no original term is used twice for the same purpose. Since $\tilde{x}_\pm$ is multiplied with clearly distinct

components of $\tilde{\rho}$, the same term can rightfully influence the frequency $\tilde{\omega}_\pm$ directly, and the frequency $\tilde{\omega}_\mp$ indirectly via the interplay of the two radial modes. The second possibility vanishes if the other radial mode has zero amplitude, as $\tilde{\rho}^2$ is constant in this case, with the oscillatory term being absent.

In any case, the constant component of $\tilde{\rho}^{2k-2}$ is given by Equation (4.14) and the first term on the right-hand side of Equation (4.43) becomes

$$\left\langle \tilde{\rho}^{2k-2} \right\rangle_0 \tilde{x}_\pm = \tilde{x}_\pm \sum_{p=0}^{k-1} \left[\binom{k-1}{p} \right]^2 \hat{\rho}_\pm^{2p} \hat{\rho}_\mp^{2(k-1-p)} \quad . \tag{4.44}$$

The oscillatory component of $\tilde{\rho}^{2k-2}$ at the frequency $\tilde{\omega}_\mathrm{b}$ is given by Equation (4.24). With these two results, the second term on the right-hand side of Equation (4.43) becomes

$$\left\langle \left\langle \tilde{\rho}^{2k-2} \right\rangle_{\tilde{\omega}_\mathrm{b}} \tilde{x}_\mp \right\rangle_{\tilde{\omega}_\pm} = \left\langle \cos(\tilde{\chi}_\mathrm{b}) \cos(\tilde{\chi}_\mp) \right\rangle_{\tilde{\omega}_\pm} \hat{\rho}_\mp \frac{2\hat{\rho}_\pm}{\hat{\rho}_\mp} \sum_{p=0}^{k-1} \binom{k-1}{p} \binom{k-1}{p+1} \hat{\rho}_\pm^{2p} \hat{\rho}_\mp^{2(k-1-p)} \tag{4.45a}$$

$$= \tilde{x}_\pm \sum_{p=0}^{k-1} \binom{k-1}{p} \binom{k-1}{p+1} \hat{\rho}_\pm^{2p} \hat{\rho}_\mp^{2(k-1-p)} \quad . \tag{4.45b}$$

The second step uses Equation (4.39) for the product of trigonometric functions. The choice of radial amplitudes $\hat{\rho}_\pm$ is such that the prefactor $\hat{\rho}_\pm / \hat{\rho}_\mp$ cancels the amplitude $\hat{\rho}_\mp$ from $\tilde{x}_\mp$ and creates the amplitude $\hat{\rho}_\pm$ necessary to write the final result as proportional to $\tilde{x}_\pm$. As discussed before, the same mechanism also works for $\tilde{y}_\pm$ from Equation (3.101) with the help of the trigonometric identity (4.40). Basically, the substitution $\cos(\tilde{\chi}_\mp) \to -\sin(\tilde{\chi}_\mp)$ is made as $\tilde{x}_\pm$ is replaced by $\tilde{y}_\pm$.

The two terms in Equations (4.44) and (4.45b) share a common binomial coefficient. The two different binomial coefficients are added using the identity

$$\binom{k-1}{p} + \binom{k-1}{p+1} = \frac{(k-1)!}{p!(k-1-p)!} + \frac{(k-1)!}{(p+1)!(k-p-2)!} \tag{4.46a}$$

$$= \frac{(k-1)!}{(p+1)!(k-p-1)!} \left[(p+1) + (k-p-1) \right] \tag{4.46b}$$

$$= \frac{k!}{(p+1)!(k-p-1)!} = \binom{k}{p+1} \quad . \tag{4.46c}$$

Using the explicit expression with factorials for the second binomial coefficient is not fine for $p = k-1$, a case encountered at the upper limit of the sum over p in Equation (4.45b). Fortunately, Equation (4.46c) still holds in this case as

$$\binom{k-1}{k-1} + \binom{k-1}{k} = \binom{k-1}{k-1} + 0 = 1 = \binom{k}{k} \tag{4.47}$$

according to the definition (3.3) of the binomial coefficient. As $p > k-1$ always gives zero in Equations (4.46a) and (4.46c), this identity for binomial coefficients holds for $p \geq 0$ in general. Here, it is sufficient to hold in the range of the summation from 0 to $k-1$.

Finally, adding Equations (4.44) and (4.45b) yields

$$\left\langle \tilde{\rho}^{2k-2}\tilde{x}\right\rangle_{\tilde{\omega}_\pm} = \tilde{x}_\pm \sum_{p=0}^{k-1} \binom{k-1}{p}\binom{k}{p+1} \hat{\rho}_\pm^{2p}\,\hat{\rho}_\mp^{2(k-1-p)} \tag{4.48}$$

for the resonant term in Equation (4.43). With this result, the parameter $\varepsilon_\pm$ in Equation (4.42) is expressed as

$$\varepsilon_\pm = -\frac{C_{2n}}{C_2}\frac{(2n)!}{2^{2n-1}}\frac{1}{d^{2n-2}} \sum_{k=1}^{n} \frac{(-1)^k k}{[k!(n-k)!]^2} \sum_{p=0}^{k-1} \binom{k-1}{p}\binom{k}{p+1} \hat{\rho}_\pm^{2p}\,\hat{\rho}_\mp^{2(k-1-p)}\,\hat{z}^{2(n-k)} \quad . \tag{4.49}$$

The first-order frequency-shift then results from Equation (3.109b) as

$$\Delta\omega_\pm = \frac{\pm\omega_+\omega_-}{\omega_+ - \omega_-}\frac{C_{2n}}{C_2}\frac{(2n)!}{2^{2n-1}}\frac{1}{d^{2n-2}} \sum_{k=1}^{n}\sum_{p=0}^{k-1} \frac{(-1)^k\,(p+1)\,\hat{\rho}_\pm^{2p}\,\hat{\rho}_\mp^{2(k-1-p)}\,\hat{z}^{2(n-k)}}{[(n-k)!\,(k-p-1)!\,(p+1)!]^2} \quad . \tag{4.50}$$

Because the limits of the sum over p allow to express the binomial coefficients explicitly in a consistent manner with factorials, we have done so by writing

$$\binom{k-1}{p}\binom{k}{p+1} = \frac{(k-1)!}{p!\,(k-1-p)!}\frac{k!}{(p+1)!\,(k-p-1)!} \tag{4.51a}$$

$$= \frac{p+1}{k}\frac{(k!)^2}{[(k-p-1)!\,(p+1)!]^2} \quad , \tag{4.51b}$$

thereby facilitating the comparison with Equation (3.56) in Reference [99], even though the expression do not yet have the identical form. After a few transformations not shown here, including Equation (2.26) and a shift of the summation variable $p \to p-1$, there is agreement.

By sending the summation variable $p \to k-1-p$ in Equation (4.50), the exponents of the radial amplitudes $\hat{\rho}_\pm$ are swapped. The overall result

$$\Delta\omega_\pm = \frac{\pm\omega_+\omega_-}{\omega_+ - \omega_-}\frac{C_{2n}}{C_2}\frac{(2n)!}{2^{2n-1}}\frac{1}{d^{2n-2}} \sum_{k=1}^{n}\sum_{p=0}^{k-1} \frac{(-1)^k\,(k-p)\,\hat{\rho}_\mp^{2p}\,\hat{\rho}_\pm^{2(k-1-p)}\,\hat{z}^{2(n-k)}}{[(n-k)!\,p!\,(k-p)!]^2} \tag{4.52}$$

is different from the one obtained by simply substituting $\hat{\rho}_\pm \to \hat{\rho}_\mp$. It becomes clear that, unlike for the axial frequency-shift (4.36), the first-order frequency-shift to the radial frequencies $\tilde{\omega}_\pm$ is not symmetric with respect to the amplitudes $\hat{\rho}_\pm$ of the radial modes. Technically, this is a consequence of the mechanism for creating resonant terms described by Equation (4.45a). While the oscillatory components (4.24) at the fundamental frequency $\tilde{\omega}_\mathrm{b}$ of powers of radial displacement squared is still symmetric with respect to the amplitudes $\hat{\rho}_\pm$, multiplying it with $\tilde{x}_\mp$ in order to create a resonant terms proportional to $\tilde{x}_\pm$ invokes the amplitudes $\hat{\rho}_\pm$ in an asymmetric way.

Although there is no symmetry for the frequency-shift to one radial mode when the two radial amplitudes are swapped, Equations (4.50) and (4.52) show that there is a simple connection between the shifts to the two different radial modes before and after swapping. In fact, the shift

to the reduced cyclotron-frequency before swapping the amplitudes differs from the shift to the magnetron frequency after the swapping operation only by a sign. The absolute value is the same. As a formula, this statement reads

$$\Delta\omega_+(\hat{\rho}_{\text{set}}, \hat{\rho}_{\text{cool}}, \hat{z}) = -\Delta\omega_-(\hat{\rho}_{\text{cool}}, \hat{\rho}_{\text{set}}, \hat{z}) \quad . \tag{4.53}$$

The arguments in brackets are the amplitudes $\hat{\rho}_+, \hat{\rho}_-, \hat{z}$ of the reduced cyclotron mode, the magnetron mode, and the axial mode in this particular order. The peculiar subscripts will be motivated in the next paragraph. Here, they merely serve to differentiate the variables $\hat{\rho}_\pm$ from specific values because using $\hat{\rho}_\pm$ after swapping the values of the two radial amplitudes is confusing.

The cyclotron sideband The cyclotron sideband is defined in Equation (2.25) as the sum of the two radial frequencies. Consequently, the shift to the cyclotron-sideband frequency is given by

$$\Delta\omega_{\text{c}} = \Delta\omega_+ + \Delta\omega_- \quad . \tag{4.54}$$

Adding Equation (4.50) for $\Delta\omega_+$ and Equation (4.52) for $\Delta\omega_-$ yields

$$\Delta\omega_{\text{c}} = \frac{\omega_+\omega_-}{\omega_+ - \omega_-}\frac{C_{2n}}{C_2}\frac{(2n)!}{2^{2n-1}}\frac{1}{d^{2n-2}}\sum_{k=1}^{n}\frac{(-1)^k\hat{z}^{2(n-k)}}{[(n-k)!]^2}\sum_{p=0}^{k-1}\frac{\hat{\rho}_+^{2p}\hat{\rho}_-^{2(k-1-p)}}{[p!\,(k-p-1)!]^2}\left[\frac{1}{p+1}-\frac{1}{k-p}\right] \quad . \tag{4.55}$$

Sending the summation variable $p \to k-1-p$ swaps the exponent of the radial amplitudes. Again, the result

$$\Delta\omega_{\text{c}} = -\frac{\omega_+\omega_-}{\omega_+ - \omega_-}\frac{C_{2n}}{C_2}\frac{(2n)!}{2^{2n-1}}\frac{1}{d^{2n-2}}\sum_{k=1}^{n}\frac{(-1)^k\hat{z}^{2(n-k)}}{[(n-k)!]^2}\sum_{p=0}^{k-1}\frac{\hat{\rho}_-^{2p}\hat{\rho}_+^{2(k-1-p)}}{[p!\,(k-p-1)!]^2}\left[\frac{1}{p+1}-\frac{1}{k-p}\right] \tag{4.56}$$

is not the same obtained by simply substituting $\hat{\rho}_\pm \to \hat{\rho}_\mp$, but, this time, the only difference is a sign. Thus, the shift to the sideband cyclotron-frequency is antisymmetric with respect to the radial amplitudes. In particular, the shift vanishes for equal radial amplitudes. In the explicit expressions for the first few C_{2n} in References [18, 99], the root $(\hat{\rho}_+^2 - \hat{\rho}_-^2)$ of the polynomial for the frequency-shift is factored out, and the practical importance of the antisymmetry is discussed in Reference [12]. The asymmetry is also seen in Reference [22]. Thanks to the general treatment here, the antisymmetry is now understood as a general feature of the first-order frequency-shift caused by cylindrically-symmetric electrostatic imperfections. Going back to Equation (4.53), the antisymmetry of the shift to the sideband cyclotron-frequency with respect to the radial amplitudes should come as no surprise. Swapping the radial amplitudes in the shifts to the two frequencies that make up the sideband leads to

$$\Delta\omega_{\text{c}}(\hat{\rho}_{\text{set}}, \hat{\rho}_{\text{cool}}, \hat{z}) = \Delta\omega_+(\hat{\rho}_{\text{set}}, \hat{\rho}_{\text{cool}}, \hat{z}) + \Delta\omega_-(\hat{\rho}_{\text{set}}, \hat{\rho}_{\text{cool}}, \hat{z}) \tag{4.57a}$$

$$= -\Delta\omega_-(\hat{\rho}_{\text{cool}}, \hat{\rho}_{\text{set}}, \hat{z}) - \Delta\omega_+(\hat{\rho}_{\text{cool}}, \hat{\rho}_{\text{set}}, \hat{z}) = -\Delta\omega_{\text{c}}(\hat{\rho}_{\text{cool}}, \hat{\rho}_{\text{set}}, \hat{z}) \quad . \tag{4.57b}$$

The interest in, or obsession with, swapping the amplitudes of the radial modes is well motivated by the experimental techniques exploiting the sideband identity (2.25). The time-of-flight ion cyclotron-resonance technique [62] scans the conversion of an initial magnetron amplitude into the amplitude of the modified cyclotron-motion. For a quadrupole coupling scheme, be it single pulse [87] or Ramsey [91], the parameters are typically chosen such that the conversion is complete if the frequency of the coupling pulse coincides with the sideband frequency of the trapped ion.

As an upgrade of the traditional method, the two radial frequencies have recently been measured sequentially [42] by means of a phase-sensitive method [43] which images the ion's radial position in the trap at the moment of ejection. The two individually measured radial frequencies are then added to determine the free-space cyclotron-frequency ω_c via the sideband identity (2.25). For measuring the radial frequency $\tilde{\omega}_\pm$, the corresponding radial mode is excited to the amplitude $\hat{\rho}_\pm = \hat{\rho}_{\text{set}}$, and the phase is then allowed to evolve freely for some time. During this evolution time, the amplitude of the other radial mode remains $\hat{\rho}_\mp = \hat{\rho}_{\text{cool}}$. If the relevant amplitudes are equal for both measurements, the identity (4.53) holds, and the anharmonic shifts caused by cylindrically-symmetric electrostatic imperfections cancel in the sideband identity

$$\omega_c = \omega_+(\hat{\rho}_{\text{set}}, \hat{\rho}_{\text{cool}}, \hat{z}) + \omega_-(\hat{\rho}_{\text{cool}}, \hat{\rho}_{\text{set}}, \hat{z}) \quad . \tag{4.58}$$

Of course, the sequential measurement offers no protection against harmonic frequency-shifts, for instance caused by voltage drifts or fluctuations of the magnetic field. The anharmonic shifts also depend on the harmonic frequencies in the ideal trap, but both the anharmonic shifts and the harmonic shifts caused by fluctuations are expected to be small. Therefore, controlling the amplitudes is probably the major challenge in maintaining the perfect cancellation of anharmonic shifts in Equation (4.58). Depending on the scheme for biasing the trap electrodes, the effective C_η may be a function of voltages and hence be effected by voltage drifts, too. However, the anharmonic frequency-shifts depend most strongly, at least quadratically, on the amplitudes.

4.1.3. Magnetostatic imperfections

Conceptually, the calculation of the first-order frequency-shifts caused by static cylindrically-symmetric magnetic imperfections is very similar to the calculation for electrostatic imperfections in Section 4.1.2. In fact, the mechanisms for producing naturally-resonant terms are the same, but, technically, deriving the expressions for the frequency-shifts is slightly more complicated. Because the Lorentz force (2.13) created by a magnetic field depends on the velocity of the charged particle, plugging in the zeroth-order velocity components (3.97)–(3.99) results in additional factors of $\tilde{\omega}_i$ for each eigenmode. This complication is not present for electrostatic imperfections, where the additional terms contain coordinates, but not velocities. Nevertheless, the calculation in this section is not just about velocities. The zeroth-order trajectories (3.94)–(3.96) will be equally important, because the additional magnetic field is a function of coordinates, too.

With the additional magnetic field $\vec{B}_\eta$ from Equation (2.77), the original equations of mo-

tion (2.16) in the ideal PENNING trap become

$$\begin{pmatrix}\ddot{x}\\ \ddot{y}\\ \ddot{z}\end{pmatrix} = \omega_\mathrm{c}\begin{pmatrix}\dot{y}\\ -\dot{x}\\ 0\end{pmatrix} + \frac{\omega_\mathrm{c}}{B_0}\begin{pmatrix}\dot{y}B_\eta^{(z)} - \dot{z}B_\eta^{(y)}\\ \dot{z}B_\eta^{(x)} - \dot{x}B_\eta^{(z)}\\ \dot{x}B_\eta^{(y)} - \dot{y}B_\eta^{(x)}\end{pmatrix} + \frac{\omega_z^2}{2}\begin{pmatrix}x\\ y\\ -2z\end{pmatrix} \quad . \tag{4.59}$$

The unperturbed axial frequency ω_z is given by Equation (2.17). In order to move closer to the form of the effective radial equations of motion (3.105), we have written the charge-to-mass ratio as $q/m = \omega_\mathrm{c}/B_0$, in agreement with the definition (2.17) of the free-space cyclotron-frequency ω_c. By writing the radial unit vector with Cartesian coordinates as in Equation (4.29), the radial magnetic field $B_\eta^{(\rho)}$ from Equation (2.80) is related to its two Cartesian components as

$$\begin{pmatrix}B_\eta^{(x)}\\ B_\eta^{(y)}\end{pmatrix} = \frac{B_\eta^{(\rho)}(\rho,z)}{\rho}\begin{pmatrix}x\\ y\end{pmatrix} = B_\eta \sum_{k=1}^{\left\lfloor\frac{\eta+1}{2}\right\rfloor} \tilde{a}_\eta(k)\, z^{\eta-2k+1}\rho^{2k-2}\begin{pmatrix}x\\ y\end{pmatrix} \quad . \tag{4.60}$$

Like for the radial electric field (4.30), there are only even powers of radial displacement. Consequently, the identities from Section 4.1.1 for powers of radial displacement squared apply. As with electrostatic imperfections, we will deal with the axial and the radial modes separately.

Shifts to the axial mode

With the radial magnetic field (4.60), the axial equation of motion is read off from the third component of Equation (4.59) as

$$\ddot{z} + \omega_z^2 z - \omega_\mathrm{c}\frac{B_\eta}{B_0}\left(\sum_{k=1}^{\left\lfloor\frac{\eta+1}{2}\right\rfloor} \tilde{a}_\eta(k)\, z^{\eta-2k+1}\rho^{2k-2}\right)(\dot{x}y - \dot{y}x) = 0 \quad . \tag{4.61}$$

As usual, we will now plug in the zeroth-order trajectories (3.94)–(3.96) and velocities (3.97)–(3.99), looking for terms that are proportional to these zeroth-order solutions. For the second term in brackets, the cross-product of coordinates and velocities, we define and evaluate the abbreviation

$$\tilde{\xi}(t) = \dot{\tilde{x}}(t)\tilde{y}(t) - \dot{\tilde{y}}(t)\tilde{x}(t) \tag{4.62}$$

$$= \hat{\rho}_+^2\tilde{\omega}_+ + \hat{\rho}_-^2\tilde{\omega}_- + \hat{\rho}_+\hat{\rho}_-(\tilde{\omega}_+ + \tilde{\omega}_-)\cos(\tilde{\chi}_+ - \tilde{\chi}_-) \quad . \tag{4.63}$$

It has a constant term and an oscillatory term at the difference frequency $\tilde{\omega}_\mathrm{b} = \tilde{\omega}_+ - \tilde{\omega}_-$ of the radial modes. Originating from the radial modes, there is no term related to the axial frequency $\tilde{\omega}_z$. As for electrostatic imperfections, naturally-resonant terms at the axial frequency arise from the axial motion, and these terms need to be preserved by multiplying them only with the constant contribution from the radial modes. As a formula, this mechanism reads

$$\left\langle \tilde{z}^{\eta-2k+1}\tilde{\rho}^{2k-2}\tilde{\xi}\right\rangle_{\tilde{\omega}_z} = \left\langle \tilde{z}^{\eta-2k+1}\right\rangle_{\tilde{\omega}_z}\left\langle \tilde{\rho}^{2k-2}\tilde{\xi}\right\rangle_0 \quad . \tag{4.64}$$

According to Equations (3.2) and (3.5), only odd powers of $\tilde{z}$ possess an oscillatory term at the axial frequency $\tilde{\omega}_z$. Thus, η has to be even for the exponent $\eta - 2k + 1$ to be odd, and we ensure

this property by writing $\eta = 2n$. The additional resonant terms in the effective axial equation of motion (3.85) are then given by

$$\varepsilon_z \tilde{z} = -\frac{\omega_\mathrm{c}}{\omega_z^2}\frac{B_{2n}}{B_0}\sum_{k=1}^{n}\tilde{a}_{2n}(k)\left\langle \tilde{z}^{2(n-k)+1}\right\rangle_{\tilde{\omega}_z}\left\langle \tilde{\rho}^{2(k-1)}\tilde{\xi}\right\rangle_0 \quad . \tag{4.65}$$

The factor of ω_z^2 in the denominator was introduced because the anharmonic term in Equation (4.61) does not contain the axial frequency, whereas Equation (3.85) does in $\omega_z^2\varepsilon_z\tilde{z}$. The coefficient $\tilde{a}_{2n}(k)$ is defined in Equation (2.81); the contribution by the axial motion is determined from Equation (3.7). It is the second term in angle brackets that needs a closer look. Both $\tilde{\rho}^{2(k-1)}$ and $\tilde{\xi}$ have a constant component. For $k > 1$, they both have an oscillatory term at the frequency $\tilde{\omega}_\mathrm{b}$, and these oscillatory terms may produce a constant component by mixing, too. Formally, the mechanism for producing constant terms is written as

$$\left\langle \tilde{\rho}^{2(k-1)}\tilde{\xi}\right\rangle_0 = \left\langle \tilde{\rho}^{2(k-1)}\right\rangle_0\left\langle \tilde{\xi}\right\rangle_0 + \left\langle \left\langle \tilde{\rho}^{2(k-1)}\right\rangle_{\tilde{\omega}_\mathrm{b}}\left\langle \tilde{\xi}\right\rangle_{\tilde{\omega}_\mathrm{b}}\right\rangle_0 \quad . \tag{4.66}$$

The first-term on the right-hand side becomes

$$\left\langle \tilde{\rho}^{2(k-1)}\right\rangle_0\left\langle \tilde{\xi}\right\rangle_0 = \tilde{\omega}_+\hat{\rho}_+^2\left\{\sum_{p=0}^{k-1}\left[\binom{k-1}{p}\right]^2\hat{\rho}_+^{2p}\hat{\rho}_-^{2(k-1-p)}\right\} + \tilde{\omega}_-\hat{\rho}_-^2\left\{\sum_{p=0}^{k-1}\left[\binom{k-1}{p}\right]^2\hat{\rho}_-^{2p}\hat{\rho}_+^{2(k-1-p)}\right\} \tag{4.67}$$

with Equations (4.14) and (4.63). The choice of the radial amplitudes $\hat{\rho}_\pm$ in Equation (4.14) is such that both terms on the right-hand side of Equation (4.67) have an identical structure with respect to the substitution $\pm \rightarrow \mp$, which would convert one term into the other.

With Equations (4.24) and (4.63), and the trigonometric identity

$$[\cos(\tilde{\chi}_\mathrm{b})]^2 = \frac{1}{2}\left[1 + \cos(2\tilde{\chi}_\mathrm{b})\right] \tag{4.68}$$

as a special case of Equation (3.2) or Equation (3.6) for $n = 0$, the second term on the right-hand side of Equation (4.66) becomes

$$\begin{aligned}\left\langle \left\langle \tilde{\rho}^{2(k-1)}\right\rangle_{\tilde{\omega}_\mathrm{b}}\left\langle \tilde{\xi}\right\rangle_{\tilde{\omega}_\mathrm{b}}\right\rangle_0 = \tilde{\omega}_+\hat{\rho}_+^2&\left\{\sum_{p=0}^{k-1}\binom{k-1}{p}\binom{k-1}{p+1}\hat{\rho}_+^{2p}\hat{\rho}_-^{2(k-1-p)}\right\}\\ &+ \tilde{\omega}_-\hat{\rho}_-^2\left\{\sum_{p=0}^{k-1}\binom{k-1}{p}\binom{k-1}{p+1}\hat{\rho}_-^{2p}\hat{\rho}_+^{2(k-1-p)}\right\} \quad .\end{aligned} \tag{4.69}$$

Again, the choice of radial amplitudes $\hat{\rho}_\pm$ in Equation (4.24) is such that the two resulting terms on the right-hand side of Equation (4.69) have an identical structure upon the substitution $\pm \rightarrow \mp$. For this particular choice, the prefactor $\hat{\rho}_\pm/\hat{\rho}_\mp$ from Equation (4.24) cancels a factor of $\hat{\rho}_\mp$ in Equation (4.63). Hence, the prefactors of the sums in Equation (4.69) are $\tilde{\omega}_\pm\hat{\rho}_\pm^2$, like

in Equation (4.67). Aided by the similar form of the sums, adding these two equations is straightforward and yields

$$\left\langle \tilde{\rho}^{2(k-1)}\tilde{\xi}\right\rangle_0 = \tilde{\omega}_+\hat{\rho}_+^2\left\{\sum_{p=0}^{k-1}\binom{k-1}{p}\binom{k}{p+1}\hat{\rho}_+^{2p}\hat{\rho}_-^{2(k-1-p)}\right\} + \tilde{\omega}_-\hat{\rho}_-^2\left\{\sum_{p=0}^{k-1}\binom{k-1}{p}\binom{k}{p+1}\hat{\rho}_-^{2p}\hat{\rho}_+^{2(k-1-p)}\right\} \quad . \tag{4.70}$$

The common binomial coefficient in Equations (4.67) and (4.69) remains. The other two binomial coefficients were combined using the identity (4.46c).

So far, the particular choice of the radial amplitudes $\hat{\rho}_\pm$ has enabled an easy summation of the terms with the common prefactor $\tilde{\omega}_\pm\hat{\rho}_\pm^2$. At this point, the two sums on the right-hand side of Equation (4.70) should be combined to give a polynomial with terms that will turn out to be of the kind $\hat{\rho}_+^{2p}\hat{\rho}_-^{2(k-p)}$. To this end, the summation variable is transformed as $p \to p-1$ in the first term

$$\tilde{\omega}_+\hat{\rho}_+^2\sum_{p=0}^{k-1}\binom{k-1}{p}\binom{k}{p+1}\hat{\rho}_+^{2p}\hat{\rho}_-^{2(k-1-p)} = \tilde{\omega}_+\sum_{p=0}^{k}\binom{k-1}{p-1}\binom{k}{p}\hat{\rho}_+^{2p}\hat{\rho}_-^{2(k-p)} \tag{4.71}$$

and as $p \to k-p-1$ in the second term

$$\tilde{\omega}_-\hat{\rho}_-^2\sum_{p=0}^{k-1}\binom{k-1}{p}\binom{k}{p+1}\hat{\rho}_-^{2p}\hat{\rho}_+^{2(k-1-p)} = \tilde{\omega}_-\sum_{p=0}^{k}\binom{k-1}{p}\binom{k}{p}\hat{\rho}_+^{2p}\hat{\rho}_-^{2(k-p)} \quad . \tag{4.72}$$

Apart from using the identity (3.4) for the binomial coefficients in Equation (4.72), we have included vanishing contributions at the lower and upper limits of the summation in Equations (4.71) and (4.72), respectively. In this way, the limits of the summation are equal, and both sums are combined easily, finally completing Equation (4.66) for the constant contribution from the radial modes as

$$\left\langle \tilde{\rho}^{2(k-1)}\tilde{\xi}\right\rangle_0 = \sum_{p=0}^{k}\binom{k}{p}\left[\tilde{\omega}_+\binom{k-1}{p-1} + \tilde{\omega}_-\binom{k-1}{p}\right]\hat{\rho}_+^{2p}\hat{\rho}_-^{2(k-p)} \quad . \tag{4.73}$$

Finally, the parameter ε_z in Equation (4.65) is given by

$$\varepsilon_z = -\frac{B_{2n}}{B_0}\frac{\omega_\mathrm{c}}{\omega_z^2}\frac{(2n)!}{2^{2n-1}}\sum_{k=1}^{n}\frac{(-1)^k\,k}{[k!(n-k)!]^2}\frac{\hat{z}^{2(n-k)}}{n-k+1}\sum_{p=0}^{k}\binom{k}{p}\left[\tilde{\omega}_+\binom{k-1}{p-1} + \tilde{\omega}_-\binom{k-1}{p}\right]\hat{\rho}_+^{2p}\hat{\rho}_-^{2(k-p)} \tag{4.74}$$

and it is related to the first-order frequency-shift by Equation (3.86), which would still contain perturbed frequencies (namely $\tilde{\omega}_\pm$) and ideal ones (notably ω_z and ω_c) at this point. However, we are allowed to make the switch $\tilde{\omega}_\pm \to \omega_\pm$ without incurring an error of first order in the

frequency-shift. Since the presence of the perturbation parameter B_{2n} signals that ε_z is at least of first order right away, only the zeroth-order contribution in the perturbed frequencies $\tilde{\omega}_\pm$ will contribute to the first-order frequency-shift. What is the zeroth-order part of the perturbed frequency $\tilde{\omega}_i$? Well, that is the unperturbed frequency ω_i.

More practically, the argument concerning the replacement also works in the opposite direction. For the calculation of first-order frequency-shifts, the frequencies ω_i the ion would have in the ideal trap are allowed to be replaced by the perturbed frequencies $\tilde{\omega}_i$. Whereas the latter are measured in the experiment, the former may not be known right away. If they were known precisely enough, for instance from design considerations (and a superior mass model or a different mass-measurement technique), there would be no point in measuring them. Experiments work the other way around, inferring physical quantities from the measured frequencies, possibly with a little help from corrections. The ideal frequencies are typically not known until these corrections are applied.

Probably because the starting point of the theoretical treatment is the ideal Penning trap, with imperfections being considered an addition rather than a nuisance to be removed by correcting for its effect, it is common to show the frequency-shifts in terms of the unperturbed frequencies. In this tradition, the first-order axial frequency-shift caused by a static cylindrically-symmetric magnetic imperfection becomes

$$\begin{aligned}\frac{\Delta\omega_z}{\omega_z} = -\frac{B_{2n}}{B_0}\frac{\omega_+ + \omega_-}{\omega_+\omega_-}\frac{(2n)!}{2^{2n+1}}\sum_{k=1}^{n}\frac{(-1)^k\,k}{[k!(n-k)!]^2}\frac{\hat{z}^{2(n-k)}}{n-k+1} \\ \cdot\sum_{p=0}^{k}\binom{k}{p}\left[\omega_+\binom{k-1}{p-1}+\omega_-\binom{k-1}{p}\right]\hat{\rho}_+^{2p}\hat{\rho}_-^{2(k-p)} \quad ,\end{aligned} \tag{4.75}$$

where we have used Equations (2.25) and (2.26) in order to express all the frequencies on the right-hand side in terms of the radial frequencies $\omega_\pm$. Unlike for the frequency-shifts caused by electrostatic imperfections, we will not use the explicit expression (3.3) for the binomial coefficients because two cases would have to be treated separately, for instance by splitting the sum over p. The binomial coefficient associated with the reduced cyclotron-frequency ω_+ vanishes for $p = 0$, and the binomial coefficient associated with the magnetron frequency ω_- vanishes for $p = k$. Using the binomial coefficients rather than an explicit expression with factorials has these exceptions covered conveniently with a single sum.

Because the binomial coefficient with ω_+ vanishes for $p = 0$, the dependence on the amplitudes would not be approximated correctly, if the binomial coefficient with ω_- were dropped altogether in general. Of course, it is tempting to neglect the term with ω_- against the one with ω_+ (provided the second one exists), because a typical experiment often has $|\omega_+| \gg |\omega_-|$. However, the relative scaling of the two binomial coefficients works against this property for large k and small p. Since for $1 \leq p \leq k-1$, the ratio of the binomial coefficients inside the square brackets in Equation (4.75) is given by

$$\frac{\binom{k-1}{p}}{\binom{k-1}{p-1}} = \frac{\dfrac{(k-1)!}{p!\,(k-1-p)!}}{\dfrac{(k-1)!}{(p-1)!\,(k-p)!}} = \frac{k-p}{p} = \frac{k}{p} - 1 \quad , \tag{4.76}$$

the largest boost for a given k is achieved for the smallest p, the maximum boost factor being $k-1$ in the case of $p=1$. Thus, a general approximation, for large n in particular, is impossible. We will stick with the full expression (4.75), leaving possible approximations in a specific case to the reader's discretion.

Sending the summation variable $p \to k-p$ in Equation (4.75) swaps the exponents of the radial amplitudes $\hat{\rho}_\pm$ and $\hat{\rho}_\mp$, but the obtained frequency-shift

$$\begin{aligned}\frac{\Delta\omega_z}{\omega_z} = &-\frac{B_{2n}}{B_0}\frac{\omega_+ + \omega_-}{\omega_+\omega_-}\frac{(2n)!}{2^{2n+1}}\sum_{k=1}^{n}\frac{(-1)^k\,k}{[k!(n-k)!]^2}\frac{\hat{z}^{2(n-k)}}{n-k+1} \\ &\cdot\sum_{p=0}^{k}\binom{k}{p}\left[\omega_+\binom{k-1}{p}+\omega_-\binom{k-1}{p-1}\right]\hat{\rho}_-^{2p}\,\hat{\rho}_+^{2(k-p)} \quad ,\end{aligned} \tag{4.77}$$

is not reproduced by simply substituting $\hat{\rho}_\pm \to \hat{\rho}_\mp$. Thus, unlike the axial frequency-shift (4.36) caused by cylindrically-symmetric electrostatic imperfections, this frequency-shift is not symmetric with respect to the radial modes. Given that velocities matter for the forces created by magnetic imperfections, this lack of symmetry comes as no surprise, because amplitudes typically enter with an additional factor of frequency for the corresponding mode. Mathematically, Equation (4.75) transforms into Equation (4.77) and vice versa upon the substitutions $\hat{\rho}_\pm \to \hat{\rho}_\mp$ and $\omega_\pm \to \omega_\mp$, because these two quantities entirely characterize the effect of the radial modes on the axial frequency-shift. When the frequencies are swapped, the amplitudes change their meaning as well. Confirming this experimentally useless symmetry serves as a minor cross-check of the frequency-shift.

The more comprehensive test would be Equation (3.73) in Reference [99]. Unfortunately, the general expression for frequency-shift does not depend on the perturbation parameter b_{2n}, the equivalent of B_{2n}, and it does not have the unit of frequency. Moreover, the expression $\overline{W_1}^{(2n,k)}$ does not seem to be defined, the closest matches being $\overline{W_1}^{(2n)}$, $\overline{W}_\pm^{(2n,k)}$ or $S^{(2n,k)}$.

In our case, Equations (4.75) and (4.77) are summarized as

$$\begin{aligned}\frac{\Delta\omega_z}{\omega_z} = &-\frac{B_{2n}}{B_0}\frac{\omega_+ + \omega_-}{\omega_+\omega_-}\frac{(2n)!}{2^{2n+1}}\sum_{k=1}^{n}\frac{(-1)^k\,k}{[k!(n-k)!]^2}\frac{\hat{z}^{2(n-k)}}{n-k+1} \\ &\cdot\sum_{p=0}^{k}\binom{k}{p}\left[\omega_\pm\binom{k-1}{p-1}+\omega_\mp\binom{k-1}{p}\right]\hat{\rho}_\pm^{2p}\,\hat{\rho}_\mp^{2(k-p)} \quad .\end{aligned} \tag{4.78}$$

Even though there is no obvious application for the two choices of subscripts here, this expression will be beneficial for calculating the shifts under lock in Section 4.3.1.

Some of the specific shifts to the axial frequency in this section have also been estimated from the axial magnetic field alone without considering the equations of motion in the radial magnetic field [96]. In this framework, the effect of the radial modes on the axial frequency is modeled as the interaction of their magnetic moment with the imperfections of the axial magnetic field, which works well for B_2 [150]. However, this method is hard to generalize. In the case of B_2, the method profits from the quadratic dependence on z of the additional axial field. The energy of a magnetic moment in this field then gives rise to an axial force that is

proportional to z, like the axial force caused by the electrostatic quadrupole potential of the ideal PENNING trap. Thus, there are no anharmonic terms with respect to the axial amplitude, which is no longer the case for higher-order terms in the magnetic field. Chapter F in the appendix takes a critical look at the model. Fortunately, the concept of a magnetic moment is not required when the axial equation of motion with the radial magnetic field is considered. It is this field, not the axial one, that couples the radial modes to the axial motion. Of course, the axial and the radial magnetic fields are related because, together, they have to fulfill MAXWELL's equation. Mathematically, this connection is expressed by the fact that both fields are derived from the same scalar potential (2.75).

Coming back to the anharmonic frequency-shift as a function of the axial amplitude $\hat{z}$, it is worth noting that the sum over k in Equation (4.78) starts at 1 rather than 0. For $k = p = 0$, there is no dependence on the radial amplitudes $\hat{\rho}_{\pm}$ and $\hat{\rho}_{\mp}$. In all other cases, either p or $k - p$ is different from zero, and at least one of the two radial amplitudes remains. This means that the axial amplitude $\hat{z}$ always shows up in a product with at least one radial amplitude (both to some power of at least 2). Thus, the axial amplitude $\hat{z}$ never reaches the maximum exponent $2n$ the two radial amplitudes have, when they show up on their own. In other words, there is no solo $\hat{z}^{2n}$ term, and the frequency-shift vanishes if the amplitudes of the radial modes are zero. A look at the spatial dependence of radial magnetic field (2.80) or Equation (4.60) explains why the axial amplitude $\hat{z}$ must enter as a product with the amplitude of a radial mode. As the radial magnetic field vanishes on the z-axis, an excursion in the radial direction is required in order to sample the effects of this field.

Shifts to the radial modes

The radial equations of motion are the first two components of Equation (4.59). They contain the axial magnetic field $B_{\eta}^{(z)}$ from Equation (2.78) and the two components of the radial magnetic field from Equation (4.60). The axial magnetic field is combined with a velocity component in the radial plane; the radial magnetic field is multiplied with the axial velocity. Both combinations will be examined for resonant terms at the radial frequencies separately. We have seen before that naturally-resonant terms at the radial frequencies originate from the radial modes. Because mixing such a resonant term with an oscillatory component at the axial frequency and its higher harmonics generally leads to nonresonant terms, a constant contribution from the axial mode is required to preserve the terms at the radial frequencies.

For the terms associated with the radial magnetic field (4.60), the dependence on the axial coordinate and velocity takes the form

$$\dot{z} z^{\eta-2k+1} = \frac{1}{\eta - 2k + 2} \frac{\mathrm{d}}{\mathrm{d}t} z^{\eta-2k+2} \quad . \tag{4.79}$$

We have introduced the time-derivative in order to facilitate the frequency-analysis, after plugging in the zeroth-order trajectory (3.96). With $\tilde{z}$ oscillating at the axial frequency $\tilde{\omega}_z$, taking $\tilde{z}^{\eta-2k+2}$ leads to higher harmonics, and to a constant term, if the exponent $\eta - 2k + 2$ is even, as shown by Equations (3.2) and (3.5). In any case, the constant, or time-independent, term is removed by the time-derivative, whereas the frequencies of the individual oscillatory terms are left unchanged. Therefore, $\dot{\tilde{z}} \tilde{z}^{\eta-2k+1}$ does not possess a constant contribution, which

excludes the radial magnetic field as a source of naturally-resonant terms, because oscillatory terms at the radial frequencies cannot be preserved. This leaves the additional axial magnetic field (2.78) as the remaining source of first-order frequency-shifts, and the radial equations of motion simplify to

$$\begin{pmatrix}\ddot{x}\\ \ddot{y}\end{pmatrix} = \omega_\mathrm{c}\begin{pmatrix}\dot{y}\\ -\dot{x}\end{pmatrix}\left[1 + \frac{B_\eta}{B_0}\sum_{k=0}^{\lfloor \eta/2\rfloor} a_\eta(k)\, z^{\eta-2k}\rho^{2k}\right] + \frac{\omega_z^2}{2}\begin{pmatrix}x\\ y\end{pmatrix} \tag{4.80}$$

for the search of naturally-resonant terms. As before, we will now plug in the zeroth-order trajectories (3.94)–(3.96), and velocities (3.97) and (3.98), while looking for terms proportional to the components $\dot{\tilde{x}}_\pm$ and $\dot{\tilde{y}}_\pm$, defined in Equation (3.102) and (3.103). The mechanism for creating and preserving oscillatory terms at the radial frequencies is formally expressed as

$$\left\langle \tilde{z}^{\eta-2k}\tilde{\rho}^{2k}\dot{\tilde{y}}\right\rangle_{\tilde{\omega}_\pm} = \left\langle \tilde{z}^{\eta-2k}\right\rangle_0 \left\langle \tilde{\rho}^{2k}\dot{\tilde{y}}\right\rangle_{\tilde{\omega}_\pm} \quad . \tag{4.81}$$

The naturally-resonant terms are preserved by multiplying them with the constant contribution from the axial mode. For $\tilde{z}^{\eta-2k}$ to have such a constant contribution, Equations (3.2) and (3.5) require the exponent $\eta - 2k$ be even. The obvious choice to guarantee this parity is $\eta = 2n$. The additional terms in the effective equations of motion (3.105) are then given by

$$\beta_\pm\dot{\tilde{y}}_\pm = \frac{B_{2n}}{B_0}\sum_{k=0}^{n} a_{2n}(k)\,\left\langle \tilde{z}^{2(n-k)}\right\rangle_0 \left\langle \tilde{\rho}^{2k}\dot{\tilde{y}}\right\rangle_{\tilde{\omega}_\pm} \quad . \tag{4.82}$$

The coefficient $a_{2n}(k)$ is defined in Equation (2.71); the constant contribution by the axial mode is given by Equation (3.6). In analogy to Equation (4.43) for the radial frequency-shifts caused by electrostatic imperfections, the dual mechanism for producing resonant terms at the radial frequencies is written as

$$\left\langle \tilde{\rho}^{2k}\dot{\tilde{y}}\right\rangle_{\tilde{\omega}_\pm} = \left\langle \tilde{\rho}^{2k}\right\rangle_0 \dot{\tilde{y}}_\pm + \left\langle \left\langle \tilde{\rho}^{2k}\right\rangle_{\tilde{\omega}_\mathrm{b}} \dot{\tilde{y}}_\mp\right\rangle_{\tilde{\omega}_\pm} \quad . \tag{4.83}$$

Firstly, a resonant term at the frequency $\tilde{\omega}_\pm$ is preserved by multiplying it with the constant contribution in $\tilde{\rho}^{2k}$. Secondly, mixing a resonant term at the frequency $\tilde{\omega}_\mp$ with a term at the frequency $\tilde{\omega}_\mathrm{b} = \tilde{\omega}_+ - \tilde{\omega}_-$ results in a resonant term at the other radial frequency $\tilde{\omega}_\pm$. The first term in Equation (4.83) is directly evaluated with Equation (4.14) for the constant component of $\tilde{\rho}^{2k}$. The second term requires Equation (4.24) for the oscillatory component of $\tilde{\rho}^{2k}$, and the trigonometric identity (4.39) to give

$$\left\langle \left\langle \tilde{\rho}^{2k}\right\rangle_{\tilde{\omega}_\mathrm{b}} \dot{\tilde{y}}_\mp\right\rangle_{\tilde{\omega}_\pm} = -\left\langle \cos(\tilde{\chi}_\mathrm{b})\cos(\tilde{\chi}_\mp)\right\rangle_{\tilde{\omega}_\pm} \tilde{\omega}_\mp\hat{\rho}_\mp\frac{2\hat{\rho}_\pm}{\hat{\rho}_\mp}\sum_{p=0}^{k}\binom{k}{p}\binom{k}{p+1}\hat{\rho}_\pm^{2p}\hat{\rho}_\mp^{2(k-p)} \tag{4.84a}$$

$$= \dot{\tilde{y}}_\pm\frac{\tilde{\omega}_\mp}{\tilde{\omega}_\pm}\sum_{p=0}^{k}\binom{k}{p}\binom{n}{p+1}\hat{\rho}_\pm^{2p}\hat{\rho}_\mp^{2(k-p)} \quad . \tag{4.84b}$$

Like in the corresponding Equation (4.45a) for electrostatic imperfections, the prefactor $\hat{\rho}_\pm/\hat{\rho}_\mp$ from Equation (4.24) is used to express the final result, which initially starts out with $\dot{\tilde{y}}_\mp$, as

proportional to the velocity $\dot{\tilde{y}}_\pm$ of the other radial mode. Because of the velocities involved here, the additional factor of $\tilde{\omega}_\mp/\tilde{\omega}_\pm$ originates from the amplitudes of $\dot{\tilde{y}}_\pm = -\tilde{\omega}_\pm\hat{\rho}_\pm\cos(\tilde{\chi}_\pm)$. Thanks to the trigonometric identity (4.40), the mechanism carries over to $\dot{\tilde{x}}_\pm = -\tilde{\omega}_\pm\hat{\rho}_\pm\sin(\tilde{\chi}_\pm)$ and hence applies to the second component in the equations of motion (4.80), too.

With these results for the two terms on the right-hand side of Equation (4.83), the resonant terms at the radial frequencies are

$$\left\langle\tilde{\rho}^{2k}\dot{\tilde{y}}\right\rangle_{\tilde{\omega}_\pm} = \dot{\tilde{y}}_\pm\sum_{p=0}^{k}\binom{k}{p}\left[\binom{k}{p}+\frac{\tilde{\omega}_\mp}{\tilde{\omega}_\pm}\binom{k}{p+1}\right]\hat{\rho}_\pm^{2p}\,\hat{\rho}_\mp^{2(k-p)} \quad . \tag{4.85}$$

The parameter $\beta_\pm$ in Equation (4.82) is then identified as

$$\beta_\pm = \frac{B_{2n}}{B_0}\frac{(2n)!}{2^{2n}}\sum_{k=0}^{n}\frac{(-1)^k\,\hat{z}^{2(n-k)}}{[k!(n-k)!]^2}\sum_{p=0}^{k}\binom{k}{p}\left[\binom{k}{p}+\frac{\tilde{\omega}_\mp}{\tilde{\omega}_\pm}\binom{k}{p+1}\right]\hat{\rho}_\pm^{2p}\,\hat{\rho}_\mp^{2(k-p)} \tag{4.86}$$

and related to the first-order frequency-shift

$$\Delta\omega_\pm = \pm\frac{B_{2n}}{B_0}\frac{\omega_+ + \omega_-}{\omega_+ - \omega_-}\frac{(2n)!}{2^{2n}}\sum_{k=0}^{n}\frac{(-1)^k\,\hat{z}^{2(n-k)}}{[k!(n-k)!]^2}\sum_{p=0}^{k}\binom{k}{p}\left[\omega_\pm\binom{k}{p}+\omega_\mp\binom{k}{p+1}\right]\hat{\rho}_\pm^{2p}\,\hat{\rho}_\mp^{2(k-p)} \tag{4.87}$$

with the help of Equation (3.109b). As for the axial frequency-shift (4.75) before, we have made the switch $\tilde{\omega}_\pm \to \omega_\pm$ from the perturbed frequencies to the frequencies in the ideal Penning trap. The frequency-shift remains correct to first order.

By sending the summation variable $p \to k - p$, the exponents of the radial amplitudes $\hat{\rho}_\pm$ are swapped. Rewritten in this way, it becomes obvious that the frequency-shift

$$\Delta\omega_\pm = \pm\frac{B_{2n}}{B_0}\frac{\omega_+ + \omega_-}{\omega_+ - \omega_-}\frac{(2n)!}{2^{2n}}\sum_{k=0}^{n}\frac{(-1)^k\,\hat{z}^{2(n-k)}}{[k!(n-k)!]^2}\sum_{p=0}^{k}\binom{k}{p}\left[\omega_\pm\binom{k}{p}+\omega_\mp\binom{k}{p-1}\right]\hat{\rho}_\mp^{2p}\,\hat{\rho}_\pm^{2(k-p)} \tag{4.88}$$

is not symmetric with respect to the radial amplitudes, because the result is not obtained from Equation (4.87) by simply substituting $\hat{\rho}_\pm \to \hat{\rho}_\mp$. The same was noted for the radial frequency-shift (4.52) caused by electrostatic imperfections, and the technical explanation carries over from there. Here, Equation (4.84a) shows that creating the resonant term $\dot{\tilde{y}}_\pm$ at the frequency $\tilde{\omega}_\pm$ by mixing $\dot{\tilde{y}}_\mp$ at $\tilde{\omega}_\mp$ with an oscillatory component at $\tilde{\omega}_\mathrm{b}$ does away with the symmetry that is still present for the oscillatory component (4.24) at $\tilde{\omega}_\mathrm{b}$ in powers of the radial displacement squared. Moreover, velocities matter for the additional forces created by magnetic imperfections, and the velocities associated with the individual modes depend on the respective frequencies in addition to the amplitudes. Therefore, a symmetry with respect to the amplitude of the radial modes alone would be dubious.

Of course, there is the technical symmetry of swapping the meaning of the modes, expressed by the substitution $\hat{\rho}_\pm \to \hat{\rho}_\mp$ and $\omega_\pm \to \omega_\mp$. This symmetry is expressed by the two alternatives in Equations (4.87) and (4.88). It can be exploited when evaluating the general formula for specific shifts. Suppose the shift to the reduced cyclotron-frequency has been coded as a function $\Delta\omega_+(\omega_+, \hat{\rho}_+, \omega_-, \hat{\rho}_-, \hat{z})$, with the five variables having their obvious meanings. The first

two terms in brackets describe the modified cyclotron-mode, the following two the magnetron mode, and the last one is the placeholder for the axial amplitude. Then, the shift to the magnetron frequency for these conditions is calculated by evaluating $\Delta\omega_+(\omega_-, \hat{\rho}_-, \omega_+, \hat{\rho}_+, \hat{z})$. In other words, the values for the frequencies and amplitudes of the radial modes are plugged in at the opposite spot for the other radial mode, which yields the shift to the other radial frequency. This behavior is essentially the equivalent of Equation (4.53) for the shifts caused by electrostatic imperfections to the radial frequencies. Equation (4.53) has an extra minus, because swapping the frequencies was not considered back then with the frequencies showing up as a global prefactor. In Equations (4.50) and (4.87), the term $\omega_+ - \omega_-$ in the denominator inverts the sign upon swapping the frequencies such that the $\pm$ sign for the shifts $\Delta\omega_\pm$ to the two radial frequencies is correctly reproduced from the single function $\Delta\omega_+(\omega_+, \hat{\rho}_+, \omega_-, \hat{\rho}_-, \hat{z})$. For these considerations and exploitations of symmetries, it is of course crucial not to approximate the denominator with ω_+ or ω_c, which provides one good reason for dropping the approximation $|\omega_+| \gg |\omega_-|$.

When comparing with Equation (3.74) from Reference [99] as a general test case, we face the same problem as for the shift caused by magnetic imperfections to the axial frequency: the general expression does not depend on the perturbation parameter and it fails dimensional analysis.

Because the binomial coefficients nicely handle the exceptions for $p = k$ and $p = 0$ in Equations (4.87) and (4.88), respectively, we will not switch to the explicit expressions (3.3). Partly because of these exceptions, we will not attempt any approximations despite the typical relation $|\omega_+| \gg |\omega_-|$ between the radial frequencies. Additionally, the scaling of the two binomial coefficients that are multiplied with the radial frequencies $\omega_\pm$ and $\omega_\mp$ in Equations (4.87) works against this relation for large k, which implies large n. According to Equation (4.76), the most extreme ratios occur either for small or large p. The details about which of the two binomial coefficients dominates in which of two cases are of little interest here. Having ruled out an approximation valid for all n, we stick with the most general expression here, just like for the axial frequency-shift (4.78) caused by magnetic imperfections.

The cyclotron sideband According to the sideband identity (2.25), the shift to the cyclotron-sideband frequency is given by the sum of the individual shifts to the radial modes. Thus, adding Equation (4.87) for $\Delta\omega_+$ and Equation (4.88) for $\Delta\omega_-$ leads to

$$\begin{aligned}\Delta\omega_\mathrm{c} = \frac{B_{2n}}{B_0}\frac{\omega_\mathrm{c}}{\omega_+ - \omega_-}\frac{(2n)!}{2^{2n}}\sum_{k=0}^{n}\frac{(-1)^k\,\hat{z}^{2(n-k)}}{[k!(n-k)!]^2}\sum_{p=0}^{k}\binom{k}{p} \\ \cdot\left\{\omega_+\left[\binom{k}{p} - \binom{k}{p-1}\right] + \omega_-\left[\binom{k}{p+1} - \binom{k}{p}\right]\right\}\hat{\rho}_+^{2p}\,\hat{\rho}_-^{2(k-p)}\quad .\end{aligned} \tag{4.89}$$

Alternately, adding Equation (4.87) for $\Delta\omega_-$ and Equation (4.88) for $\Delta\omega_+$ leads to

$$\begin{aligned}\Delta\omega_\mathrm{c} = -\frac{B_{2n}}{B_0}\frac{\omega_\mathrm{c}}{\omega_+ - \omega_-}\frac{(2n)!}{2^{2n}}\sum_{k=0}^{n}\frac{(-1)^k\,\hat{z}^{2(n-k)}}{[k!(n-k)!]^2}\sum_{p=0}^{k}\binom{k}{p} \\ \cdot\left\{\omega_-\left[\binom{k}{p}-\binom{k}{p-1}\right]+\omega_+\left[\binom{k}{p+1}-\binom{k}{p}\right]\right\}\hat{\rho}_-^{2p}\,\hat{\rho}_+^{2(k-p)}\quad,\end{aligned} \tag{4.90}$$

which is also obtained by sending the summation variable $p \to k-p$ in Equation (4.89). Together, the Equations (4.89) and (4.90) show that the frequency-shift is symmetric under the combined substitution $\omega_\pm \to \omega_\mp$ and $\hat{\rho}_\pm \to \hat{\rho}_\mp$ for radial frequencies and amplitudes. In this case, the additional minus is compensated for by the denominator $\omega_+ - \omega_-$. Mathematically speaking, the variables are simply placeholders. They do not know which physical mode they are associated with here because the sideband frequency treats shifts to both radial modes equally.

Although the symmetry provides no general test, it is tremendously helpful for spotting dubious specific results. In our notation, Equation (3.79) from Reference [99] for the shift $\Delta\omega_\mathrm{c}$ caused by B_4 contains a term like $\hat{\rho}_-^4 + \hat{\rho}_+^4$, which will not switch sign when swapping the radial amplitudes. Thus, it will not undo the change of sign in the denominator $\omega_+ - \omega_-$, and we wonder about a misprint. A term like $\hat{\rho}_-^4 - \hat{\rho}_+^4$ preserves the symmetry. Similarly, the same shift in Reference [22] contains a term like $\omega_+\hat{\rho}_+^4 + \omega_-\hat{\rho}_-^4$, which faces the same problem.

4.2. Relativistic effects

This section applies the classical perturbative method outlined in Chapter 3 to the relativistic frequency-shifts caused by the motional degrees of freedom in the ideal Penning trap. Although the particular first-order formalism in Section 3.4.2 was originally conceived with cylindrically-symmetric imperfections in mind, it extends to imperfections that do not break cylindrical symmetry. Since special relativity does not introduce a preferred direction, the cylindrical symmetry of the ideal Penning trap is preserved, and this configuration, always considered in the nonrelativistic classical limit so far, is the starting point for the perturbative treatment.

Speaking of the classical limit is ambiguous when considering the effects of special relativity and quantum mechanics together, and a clarification is in order here. In the nonrelativistic limit, the velocity of the particle is much smaller than the speed of light c, which means the particle's motion is described sufficiently well by the classical Newtonian equations of motion. As there is no threshold for the onset of relativistic effects, an entirely classical regime does not exist. It is merely characterized by the fact that relativistic effects are too small to be observed. When trying to move further into the classical domain by reducing the particle's velocity, or equivalently its motional amplitudes in the Penning trap, quantization would eventually set in. For the quantum-mechanical calculation, the classical limit means that the quantum numbers are high enough such that quantization remains unobservable. Instead, the classical notion of a trajectory holds, and the eigenmotions in the Penning trap are characterized by their amplitudes rather than their quantum numbers. The eigenfrequencies are important in both cases.

In contrast to the cylindrically-symmetric imperfections, the motivation behind the calculation of relativistic frequency-shifts is not immediately obvious, neither from a mathematical nor

from a physical perspective. The relativistic shifts have been calculated before [20, 61, 99, 132], and as there is only one set of first-order frequency-shifts here, a more general result is not to be expected. Quite on the contrary, the result will even be less general, because a classical method fails to account for spin and quantization. Furthermore, the discussion in the previous paragraph raises the question whether the classical limits for relativistic and quantum-mechanical effects overlap. Indeed, most of the aforementioned references give the energy-shift of the particle as a function of its quantum numbers rather than a frequency-shift as a function of the particle's total energy or amplitudes. Of course, spin is quantized, but for the motional degrees of freedom, possible reservations against the classical limit are never made explicit. If the particle were already highly relativistic when quantization begins to fade, a perturbative treatment based on classical trajectories rather than operators and eigenstates would have little predictive power. In this case, quantization would have to be included when a perturbative treatment is justified, and once it could be neglected, the perturbative approach would become doubtful. Fortunately, this is not the case.

The importance of relativistic frequency-shifts in Penning traps is due to the precision with which frequencies can be measured rather than the extreme energy of the trapped particle. A small relativistic shift to the reduced cyclotron-frequency had to be accounted for in determining the mass of the antiproton [55]. Even when quantum numbers are high enough for a description with classical trajectories, the particle is barely relativistic, and a perturbative treatment is justified. In this classical limit of the quantum-mechanical result, Reference [20] expresses the relativistic energy-shift, given as a function of the quantum numbers, as a relativistic frequency-shift in terms of the particle's energy with the approximation $|\omega_+| \gg |\omega_-|$. Like for the shifts caused by C_4 and B_2, the quantum-mechanical result [20] is the starting point for expressing the relativistic shifts in the classical limit without this approximation [44] (see Section 4.2.4). Since a non-quantized result itself is useful for many experiments on light or highly-charged ions [7, 17, 151] and there seems to be only one major source, a check via a different method is worthwhile. In the best case, it would serve as an independent confirmation of the classical limit.

Unlike the perturbation parameters C_η and B_η associated with the cylindrically-symmetric imperfections, the relativistic perturbation cannot be tuned, and the resulting frequency-shift is determined by the eigenfrequencies and the motional amplitudes alone. On the one hand, even the ideal classical Penning trap will possess some degree of anharmonicity. On the other hand, relativistic shifts allow for a measurement of motional amplitudes—most notably the amplitude of the modified cyclotron motion [107, 130]—in the absence of other imperfections. Here, the speed of light c as the perturbation parameter is set by nature, whereas it has be determined separately for other imperfections. This determination from a measurement alone is difficult because, even with only a single eigenmode involved, the measurable frequency-shift depends on a product the perturbation parameter and powers of the amplitude.

So far, the treatment of relativistic frequency-shifts has mainly relied on quantum-mechanical operator methods. When the treatment included equations of motion, the focus was more on the excitation of the modified cyclotron-mode than on the frequency-shifts when the motional amplitudes are static. In References [52, 80], a damping term due to the emission of synchrotron radiation is considered for the modified cyclotron-motion of an electron in combination with an external drive. Reference [64] from the field of FT-ICR deals with the resonant excitation of

the modified cyclotron-motion despite relativistic mass-increase. In both cases, only one of the three eigenmodes in a PENNING trap is considered. The effect of relativistic shifts on the mass determination in an FT-ICR spectrometer is mentioned in Reference [154] without going into detail about the frequency-shifts involved. In short, I have not been able to find in the literature a general calculation of all the relativistic frequency-shifts associated with the motional degrees of freedom in the manner presented in this section.

In order to employ classical perturbation theory based on the trajectories of the nonrelativistic case as the zeroth-order solution, the relativistic equations of motion will have to be approximated in Section 4.2.1 by a power series of some perturbation parameter. Quite naturally, the speed of light c takes this role. After calculating to first order the relativistic frequency-shifts to the axial mode and the radial modes in Sections 4.2.2 and 4.2.3, respectively, Section 4.2.5 contemplates on the more familiar and intuitive picture of relativistic mass-increase.

4.2.1. Relativistic equations of motion

In close connection to the experiment, we will consider the particle in the laboratory frame, where the electromagnetic fields of the ideal PENNING trap are known right away without any LORENTZ transformations. This is the case in the rest frame of the PENNING trap, not of the particle. With this choice, the time-derivatives shown in the following (including the implicit ones hidden in velocities) are with respect to time in the lab, not to the particle's proper time. Not only are the electromagnetic fields known in the lab frame, they are also time-independent, which eliminates the complications of retardation.[13] Furthermore, we will ignore radiation damping, for instance by the emission of synchrotron radiation, which is a good assumption for particles heavier than electrons [20].

In this framework, the relativistic equation of motion for a pointlike spinless particle of charge q in electromagnetic fields is given by

$$\dot{\vec{p}} = \frac{\mathrm{d}}{\mathrm{d}t}\vec{p} = \frac{\mathrm{d}}{\mathrm{d}t}(\gamma m\vec{v}) = \dot{\gamma} m\vec{v} + \gamma m\dot{\vec{v}} = q(\vec{E} + \vec{v} \times \vec{B}) \quad , \tag{4.91}$$

where $\vec{p}$ is the particle's relativistic momentum. In addition to the *rest* mass m and the velocity $\vec{v}$, both known from the classical momentum, it comes with the LORENTZ factor

$$\gamma = \frac{1}{\sqrt{1 - v^2/c^2}} \quad , \tag{4.92}$$

where c is the speed of light. We will use $v = |\vec{v}|$ and $p = |\vec{p}|$ as an abbreviation for the length of the corresponding vectors. The right-hand side of Equation (4.91) is the LORENTZ force (2.13). In addition to the time-derivative $\dot{\vec{v}}$ of the velocity $\vec{v}$, which gives the acceleration known from NEWTON's third law (2.15), the left-hand side contains a time-derivative of the LORENTZ factor. It is conveniently related to the right-hand side of the equation of motion (4.91) by calculating

[13] This is no longer true for the fields caused by the image charges the particle induces in the trap electrodes. However, this effect may be treated as an additional perturbation. Moreover, for typical trap sizes and frequencies, the instantaneous component dominates unless for electrons [21, 67]. In any case, the shift discussed in this section is the more fundamental one, since it does not depend on the cavity that forms the PENNING trap.

the time-derivative of the particle's total energy $\mathcal{E} = \gamma mc^2$. With relativistic energy–momentum relation, the result is

$$\dot{\gamma} = \frac{1}{mc^2}\frac{\mathrm{d}}{\mathrm{d}t}\mathcal{E} = \frac{1}{mc^2}\frac{\mathrm{d}}{\mathrm{d}t}\left[\sqrt{(mc^2)^2 + (pc)^2}\right] = \frac{\dot{\vec{p}}\cdot\vec{p}}{\gamma m^2 c^2} \tag{4.93}$$

in terms of a scalar product of the particle's momentum $\vec{p}$ and its time-derivative $\dot{\vec{p}}$. The latter is given by the right-hand side of Equation (4.91). Taking into account that the force by the magnetic field is always perpendicular to the particle's momentum, or equivalently $\vec{v}\cdot(\vec{v}\times\vec{B}) = 0$, only the electric field contributes to the change of the Lorentz factor, and hence to a change of the particle's total energy. The magnetic field changes the direction of the particle's momentum, but not its magnitude. In the electromagnetic fields, the derivative of the Lorentz factor becomes

$$\dot{\gamma} = \frac{q}{\gamma mc^2}\,\vec{E}\cdot\vec{v} \tag{4.94}$$

and the relativistic equation of motion (4.91) is rewritten as

$$\dot{\vec{v}} = \frac{q}{\gamma m}\left(\vec{E} + \vec{v}\times\vec{B}\right) - \frac{q}{\gamma mc^2}\vec{v}\left(\vec{E}\cdot\vec{v}\right) \quad . \tag{4.95}$$

The classical Newtonian equation of motion is recovered in the limit of $c \to \infty$, and consequently $\gamma \to 1$. Clearly, c^{-2} would make for a good perturbation parameter, but at this point, the Lorentz factor is a still a function of c^{-2}, rather than a power series in c^{-2}. For small velocities $v \ll c$, the remedy is to expand the inverse Lorentz factor as

$$\frac{1}{\gamma} = \sqrt{1 - \frac{v^2}{c^2}} \approx 1 - \frac{v^2}{2c^2} - \cdots \quad . \tag{4.96}$$

For an ion in a Penning trap, the first-order approximation will typically do. With the expansion (4.96), the exact relativistic equations of motion (4.95) is then approximated to first-order as

$$\dot{\vec{v}} = \frac{q}{m}\left(1 - \frac{v^2}{2c^2}\right)\left(\vec{E} + \vec{v}\times\vec{B}\right) - \frac{q}{mc^2}\vec{v}\left(\vec{E}\cdot\vec{v}\right) \quad . \tag{4.97}$$

Because the last term is a relativistic correction, it came with a factor of c^{-2} from the beginning. Therefore, only the zeroth-order contribution of the inverse Lorentz factor has to be considered. With the presence of c^{-2}, its first-order correction gives rise to a term of second order—that is, c^{-4}—which we have neglected here.

So far, the treatment was general and did not assume any particular shape of the electromagnetic fields. At this point, we will plug in the electric and magnetic fields of the ideal Penning trap: $\vec{E}_2$ from Equation (2.14) and $\vec{B}_0$ from Equation (2.1). The first-order relativistic equations of motion then take the form

$$\begin{pmatrix}\ddot{x}\\ \ddot{y}\\ \ddot{z}\end{pmatrix} = \left[1 - \frac{v^2}{2c^2}\right]\frac{\omega_z^2}{2}\begin{pmatrix}x\\ y\\ -2z\end{pmatrix} + \left[1 - \frac{v^2}{2c^2}\right]\omega_\mathrm{c}\begin{pmatrix}\dot{y}\\ -\dot{x}\\ 0\end{pmatrix} - \frac{1}{c^2}\frac{\omega_z^2}{2}\begin{pmatrix}\dot{x}\\ \dot{y}\\ \dot{z}\end{pmatrix}[\dot{x}x + \dot{y}y - 2\dot{z}z] \tag{4.98}$$

with the velocity squared

$$v^2 = \dot{x}^2 + \dot{y}^2 + \dot{z}^2 \tag{4.99}$$

given by the quadratic sum of the components of the velocity vector $\vec{v}$. The axial frequency ω_z and the free-space cyclotron-frequency ω_c from the nonrelativistic case are defined in Equations (2.17) and (2.18), respectively. The dependence on the velocity squared results from the expansion of the LORENTZ factor; the last term on the right-hand side of the equations of motion (4.98) essentially results from its time-derivative.

Frequently used identities

For the calculation of the frequency-shifts caused by cylindrically-symmetric imperfections of the magnetic and electric fields in Section 4.1, powers of radial displacement squared played a crucial role. As the equations of motion (4.98) show, the velocity squared takes over this role for the relativistic frequency-shifts considered here. Therefore, we will derive some identities to be used universally throughout the calculation. Fortunately, arbitrary powers as for the radial displacement squared do not have to be considered here.

In analogy to Equation (2.45), the radial contribution to the zeroth-order velocity squared is given by

$$\dot{\tilde{x}}^2 + \dot{\tilde{y}}^2 = (\tilde{\omega}_+\hat{\rho}_+)^2 + (\tilde{\omega}_-\hat{\rho}_-)^2 + 2\tilde{\omega}_+\tilde{\omega}_-\hat{\rho}_+\hat{\rho}_- \cos(\tilde{\chi}_\mathrm{b}) \quad \text{with} \quad \tilde{\chi}_\mathrm{b} = \tilde{\chi}_+ - \tilde{\chi}_- \quad , \tag{4.100}$$

where the unperturbed frequencies ω_i have been replaced by the perturbed or relativistic[14] ones $\tilde{\omega}_i$. There is the constant component

$$\left\langle \dot{\tilde{x}}^2 + \dot{\tilde{y}}^2 \right\rangle_0 = (\tilde{\omega}_+\hat{\rho}_+)^2 + (\tilde{\omega}_-\hat{\rho}_-)^2 \tag{4.101}$$

and the oscillatory component

$$\left\langle \dot{\tilde{x}}^2 + \dot{\tilde{y}}^2 \right\rangle_{\tilde{\omega}_\mathrm{b}} = 2\tilde{\omega}_+\tilde{\omega}_-\hat{\rho}_+\hat{\rho}_- \cos(\tilde{\omega}_\mathrm{b} t + \tilde{\varphi}_\mathrm{b}) \tag{4.102}$$

at the difference frequency $\tilde{\omega}_\mathrm{b} = \tilde{\omega}_+ - \tilde{\omega}_-$. As a reminder of the abbreviation $\tilde{\chi}_i$ defined in Equation (3.104) for the total phase, we have shown the explicit time-dependence for the argument of the trigonometric function here. We have also used the notation $\langle\cdot\rangle_\omega$ to retrieve the oscillatory term at the frequency ω from the term in angle brackets.

The last term in the equations of motion (4.98) contains products of the three coordinates with their corresponding velocity components. As a special case of Equation (4.79), these terms are expressed as

$$\dot{x}x = \frac{1}{2}\frac{\mathrm{d}}{\mathrm{d}t}x^2 \tag{4.103}$$

[14] Since, unlike the cylindrically-symmetric imperfections, relativistic effects cannot be eliminated, referring to them as perturbations in the true sense of the word might not be doing them true justice. Perhaps, the classical limit should instead be denounced as an effective theory that is far less general. However, the relativistic terms are perturbations in the sense of perturbation theory, and we will therefore use perturbed and relativistic frequencies interchangeably.

with a time-derivative, where x is used as an example here. Of course, the same expression also holds for y and z. For analyzing the frequency spectrum of these terms after plugging in the zeroth-order trajectory (3.94)–(3.96) and velocity (3.97)–(3.99), the same argument as before applies. Any constant (or time-independent) term in, say, $\tilde{x}^2$ is removed by taking the time-derivative, whereas the frequency of the oscillatory terms is not affected. The oscillatory terms will have to be calculated; the constant contribution does not exist:

$$\left\langle \dot{\tilde{x}}\tilde{x} \right\rangle_0 = \left\langle \dot{\tilde{y}}\tilde{y} \right\rangle_0 = \left\langle \dot{\tilde{z}}\tilde{z} \right\rangle_0 = 0 \quad . \tag{4.104}$$

The overall contribution

$$\dot{\tilde{x}}\tilde{x} + \dot{\tilde{y}}\tilde{y} = -\hat{\rho}_+\hat{\rho}_- \left(\tilde{\omega}_+ - \tilde{\omega}_-\right) \sin(\tilde{\chi}_+ - \tilde{\chi}_-) \tag{4.105}$$

from the radial modes oscillates at the difference frequency $\tilde{\omega}_\mathrm{b}$. As predicted by Equation (4.104), there is no constant term in the sum, because there is none in the two individual terms.

4.2.2. Shifts to the axial mode

The axial equation of motion

$$\ddot{z} + \omega_z^2 \left[z \left(1 - \frac{v^2}{2c^2} \right) + \frac{\dot{z}(\dot{x}x + \dot{y}y - 2\dot{z}z)}{2c^2} \right] = 0 \tag{4.106}$$

is the third component of Equation (4.98). As usual, we will now insert the zeroth-order trajectories (3.94)–(3.96) and velocities (3.97)–(3.99), looking for terms that fit into the effective axial equation of motion (3.85). For the axial mode, these are terms proportional to $\tilde{z}$. The identities derived at the end of the last subsection will provide some shortcuts.

Naturally-resonant terms at the axial frequency $\tilde{\omega}_z$ originate from the axial motion itself, while including the frequencies of the radial modes by means of mixing typically leads to nonresonant contributions. In order to preserve terms at the axial frequency, a constant contribution is required from the radial modes, whenever they are involved here. For the last term inside the square brackets in the axial equation of motion (4.106), the mechanism for generating naturally-resonant terms at the axial frequency $\tilde{\omega}_z$ is formally expressed as

$$\left\langle \dot{\tilde{z}} \left(\dot{\tilde{x}}\tilde{x} + \dot{\tilde{y}}\tilde{y} - 2\dot{\tilde{z}}\tilde{z} \right) \right\rangle_{\tilde{\omega}_z} = \left\langle \dot{\tilde{z}} \right\rangle_{\tilde{\omega}_z} \left\langle \dot{\tilde{x}}\tilde{x} + \dot{\tilde{y}}\tilde{y} \right\rangle_0 - 2 \left\langle \tilde{z}\dot{\tilde{z}}^2 \right\rangle_{\tilde{\omega}_z} \quad . \tag{4.107}$$

As Equation (4.105) shows that there is no constant contribution from the radial modes, only the last term remains. Its time-dependence is of the form

$$\cos(\tilde{\chi}_z)[\sin(\tilde{\chi}_z)]^2 = \cos(\tilde{\chi}_z) - [\cos(\tilde{\chi}_z)]^3 = \frac{\cos(\tilde{\chi}_z) - \cos(3\tilde{\chi}_z)}{4} \quad , \tag{4.108}$$

where we have used Equation (3.5) in order to express cosine cubed as a sum of oscillatory terms. The component at the fundamental axial frequency $\tilde{\omega}_z$ is

$$\left\langle \tilde{z}\,\dot{\tilde{z}}^2 \right\rangle_{\tilde{\omega}_z} = \frac{1}{4}\tilde{\omega}_z^2\hat{z}^3 \cos(\tilde{\omega}_z t + \tilde{\varphi}_z) = \frac{1}{4}(\tilde{\omega}_z\hat{z})^2\,\tilde{z} \quad . \tag{4.109}$$

We have absorbed one factor of $\hat{z}$ in the zeroth-order solution $\tilde{z}$ from Equation (3.96). Overall, Equation (4.107) evaluates to

$$\left\langle \dot{\tilde{z}} \left(\dot{\tilde{x}}\tilde{x} + \dot{\tilde{y}}\tilde{y} - 2\dot{\tilde{z}}\tilde{z} \right) \right\rangle_{\tilde{\omega}_z} = -2 \left\langle \tilde{z}\dot{\tilde{z}}^2 \right\rangle_{\tilde{\omega}_z} = -\frac{1}{2}(\tilde{\omega}_z \hat{z})^2 \, \tilde{z} \quad . \tag{4.110}$$

Next, we examine the term $v^2 z$ in axial equation of motion (4.106). Naturally-resonant terms at the axial frequency $\tilde{\omega}_z$ are produced in the same way as before. Formally, this mechanism reads

$$\left\langle \tilde{z} \left(\dot{\tilde{x}}^2 + \dot{\tilde{y}}^2 + \dot{\tilde{z}}^2 \right) \right\rangle_{\tilde{\omega}_z} = \left\langle \dot{\tilde{x}}^2 + \dot{\tilde{y}}^2 \right\rangle_0 \left\langle \tilde{z} \right\rangle_{\tilde{\omega}_z} + \left\langle \tilde{z}\, \dot{\tilde{z}}^2 \right\rangle_{\tilde{\omega}_z} \tag{4.111a}$$

$$= \left[(\tilde{\omega}_+ \hat{\rho}_+)^2 + (\tilde{\omega}_- \hat{\rho}_-)^2 \right] \tilde{z} + \frac{(\tilde{\omega}_z \hat{z})^2}{4} \tilde{z} \quad . \tag{4.111b}$$

The final step uses the constant contribution (4.101) from the radial modes, and Equation (4.109) for the contribution by the axial mode.

Collecting the resonant terms from Equations (4.110) and (4.111b) leads to the effective equation of motion

$$\ddot{\tilde{z}} + \omega_z^2 \tilde{z} \left[1 - \frac{(\tilde{\omega}_+ \hat{\rho}_+)^2 + (\tilde{\omega}_- \hat{\rho}_-)^2 + \frac{(\tilde{\omega}_z \hat{z})^2}{4}}{2c^2} - \frac{\frac{(\tilde{\omega}_z \hat{z})^2}{2}}{2c^2} \right] = 0 \quad , \tag{4.112}$$

from which the parameter

$$\varepsilon_z = -\frac{1}{2c^2} \left[(\tilde{\omega}_+ \hat{\rho}_+)^2 + (\tilde{\omega}_- \hat{\rho}_-)^2 + \frac{3}{4}(\tilde{\omega}_z \hat{z})^2 \right] \tag{4.113}$$

in Equation (3.85) is read off. With the help of Equation (3.86), the parameter ε_z is related to the first-order frequency-shift

$$\frac{\Delta\omega_z}{\omega_z} = \frac{\varepsilon_z}{2} = -\frac{1}{4c^2} \left[(\omega_+ \hat{\rho}_+)^2 + (\omega_- \hat{\rho}_-)^2 + \frac{3}{4}(\omega_z \hat{z})^2 \right] \quad . \tag{4.114}$$

Here, we have switched from the relativistic frequencies $\tilde{\omega}_i$ to the frequencies ω_i in the classical limit.[15] As the difference between the two is at least of first order in the perturbation parameter c^{-2}, this switch affects the frequency-shift only in the next order. Because of the perturbation parameter c^{-2} as a prefactor, the frequency-shift as such is of at least of first order right from the start, regardless of the frequencies its expression contains. This argument was the same in Section 4.1.3 when switching from perturbed frequencies in Equation (4.74) to unperturbed frequencies in Equation (4.75) for the axial frequency-shifts caused by magnetic imperfections. The same switch is also made from Equation (4.86) to Equation (4.87) for the shifts to the radial modes.

Since the relativistic effect of the radial modes on the axial frequency is mediated nonresonantly via the first-order approximation of the Lorentz factor, the functional dependence of Equation (4.114) on both radial modes is the same. Essentially, the velocity of each radial mode matters. Section 4.2.5 will revisit this behavior in terms of relativistic mass-increase.

[15] In Reference [83], this switch is made a little early without announcing it. In Equations (44) and (45), which correspond to Equations (4.111b) and (4.112), respectively, the tilde on top of the axial frequency is missing.

4.2.3. Shifts to the radial modes

The radial equations of motions are the first two components of Equation (4.98). Three terms need to be considered as a source of additional resonant terms when inserting the zeroth-order trajectory (3.94)–(3.96) and velocity (3.97)–(3.99). Naturally-resonant terms at the radial frequencies $\tilde{\omega}_\pm$ result from the radial modes themselves. Including oscillatory components at the axial frequency $\tilde{\omega}_z$ and its higher harmonics typically leads to nonresonant terms. Terms at the radial frequencies $\tilde{\omega}_\pm$ are preserved by multiplying them only with the constant contribution from the axial mode.

We will begin the search for naturally-resonant terms by examining the product of velocity squared and radial coordinates, that is, v^2x and v^2y. Picking $\tilde{x}$ as the example, the naturally-resonant terms at the radial frequencies $\tilde{\omega}_\pm$ are given by

$$\left\langle \left(\dot{\tilde{x}}^2 + \dot{\tilde{y}}^2 + \dot{\tilde{z}}^2\right)\tilde{x}\right\rangle_{\tilde{\omega}_\pm} = \left\langle \left(\dot{\tilde{x}}^2 + \dot{\tilde{y}}^2\right)\tilde{x}\right\rangle_{\tilde{\omega}_\pm} + \left\langle \dot{\tilde{z}}^2\right\rangle_0 \left\langle \tilde{x}\right\rangle_{\tilde{\omega}_\pm} \quad . \tag{4.115}$$

With the trigonometric identity

$$[\sin(\tilde{\chi}_z)]^2 = 1 - [\cos(\tilde{\chi}_z)]^2 = \frac{1}{2}\left[1 - \cos(2\tilde{\chi}_z)\right] \quad , \tag{4.116}$$

which is a variant of Equation (4.68), and ultimately Equation (3.2), the constant contribution from the axial mode becomes

$$\left\langle \dot{\tilde{z}}^2\right\rangle_0 = (\tilde{\omega}_z\hat{z})^2 \left\langle [\sin(\tilde{\chi}_z)]^2\right\rangle_0 = \frac{1}{2}(\tilde{\omega}_z\hat{z})^2 \quad . \tag{4.117}$$

Thus, the second term on the right-hand side of Equation (4.115) is

$$\left\langle \dot{\tilde{z}}^2\right\rangle_0 \left\langle \tilde{x}\right\rangle_{\tilde{\omega}_\pm} = \frac{1}{2}(\tilde{\omega}_z\hat{z})^2\tilde{x}_\pm \quad , \tag{4.118}$$

where we have used the abbreviation (3.100) for the resonant term $\tilde{x}_\pm$ from the radial mode. This result remains valid with the substitutions $\tilde{x} \to \tilde{y}$ and $\tilde{x}_\pm \to \tilde{y}_\pm$, and it is applicable to the $\tilde{v}^2\tilde{y}$ term in the second component of the radial equations of motion.

Evaluating the first term on the right-hand side of Equation (4.115) is trickier, because $\tilde{x}$ comes with two oscillatory terms—one at each radial frequency $\tilde{\omega}_\pm$. Of course, these terms are resonant, and they give a resonant contribution because the radial part (4.100) of the velocity squared comes with a constant term. However, it also comes with an oscillatory component at the difference frequency $\tilde{\omega}_\mathrm{b}$ of the radial modes. These two contributions are given by Equations (4.101) and (4.102), respectively. As Equation (4.39) demonstrates, mixing an oscillatory term at $\tilde{\omega}_\mathrm{b}$ with a term at the radial frequency $\tilde{\omega}_\mp$ results in an oscillatory term at the other radial frequency $\tilde{\omega}_\pm$. Both mechanism combine, yielding the resonant terms

$$\left\langle \left(\dot{\tilde{x}}^2 + \dot{\tilde{y}}^2\right)\tilde{x}\right\rangle_{\tilde{\omega}_\pm} = \left\langle \dot{\tilde{x}}^2 + \dot{\tilde{y}}^2\right\rangle_0 \left\langle \tilde{x}\right\rangle_{\tilde{\omega}_\pm} + \left\langle \left\langle \dot{\tilde{x}}^2 + \dot{\tilde{y}}^2\right\rangle_{\tilde{\omega}_\mathrm{b}} \tilde{x}_\mp\right\rangle_{\tilde{\omega}_\pm} \tag{4.119a}$$

$$= \left[(\tilde{\omega}_+\hat{\rho}_+)^2 + (\tilde{\omega}_-\hat{\rho}_-)^2\right]\tilde{x}_\pm + \tilde{\omega}_+\tilde{\omega}_-\hat{\rho}_+\hat{\rho}_-\,\hat{\rho}_\mp\cos(\tilde{\chi}_\pm) \tag{4.119b}$$

$$= \left[(\tilde{\omega}_+\hat{\rho}_+)^2 + (\tilde{\omega}_-\hat{\rho}_-)^2 + \tilde{\omega}_+\tilde{\omega}_-\hat{\rho}_\mp^2\right]\tilde{x}_\pm \quad . \tag{4.119c}$$

In the last step, a factor of $\hat{\rho}_\pm$ is used to provide the amplitude of $\tilde{x}_\pm = \hat{\rho}_\pm \cos(\tilde{\chi}_\pm)$. With the replacement $\cos(\tilde{\chi}_\pm) \to -\sin(\tilde{\chi}_\pm)$ and the trigonometric identity (4.40), the above transformations also hold for $\tilde{y}$ and $\tilde{y}_\pm = -\hat{\rho}_\pm \sin(\tilde{\chi}_\pm)$ in

$$\left\langle \left(\dot{\tilde{x}}^2 + \dot{\tilde{y}}^2\right) \tilde{y} \right\rangle_{\tilde{\omega}_\pm} = \left[(\tilde{\omega}_+\hat{\rho}_+)^2 + (\tilde{\omega}_-\hat{\rho}_-)^2 + \tilde{\omega}_+\tilde{\omega}_-\hat{\rho}_\mp^2\right] \tilde{y}_\pm \quad . \tag{4.120}$$

Second, we tackle the $v^2\dot{\tilde{y}}$ and $v^2\dot{\tilde{x}}$ terms in the radial equations of motion. Because the zeroth-order velocities contain the same frequencies as the corresponding zeroth-order trajectories, the treatment is essentially the same as for the $\tilde{v}^2\tilde{x}$ term in Equation (4.115). The only complication is that the zeroth-order velocities come with an additional factor of frequency that is not present in the coordinates. Naturally-resonant terms at the radial frequencies $\tilde{\omega}_\pm$ are written as

$$\left\langle \left(\dot{\tilde{x}}^2 + \dot{\tilde{y}}^2 + \dot{\tilde{z}}^2\right) \dot{\tilde{y}} \right\rangle_{\tilde{\omega}_\pm} = \left\langle \left(\dot{\tilde{x}}^2 + \dot{\tilde{y}}^2\right) \dot{\tilde{y}} \right\rangle_{\tilde{\omega}_\pm} + \left\langle \dot{\tilde{z}}^2 \right\rangle_0 \left\langle \dot{\tilde{y}} \right\rangle_{\tilde{\omega}_\pm} \quad . \tag{4.121}$$

With the help of Equation (4.117) and the short-hand notation (3.103) for the resonant contribution $\dot{\tilde{y}}_\pm$ from the zeroth-order solution $\dot{\tilde{y}}$, the second term on the right-hand side becomes

$$\left\langle \dot{\tilde{z}}^2 \right\rangle_0 \left\langle \dot{\tilde{y}} \right\rangle_{\tilde{\omega}_\pm} = \frac{1}{2}(\tilde{\omega}_z\hat{z})^2 \dot{\tilde{y}}_\pm \quad . \tag{4.122}$$

This result also applies with the substitutions $\dot{\tilde{y}} \to \dot{\tilde{x}}$ and $\dot{\tilde{y}}_\pm \to \dot{\tilde{x}}_\pm$. In complete analogy to Equation (4.119a), the first term on the right-hand side of Equation (4.121) is written as

$$\left\langle \left(\dot{\tilde{x}}^2 + \dot{\tilde{y}}^2\right) \dot{\tilde{y}} \right\rangle_{\tilde{\omega}_\pm} = \left\langle \dot{\tilde{x}}^2 + \dot{\tilde{y}}^2 \right\rangle_0 \left\langle \dot{\tilde{y}} \right\rangle_{\tilde{\omega}_\pm} + \left\langle \left\langle \dot{\tilde{x}}^2 + \dot{\tilde{y}}^2 \right\rangle_{\tilde{\omega}_\mathrm{b}} \dot{\tilde{y}}_\mp \right\rangle_{\tilde{\omega}_\pm} \tag{4.123a}$$

$$= \left[(\tilde{\omega}_+\hat{\rho}_+)^2 + (\tilde{\omega}_-\hat{\rho}_-)^2\right] \dot{\tilde{y}}_\pm - \tilde{\omega}_+\tilde{\omega}_-\hat{\rho}_+\hat{\rho}_-\,\tilde{\omega}_\mp\hat{\rho}_\mp \cos(\tilde{\chi}_\pm) \tag{4.123b}$$

$$= \left[(\tilde{\omega}_+\hat{\rho}_+)^2 + (\tilde{\omega}_-\hat{\rho}_-)^2\right] \dot{\tilde{y}}_\pm + (\tilde{\omega}_\mp\hat{\rho}_\mp)^2\, \dot{\tilde{y}}_\pm \tag{4.123c}$$

$$= \left[(\tilde{\omega}_\pm\hat{\rho}_\pm)^2 + 2(\tilde{\omega}_\mp\hat{\rho}_\mp)^2\right] \dot{\tilde{y}}_\pm \quad . \tag{4.123d}$$

In the second step, we have used a factor of $-\tilde{\omega}_\pm\hat{\rho}_+$ as the amplitude of the zeroth-order velocity $\dot{\tilde{y}}_\pm = -\tilde{\omega}_\pm\hat{\rho}_+ \cos(\tilde{\chi}_\pm)$. With the substitution $\cos(\tilde{\chi}_\pm) \to \sin(\tilde{\chi}_\pm)$ and the trigonometric identity (4.40) in lieu of Equation (4.39), the transformations work accordingly for $\dot{\tilde{x}}$ and $\dot{\tilde{x}}_\pm = -\tilde{\omega}_\pm\hat{\rho}_\pm \sin(\tilde{\chi}_\pm)$ with the result

$$\left\langle \left(\dot{\tilde{x}}^2 + \dot{\tilde{y}}^2\right) \dot{\tilde{x}} \right\rangle_{\tilde{\omega}_\pm} = \left[(\tilde{\omega}_\pm\hat{\rho}_\pm)^2 + 2(\tilde{\omega}_\mp\hat{\rho}_\mp)^2\right] \dot{\tilde{x}}_\pm \quad . \tag{4.124}$$

Third, we deal with the term that contains a product of velocity and coordinate. In the first component of the radial equations of motion, naturally-resonant terms at the radial frequencies $\tilde{\omega}_\pm$ are written as

$$\left\langle \left(\dot{\tilde{x}}\tilde{x} + \dot{\tilde{y}}\tilde{y} - 2\dot{\tilde{z}}\tilde{z}\right) \dot{\tilde{x}} \right\rangle_{\tilde{\omega}_\pm} = \left\langle \left(\dot{\tilde{x}}\tilde{x} + \dot{\tilde{y}}\tilde{y}\right) \dot{\tilde{x}} \right\rangle_{\tilde{\omega}_\pm} - 2\left\langle \dot{\tilde{z}}\tilde{z} \right\rangle_0 \left\langle \dot{\tilde{x}} \right\rangle_{\tilde{\omega}_\pm} \quad . \tag{4.125}$$

According to Equation (4.104), there is no constant contribution from the axial mode, and only the first term on the right-hand side remains. The term in round brackets is shown in Equation (4.105), and it oscillates at the difference frequency $\tilde{\omega}_\mathrm{b}$ of the radial modes. As there is no constant term, resonant contributions at the radial frequencies $\tilde{\omega}_\pm$ are only created

from the component $\dot{\tilde{x}}_\mp$ at the other radial frequency $\tilde{\omega}_\mp$. With the trigonometric identity (see Equation (C.12) in the appendix)

$$\left\langle \sin(\tilde{\chi}_+ - \tilde{\chi}_-)\sin(\tilde{\chi}_\mp)\right\rangle_{\tilde{\omega}_\pm} = \mp\frac{1}{2}\cos(\tilde{\chi}_\pm) \quad , \tag{4.126}$$

the resonant terms become

$$\begin{aligned}
\left\langle \left(\dot{\tilde{x}}\tilde{x} + \dot{\tilde{y}}\tilde{y}\right)\dot{\tilde{x}}\right\rangle_{\tilde{\omega}_\pm} &= \left\langle \left(\dot{\tilde{x}}\tilde{x} + \dot{\tilde{y}}\tilde{y}\right)\dot{\tilde{x}}_\mp\right\rangle_{\tilde{\omega}_\pm} && \text{(4.127a)}\\
&= \left\langle [-\hat{\rho}_+\hat{\rho}_-(\tilde{\omega}_+ - \tilde{\omega}_-)\sin(\tilde{\chi}_+ - \tilde{\chi}_-)]\,[-\tilde{\omega}_\mp\hat{\rho}_\mp\sin(\tilde{\chi}_\mp)]\right\rangle_{\tilde{\omega}_\pm} && \text{(4.127b)}\\
&= \mp\frac{1}{2}\hat{\rho}_+\hat{\rho}_-\hat{\rho}_\mp\,\tilde{\omega}_\mp(\tilde{\omega}_+ - \tilde{\omega}_-)\cos(\tilde{\chi}_\pm) && \text{(4.127c)}\\
&= \mp\frac{1}{2}\hat{\rho}_\mp^2\,\tilde{\omega}_\mp(\tilde{\omega}_+ - \tilde{\omega}_-)\,\tilde{x}_\pm \quad . && \text{(4.127d)}
\end{aligned}$$

For $\dot{\tilde{y}}$ instead of $\dot{\tilde{x}}$, as is the case in the second component of the radial equations of motion, the relevant trigonometric identity (see Equation (C.11) in the appendix) is

$$\left\langle \sin(\tilde{\chi}_+ - \tilde{\chi}_-)\cos(\tilde{\chi}_\mp)\right\rangle_{\tilde{\omega}_\pm} = \pm\frac{1}{2}\sin(\tilde{\chi}_\pm) \quad , \tag{4.128}$$

and the result is

$$\begin{aligned}
\left\langle \left(\dot{\tilde{x}}\tilde{x} + \dot{\tilde{y}}\tilde{y}\right)\dot{\tilde{y}}\right\rangle_{\tilde{\omega}_\pm} &= \left\langle \left(\dot{\tilde{x}}\tilde{x} + \dot{\tilde{y}}\tilde{y}\right)\dot{\tilde{y}}_\mp\right\rangle_{\tilde{\omega}_\pm} && \text{(4.129a)}\\
&= \left\langle [-\hat{\rho}_+\hat{\rho}_-(\tilde{\omega}_+ - \tilde{\omega}_-)\sin(\tilde{\chi}_+ - \tilde{\chi}_-)]\,[-\tilde{\omega}_\mp\hat{\rho}_\mp\cos(\tilde{\chi}_\mp)]\right\rangle_{\tilde{\omega}_\pm} && \text{(4.129b)}\\
&= \pm\frac{1}{2}\hat{\rho}_+\hat{\rho}_-\hat{\rho}_\mp\,\tilde{\omega}_\mp(\tilde{\omega}_+ - \tilde{\omega}_-)\sin(\tilde{\chi}_\pm) && \text{(4.129c)}\\
&= \mp\frac{1}{2}\hat{\rho}_\mp^2\,\tilde{\omega}_\mp(\tilde{\omega}_+ - \tilde{\omega}_-)\,\tilde{y}_\pm \quad . && \text{(4.129d)}
\end{aligned}$$

In each of the last steps, we have absorbed a factor of $\hat{\rho}_\pm$ and $-\hat{\rho}_\pm$ as the amplitudes of $\tilde{x}_\pm$ and $\tilde{y}_\pm$, respectively. In the beginning, the last term in the equations of motion (4.98) did not look like any of the other terms to be fit into the effective equations of motion (3.105). Therefore, its connection to a frequency-shift in the framework of cylindrical symmetry may have appeared doubtful. As it turns out here at the end of the calculation, the resonant contribution from the term fits nicely into the effective equations of motion. This compliance could have been guessed beforehand. The relativistic effects considered here do not break the cylindrical symmetry of the ideal Penning trap, because the Lorentz factor γ as the only addition is isotropic, and hence does not favor a velocity component.

With all the resonant contributions, the effective equations of motion (3.105) take the form

$$\begin{aligned}
\begin{pmatrix}\ddot{\tilde{x}}_\pm\\ \ddot{\tilde{y}}_\pm\end{pmatrix} = &\left[1 - \frac{(\tilde{\omega}_+\hat{\rho}_+)^2 + (\tilde{\omega}_-\hat{\rho}_-)^2 + \tilde{\omega}_+\tilde{\omega}_-\hat{\rho}_\mp^2 + \frac{1}{2}(\tilde{\omega}_z\hat{z})^2}{2c^2} - \frac{\mp\hat{\rho}_\mp^2\,\tilde{\omega}_\mp(\tilde{\omega}_+ - \tilde{\omega}_-)}{2c^2}\right]\frac{\omega_z^2}{2}\begin{pmatrix}\tilde{x}_\pm\\ \tilde{y}_\pm\end{pmatrix}\\
&+\left[1 - \frac{(\tilde{\omega}_\pm\hat{\rho}_\pm)^2 + 2(\tilde{\omega}_\mp\hat{\rho}_\mp)^2 + \frac{1}{2}(\tilde{\omega}_z\hat{z})^2}{2c^2}\right]\omega_\mathrm{c}\begin{pmatrix}\dot{\tilde{y}}_\pm\\ -\dot{\tilde{x}}_\pm\end{pmatrix} \quad .
\end{aligned} \tag{4.130}$$

The first line contains the contributions from Equations (4.118), (4.119c) and (4.120) in the first fraction, and Equations (4.127d), and (4.129d) in the second one. The second line comprises Equations (4.122), (4.123d) and (4.124). Using $\mp\tilde{\omega}_\mp(\tilde{\omega}_+ - \tilde{\omega}_-) = \tilde{\omega}_\mp^2 - \tilde{\omega}_+\tilde{\omega}_-$, the parameters in the effective equations of motion (3.105) are read off as

$$\beta_\pm = \varepsilon_\pm = -\frac{1}{2c^2}\left[(\tilde{\omega}_\pm\hat{\rho}_\pm)^2 + 2(\tilde{\omega}_\mp\hat{\rho}_\mp)^2 + \frac{1}{2}(\tilde{\omega}_z\hat{z})^2\right] \quad . \tag{4.131}$$

Because the two parameters $\beta_\pm$ and $\varepsilon_\pm$ are equal, the numerators in Equation (3.109b) for the first-order frequency-shift are simply added with the help of

$$\pm\omega_\pm\omega_\mathrm{c} \mp \omega_+\omega_- = \pm\omega_\pm(\omega_+ + \omega_-) \mp \omega_+\omega_- = \pm\omega_\pm^2 \quad , \tag{4.132}$$

and the expression (3.109b) for the frequency-shift simplifies to

$$\Delta\omega_\pm = \pm\frac{\omega_\pm^2}{\omega_+ - \omega_-}\beta_\pm = \pm\frac{\omega_\pm^2}{\omega_+ - \omega_-}\varepsilon_\pm \quad . \tag{4.133}$$

Specifically, the relativistic frequency-shift to the radial modes is given by

$$\frac{\Delta\omega_\pm}{\omega_\pm} = \mp\frac{\omega_\pm}{\omega_+ - \omega_-}\frac{(\omega_\pm\hat{\rho}_\pm)^2 + 2(\omega_\mp\hat{\rho}_\mp)^2 + \frac{1}{2}(\omega_z\hat{z})^2}{2c^2} \quad . \tag{4.134}$$

Like for the relativistic shift to the axial frequency at the end of Section 4.2.2, we have replaced the relativistic frequencies $\tilde{\omega}_i$ in the parameters $\beta_\pm$ and $\varepsilon_\pm$ by the frequencies ω_i in the classical limit. This replacement is good to zeroth-order in the frequencies, but fine to first order in the frequency-shift.

Ignoring the factor of 2 between the dependence on the amplitudes of the radial modes, the absolute shift to the reduced cyclotron-frequency is approximately a factor of ω_+^2/ω_-^2 larger than the shift to the magnetron frequency. Consequently, the shift to the sideband cyclotron-frequency (2.25), obtained by adding the shifts to the two radial modes, is largely dominated by $\Delta\omega_+$:

$$\Delta\omega_\mathrm{c} = -\frac{(\omega_+^2 - 2\omega_-^2)(\omega_+\hat{\rho}_+)^2 + (2\omega_+^2 - \omega_-^2)(\omega_-\hat{\rho}_-)^2 + (\omega_+^2 - \omega_-^2)(\omega_z\hat{z})^2}{(\omega_+ - \omega_-)\,2c^2} \tag{4.135a}$$

$$= -\left[\omega_\mathrm{c} - \frac{\omega_-^2}{\omega_+ - \omega_-}\right]\frac{(\omega_+\hat{\rho}_+)^2}{2c^2} - \left[2\omega_\mathrm{c} + \frac{\omega_-^2}{\omega_+ - \omega_-}\right]\frac{(\omega_-\hat{\rho}_-)^2}{2c^2} - \omega_\mathrm{c}\frac{(\omega_z\hat{z})^2}{4c^2} \quad . \tag{4.135b}$$

The last step uses the third binomial formula on $\omega_+^2 - \omega_-^2 = (\omega_+ + \omega_-)(\omega_+ - \omega_-) = \omega_\mathrm{c}(\omega_+ - \omega_-)$.

The technical symmetry between the shifts to the two radial frequencies is present once again. Thus, knowing the functional dependence of the relativistic shift $\Delta\omega_+(\omega_+, \hat{\rho}_+, \omega_-, \hat{\rho}_-, \omega_z, \hat{z})$ to the modified cyclotron-frequency, the relativistic shift $\Delta\omega_-$ to the magnetron frequency is calculated from the same function as $\Delta\omega_+(\omega_-, \hat{\rho}_-, \omega_+, \hat{\rho}_+, \omega_z, \hat{z})$. This evaluation based on the change of the arguments corresponds to the combined substitution $\omega_\pm \to \omega_\mp$ and $\hat{\rho}_\pm \to \hat{\rho}_\mp$ for the radial frequencies and amplitudes. The relativistic shift $\Delta\omega_\mathrm{c}$ to the sideband frequency is invariant under this substitution.

4.2.4. Comparison with other results

For easier comparison with results from the literature, it is useful to express the relativistic frequency-shifts (4.114) and (4.134) as a function of the energies (2.49)–(2.51) associated with the three eigenmotions instead of their amplitudes. The relativistic frequency-shifts then take the form[16]

$$\frac{\Delta\omega_+}{\omega_+} = \frac{-1}{mc^2}\left[\frac{\omega_+^2\,\mathcal{E}_+}{(\omega_+-\omega_-)^2} + \frac{\omega_+\,\mathcal{E}_z}{2(\omega_+-\omega_-)} - \frac{\omega_z^2\,\mathcal{E}_-}{(\omega_+-\omega_-)^2}\right] \quad , \tag{4.136}$$

$$\frac{\Delta\omega_z}{\omega_z} = \frac{-1}{mc^2}\left[\frac{\omega_+\,\mathcal{E}_+}{2(\omega_+-\omega_-)} + \frac{3}{8}\mathcal{E}_z - \frac{\omega_z^2\,\mathcal{E}_-}{4\omega_+(\omega_+-\omega_-)}\right] \quad , \tag{4.137}$$

$$\frac{\Delta\omega_-}{\omega_-} = \frac{1}{mc^2}\left[\frac{\omega_z^2\,\mathcal{E}_+}{(\omega_+-\omega_-)^2} + \frac{\omega_-\,\mathcal{E}_z}{2(\omega_+-\omega_-)} - \frac{\omega_-^2\,\mathcal{E}_-}{(\omega_+-\omega_-)^2}\right] \quad . \tag{4.138}$$

With the approximation $\omega_+ - \omega_- \approx \omega_+$ for $|\omega_+| \gg |\omega_-|$, the result agrees with the classical limit given in Reference [20], after applying the identity (2.26) multiple times. The same reference also shows the quantum mechanical result in terms of quantum numbers, a result picked up and expressed as a function of the energies $\mathcal{E}_i$ in Reference [44] without any assumptions about the frequencies. Apart from the frequency-shifts caused by spin and the zero-point shift caused by the fact that even the quantum-mechanical ground-state of each eigenmode has nonzero energy—both being effects which our entirely classical treatment simply cannot reproduce—there is agreement.

4.2.5. Estimates based on relativistic mass-increase

Because of the additional time-derivative of the Lorentz factor, the relativistic equations of motion (4.91) do not result from the classical ones by simply making the replacement $m \to \gamma m$ for the mass. Nevertheless, the concept of relativistic mass-increase at slow speeds [49] is widely used to introduce the most important relativistic frequency-shifts, for which it turns out to work nicely. This section explores why this model is tempting in the context of the Penning trap, and compares its estimates with the first-order result.

Without an electric field, the time-derivative (4.94) of the Lorentz factor γ vanishes, and the relativistic equations of motion (4.91) look like the classical equations of motion for particle of mass γm. Consequently, the motion in an entirely magnetic field supports the notion of relativistic mass-increase as the major relativistic effect. In fact, it is the only one in this setting. In a homogeneous magnetic field, the expression

$$\tilde{\omega}_\mathrm{c} = \frac{qB_0}{\gamma m} \tag{4.139}$$

for the relativistic free-space cyclotron-frequency $\tilde{\omega}_\mathrm{c}$ is exact. No approximations are required to calculate the frequency-shift with respect to the classical case. However, the relativistic frequency-shift is typically derived by starting from the classical case without discussing the

[16] Now, the substitution for making the switch $\Delta\omega_\pm \to \Delta\omega_\mp$ is $\omega_\pm \to \omega_\mp$ and $\mathcal{E}_\pm \to -\mathcal{E}_\mp$.

relativistic solution. This approach will be extended to the three eigenfrequencies in the PENNING trap. For small velocities, the relativistic mass of the particle is expanded as

$$\gamma m = \frac{m}{\sqrt{1 - v^2/c^2}} \approx m\left(1 + \frac{v^2}{2c^2} + \cdots\right) \quad , \tag{4.140}$$

which results in the velocity-dependent mass-increase

$$\frac{\Delta m}{m} = \frac{v^2}{2c^2} \quad . \tag{4.141}$$

Next, the mass-dependence of classical free-space cyclotron-frequency (2.18)

$$\frac{\mathrm{d}\omega_\mathrm{c}}{\mathrm{d}m} = -\frac{\omega_\mathrm{c}}{m} \tag{4.142}$$

is related to the relativistic frequency-shift by plugging in the velocity-dependence (4.141) of the mass as

$$\frac{\Delta\omega_\mathrm{c}}{\omega_\mathrm{c}} = -\frac{\Delta m}{m} = -\frac{v^2}{2c^2} = -\frac{(\omega_\mathrm{c}\hat{\rho}_\mathrm{c})^2}{2c^2} \quad . \tag{4.143}$$

The velocity squared is the one of a circular motion at the free-space cyclotron-frequency ω_c with cyclotron-radius $\hat{\rho}_\mathrm{c}$. As usual, we do not distinguish between the relativistic frequencies $\tilde{\omega}$ and the classical ones ω to first-order in the frequency-shift. Of course, the particle is free to drift along the magnetic field-lines with constant velocity, but we do not show this contribution to v^2 here, because it would eventually lead to a loss of the particle. It is for this reason that the PENNING trap employs an electric field for axial confinement. In turn, the situation becomes more complicated to the extent that an analytic solution of the relativistic equations of motion (4.95) is impossible, because the time-derivative (4.94) of the LORENTZ factor does not vanish. Instead, the time-dependent LORENTZ factor turns the relativistic equations of motions into nonlinear ones. Nevertheless, the prediction (4.143) for the relativistic free-space cyclotron-frequency ω_c is assumed to be valid for the shift to the modified cyclotron-frequency ω_+. When the trap is operated in the usual regime $|\omega_\mathrm{c}| \gtrsim |\omega_+| \gg \omega_z \gg |\omega_-|$, the magnetic field is expected to dominate the modified cyclotron-mode, while the other, slower, modes give negligible contributions to the total velocity, assuming similar amplitudes. If, furthermore, the amplitudes of the other modes can be neglected, the main motion in the PENNING trap is still a circular one.

The simple model of mass-increase will be applied more rigorously in the following. Generally, the radial frequencies $\omega_\pm$ defined in Equation (2.23) depend on mass as

$$\frac{\mathrm{d}\omega_\pm}{\mathrm{d}m} = \frac{\partial\omega_\pm}{\partial\omega_\mathrm{c}}\frac{\partial\omega_\mathrm{c}}{\partial m} + \frac{\partial\omega_\pm}{\partial\omega_z^2}\frac{\partial\omega_z^2}{\partial m} \tag{4.144a}$$

$$= \frac{\pm\omega_+}{\omega_+ - \omega_-}\frac{-\omega_\mathrm{c}}{m} \mp \frac{1}{2(\omega_+ - \omega_-)}\frac{-\omega_z^2}{m} = -\frac{1}{m}\frac{\pm\omega_\pm\omega_\mathrm{c} \mp \omega_+\omega_-}{\omega_+ - \omega_-} \tag{4.144b}$$

$$= \mp\frac{1}{m}\frac{\omega_\pm^2}{\omega_+ - \omega_-} \quad . \tag{4.144c}$$

The derivatives of the radial frequencies with respect to the free-space cyclotron-frequency ω_c and the axial frequency squared use Equations (3.107) and (3.108). The derivatives of the frequencies with respect to mass are calculated from Equations (2.18) (or directly Equation (4.142)) and Equation (2.17), respectively. In both cases, it is more convenient to use the axial frequency squared as a variable, because the radial frequencies $\omega_\pm$ are a function of ω_z^2, and taking ω_z^2 eliminates the square root in the functional dependence of ω_z on mass m. In the second-to-last step, the axial frequency squared is expressed as a product of the radial frequencies via Equation (2.26). In the last step, the numerator is summed with the help of Equation (4.132).

With Equation (4.141), the mass-dependence (4.141) of the radial frequencies is linked to the estimate

$$\frac{\Delta\omega_\pm}{\omega_\pm} = \mp\frac{\omega_\pm}{\omega_+ - \omega_-}\frac{\Delta m}{m} = \mp\frac{\omega_\pm}{\omega_+ - \omega_-}\frac{v^2}{2c^2} \tag{4.145}$$

for the relativistic frequency-shift. In an ideal Penning trap, the kinetic energy (2.47) is not constant, unless the trapped particle has no axial amplitude, and only one of its two radial modes has nonzero amplitude. Thus, the velocity squared is generally a function of time. For the estimate of the relativistic frequency-shift by means of relativistic mass-increase, we consider the constant (or time-averaged) component

$$\left\langle \tilde{v}^2 \right\rangle_0 = (\tilde{\omega}_+\hat{\rho}_+)^2 + (\tilde{\omega}_-\hat{\rho}_-)^2 + \frac{1}{2}(\tilde{\omega}_z\hat{z})^2 \quad , \tag{4.146}$$

taken from Equations (4.101) and (4.117). To first order in the frequency-shift, the relativistic frequencies $\tilde{\omega}$ may be replaced by the frequencies ω from the classical case. Since we do not want to show an incorrect formula for the relativistic frequency-shifts, we will not plug this result into Equation (4.145) explicitly. As it turns out, the simple model of relativistic mass-increase fails to account for the factor of 2 in the dependence of the radial frequency $\omega_\pm$ on the amplitude squared $\hat{\rho}_\mp^2$ of the other radial motion. Apart from missing this factor, the exact first-order result (4.134) is reproduced, and the order of magnitude is certainly correct.

According to Equation (2.17), the dependence on the axial frequency on mass evaluates to

$$\frac{\mathrm{d}\omega_z}{\mathrm{d}m} = -\frac{\omega_z}{2m} \quad . \tag{4.147}$$

With Equation (4.141), this result is related to the estimate

$$\frac{\Delta\omega_z}{\omega_z} = -\frac{\Delta m}{2m} = -\frac{v^2}{4c^2} \tag{4.148}$$

for the relativistic frequency-shift. Again, we refrain from showing the full expression after plugging in Equation (4.146) for the estimate of velocity squared because the exact first-order result (4.114) is not completely reproduced. This time, the simple model of relativistic mass-increase underestimates the dependence on axial amplitude squared by a factor of $3/2$, but it does not miss out on the right order of magnitude. Moreover, the dependence of the relativistic frequency-shift on the radial modes is reproduced correctly.

Table 4.1 summarizes the successes and the pitfalls of the simple model based on relativistic mass-increase. Because of the hierarchy $|\omega_+| \gg \omega_z \gg |\omega_-|$ for the eigenfrequencies, relativistic

Table 4.1.: Comparison of the simple estimate based on relativistic mass-increase with the exact first-order calculation for the dependence of the relativistic frequency-shift $\Delta\omega_i$ on the amplitudes of the three eigenmotions. The checkmark (✓) indicates agreement; the cross (×) indicates a discrepancy. Even in case of a discrepancy, the order of magnitude is correct.

	$\hat{\rho}_+$	$\hat{z}$	$\hat{\rho}_-$
$\Delta\omega_+$	✓	✓	×
$\Delta\omega_z$	✓	×	✓
$\Delta\omega_-$	×	✓	✓

shifts to and by the modified cyclotron-mode are typically the most important ones, assuming similar amplitudes. Apart from the least important shift to the magnetron mode, the simple model agrees with the complete first-order result for these. Because of this coincidence or authors' awareness, the discrepancies have not played an important role. The discrepancy for the dependence of the axial frequency on the amplitude of the axial motion is probably the first one that could be of experimental relevance. However, corrections for this relativistic frequency-shift seem to have been applied correctly, mainly because of the availability of the earlier results based on operator methods. The only paper that I am aware of for incorrectly using the simple model of relativistic mass-increase in this case is a theoretical one [110] without any direct interpretation of experimental data.

It is worth noting that even if we hypothetically sought to eliminate the relativistic effects beyond mass-increase from the equations of motion by ignoring the time-derivative of the Lorentz factor, the first-order result would not agree with the simple model presented in this section. If the time-derivative of the Lorentz factor were dropped from the axial equation of motion (4.106), the simple model of mass-increase would still not get the dependence of the relativistic shift $\Delta\omega_z$ on the axial amplitude right. In this case, the last term in square brackets in Equation (4.112) would be missing and the factor of $3/4$ in the frequency-shift (4.114) would read $1/4$ rather than $1/2$ as predicted by the estimate of velocity (4.146). The discrepancy arises from the fact that the relativistic mass is dynamical, rather than constant. When searching for resonant terms that drive the first-order frequency-shift, terms like $v^2 z$ need to be analyzed as a whole, not just as individual factors. Although these mechanism of resonant mixing are even more pronounced for the radial modes, we will not go into detail of what the first-order frequency-shift would look like if the term $\mp\hat{\rho}_\mp^2\,\tilde{\omega}_\mp(\tilde{\omega}_+ - \tilde{\omega}_-)$, which results from the time-derivative of the Lorentz factor, were missing in the effective radial equations of motion (4.130). At a first glance, the contributions that look like (time-averaged) mass-increase remain unchanged, while the dependence of the shift $\Delta\omega_\pm$ on the amplitude $\hat{\rho}_\mp$ of the other radial motion would still disagree with the estimate from the model of mass-increase. In reality, the time-derivative of the Lorentz factor is here to stay as a relativistic effect. The goal of this academic discussion was to highlight the importance of correctly averaging the forces on the particle for the calculation of first-order frequency-shifts.

4.3. Shifts in axial lock

This section examines anharmonic frequency-shifts to the radial modes when the axial frequency is held constant. This mode of operation is referred to as axial (frequency) lock, and the axial frequency $\tilde{\omega}_z$ is called locked, in contrast to the free-running mode. Assuming a perfect locked loop, the effective axial equation of motion (3.85) shows that $\omega_z^2(1+\varepsilon_z)$ has to be kept constant for the axial frequency $\tilde{\omega}_z$ to stay constant. Although the effective radial equations of motion (3.105) also contain ω_z, this quantity is not equal to the actual axial frequency in the perturbed PENNING trap. The radial frequencies $\tilde{\omega}_\pm$ depend on the effective curvature of the electrostatic potential in the radial direction, just like the axial frequency $\tilde{\omega}_z$ depends on the effective curvature of the electrostatic potential in the axial direction. Only in the case of the ideal PENNING trap are these two curvatures related in a simple manner. If this relation is preserved by the imperfections, the frequency-shifts cancel in the invariance theorem [25]. The parameters $\varepsilon_\pm$ in the effective radial equations of motion (3.105) show that the effective curvature in the radial directions may differ for the two radial modes. If they are the same—that is, $\varepsilon_+ = \varepsilon_-$—the first-order frequency-shifts (3.109b) cancels in the sideband-identity (2.25).[17]

From the mathematical point of view, the actual axial frequency in lock is readily included in the effective curvature of the radial electrostatic potential by means of

$$\omega_z^2(1+\varepsilon_\pm) = \frac{\omega_z^2(1+\varepsilon_z)(1+\varepsilon_\pm)}{(1+\varepsilon_z)} = \frac{\check{\omega}_z^2(1+\varepsilon_\pm)}{(1+\varepsilon_z)} \tag{4.149a}$$

$$\approx \check{\omega}_z^2(1+\varepsilon_\pm)(1-\varepsilon_z+\cdots) \tag{4.149b}$$

$$\approx \check{\omega}_z^2(1+\varepsilon_\pm-\varepsilon_z+\cdots) \quad . \tag{4.149c}$$

In the first step, we have expanded with $1+\varepsilon_z$ to write the actual axial frequency in lock as

$$\check{\omega}_z = \omega_z\sqrt{1+\varepsilon_z} \quad . \tag{4.150}$$

From this point on, we will indicate frequencies in lock with the inverted hat as $\check{\omega}_i$. Under lock, the axial frequency-shift vanishes: $\Delta\check{\omega}_z = 0$, in contrast to the free-running mode. We have then approximated the denominator for $|\varepsilon_z| \ll 1$. The cross-term $\varepsilon_\pm\varepsilon_z$ has been neglected because it is of higher order. If either $\varepsilon_\pm$ or ε_z were correct up to, say, second order, the second-order contribution of the cross-term $\varepsilon_\pm\varepsilon_z$ would have to be retained, in order to stay correct to second order. However, all the frequency-shifts considered in this chapter are of first order only.

Substituting Equation (4.149c) into the effective radial equations of motion (3.105) in free-running mode results in the effective radial equations of motion

$$\begin{pmatrix}\ddot{\tilde{x}}_\pm\\ \ddot{\tilde{y}}_\pm\end{pmatrix} = \omega_c(1+\beta_\pm)\begin{pmatrix}\dot{\tilde{y}}_\pm\\ -\dot{\tilde{x}}_\pm\end{pmatrix} + \frac{\check{\omega}_z^2(1+\varepsilon_\pm-\varepsilon_z)}{2}\begin{pmatrix}\tilde{x}_\pm\\ \tilde{y}_\pm\end{pmatrix} \tag{4.151}$$

under lock. The two differences are the substitution $\omega_z^2 \to \check{\omega}_z^2$, and the addition of the parameter $-\varepsilon_z$. The shift to the radial frequencies $\omega_\pm$ under lock is now calculated according to

[17] This is not the case for $\beta_+ = \beta_- \equiv \beta$. Rather, the associated two shifts would combine to increase the sideband cyclotron-frequency by $\omega_c\beta$ to the value of the effective cyclotron-frequency $\omega_c(1+\beta)$.

Equation (3.105) for the free-running mode[18] with the result

$$\Delta\check{\omega}_\pm = \pm\frac{\omega_\pm\omega_\mathrm{c}}{\omega_+-\omega_-}\beta_\pm \mp \frac{\omega_+\omega_-}{\omega_+-\omega_-}(\varepsilon_\pm-\varepsilon_z) \tag{4.152a}$$

$$= \Delta\omega_\pm \pm \frac{\omega_+\omega_-}{\omega_+-\omega_-}\varepsilon_z \tag{4.152b}$$

$$= \Delta\omega_\pm \pm \frac{2\omega_+\omega_-}{\omega_+-\omega_-}\frac{\Delta\omega_z}{\omega_z} \quad . \tag{4.152c}$$

The last step relates the parameter ε_z to the axial frequency-shift in free-running mode via Equation (3.86). This is the same result as in Reference [44]. Without any specific expression for the frequency-shifts, Equation (4.152c) shows that the shift to the sideband cyclotron-frequency (2.25) is the same under lock as in free-running mode:

$$\Delta\check{\omega}_\mathrm{c} = \Delta\check{\omega}_+ + \Delta\check{\omega}_- = \Delta\omega_+ + \Delta\omega_- = \Delta\omega_\mathrm{c} \quad . \tag{4.153}$$

Next, we consider shifts to the frequency determined via the invariance theorem (2.27). In the ideal case and for some imperfections covered by the invariance theorem, such as an elliptic quadrupole potential and a misalignment of this potential with respect to the magnetic field, summing the three eigenfrequencies in the trap in quadrature yields the free-space cyclotron-frequency (2.18) squared. However, the cancellation in the quadratic sum does not work for arbitrary frequency-shifts. Consequently, the frequency determined by plugging the shifted frequencies, which have not been corrected for that very shift, into the invariance theorem will in general differ from the ideal free-space cyclotron-frequency ω_c given by Equation (2.18).

The free-space cyclotron-frequency ω_c depends differentially on the three eigenfrequencies ω_i in the trap as

$$\frac{\partial\omega_\mathrm{c}}{\partial\omega_i} = \frac{\partial}{\partial\omega_i}\sqrt{\omega_+^2+\omega_z^2+\omega_-^2} = \frac{\omega_i}{\sqrt{\omega_+^2+\omega_z^2+\omega_-^2}} = \frac{\omega_i}{\omega_\mathrm{c}} \quad , \tag{4.154}$$

when it is determined via the invariance theorem. Thus, shifts $\Delta\omega_i$ to these frequencies result in the shift

$$\omega_\mathrm{c}\Delta\omega_\mathrm{c} = \omega_+\Delta\omega_+ + \omega_z\Delta\omega_z + \omega_-\Delta\omega_- \tag{4.155}$$

to the calculated free-space cyclotron-frequency.[19] Since estimating the shift $\Delta\omega_\mathrm{c}$ with only the first derivative neglects cross-terms and powers in the shifts $\Delta\omega_i$, we are free to switch between the perturbed frequencies, $\tilde{\omega}_i$ and $\check{\omega}_i$, and the unperturbed ones in this approximation. Taking the difference between these frequencies into account would lead to powers in the shifts $\Delta\omega_i$, too. When higher-order derivatives are not considered, dropping these terms of higher order is the honest thing to do.

[18] Because the effective radial equation of motion (4.151) under lock contain the locked axial frequency $\check{\omega}_z$ rather than the axial frequency ω_z in the ideal trap, a little care has to be taken. The original calculation uses Equation (2.26), $\omega_z^2 = 2\omega_+\omega_-$, whereas now $\check{\omega}_z^2 = \omega_z^2(1+\varepsilon_z)$ according to Equation (4.150). However, the difference is of higher order and will hence be neglected here.

[19] We are talking about shifts in the sense of applying corrections. Propagating the uncertainties of these shifts is a different matter.

For shifts $\Delta\breve{\omega}_i$ under lock, which ideally means $\Delta\tilde{\omega}_z = 0$ as the axial frequency is held constant, the shift to the calculated free-space cyclotron-frequency becomes

$$\omega_c \Delta\breve{\omega}_c = \omega_+ \Delta\breve{\omega}_+ + \omega_- \Delta\breve{\omega}_- \tag{4.156a}$$

$$= \omega_+ \left(\Delta\omega_+ + \frac{\omega_z}{\omega_+ - \omega_-} \Delta\omega_z \right) + \omega_- \left(\Delta\omega_- - \frac{\omega_z}{\omega_+ - \omega_-} \Delta\omega_z \right) \tag{4.156b}$$

$$= \omega_+ \Delta\omega_+ + \omega_z \Delta\omega_z + \omega_- \Delta\omega_- \quad . \tag{4.156c}$$

The second step uses Equation (4.152c) in conjunction with Equation (2.26), $\omega_z^2 = 2\omega_+\omega_-$. The final result is the same as in Equation (4.155) without lock.

When it comes to the invariance theorem (2.27), applying the shifts to the radial frequencies under lock without correcting the locked axial frequency is equivalent to applying the shifts for free-running mode to all three eigenfrequencies. While locking the axial frequency seems like a clever alternative to measuring it, there is no guarantee that the frequency to which the particle locks is the unperturbed axial frequency the particle would have in the ideal trap. Consequently, corrections of the axial frequency have to be implemented in the invariance theorem, even under lock. This fact is expressed very clearly by Equation (4.156c), whereas these corrections in Equation (4.156a) are hidden in the shifts $\Delta\breve{\omega}_\pm$ to the radial frequencies under lock.

At this point, we turn from the general relations for shifts to the specific frequency-shifts from Sections 4.1 and 4.2 for cylindrically-symmetric imperfections and relativistic effects, respectively, in order to calculate the corresponding shifts in lock in the following two subsections.

4.3.1. Cylindrically-symmetric imperfections

As in this whole chapter, the results will be kept general when possible. Explicit expressions for the frequency-shifts caused by the lowest-order imperfections are shown in Chapter E of the appendix.

Electrostatic imperfections

The exponent of the amplitude $\hat{\rho}_\pm$ is not the same in the axial frequency-shift (4.36) as in the shift (4.50) to the radial frequencies. Consequently, combining these shifts directly according to Equation (4.152c) for the shift in lock would yield an unnecessarily complicated expression. By transforming the summation variable in Equation (4.36) as $k \to k - 1$, the axial frequency-shift is rewritten as

$$\frac{\Delta\omega_z}{\omega_z} = -\frac{C_{2n}}{C_2} \frac{(2n)!}{2^{2n}} \sum_{k=1}^{n} \sum_{p=0}^{k-1} \frac{(-1)^k (n+1-k)\, \hat{\rho}_\pm^{2p}\, \hat{\rho}_\mp^{2(k-1-p)}\, \hat{z}^{2(n-k)}}{[(n+1-k)!\, p!\, (k-1-p)!]^2\, d^{2n-2}} \tag{4.157}$$

with the same exponents for the amplitudes as in the shift (4.50) to the radial frequencies. Moreover, the sums now have the same limits. Overall, the frequency-shifts are in the right shape to plug them into Equation (4.152c), where the two expressions on the right-hand side turn out to be almost equal up to factors of

$$\frac{p+1}{[(n-k)!\,(p+1)!]^2} - \frac{n-k+1}{[(n+1-k)!\,p!]^2} = \frac{1}{[(n-k)!\,p!]^2} \left[\frac{1}{p+1} - \frac{1}{n+1-k} \right] \quad . \tag{4.158}$$

The first term is from the radial modes; the second one from the axial mode. The signs shown here reflect the situation for the modified cyclotron-frequency $\check{\omega}_+$ under axial lock. For the shift to the magnetron frequency ω_-, there is a global minus sign.

Considering all the common factors not shown in Equation (4.158), the shift to the radial frequencies in lock becomes

$$\begin{aligned}\Delta\check{\omega}_\pm = \pm\frac{\omega_+\omega_-}{\omega_+ - \omega_-}\frac{C_{2n}}{C_2}\frac{(2n)!}{2^{2n-1}}\frac{1}{d^{2n-2}}\sum_{k=1}^{n}\frac{(-1)^k\,\hat{z}^{2(n-k)}}{[(n-k)!]^2} \\ \cdot\sum_{p=0}^{k-1}\frac{\hat{\rho}_\pm^{2p}\,\hat{\rho}_\mp^{2(k-1-p)}}{[p!\,(k-p-1)!]^2}\left(\frac{1}{p+1}-\frac{1}{n+1-k}\right) \quad .\end{aligned} \tag{4.159}$$

It vanishes for $p = n - k$, which means that there are no terms with $\hat{z}$ and $\hat{\rho}_\pm$ having the same exponent. Moreover, the term $\hat{\rho}_\mp^{2(n-1)}$ with the strongest possible dependence on the amplitude of the other radial mode is gone, because reaching this exponent requires $k = n$ and $p = 0$, which satisfies $p = n - k$.

Inserting the condition $k = n - p$ for a vanishing contribution into the limits $0 \le p \le k - 1$ for the summation variable p yields the condition $0 \le 2p \le n - 1$ for all possible values of p that lead to a vanishing contribution. Overall, the shift (4.159) to the radial frequencies under axial lock contains $1 + \lfloor (n-1)/2 \rfloor = \lfloor (n+1)/2 \rfloor$ fewer terms with distinct dependencies on amplitudes than the corresponding shift (4.50) in free-running mode.

Static magnetic imperfections

For magnetostatic imperfections, the expressions for the shift (4.78) to the axial mode and for the shift (4.87) to the radial modes have the right form to combine them according to Equation (4.152c) for the frequency-shift in lock without any transformation of summation variables. Although the lower limits of the summation over k are not the same yet, they are matched readily, because both binomial coefficients inside the square brackets in Equation (4.78) vanish at the new lower limit $k = 0$, where there is no additional contribution to be considered. The frequency-shift in lock then becomes

$$\begin{aligned}\Delta\check{\omega}_\pm = \pm\frac{B_{2n}}{B_0}\frac{\omega_+ + \omega_-}{\omega_+ - \omega_-}\frac{(2n)!}{2^{2n}}\sum_{k=0}^{n}\frac{(-1)^k\,\hat{z}^{2(n-k)}}{[k!(n-k)!]^2} \\ \cdot\sum_{p=0}^{k}\binom{k}{p}\left\{\omega_\pm\left[\binom{k}{p}-\frac{k}{n-k+1}\binom{k-1}{p-1}\right]\right. \\ \left.+\,\omega_\mp\left[\binom{k}{p+1}-\frac{k}{n-k+1}\binom{k-1}{p}\right]\right\}\hat{\rho}_\pm^{2p}\,\hat{\rho}_\mp^{2(k-p)} \quad .\end{aligned} \tag{4.160}$$

Like for the magnetic shifts in free-running mode, we will not use the explicit expression (3.3) for the binomial coefficients, because of the special cases for $p = 0$, $p = k$, and $k = 0$. These vanishing contributions are included in the binomial coefficients without having to split the sums. Anyway, the binomial coefficients do not subtract nicely and possible cancellations are

much harder to spot. Moreover, two cancellations are required for a particular dependence on amplitudes to vanish. Thus, we will not attempt a general survey here, going with a specific example instead. For the lowest-order term B_2, the shift $\Delta\check{\omega}_\pm$ does not depend on the amplitude $\hat{\rho}_\mp$ of the other radial motion.

4.3.2. Relativistic effects

For the frequency-shifts in lock, Equation (4.152c) combines the frequency-shifts in free-running mode: Equation (4.114) for the axial frequency and Equation (4.134) for the radial frequencies. The resulting shift

$$\begin{aligned}\Delta\check{\omega}_+ = -\frac{1}{2c^2}\frac{\omega_+^2}{\omega_+ - \omega_-}\Bigg\{&(\omega_+\hat{\rho}_+)^2\left[1+\frac{\omega_-}{\omega_+}\right] + 2(\omega_-\hat{\rho}_-)^2\left[1+\frac{\omega_-}{2\omega_+}\right] \\ &+ \frac{(\omega_z\hat{z})^2}{2}\left[1+\frac{3\omega_-}{2\omega_+}\right]\Bigg\}\end{aligned} \tag{4.161}$$

to the reduced cyclotron-frequency is largely dominated by the shift to that frequency in free-running mode. Conversely, the shift

$$\begin{aligned}\Delta\check{\omega}_- = \frac{1}{2c^2}\frac{\omega_+\omega_-}{\omega_+ - \omega_-}\Bigg\{&(\omega_-\hat{\rho}_-)^2\left[1+\frac{\omega_-}{\omega_+}\right] + (\omega_+\hat{\rho}_+)^2\left[1+2\frac{\omega_-}{\omega_+}\right] \\ &+ \frac{3(\omega_z\hat{z})^2}{4}\left[1+\frac{2\omega_-}{3\omega_+}\right]\Bigg\}\end{aligned} \tag{4.162}$$

to the magnetron frequency is dominated by the shift to the axial frequency that lock will undo. In typical experiments, the factors of ω_-/ω_+ may safely be neglected.

5. Calculating other frequency-shifts

This chapter deals with two sources of frequency-shifts that did not fit into the context of Chapter 4, either because no truly perturbative method is required as is the case in Section 5.1 on the frequency-shift caused by image charges, or because second-order perturbation theory is required. In this regard, Section 5.2 on a modulation of the trapping potential extends Section 3.3 on second-order effects to the treatment of a time-dependent perturbation. The general methods of Chapter 3, in particular Section 3.4, come in handy for Section 5.1, too.

5.1. Image-charge frequency-shift

Section 2.2.1 on the electrostatic potential in a Penning trap mentioned the self-interaction of an ion via the charges its electric field induces in the electrodes. This interaction is a consequence of the electrodes being equipotential surfaces. Because the ion creates a nonzero potential there, which depends inversely on the distance from the ion, there has to be an additional potential with a nontrivial spatial dependence. This potential compensates for the ion's Coulomb potential on the electrodes, and it is present everywhere, in particular at the ion's position. For the overall electric field, the electrode being an equipotential surface means that the field lines have to be perpendicular to it, or else the remaining parallel component would move charges along the surface, until a new equilibrium is reached.

For particular geometries, the boundary conditions on the electrodes are satisfied by the strategic placement of fictitious charges, and the electric potential and field are calculated from this configuration. A point charge in front of an infinite conducting plate is the textbook example. The fictitious charge which ensures that the plate remains an equipotential surface is the mirror image of the original charge—opposite in sign and opposite the plate. That is why the method for solving this boundary-value problem is called method of image charges.

As is customary in Penning-trap physics, we will sloppily refer to the charge distribution on the electrodes as image charges, even though no pointlike charges can be singled out there. Mathematically, one would be hard-pressed to compensate for the ion's finite potential on the electrodes by placing pointlike charges, whose potential diverges at their location, right on the electrodes.

Due to the ion's motion in the Penning trap, the image charges are not static. Section 4.2.1 mentioned the complication of retardation for the modified cyclotron-mode of electrons [21, 67] when deriving relativistic equations of motion. The classical formalism of instantaneous fields suffices for ions because the wavelengths associated with their eigenfrequencies are much larger than the dimension of the trap. When neglecting the insignificant magnetic field created by the orbiting ion and by the oscillating image-charges, the time-derivatives in Maxwell's equations (2.53) and (2.54) play no role, and the problem looks like the electrostatic one again. The ion's position acts as a parameter whose time-dependence comes into play only after having

solved the electrostatic problem for the image-charge field and potential as a function of that parameter without considering the ion's motion yet. The ion's trajectory is then determined from the equation of motion that includes the force by the image charges.

The method of images has been employed multiple times to estimate the additional electric field due to image charges in a Penning trap with the goal of translating this field into frequency-shifts [162, 191, 194]. We will skip the first part of determining the image-charge field for a particular trap geometry, calculating the frequency-shifts for the generic lowest-order form this field may have. Honoring the particularity of THe-Trap, we devote special attention to the shifts under lock. In doing so, we extend the work of Reference [162] beyond an image-charge field of spherical symmetry. Reference [124] gives corresponding formulas with going into detail about their derivation. Shifts in free-running mode with the major focus on the modification of the invariance theorem (2.27) are discussed by References [127, 152].

For an ion of charge $q = ne$, with n elementary charges e, that is,[1] the field of the image charges at the position of this very ion is given by

$$\vec{E}_{\mathrm{ic}} = n(E'_x x\vec{e}_x + E'_y y\vec{e}_y + E'_z z\vec{e}_z) \tag{5.1}$$

to lowest order. This field is linear in the position of the ion—not the general coordinates—and the E'_i describe the field's gradient for one (positive) elementary charge e in the trap.[2]

When considering the image-charge potential, keeping track of two different sets of coordinates is crucial. This potential depends on the position of the ion, but it is defined everywhere. The electric field at any position is calculated by taking the negative gradient with respect to the general coordinates, while the position of the ion is treated as a parameter. The electric field at the position of the ion then follows by evaluating the resulting expression at the position of the ion [127]. This operation is not equal to plugging in the position of the ion into the general coordinate of the potential and then taking the negative gradient with respect to the position of the ion. Even though a factor of ½ cures the shortcoming of the second method [157], the difference between the image-charge potential as a function of general coordinates with the position of the ion as a parameter and the same potential evaluated at the position of the ion has profound consequences. While the former fulfills the Laplace equation (2.57) (with the Laplace operator working on the general coordinates), the latter typically does not (with respect to the position of the ion—the only variable that is left). Thus, the constraint $E'_x + E'_y + E'_z = 0$ for an electric field which is derived from a potential that is quadratic in the coordinates and satisfies the Laplace equation is lifted. Other, less fundamental relations are established by the symmetry of the trap.

A constant term in the image-charge field (5.1) is ruled out by the symmetry under point reflection about the center of the trap. If cylindrical symmetry is present, as we shall assume

[1] For N ions of the same species, assumed to occupy the same spot, the formulas in this section should hold with the replacement $n \to Nn$, as long as the ion–ion interaction is neglected.

[2] We are running short of symbols to distinguish the notation, the ordinary $E_\eta^{(i)}$ being used for the electric field. The calligraphic $\mathcal{E}$ denotes the energy of the particle (Section 2.1.2). The two variants ϵ and ε of the Greek letter epsilon are used as the perturbation parameter (3.1) and as a relative change of effective electric field (Equations (3.85) and (3.105)), respectively, both being related to frequency-shifts. Unfortunately, the capital epsilon looks like a Latin E, and for the ease of copying the formulas by hand we do not want to switch to the Fraktur or blackboard letters, $\mathfrak{E}$ or $\mathbb{E}$, LaTeX has to offer from its math alphabets. Since the E'_i describe a field gradient, the prime serves as a reminder of the derivative.

here for the moment before getting to the most general case, the gradients in the radial directions are described by the same parameter $E'_\rho \equiv E'_x = E'_y$.

In the case of spherical symmetry, all three gradients are the same: $E'_r \equiv E'_\rho = E'_z$. Even though the trap is not spherical, this case makes for an interesting model because of the analytic solution [162]

$$E'_r = \frac{1}{4\pi\varepsilon_0}\frac{e}{a^3} \tag{5.2}$$

for the gradient[3] in a sphere of radius a. Analytic expressions for some other geometries exist [157]. Unfortunately, traps with hyperboloidal electrodes are not among them, and determining the gradients relies on a semi-analytic approach [127] or simulations [140].

As a general statement, we expect the particle to be attracted by the opposite-sign charges on the electrodes (fractions of elementary charge actually), which is reflected by positive or zero gradients E'_ρ and E'_z. The gradient for one direction is zero when there is translational invariance in this direction, for instance $E'_z = 0$ in an infinite cylinder stretching along the z-axis, or $E'_\rho = 0$ for an infinite plate perpendicular to the z-axis.

Like for the imperfections of the electric and magnetic field, we will calculate the image-charge frequency-shifts in general terms, assuming that the relevant coefficients—the gradients E'_ρ and E'_z in the case of cylindrical symmetry—can be procured from other sources. Turning things around, the gradients might of course be determined from a measurement of the image-charge frequency-shift. However, we shall see that such a measurement is virtually impossible with one single ion because, for one species in a given trap, there are no suitable parameters to sample. Unlike the imperfections of the electric and magnetic trapping fields, which can be varied and whose frequency-shift depends on the amplitude of the particle, the image-charge effect is much harder to tune. In short, it is hard to extrapolate to zero image-charge frequency-shift for a single ion.

Axial mode

The additional axial acceleration $\ddot{z}_{\mathrm{ic}} = (q/m)nE'_z z$ by the image-charge field (5.1) is incorporated into the axial equation of motion (3.85) with the parameter

$$\varepsilon_z = -n\frac{q}{m}\frac{E'_z}{\omega_z^2} \tag{5.3}$$

and translated into the relative frequency-shift

$$\frac{\Delta\omega_z}{\omega_z} = -n\frac{q}{m}\frac{E'_z}{2\omega_z^2} \tag{5.4}$$

via Equation (3.86) for $|\varepsilon_z| \ll 1$. Since the axial image-charge field (5.1) has the same spatial dependence as the axial electric field (2.14) in the ideal Penning trap, both being proportional to z, perturbation theory is actually unnecessary, and the axial frequency squared is read off directly from the equations of motion as

$$\tilde{\omega}_z^2 = \omega_z^2(1 + \varepsilon_z) \tag{5.5}$$

[3] References [162] and [127] use Gaussian units, rather than SI units. We have included the vacuum permittivity ε_0 together with a factor of 4π here.

without searching for resonant terms.[4] The axial frequency-shift due to image charges is a harmonic one, which means that it does not depend on the motional amplitudes of the particle, at least for the lowest-order image-charge field considered here.

For $E_z' > 0$ as expected for typical geometries, we have $\varepsilon_z < 0$, and the axial frequency-shift is negative.[5] Thus, the actual axial frequency is smaller than it would be if the image charges were magically turned off.

Radial modes

For the radial modes, the additional acceleration

$$\begin{pmatrix} \ddot{x}_{\mathrm{ic}} \\ \ddot{y}_{\mathrm{ic}} \end{pmatrix} = n\frac{q}{m}E_\rho' \begin{pmatrix} x \\ y \end{pmatrix} \tag{5.6}$$

by the image charges fits into the radial equations of motion (3.105) with the parameter

$$\varepsilon_\rho = \varepsilon_\pm = n\frac{q}{m}\frac{2E_\rho'}{\omega_z^2} \quad . \tag{5.7}$$

Like in the axial case, the spatial dependence of the cylindrically-symmetric radial image-charge field (5.1) is the same as for the electric field (2.14) in the ideal PENNING trap. However, the prefactors of the additional axial and radial acceleration are unrelated because there is no fundamental link between the gradients E_z' and E_ρ', their ratio depending on the geometry of the trap electrodes. With the radial image-charge field easily incorporated into the equations of motion (3.105) without an explicit search for resonant terms,[6] the modified radial frequencies (2.23) become

$$\tilde{\omega}_\pm = \frac{1}{2}\left[\omega_\mathrm{c} \pm \frac{\omega_\mathrm{c}}{|\omega_\mathrm{c}|}\sqrt{\omega_\mathrm{c}^2 - 2\omega_z^2(1+\varepsilon_\rho)}\right] \quad . \tag{5.8}$$

For $|\varepsilon_\rho| \ll 1$, Equation (3.109b) gives the image-charge frequency-shift as

$$\Delta\omega_\pm = \mp\frac{q}{m}\frac{nE_\rho'}{\omega_+ - \omega_-} = \mp\frac{nE_\rho'}{B_0}\frac{\omega_+ + \omega_-}{\omega_+ - \omega_-} \approx \mp\frac{nE_\rho'}{B_0}\left(1 + 2\frac{\omega_-}{\omega_+}\right) \approx \mp\frac{nE_\rho'}{B_0} \quad . \tag{5.9}$$

We have used the definition (2.18) of the free-space cyclotron-frequency ω_c and the cyclotron-sideband identity (2.25), before approximating the frequency-shift in the limit of $\omega_-/\omega_+ \ll 1$. When dropping the factor altogether, the image-charge frequency-shift is (approximately) independent of the mass of the particle, depending only on its charge and two parameters of the trap. This dependence also explains why the shift to radial frequencies is almost impossible to measure with a single ion, in which case the only parameter to be varied would be magnetic field. However, the radial frequencies $\omega_\pm$ as such, and not just their shift, depend on the magnetic

[4] We have made the reference to the effective axial equation of motion (3.86) though, because we did not want to reprint a slightly modified version here, with just the tilde removed from $\tilde{z}$ and $\ddot{\tilde{z}}$.

[5] For a negative charge, both $q = ne$ and n are negative. Thus, the product nq in Equation (5.3) is unchanged.

[6] As for the axial mode, we could have modified the original equations of motion (2.16) in the ideal PENNING trap with x and y rather than the zeroth-order trajectories $\tilde{x}$ and $\tilde{y}$, but the effective equations of motion (3.105) already contain the parameter $\varepsilon_\pm$, to which we have assigned the meaning of ε_ρ.

field, too. Even if the magnetic field were readily adjusted, which is difficult for superconducting magnets in persistent mode, the change due the principal dependence (2.23) on the magnetic field would overshadow the change in the image-charge frequency-shift.

For a radial gradient $E'_\rho > 0$, which describes an attraction by the image-charge distribution on the electrodes, the absolute value of the reduced cyclotron-frequency ω_+ decreases, while the absolute value of magnetron frequency ω_- increases.[7] This behavior is expected for a stronger radial electric field. Since the image-charge shift (5.9) is caused by a rescaling of the radial electric field, which is equivalent to a change of the trapping voltage V_0 when there is cylindrical symmetry, the shift vanishes upon summing both radial frequencies in the cyclotron-sideband identity (2.25).

Modified invariance theorem

As discussed in the introduction to this section, the electric field (5.1) of the image charges does not have to originate from a potential that fulfills the Laplace equation (2.57) with respect to the coordinates of the ion. Therefore, the overall effect of the image-charge field is not described by a change of the effective trapping voltage V_0 in the quadrupole potential (2.2) of the ideal trap, unless the gradients satisfy $E'_z = -2E'_\rho$. As a consequence, the invariance theorem (2.27) is violated, when the image-charge frequency-shift has to be taken into account.

Summing the full expressions for the shifted axial frequency (5.5) and the shifted radial frequencies (5.8) in quadrature yields

$$\tilde{\omega}_\mathrm{c}^2 = \tilde{\omega}_+^2 + \tilde{\omega}_-^2 + \tilde{\omega}_z^2 \tag{5.10a}$$

$$= +\frac{1}{4}\left[\omega_\mathrm{c}^2 + 2\omega_\mathrm{c}\sqrt{\omega_\mathrm{c}^2 - 2\omega_z^2(1+\varepsilon_\rho)} + \omega_\mathrm{c}^2 - 2\omega_z^2(1+\varepsilon_\rho)\right] + \frac{1}{4}\left[\omega_\mathrm{c}^2 - 2\omega_\mathrm{c}\sqrt{\omega_\mathrm{c}^2 - 2\omega_z^2(1+\varepsilon_\rho)} + \omega_\mathrm{c}^2 - 2\omega_z^2(1+\varepsilon_\rho)\right] + \omega_z^2(1+\varepsilon_z) \tag{5.10b}$$

$$= \omega_\mathrm{c}^2 - \omega_z^2(\varepsilon_\rho - \varepsilon_z) = \omega_\mathrm{c}^2 - n\frac{q}{m}(2E'_\rho + E'_z) \quad . \tag{5.10c}$$

In the last step, we have used Equations (5.3) and (5.7) for ε_z and ε_ρ, respectively. The shifted free-space cyclotron-frequency $\tilde{\omega}_\mathrm{c}$ is not an actual frequency in the trap, and in general it is not equal[8] to the true free-space cyclotron-frequency, with which the ion would orbit around the magnetic field lines if there were no trap. The frequency $\tilde{\omega}_\mathrm{c}$ merely results from stubbornly applying the invariance theorem (2.27) beyond its scope. Consequently, the frequency determined in this way is shifted from the coveted one by

$$\Delta\omega_\mathrm{c} = \tilde{\omega}_\mathrm{c} - \omega_\mathrm{c} = \frac{\tilde{\omega}_\mathrm{c}^2 - \omega_\mathrm{c}^2}{\tilde{\omega}_\mathrm{c} + \omega_\mathrm{c}} \approx -\frac{n\frac{q}{m}(2E'_\rho + E'_z)}{2\omega_\mathrm{c}} = -n\frac{2E'_\rho + E'_z}{2B_0} \quad . \tag{5.11}$$

There is an approximate sign in between because we have used $\tilde{\omega}_\mathrm{c} \approx \omega_\mathrm{c}$ in the denominator after expanding with the sum of these two frequencies. For $2E'_\rho + E'_z > 0$, which we expect

[7] This statement is true regardless of the signs of n and B_0, because these two also determine the sign of the free-space cyclotron-frequency ω_c and hence the sign of the radial frequencies $\omega_\pm$. Thus the shift $\Delta\omega_+$ has the opposite sign of ω_+, whereas $\Delta\omega_-$ has the same sign as ω_-.

[8] As predicted, equality holds for $E'_z = -2E'_\rho$, when the effect of the image-charge field mimics a change of the trapping voltage V_0.

to be the usual case for the attraction by the image charges on the electrodes, the determined frequency $\tilde{\omega}_\mathrm{c}$ has a smaller absolute value[9] than the "true" free-space cyclotron-frequency ω_c.

Defining $\Delta\omega_e$ as the shift per elementary charge, the correction (5.11) is written as

$$\omega_\mathrm{c} = \tilde{\omega}_\mathrm{c} + n\Delta\omega_e \quad \text{with} \quad \Delta\omega_e = \frac{2E'_\rho + E'_z}{2B_0} \quad . \tag{5.12}$$

The shift $\Delta\omega_e$ per elementary charge depends on the magnetic field B_0 and the two gradients E'_ρ and E'_z of the image-charge field (5.1), which are a function of the trap's geometry. The result is independent of ion's mass. Moreover, there a no parameters, which are easy to vary for one ion in a specific trap, which precludes a measurement of the shift without changing the ion content of the trap, that is, varying the number of ions or the species. On the other hand, the simple dependence on such a low number of parameters with very little temporal variation is a blessing, provided the theoretical prediction is trustworthy.

Axial lock

Here we apply the methods of Section 4.3 for frequency-shifts to the radial modes when the axial mode is held constant ("locked") to the image-charge frequency-shifts. According to Equation (4.150), the lock keeps $\check{\omega}_z^2 = \omega_z^2(1+\varepsilon_z)$ constant, where the inverted hat on the frequencies $\check{\omega}_i$ indicates lock mode, in contrast to the perturbed frequencies $\tilde{\omega}_+$ with a tilde in free-running mode.

Expressing the radial frequencies (5.8) as a function of the locked axial frequency $\check{\omega}_z$ rather than the unperturbed axial frequency ω_z yields

$$\check{\omega}_\pm = \frac{1}{2}\left(\omega_\mathrm{c} \pm \frac{\omega_\mathrm{c}}{|\omega_\mathrm{c}|}\sqrt{\omega_\mathrm{c}^2 - 2\check{\omega}_z^2\frac{1+\varepsilon_\rho}{1+\varepsilon_z}}\right) \tag{5.13}$$

for the radial frequencies under lock. Making the corresponding substitutions in Equation (5.10b) is now straightforward, and the shift in the quadrature relation, the invariance theorem (2.27), becomes

$$\begin{aligned}
\check{\omega}_\mathrm{c}^2 - \omega_\mathrm{c}^2 &= \check{\omega}_+^2 + \check{\omega}_-^2 + \check{\omega}_z^2 - \omega_\mathrm{c}^2 && (5.14a)\\
&= -\check{\omega}_z^2\frac{1+\varepsilon_\rho}{1+\varepsilon_z} + \check{\omega}_z^2 = -\omega_z^2(1+\varepsilon_\rho) + \omega_z^2(1+\varepsilon_z) && (5.14b)\\
&= -\omega_z^2(\varepsilon_\rho - \varepsilon_z) = -n\frac{q}{m}(2E'_\rho + E'_z) \quad . && (5.14c)
\end{aligned}$$

As before, we have used Equations (5.3) and (5.7) for ε_z and ε_ρ, respectively, in the last step. The result is the same as in Equation (5.10c) for free-running mode, and hence Equations (5.11) and (5.12) also hold under lock with the replacement $\tilde{\omega}_\mathrm{c} \to \check{\omega}_\mathrm{c}$. Of course, the conclusions apply, too.

The agreement is in line with Equations (4.155) and (4.156c), and we could have relied on their statement. However, for the cylindrically-symmetric image-charge field (5.1), the shift to the frequency determined via the invariance theorem is calculated here without having to

[9] The statement about n and B_0 determining the sign of ω_c applies here again. Thus, the shift has the opposite sign of ω_c (and $\tilde{\omega}_\mathrm{c}$).

express the shifts $\Delta\omega_i$ to the individual frequencies, which involves first-order approximations. Moreover, no additional approximations, such as the differential dependence (4.154) of the free-space cyclotron-frequency ω_c, had to be used with the approach including the full quadrature relation here.[10]

The shift to the radial frequencies under lock is calculated by plugging Equations (5.3) and (5.9) into Equation (4.152b), or Equations (5.3) and (5.7) into Equation (4.152a). Both alternatives use Equation (2.26), $\omega_z^2 = 2\omega_+\omega_-$, and they neglect the difference between the perturbed and unperturbed frequencies in the prefactor. Using the same steps as in Equation (5.9)—the definition (2.18) of the free-space cyclotron-frequency ω_c, the cyclotron-sideband identity (2.25) and the approximation $\omega_-/\omega_+ \ll 1$—yields

$$\Delta\check{\omega}_\pm = \mp\frac{n}{2}\frac{q}{m}\frac{2E'_\rho + E'_z}{\omega_+ - \omega_-} = \mp n\frac{2E'_\rho + E'_z}{2B_0}\frac{\omega_+ + \omega_-}{\omega_+ - \omega_-} \tag{5.15a}$$

$$\approx \mp n\frac{2E'_\rho + E'_z}{2B_0}\left(1 + 2\frac{\omega_-}{\omega_+}\right) \approx \mp n\frac{2E'_\rho + E'_z}{2B_0} \quad . \tag{5.15b}$$

Thus, the shift to the radial frequencies under lock has about the same magnitude as the shift (5.11) to the free-space cyclotron-frequency determined via the invariance theorem (in either operating mode of the trap, with our without lock). Taking the signs into account, we have $\Delta\check{\omega}_\pm \approx \pm\Delta\omega_\mathrm{c}$. In addition to the approximate equality, the common sign for $\Delta\check{\omega}_+$ and $\Delta\omega_\mathrm{c}$ reflects that, under lock, the image-charge frequency-shift via the invariance theorem (2.27) is dominated by the shift to the modified cyclotron-frequency.

This relation also explains why References [162] and [127] compare so favorably, almost fortuitously, without a closer inspection of the operating mode in which their results were obtained. The former measures the image-charge frequency-shift to the radial modes under lock; the latter estimates the image-charge frequency-shift to the free-space cyclotron-frequency determined via the invariance theorem for that particular trap in order to test the theoretical method developed in the paper.

Beyond cylindrical symmetry

So far, we have treated the problem of frequency-shifts by image charges as a cylindrically-symmetric one. Fortunately, the generalization to a more complex situation with two different radial gradients of the image-charge field, $E'_x \neq E'_y$, is straightforward by defining

$$E'_\rho = \frac{1}{2}\left(E'_y + E'_x\right) \qquad \text{and} \qquad E'_\epsilon = \frac{1}{2}\left(E'_y - E'_x\right) \quad . \tag{5.16}$$

The first gradient, E'_ρ, has the same meaning as before. In this more general setting, it describes a kind of effective or average cylindrical symmetry. The second gradient, E'_ρ, describes a kind of ellipticity in the sense of Section 3.4.4. By rewriting the additional radial field (5.1) by the

[10] The full quadrature relation would be inconvenient in Section 4.3 because in general the square root for the perturbed radial frequencies (5.8) contains $\omega_\mathrm{c}^2(1+\beta_\pm)^2 - 2\omega_z^2(1+\varepsilon_\pm)$. When the parameters $\beta_\pm$ and $\varepsilon_\pm$ from the effective equation of motion (3.105) differ for the two radial modes, the square roots in Equation (5.10b) would not subtract to zero, thereby necessitating an approximation to deduce a practical statement.

image charges as

$$\begin{pmatrix} E_{\mathrm{ic}}^{(x)} \\ E_{\mathrm{ic}}^{(y)} \end{pmatrix} = n \begin{pmatrix} E_x' x \\ E_y' y \end{pmatrix} = n E_\rho' \begin{pmatrix} x \\ y \end{pmatrix} + n E_\epsilon' \begin{pmatrix} -x \\ y \end{pmatrix} \tag{5.17}$$

and by comparing the result with Equation (3.116), we identify the ellipticity parameter

$$\epsilon = n \frac{q}{m} \frac{2}{\omega_z^2} E_\epsilon' = n \frac{q}{m} \frac{E_\epsilon'}{\omega_+ \omega_-} \quad . \tag{5.18}$$

In the last step, we have used Equation (2.26) for the axial frequency squared in the ideal Penning trap. Actually, we should redefine the frequencies via Equations (5.5) and (5.8), thereby accounting for the cylindrically-symmetric contribution by the image charges. However, we will ignore the small image-charge shift in the frequencies that show up in prefactors because the shift is treated as a perturbation rather than a major modification of the ideal Penning trap. The magnitude of the image-charge frequency-shift is essentially given by the gradients E_i' of the image-charge field. Corrections to the prefactor are viewed as of higher order, and we are more interested in shifts than absolute frequencies.

In principle, Equation (3.129) allows to calculate the radial frequencies exactly in the presence of ellipticity, but again care must be taken how to incorporate the cylindrically-symmetric contribution of the image-charge field in the radial frequencies. This is not trivial because the axial and the radial field may be affected differently from what the constraint of a common quadrupole potential (2.2) would permit. As a typical consequence, the uncorrelated change invalidates the relation (2.26) and the invariance theorem (2.27), both of which were used to rewrite Equations (25) and (26) of Reference [92] as Equation (3.129). The replacement $\omega_z^2 \to \omega_z^2(1 + \varepsilon_\rho)$ in all the terms related to the radial motions that do not contain the ellipticity parameter ϵ should correctly adapt the original version. Thus, the replacement excludes the term $\epsilon^2 \omega_z^4$. This recipe is equivalent to the general replacement $\omega_z^2 \to \omega_z^2(1 + \varepsilon_\rho)$ and the redefinition $\epsilon \to \epsilon/(1 + \varepsilon_\rho)$ of the ellipticity parameter. The characteristic equation (13) of Reference [46] for the radial frequencies provides a suitable alternative because the axial frequency is not used as a symbol in the radial equations of motion, which minimizes confusion.

However, it may not be necessary to recalculate the perturbed eigenfrequencies individually because the effect of ellipticity is removed by the invariance theorem. Thus, Equations (5.10c), (5.11), (5.12) and (5.14c) all remain valid [152] with the replacement $2E_\rho' \to E_x' + E_y'$, which is the use of E_ρ' from Equation (5.16). In that sense, the average cylindrical symmetry counts, and the dominant shifts (5.9) and (5.15b) to the radial frequencies in free-running mode and lock, respectively, result from the same averaging procedure for the two radial gradients of the image-charge field. The shift by the elliptic component is subdominant in trap geometries with near cylindrical symmetry. Equation (3.128) and (5.18) produce the second-order estimate

$$\Delta\omega_\pm(\epsilon) = \pm \frac{\omega_\pm}{2} \frac{\omega_\mp^2}{\omega_+^2 - \omega_-^2} \left(\frac{nqE_\epsilon'}{m\omega_+\omega_-} \right)^2 = \frac{\pm 1}{2\omega_\pm} \frac{1}{\omega_+^2 - \omega_-^2} \left(\frac{nqE_\epsilon'}{m} \right)^2 = \frac{\pm 1}{2\omega_\pm} \frac{\omega_\mathrm{c}}{\omega_+ - \omega_-} \left(n \frac{E_\epsilon'}{B_0} \right)^2 \tag{5.19}$$

for the shift due to the elliptic image-charge gradient E_ϵ' from Equation (5.16). We have introduced the free-space cyclotron-frequency (2.18) in the last step and used the sideband identity (2.25).

Assuming that the image-charge field has a cylindrical component—that is, $E'_\rho \neq 0$—the second-order elliptic shift becomes

$$\Delta\omega_\pm(\epsilon) = \pm\frac{1}{2\omega_\pm}\frac{\omega_+ + \omega_-}{\omega_+ - \omega_-}\left(\frac{\omega_+ - \omega_-}{\omega_+ + \omega_-}\frac{E'_\epsilon}{E'_\rho}\right)^2\left(\frac{nE'_\rho}{B_0}\frac{\omega_+ + \omega_-}{\omega_+ - \omega_-}\right)^2 = \pm\frac{\omega_+ - \omega_-}{\omega_+ + \omega_-}\left(\frac{E'_\epsilon}{E'_\rho}\right)^2\frac{(\Delta\omega_\pm)^2}{2\omega_\pm} \quad (5.20)$$

when related to the image-charge shift (5.9) due to average cylindrical symmetry. Apart from expanding in order to introduce the dominant shift, we have used the sideband identity (2.25) for the free-space cyclotron-frequency ω_c.

Because the image-charge shift to the radial modes is equal in magnitude for cylindrical symmetry ($|\Delta\omega_+| = |\Delta\omega_-|$), the magnetron frequency is affected more strongly here by the particular breaking of that symmetry. However, there are two suppression factors, which would probably render the shift irrelevant taken on their own: $\Delta\omega_\pm/\omega_\pm$, the ratio of the dominant image-charge shift and the radial frequency, which may just be large enough for this relative shift to be relevant, and $(E'_\epsilon/E'_\rho)^2$, a measure of the departure from cylindrical symmetry. Because the axial mode is not effected by ellipticity, there is no additional shift under axial lock.

Impact on cyclotron-frequency ratio

Finally, we discuss the impact of the image-charge shift on a ratio of cyclotron-frequencies. Suppose $\omega_\mathrm{c}(i)$ represent the true free-space cyclotron-frequencies, with the ion species indicated in brackets. Furthermore, suppose the frequency $\tilde{\omega}_\mathrm{c}(i)$ has been determined via the invariance theorem (2.27) after a measurement of the three eigenfrequencies in the trap, which were corrected for all systematic effects apart from image-charge frequency-shifts. With these accounted for by Equation (5.12), where the ions carry n_i elementary charges e, the true ratio R is expressed a function of the measured (and partially corrected) ratio $\tilde{R}$ as

$$R = \frac{\omega_\mathrm{c}(2)}{\omega_\mathrm{c}(1)} = \frac{\tilde{\omega}_\mathrm{c}(2) + n_2\Delta\omega_e}{\tilde{\omega}_\mathrm{c}(1) + n_1\Delta\omega_e} = \frac{\tilde{\omega}_\mathrm{c}(2)}{\tilde{\omega}_\mathrm{c}(1)}\frac{1 + \frac{n_2\Delta\omega_e}{\tilde{\omega}_\mathrm{c}(2)}}{1 + \frac{n_1\Delta\omega_e}{\tilde{\omega}_\mathrm{c}(1)}} \quad (5.21a)$$

$$\approx \tilde{R}\left(1 + \frac{n_2\Delta\omega_e}{\tilde{\omega}_\mathrm{c}(2)} - \frac{n_1\Delta\omega_e}{\tilde{\omega}_\mathrm{c}(1)} + \ldots\right) \approx \tilde{R}\left(1 + \frac{\Delta\omega_e}{eB_0}(m_2 - m_1) + \ldots\right) \quad . \quad (5.21b)$$

In the approximation of the denominator for $|n_1\Delta\omega_e| \ll |\omega_\mathrm{c}(1)|$, we have neglected higher-order terms and cross-terms. Moreover, we have then used Equation (2.18) for the unperturbed free-space cyclotron-frequency to approximate the perturbed frequencies $\tilde{\omega}_\mathrm{c}(i)$ in the denominators, additionally neglecting a temporal change of the magnetic field strength B_0 between the two measurements.

While the individual correction (5.12) to the free-space cyclotron-frequency calculated via the invariance theorem[11] depends on the charge of the ion, the image-charge correction to the ratio depends on the mass difference between the two species. The correction vanishes for ions of the same mass, which means that there is essentially no correction for different charge states of ions that belong to the same atomic species, because only missing electrons (and their binding energies) constitute the mass difference. This suppression of image-charge shifts is important

[11] The shift (5.9) to the radial frequencies cancels in the sideband identity (2.25), but the invariance theorem has other advantages that back its use.

to keep in mind when doing consistency checks in this way, in which case the image-charge shift remains hidden, until it shows up as a systematic between ions of different mass [164]. On the bright side, a measurement of cyclotron-frequency ratios on mass doublets, such as ^{3}H and ^{3}He, is virtually unaffected.

5.2. Modulation of the trap potential

This section calculates the frequency-shift caused by a modulation of the trapping potential. Such a modulation creates sidebands, on which the ion motion can be driven. As a practical benefit, the frequency of this external drive on the sideband differs from the frequency of the detection system, which is tuned to an eigenfrequency of the particle. In this way, the ion signal picked up by the detection system is not swamped by spurious radio-frequency feedthrough of the drive [190], thereby enabling simultaneous excitation and detection of the ion as one continuous operation.

Essentially, we will make the replacement

$$V_0 \to \tilde{V}_0(t) = V_0 + V_\sim \cos(\omega_\sim t + \varphi_\sim) = V_0 \left[1 + \epsilon \cos(\chi_\sim)\right] \tag{5.22}$$

for the voltage in the equations of motion (2.16) of the ideal Penning trap, ignoring all the terms beyond the quadrupole potential. Here, we have introduced the abbreviation (2.33) for the argument of the trigonometric function with the frequency $\omega_\sim > 0$ and an initial phase $\varphi_\sim$. The amplitude of the voltage modulation is given by $V_\sim$. The perturbation parameter $\epsilon = V_\sim / V_0$, a kind of strength of the modulation, suggests itself. For a perturbative treatment, we will demand $|\epsilon| \ll 1$ without any specific assumption for the modulation frequency $\omega_\sim$. In the course of the calculation, we will exclude specific values, either because they counteract the original purpose of modulating the trapping voltage, or because the lead to parametric excitation.

We will ignore the effect of the axial drive on the sideband, even though it represents an additional nonresonant modulation for the radial modes. However, it is not described by a global modulation of the trapping voltage V_0 because the excitation is only applied to specific electrodes. See References [90, 116] for some ideas on how to calculate the frequency-shift by the additional drive.

The oscillatory voltage $\tilde{V}_0(t)$ brings to mind the Paul trap, a storage device without magnetic field. Adding the magnetic field of the Penning trap can be thought of as creating a combined trap. In fact, magnetic fields have been superimposed on Paul traps since their inception, for instance to increase the electron-impact ionization rate by extending the path lengths of electrons [45] or to resolve magnetic sublevels of the stored ions [98, 139]. However, the magnetic field was only a small perturbation for the ions, their storage being accomplished with the radio-frequency field. For our purpose of precision mass spectrometry, we are interested in the Penning-side of the combined trap, with the modulation representing a minor perturbation, whereas radial storage is ensured by the magnetic field. Even though the combined trap has been treated quantum-mechanically [66] and classically [97], frequency-shifts are hard to extract from these results because the focus was on the stability of the device, and the effect of the radio-frequency field is modeled as an effective potential. This pseudopotential approximation requires that the modulation frequency $\omega_\sim$ be much larger than the motional frequencies of

the ion in the static fields. This restriction pertains to many publications on combined traps, even when the PENNING-trap side in the limit of $V_\sim \to 0$ is considered [2, 33], and analytic expressions for the frequencies are given [72, 74, 109]. We are explicitly interested in the case of $\omega_\sim \ll \omega_z$, that is, a modulation frequency much smaller than the axial frequency, and we will show in this section that the LINDSTEDT–POINCARÉ method from Section 3.2.2 also works for this particular time-dependent perturbation.

5.2.1. Axial mode

With the replacement (5.22) for the trapping voltage V_0, the axial equation of motion (2.16) in the ideal PENNING trap becomes

$$\ddot{z} + \omega_z^2 z \left[1 + \epsilon \cos(\chi_\sim)\right] = 0 \quad , \tag{5.23}$$

which is an equation of MATHIEU type. Rather than relying on the mathematical groundwork (see Chapter 28 in References [38, 113], for instance), we attempt a perturbative solution for $|\epsilon| \ll 1$, using the series expansion (3.19) for the trajectory and the series expansion (3.28) for the frequency squared. As usual, both are power series in the perturbation parameter ϵ. Plugging them into the axial equation of motion (5.23) yields

$$\begin{aligned} &\ddot{z}_0 + \epsilon\ddot{z}_1 + \epsilon^2\ddot{z}_2 + \ldots \\ &\qquad + \left[\Omega_z^2 - \epsilon\omega_1^2 - \epsilon^2\omega_2^2 - \ldots\right]\left[z_0 + \epsilon z_1 + \epsilon^2 z_2 + \ldots\right]\left[1 + \epsilon\cos(\chi_\sim)\right] = 0 \quad . \end{aligned} \tag{5.24}$$

For space, the time-dependence of the z_i is not indicated explicitly. The dots indicate that individual terms of third order and higher have been ignored. Of course, executing the multiplication with the terms shown will also result in terms beyond second order, but the terms shown are necessary to get the second order right. As we shall see, the first nonvanishing term in the frequency-shift is of second order, and we will not go any further.

The zeroth-order equation of motion is simply the harmonic oscillator with a characteristic frequency Ω_z. The zeroth-order solution $z_0(t) = \hat{z}_0 \cos(\Omega_z t + \varphi_z)$ from Equation (3.31) carries over. The amplitude $\hat{z}_0$ and the initial phase φ_z are determined by the initial conditions for $z(t)$. Since the second-order frequency-shift does not depend on them, we will not specify them here.

Collecting all the term of order ϵ in the axial equation of motion (5.24), the differential equation for the first-order trajectory $z_1(t)$ becomes

$$\ddot{z}_1 + \Omega_z^2 z_1 = \omega_1^2 z_0 - \Omega_z^2 z_0 \cos(\chi_\sim) \tag{5.25a}$$

$$= \omega_1^2 z_0 - \Omega_z^2 \frac{\hat{z}_0}{2}\left[\cos(\chi_z' + \chi_\sim) + \cos(\chi_z' - \chi_\sim)\right] \quad . \tag{5.25b}$$

In the last step, we have plugged in the specific form (3.31) of the zeroth-order solution $z_0(t)$, and we have used the trigonometric product-to-sum identity (C.10) from the appendix. Note the difference between the time-dependent solution z_0 and its constant amplitude $\hat{z}_0$. The abbreviation (2.33) for the total phase of the cosine in $z_0(t)$ is written with a prime here, in order

to indicate that the total phase $\chi_z' = \Omega_z t + \varphi_z$ depends on the perturbed frequency Ω_z, rather than the unperturbed one.[12]

The cosine terms in the differential equation (5.25b) for the first-order trajectory $z_1(t)$ are nonresonant—that is, with a drive-frequency different from the axial frequency Ω_z—for $\omega_\sim \neq 0$ and $\omega_\sim \neq 2\Omega_z$. The former case is easy to handle because the trapping potential $\tilde{V}_0$ loses its time-dependence. The frequency-shift then results from a change of the static potential via Equation (3.86). No perturbative approach is required. The case of $\omega_\sim = 2\Omega_z$ corresponds to parametric excitation and is much harder to deal with. When the ion is supposed to be driven on its sideband, this case has to be avoided, and we will ignore it.

With two nonresonant drive-terms, the particular solution follows from Equation (3.26) as

$$z_{1,\mathrm{p}} = -\Omega_z^2 \frac{\hat{z}_0}{2}\left[\frac{\cos(\chi_z' - \chi_\sim)}{\Omega_z^2 - (\Omega_z - \omega_\sim)^2} + \frac{\cos(\chi_z' + \chi_\sim)}{\Omega_z^2 - (\Omega_z + \omega_\sim)^2}\right] \tag{5.26a}$$

$$= -\Omega_z^2 \frac{\hat{z}_0}{2\omega_\sim}\left[\frac{\cos(\chi_z' - \chi_\sim)}{2\Omega_z - \omega_\sim} - \frac{\cos(\chi_z' + \chi_\sim)}{2\Omega_z + \omega_\sim}\right] \quad . \tag{5.26b}$$

In the last step, we have simplified the denominators. Of course, $z_1(t)$ also contains a homogeneous solution—oscillatory terms at the perturbed axial frequency Ω_z—chosen to match the initial conditions, which we have not specified. Fortunately, we shall see that the resonant terms that drive a second-order frequency-shift do not depend on the homogeneous solution of $z_1(t)$. Speaking of resonant terms, or the lack thereof in first-order, we set the frequency-shift parameter $\omega_1^2 = 0$, indicating that there is no first-order frequency-shift.[13]

Terms of order ϵ^2 in the equation of motion (5.24) are

$$\ddot{z}_2 + \Omega_z^2 z_2 = \omega_1^2 z_1 + \omega_1^2 z_0 \cos(\chi_\sim) + \omega_2^2 z_0 - \Omega_z^2 z_1 \cos(\chi_\sim) \quad . \tag{5.27}$$

This differential equation for the second-order trajectory $z_2(t)$ is simplified in the particular case of $\omega_1^2 = 0$. With the notation $\langle\cdot\rangle_\omega$, which retrieves the term at the frequency ω from the argument in angle brackets (see Section 3.1), naturally-resonant terms at the fundamental axial frequency Ω_z are written has

$$\langle z_1 \cos(\chi_\sim)\rangle_{\Omega_z} = \left\langle z_{1,\mathrm{p}} \cos(\chi_\sim)\right\rangle_{\Omega_z} = -\Omega_z^2 \frac{\hat{z}_0}{2\omega_\sim}\frac{1}{2}\left[\frac{1}{2\Omega_z - \omega_\sim} - \frac{1}{2\Omega_z + \omega_\sim}\right]\cos(\chi_z') \tag{5.28a}$$

$$= -\frac{\Omega_z^2}{2}\frac{z_0}{(2\Omega_z)^2 - \omega_\sim^2} \quad . \tag{5.28b}$$

We have used the trigonometric product-to-sum identity (C.10) from the appendix, dismissing oscillatory terms at the frequencies $2\Omega_z - \omega_\sim$ and $\omega_\sim$ as nonresonant. Therefore, the case $\Omega_z = \omega_\sim$ requires special attention mathematically. However, it is of little experimental relevance because the whole point of the modulating the trapping potential is to avoid operating a frequency-generator close to the axial frequency of the particle.

[12] In this thesis, the tilde on top of frequencies has mainly been used to include first-order shifts. The capital Omega has been reserved for frequencies with effects of higher order. However, we do not want to use a capital Xi for the total phase here because it looks like a Latin X.

[13] Such a term would indicate a phase-dependence of the frequency-shift because adjusting the phase as $\varphi_\sim \to \varphi_\sim + \pi$ emulates a sign-flip of the perturbation parameter ϵ.

In the step leading to Equation (5.28b), we have written $z_0 = \hat{z}_0 \cos(\chi_\sim)$ for the zeroth-order trajectory of the particle. Indeed, the naturally-resonant terms are proportional to z_0, and they are removed by choosing

$$\omega_2^2 = -\frac{\Omega_z^4}{2} \frac{1}{(2\Omega_z)^2 - \omega_\sim^2} = -\frac{\Omega_z^2}{8} \frac{4\Omega_z^2}{4\Omega_z^2 - \omega_\sim^2} = -\frac{\Omega_z^2}{8} \left(1 - \frac{\omega_\sim^2}{4\Omega_z^2}\right)^{-1} \tag{5.29}$$

for the second-order frequency-shift parameter. The series expansion (3.28) of the axial frequency squared is then turned into an expression for the perturbed axial frequency with the expansion (3.47) for the square root. To second order in the frequency-shift, we are allowed to substitute $\Omega_z \to \omega_z$ in ω_2^2 of Equation (5.29), and the relative frequency-shift due to the modulation becomes

$$\frac{\Delta\omega_z}{\omega_z} = \frac{\omega_2^2}{2\omega_z^2}\epsilon^2 = -\frac{\epsilon^2}{16}\left[1 - \left(\frac{\omega_\sim}{2\Omega_z}\right)^2\right]^{-1} = -\frac{\epsilon^2}{16}\frac{(2\omega_z)^2}{(2\omega_z)^2 - \omega_\sim^2} = -\frac{\epsilon^2}{16}\frac{4\omega_z^2}{4\omega_z^2 - \omega_\sim^2} \approx -\frac{\epsilon^2}{16} \quad . \tag{5.30}$$

The last approximation is valid for $\omega_\sim \ll \omega_z$, and it reproduces the result from Reference [20]. The full expression agrees[14] with Reference [90].

In the limit of $\omega_\sim \ll \omega_z$, it is tempting to include the time-dependent trapping voltage (5.22) in the axial frequency (2.17) by defining the instantaneous axial frequency

$$\omega_z(t) = \omega_z\sqrt{1 + \epsilon\cos(\chi_\sim)} \approx \omega_z\left[1 + \frac{\epsilon}{2}\cos(\chi_\sim) - \frac{\epsilon^2}{8}\left[\cos(\chi_\sim)\right]^2 + \ldots\right] \quad . \tag{5.31}$$

In the last step, we have used the Taylor expansion (3.62) of the square root. For slow changes of the trapping voltage during one oscillation period of the particle, it seems natural to average the instantaneous frequency over time, provided the change is still fast enough to go unresolved in the experiment:

$$\langle\omega_z(t)\rangle_0 = \left[1 + \frac{\epsilon}{2}\langle\cos(\chi_\sim)\rangle_0 - \frac{\epsilon^2}{8}\left\langle\left[\cos(\chi_\sim)\right]^2\right\rangle_0 + \ldots\right] = \omega_z\left[1 - \frac{\epsilon^2}{16} + \ldots\right] \quad . \tag{5.32}$$

The constant components result from Equations (3.6) and (3.7). The shift to this average axial frequency agrees with the perturbative result (5.30) in the limit of $\omega_\sim \ll \omega_z$.

5.2.2. Radial modes

Instead of the two-dimensional radial equations of motion (2.16), we will generalize the one-dimensional equation of motion (2.20) for the complex variable $u = x + \mathrm{i}y$ from Equation (2.19). With the replacement (5.22) for the trapping voltage, the equation reads

$$\ddot{u} + \mathrm{i}\omega_c\dot{u} - \frac{\omega_z^2}{2}u\left[1 + \epsilon\cos(\chi_\sim)\right] = 0 \quad . \tag{5.33}$$

[14] Reference [116] deals with a similar problem, and the last part of its Equation (39) agrees with the full result here. However, the intermediate expression does not seem to have the right unit of frequency. A factor of ω_z^3 in the denominator, rather than ω_z, would cure the discrepancy.

Because it is still linear in u, we do not expect any mixing between the two radial modes, except for very particular choices of the modulation frequency $\omega_\sim$. Therefore, we will use the two separate series expansions

$$u_\pm(t) = u_{0,\pm} + \epsilon u_{1,\pm} + \epsilon^2 u_{2,\pm} + \dots \tag{5.34}$$

for the trajectory of each radial eigenmode. Of course, the ansatz is still inspired by the series expansion (3.19) for the one-dimensional case with only one eigenmode.

Unlike for the axial mode—a harmonic oscillator in the unperturbed case—the eigenfrequencies of the radial modes are not spotted directly even in the unperturbed equation of motion (2.20). Since the modulation does not affect the magnetic field, which is contained in the free-space cyclotron-frequency ω_c here, the series expansion for the frequency is limited to the term characterized by the axial frequency in the ideal PENNING trap.[15] In analogy to the series expansion (3.28) for the axial frequency, we use

$$\Omega_{z,\pm}^2 = \omega_z^2 + \epsilon\omega_{1,\pm}^2 + \epsilon^2\omega_{2,\pm}^2 + \dots \quad , \tag{5.35}$$

where the ±-signs indicate that the frequency-shift may be different for the two radial modes.

With the two expansions (5.34) and (5.35) for the trajectory and frequencies, respectively, the equation of motion (5.33) becomes

$$\begin{aligned}\ddot{u}_{0,\pm} + \epsilon\ddot{u}_{1,\pm} + \epsilon^2\ddot{u}_{2,\pm} + \dots + \mathrm{i}\omega_\mathrm{c}\left(\dot{u}_{0,\pm} + \epsilon\dot{u}_{1,\pm} + \epsilon^2\dot{u}_{2,\pm} + \dots\right) \\ \frac{\Omega_{z,\pm}^2}{2}\left[u_{0,\pm} + \epsilon u_{1,\pm} + \epsilon^2 u_{2,\pm} + \dots\right]\left[1 + \epsilon\cos(\chi_\sim)\right] = 0 \quad .\end{aligned} \tag{5.36}$$

The dots indicate that terms which are at least of third order themselves are not shown. By the design of the perturbative ansatz, the differential equation for the zeroth-order trajectory u_0 is equivalent to Equation (2.20) for the ideal PENNING trap with the substitutions $u \to u_0$ and $\omega_z \to \Omega_{z,\pm}$. Thus, the ansatz

$$u_{0,\pm} = \hat{u}_{0,\pm}\mathrm{e}^{-\mathrm{i}(\Omega_\pm t + \varphi_\pm)} = \hat{u}_{0,\pm}\mathrm{e}^{-\mathrm{i}\chi'_\pm} \quad , \tag{5.37}$$

very similar to Equation (2.21), yields the corresponding characteristic equation (2.22) for the perturbed radial frequencies with the solutions

$$\Omega_\pm = \frac{1}{2}\left[\omega_\mathrm{c} \pm \frac{\omega_\mathrm{c}}{|\omega_\mathrm{c}|}\sqrt{\omega_\mathrm{c}^2 - 2\Omega_{z,\pm}^2}\right] \quad . \tag{5.38}$$

In contrast to the radial frequencies (2.23) in the ideal Penning trap, the argument in the square root might differ for the two radial modes due to the presence of $\Omega_{z,\pm}^2$ rather than ω_z^2. Thus, the cyclotron sideband-identity (2.25) does not have to be valid, and Equation (2.26) would be modified, too. When $\Omega_{z,\pm}$ is not equal to the actual axial frequency Ω_z, the invariance theorem (2.27) does not hold either.

[15] Keep in mind that ω_z in this context of the radial modes is no longer related to the actual axial oscillation frequency Ω_z in the perturbed PENNING trap. The symbol (2.17) is just a convenient way to summarize all the factors.

The terms of order ϵ from the equation of motion (5.36) are given by

$$\ddot{u}_{1,\pm} + \mathrm{i}\omega_\mathrm{c}\dot{u}_{1,\pm} - \frac{\Omega_{z,\pm}^2}{2} = -\frac{\omega_{1,\pm}^2}{2}u_{0,\pm} + \frac{\Omega_{z,\pm}^2}{2}u_{0,\pm}\cos(\chi_\sim) \tag{5.39a}$$

$$= -\frac{\omega_{1,\pm}^2}{2}u_{0,\pm} + \frac{\Omega_{z,\pm}^2}{4}\hat{u}_{0,\pm}\left[\mathrm{e}^{-\mathrm{i}(\chi'_\pm-\chi_\sim)} + \mathrm{e}^{-\mathrm{i}(\chi'_\pm+\chi_\sim)}\right] \quad , \tag{5.39b}$$

where we have plugged in the specific form (5.37) of the zeroth-order solution in the last step. For the analysis of frequency-components, it is convenient to express the cosine as exponential functions with imaginary arguments via Equation (C.1) from the appendix.

Before we examine the two resulting drive-terms in detail, we take a step back for some preparatory work by considering the simplified differential equation

$$\ddot{u}_{1,\pm} + \mathrm{i}\omega_\mathrm{c}\dot{u}_{1,\pm} - \frac{\Omega_{z,\pm}^2}{2}u_{1,\pm} = \hat{a}_\mathrm{d}\mathrm{e}^{-\mathrm{i}(\omega_\mathrm{d}t+\varphi_\mathrm{d})} \tag{5.40}$$

with a generic drive-term at the frequency ω_d. This drive-term on the right-hand side is characterized by the amplitude $\hat{a}_\mathrm{d}$ of the acceleration, its frequency ω_d, and a phase φ_d. For a nonresonant drive, the usual ansatz $u_1 \propto \exp[-\mathrm{i}(\omega_\mathrm{d}t + \varphi_\mathrm{d})]$ leads to the particular solution

$$u_{1_\mathrm{p},\pm} = \frac{-\hat{a}_\mathrm{d}\mathrm{e}^{-\mathrm{i}(\omega_\mathrm{d}t+\varphi_\mathrm{d})}}{\omega_\mathrm{d}^2 - \omega_\mathrm{c}\omega_\mathrm{d} + \frac{\Omega_{z,\pm}^2}{2}} \quad . \tag{5.41}$$

For $\omega_\mathrm{d} = \Omega_\pm$, that is, a resonant drive, the denominator vanishes because it is the characteristic equation for the radial frequencies. In the case of the drive-terms in Equation (5.39b) for the first-order trajectory u_1, the resonant-drive condition is excluded by demanding that $\omega_\sim \neq |\Omega_+ - \Omega_-|$. Otherwise, there is parametric excitation of the radial modes [131, 141].

Generally, the two nonresonant drive-frequencies in Equation (5.39b) are $\omega_{\sigma_\pm} = \Omega_\pm + \sigma_\pm\omega_\sim$, where $\sigma_\pm = \pm 1$. We have introduced the extra parameter $\sigma_\pm$ in order to distinguish the additional choice of sign for the sideband from the two radial frequencies $\Omega_\pm$, which are also identified by their sign. As a consequence of modulating the trapping potential, each radial motion develops an upper sideband and a lower sideband in first order. The parameter $\sigma_\pm$ is an additional degree of freedom, chosen independently of the sign that identifies the radial frequencies.

By plugging in the frequencies $\omega_{\sigma_\pm}$ for ω_d in Equation (5.41) and using the superposition principle on the linear differential equation (5.39b) for the first-order trajectory u_1, its particular solution takes the form

$$u_{1_\mathrm{p},\pm} = -\frac{\Omega_{z,\pm}^2}{4}\hat{u}_{0,\pm}\left[\frac{\mathrm{e}^{-\mathrm{i}(\chi'_\pm-\chi_\sim)}}{\omega_{\sigma_-}^2 - \omega_\mathrm{c}\omega_{\sigma_-} + \frac{1}{2}\Omega_{z,\pm}^2} + \frac{\mathrm{e}^{-\mathrm{i}(\chi'_\pm+\chi_\sim)}}{\omega_{\sigma_+}^2 - \omega_\mathrm{c}\omega_{\sigma_+} + \frac{1}{2}\Omega_{z,\pm}^2}\right] \tag{5.42}$$

$$= -\frac{\Omega_{z,\pm}^2}{4\omega_\sim}\hat{u}_{0,\pm}\left[\frac{\mathrm{e}^{-\mathrm{i}(\chi'_\pm-\chi_\sim)}}{\omega_\sim - (2\Omega_\pm - \omega_\mathrm{c})} + \frac{\mathrm{e}^{-\mathrm{i}(\chi'_\pm+\chi_\sim)}}{\omega_\sim + (2\Omega_\pm - \omega_\mathrm{c})}\right] \quad . \tag{5.43}$$

The last step simplifies the denominators as

$$\omega_{\sigma_\pm}^2 - \omega_\mathrm{c}\omega_{\sigma_\pm} + \frac{\Omega_{z,\pm}^2}{2} = (\Omega_\pm + \sigma_\pm\omega_\sim)^2 - \omega_\mathrm{c}(\Omega_\pm + \sigma_\pm\omega_\sim) + \frac{\Omega_{z,\pm}^2}{2} \tag{5.44a}$$

$$= \underbrace{\Omega_\pm^2 - \omega_\mathrm{c}\Omega_\pm + \frac{\Omega_{z,\pm}^2}{2}}_{=0} + 2\sigma_\pm\Omega_\pm\omega_\sim + \omega_\sim^2 - \sigma_\pm\omega_\mathrm{c}\omega_\sim \tag{5.44b}$$

$$= \omega_\sim\left[\omega_\sim + \sigma_\pm(2\Omega_\pm - \omega_\mathrm{c})\right] \quad , \tag{5.44c}$$

where the underbraced terms vanish because they represent the characteristic equation for the perturbed radial frequencies. Like for the axial mode, we shall see that the homogeneous solution for the first-order trajectory $u_1(t)$, which consists of oscillatory terms at the radial frequencies $\Omega_\pm$, does not give rise to naturally-resonant terms. Thus, we do not have to bother about initial conditions. Because there are no naturally-resonant terms in first order, we choose $\omega_{1,\pm}^2 = 0$ for the first-order frequency-shift parameter. Again, there is no first-order frequency-shift due to the modulation.

The second-order terms in the equation of motion (5.36) for $u_{2,\pm}$ are

$$\ddot{u}_{2,\pm} + \mathrm{i}\omega_\mathrm{c}\dot{u}_{2,\pm} - \frac{\Omega_{z,\pm}^2}{2} = -\frac{\omega_{1,\pm}^2}{2}\left[u_{1,\pm} + u_{0,\pm}\cos(\chi_\sim)\right] - \frac{\omega_{2,\pm}^2}{2}u_{0,\pm} + \frac{\Omega_{z,\pm}^2}{2}u_{1,\pm}\cos(\chi_\sim) \quad , \tag{5.45}$$

of which only two terms remain on the right-hand side because $\omega_{1,\pm}^2 = 0$. With the particular solution (5.43) for the first-order trajectory, the naturally-resonant terms at the frequencies $\Omega_\pm$ of the radial eigenmodes evaluate to

$$\left\langle u_{1,\pm}\cos(\chi_\sim)\right\rangle_{\Omega_\pm} = \frac{1}{2}\left\langle u_{1,\pm}\left[\mathrm{e}^{\mathrm{i}\chi_\sim} + \mathrm{e}^{-\mathrm{i}\chi_\sim}\right]\right\rangle_{\Omega_\pm} = \frac{1}{2}\left\langle u_{1\mathrm{p},\pm}\left[\mathrm{e}^{\mathrm{i}\chi_\sim} + \mathrm{e}^{-\mathrm{i}\chi_\sim}\right]\right\rangle_{\Omega_\pm} \tag{5.46a}$$

$$= -\frac{\Omega_{z,\pm}^2}{8\omega_\sim}\hat{u}_{0,\pm}\mathrm{e}^{-\mathrm{i}\chi'_\pm}\left[\frac{1}{\omega_\sim - (2\Omega_\pm - \omega_\mathrm{c})} + \frac{1}{\omega_\sim + (2\Omega_\pm - \omega_\mathrm{c})}\right] \tag{5.46b}$$

$$= -\frac{\Omega_{z,\pm}^2}{4}\frac{u_{0,\pm}}{\omega_\sim^2 - (2\Omega_\pm - \omega_\mathrm{c})^2} \quad . \tag{5.46c}$$

Since these naturally-resonant terms are proportional to the zeroth-order trajectory $u_{0,\pm}$ from Equation (5.37), they are removed by the choice

$$\omega_{2,\pm}^2 = -\frac{\Omega_{z,\pm}^4}{4}\frac{1}{\omega_\sim^2 - (2\Omega_\pm - \omega_\mathrm{c})^2} \approx \frac{\omega_z^4}{4}\frac{1}{(2\omega_\pm - \omega_\mathrm{c})^2 - \omega_\sim^2} = \frac{\omega_z^4}{4}\frac{1}{(\omega_+ - \omega_-)^2 - \omega_\sim^2} \tag{5.47}$$

for the second-order frequency-shift parameter. To second-order in the frequency-shift, the perturbed frequencies may be replaced with the frequencies in the ideal Penning trap here, because $\omega_{2,\pm}^2$ enters in a product with ϵ^2, which is of second order itself. In the last step, we have used the cyclotron-sideband identity (2.25) to write $2\omega_\pm - \omega_\mathrm{c} = 2\omega_\pm - (\omega_+ + \omega_-) = \pm(\omega_+ - \omega_-)$. In fact, we might now drop the ±-sign in the subscript of $\omega_{2,\pm}^2$ because the parameter is the same for both radial modes, but we will keep it in order to distinguish the parameters from the ones in Section 5.2.1 on the axial mode.

With $\omega_{1,\pm}^2 = 0$, the series expansion (5.35) for the fictitious frequency squared in a configuration with no magnetic field becomes

$$\Omega_{z,\pm}^2 = \omega_z^2 + \omega_{2,\pm}^2\epsilon^2 + \ldots = \omega_z^2\left(1 + \frac{\omega_{2,\pm}^2}{\omega_z^2}\epsilon^2 + \ldots\right) \tag{5.48}$$

to second order. This expansion describes the effective change of the electric potential, and it could be translated into the actual perturbed radial frequencies via Equation (5.38). For small frequency-shifts, it is convenient to express the effect in terms of the parameter

$$\varepsilon_\pm = \frac{\omega_{2,\pm}^2}{\omega_z^2}\epsilon^2 \tag{5.49}$$

from the effective radial equations of motion (3.105). For $|\varepsilon_\pm| \ll 1$, Equation (3.109b) yields the frequency-shift

$$\Delta\omega_\pm = \mp\frac{\omega_z^2}{2(\omega_+ - \omega_-)}\varepsilon_\pm = \mp\frac{\omega_z^4}{\omega_+ - \omega_-}\frac{1}{(\omega_+ - \omega_-)^2 - \omega_\sim^2}\frac{\epsilon^2}{8} \approx \mp\frac{\omega_z^4}{(\omega_+ - \omega_-)^3}\frac{\epsilon^2}{8} \quad , \tag{5.50}$$

where we have used Equation (2.26), $\omega_z^2 = 2\omega_+\omega_-$, on the original product of radial frequencies. The last approximation is valid for $\omega_\sim \ll |\Omega_+ - \Omega_-|$. Since the shift to the radial modes is equal in magnitude, but opposite in sign, it vanishes in the cyclotron-sideband identity (2.25).

The second-order frequency-shift (5.50) agrees with Reference [90], and it clearly disagrees with the statement from Reference [116] that "the Paul trap shift is not accompanied by changes in the cyclotron or magnetron frequencies." The classic review paper [20] on Penning traps discusses the effect of the modulation on the axial mode without elaborating on the radial modes. However, this omission is not justified with a statement that would rule out an effect entirely.

Like for the shift to the axial frequency, we define the instantaneous radial frequencies

$$\omega_\pm(t) = \frac{1}{2}\left[\omega_\mathrm{c} \pm \frac{\omega_\mathrm{c}}{|\omega_\mathrm{c}|}\sqrt{\omega_\mathrm{c}^2 - 2\omega_z^2\left[1 + \epsilon\cos(\chi_\sim)\right]}\right] \tag{5.51a}$$

$$\approx \omega_\pm \mp \frac{\omega_\mathrm{c}}{|\omega_\mathrm{c}|}\frac{\omega_z^2}{2\sqrt{\omega_\mathrm{c}^2 - 2\omega_z^2}}\epsilon\cos(\chi_\sim) \mp \frac{\omega_\mathrm{c}}{|\omega_\mathrm{c}|}\frac{\omega_z^4}{4\left(\sqrt{\omega_\mathrm{c}^2 - 2\omega_z^2}\right)^3}\epsilon^2\left[\cos(\chi_\sim)\right]^2 + \ldots \quad . \tag{5.51b}$$

The second step uses the Taylor expansion

$$\sqrt{b - a\epsilon} \approx \sqrt{b} - \frac{a}{2\sqrt{b}}\epsilon - \frac{a}{8\sqrt{b}^3}\epsilon^2 - \ldots \tag{5.52}$$

for the square root, where $b = \omega_\mathrm{c}^2 - 2\omega_z^2$ and $a = 2\omega_z^2$. In the limit of $\omega_\sim \ll |\omega_\pm|$, we may expect a decent estimate by averaging the instantaneous radial frequencies:

$$\langle\omega_\pm(t)\rangle_0 = \omega_\pm \mp \frac{\omega_\mathrm{c}}{|\omega_\mathrm{c}|}\frac{\omega_z^4}{8\left(\sqrt{\omega_\mathrm{c}^2 - 2\omega_z^2}\right)^3}\epsilon^2 = \omega_\pm \mp \frac{\omega_z^4}{8\left(\omega_+ - \omega_-\right)^3}\epsilon^2 \quad . \tag{5.53}$$

The constant components of the cosines are from Equations (3.6) and (3.7), and we have used Equation (3.106) for the square root. The result is the same as the perturbative expression (5.50) in the limit of $\omega_\sim \ll |\omega_+ - \omega_-|$. Because $|\omega_+| \gg |\omega_-|$ in typical experiments, this limit is less restrictive than the condition $\omega_\sim \ll |\omega_\pm|$, which we assumed for averaging the instantaneous radial frequencies. Since $|\omega_-| < |\omega_+|$ for a trapped particle, the last condition boils down to $\omega_\sim \ll |\omega_-|$. It is surprising that the concept of averaging the instantaneous magnetron-frequency produces a valid estimate even beyond the limit of slow changes. However, unlike for the axial mode, the modulation affects only part of the force that gives rise to the magnetron mode.

Due to the constant neglect of the shift (5.50) to the radial frequencies in the literature, we compare its magnitude with the corresponding shift (5.30) to the axial mode:

$$\Delta\omega_\pm \approx \pm\frac{2\omega_z^3}{(\omega_+ - \omega_-)^3}\frac{-\omega_z\epsilon^2}{16} \approx \pm\frac{2\omega_z^3}{(\omega_+ - \omega_-)^3}\Delta\omega_z \quad . \tag{5.54}$$

Because we have neglected the modulation frequency $\omega_\sim$, we use the approximate sign. For the typical hierarchy $|\omega_-| \ll \omega_z \ll |\omega_+|$, there is quite a strong suppression, even considering that shifts to the individual eigenfrequencies are scaled with the respective eigenfrequency when calculating the free-space cyclotron-frequency via the invariance theorem (2.27), as Equation (4.155) shows. Accordingly, the relative shift is given by

$$\frac{\Delta\omega_\mathrm{c}}{\omega_\mathrm{c}} = \frac{\omega_+\Delta\omega_+ + \omega_z\Delta\omega_z + \omega_-\Delta\omega_-}{\omega_\mathrm{c}^2} \quad . \tag{5.55}$$

This expression also holds for the frequency-shifts under lock, see Equation (4.156a). The shifts (5.30) and (5.50) due to the modulation generally do not cancel.

Assuming the major contribution of the modulation to enter through the axial mode due the suppression factor of about $(\omega_z/\omega_+)^3$ in Equation (5.54), the relative shift to the frequency determined via the invariance theorem is approximated as

$$\frac{\Delta\omega_\mathrm{c}}{\omega_\mathrm{c}} \approx -\frac{\omega_z^2}{\omega_\mathrm{c}^2}\frac{\epsilon^2}{16} = -\frac{\frac{qC_2V_0}{md^2}}{\frac{q^2B_0^2}{m^2}}\frac{V_\sim^2}{16V_0^2} = -\frac{m}{qV_0}\frac{C_2}{d^2B_0^2}\frac{V_\sim^2}{16} \tag{5.56a}$$

$$= -\frac{md^2}{qC_2V_0}\frac{C_2^2}{d^4B_0^2}\frac{V_\sim^2}{16} = -\left(\frac{C_2V_\sim}{4\omega_z d^2B_0}\right)^2 \quad . \tag{5.56b}$$

We have used the unperturbed axial frequency (2.17), the free-space cyclotron-frequency (2.18), and the definition (5.22) of the perturbation parameter ϵ. Since two different ion species are typically locked to the same axial frequency, the relative shift due to the modulation is approximately the same for them, provided the amplitude $V_\sim$ of the modulation is not changed.[16] Among the other parameters, the magnetic field is probably subject to the largest temporal variations. Because a constant relative shift to the free-space cyclotron-frequency cancels in the frequency ratio, see Equation (5.21a), corrections do not have to be applied to the two species individually.

[16] An adjustment of V_0 is typically required to end up with the same axial frequency for both species.

For completeness, we mention the shift to the radial modes under axial lock. Using Equation (4.152c) with Equation (2.26), $2\omega_+\omega_- = \omega_z^2$, to combine the shifts (5.30) and (5.50) to the axial mode and radial modes, respectively, yields

$$\Delta\check{\omega}_\pm \approx \mp\frac{\omega_z^2}{\omega_+ - \omega_-}\frac{\epsilon^2}{16}\left[1 + \frac{2\omega_z^2}{(\omega_+ - \omega_-)^2}\right] \quad . \tag{5.57}$$

In line with typical experiments, we have neglected the modulation frequency $\omega_\sim$ against ω_z and $|\omega_+ - \omega_-|$. The modulation-shift to the radial modes under axial lock is dominated by the shift to the axial mode.

5.2.3. Pseudopotential for high modulation-frequency

The perturbative approach did not require the modulation frequency $\omega_\sim$ to be small compared with the motional frequencies of the ion in the static trap. Turning to a modulation frequency much higher than all the eigenfrequencies in the static trap yields an analytic expression for the slow motional frequencies, thereby allowing a cross-check of the perturbative result for the frequency-shifts.

In this regime, the effect of a rapidly oscillating electric field $\vec{E}(t) = \vec{E}_\sim \cos(\omega_\sim t + \varphi_\sim)$ on the slower eigenmotions is described by the static pseudopotential[17] [56]

$$\bar{\Phi}_\sim = \frac{q}{m}\frac{1}{4\omega_\sim^2}\left|\vec{E}_\sim\right|^2 \quad . \tag{5.58}$$

The fast component of the motion at the frequency of the modulation ("micromotion") is supposed to be sufficiently small compared with the slow motion in the time-averaged fields ("macromotion" or "secular motion"). With the oscillatory voltage from Equation (5.22), the amplitude of the oscillatory field is given by $\vec{E}_\sim = \epsilon\vec{E}_2$, where $\vec{E}_2$ is the electrostatic field (2.14) that results from the quadrupole potential Φ_2 of the ideal Penning trap. As before in this section, we have neglected the effect of modulating higher-order potentials. With these choices, the pseudopotential becomes

$$\bar{\Phi}_\sim = \frac{m}{q}\frac{\omega_z^4}{\omega_\sim^2}\frac{\epsilon^2}{16}\left(x^2 + y^2 + 4z^2\right) \quad . \tag{5.59}$$

Clearly, it violates the Laplace equation (2.57), which is one of the reasons for calling it a *pseudo*potential. More interestingly, the pseudopotential creates a potential well in all three directions, thereby allowing confinement in three dimensions.[18]

The electric field by the pseudopotential $\bar{\Phi}_\sim$ results from taking the negative gradient. The additional acceleration

$$\begin{pmatrix}\ddot{\bar{x}}_\sim\\ \ddot{\bar{y}}_\sim\\ \ddot{\bar{z}}_\sim\end{pmatrix} = -\frac{q}{m}\vec{\nabla}\bar{\Phi}_\sim = -\frac{\omega_z^4}{\omega_\sim^2}\frac{\epsilon^2}{8}\begin{pmatrix}x\\ y\\ 4z\end{pmatrix} \tag{5.60}$$

[17] We have slightly modified the notation of Reference [56], because we want the pseudopotential $\bar{\Phi}_\sim$ to have the unit of voltage in order to be in line with the electrostatic potentials Φ_η in this thesis.

[18] Do not worry about the sign of the charge q. There is another factor of q in the potential energy $\mathcal{E}_{\text{pot}} = q\bar{\Phi}_\sim$, which has a global minimum at the origin then. Because the pseudopotential depends on the magnitude (squared) of the electric field, any field-free point constitutes a global minimum of the potential energy energy.

has to be included in the equations of motion (2.16) of the ideal PENNING trap. The spatial dependence is very similar to the acceleration by the image charges in Section 5.1, and the treatment carries over. In fact, the assumption of $|\epsilon| \ll 1$ for a perturbative treatment is no longer necessary with this pseudopotential. We could give exact expressions for the radial frequencies, like References [74, 109] do for the radial modes.[19] We will content ourselves with the limit of $|\epsilon| \ll 1$ here because we want to check our perturbative results from Sections 5.2.1 and 5.2.2.

The additional axial acceleration (5.60) is incorporated by choosing the parameter

$$\varepsilon_z = \frac{\omega_z^2}{\omega_\sim^2}\frac{\epsilon^2}{2} \tag{5.61}$$

in the axial equation of motion (3.85). According to Equation (3.86), the corresponding frequency-shift is

$$\frac{\Delta\omega_z}{\omega_z} = \frac{\varepsilon_z}{2} = \frac{\omega_z^2}{\omega_\sim^2}\frac{\epsilon^2}{4} \quad , \tag{5.62}$$

which agrees with the perturbative result (5.30) in the limit of $\omega_\sim^2 \gg 4\omega_z^4$.

The additional radial acceleration (5.60) is included in the radial equations of motion (3.105) with the choice

$$\varepsilon_\pm = -\frac{\omega_z^2}{\omega_\sim^2}\frac{\epsilon^2}{4} \quad . \tag{5.63}$$

Equation (3.109b) translates this parameter into the frequency-shift

$$\Delta\omega_\pm = \mp\frac{\omega_z^2}{2(\omega_+ - \omega_-)}\varepsilon_\pm = \pm\frac{\omega_z^4}{\omega_+ - \omega_-}\frac{1}{\omega_\sim^2}\frac{\epsilon^2}{8} \quad , \tag{5.64}$$

where we have used Equation (2.26), $2\omega_+\omega_- = \omega_z^2$. This result agrees with the frequency-shift (5.50) from the perturbative treatment in the limit of $(\omega_+ - \omega_-)^2 \ll \omega_\sim^2$.

The sign of the frequency-shifts (5.62) and (5.64) for high-frequency modulation is opposite to the case of a low modulation frequency $\omega_\sim$. In the regime here, the well-shape of the pseudopotential explains the sign intuitively. The axial frequency increases because of an additional restoring force in the axial direction. In the radial direction, the field from the pseudopotential counteracts the outward radial field of the ideal PENNING trap, thereby bringing the modified cyclotron-frequency closer to the free-space cyclotron-frequency. Conversely, the magnetron motion is slowed down due to the reduced net electric field.

[19] Because References [74, 109] consider linear combined traps, applying the oscillatory voltage only to the central part of the trap, there is no modulation in the axial component.

6. Summary and outlook

This thesis has used a classical formalism of perturbation theory in order to calculate miscellaneous frequency-shifts in Penning traps. The approach speaks the language of an experimentalist, working with equations of motions, amplitudes and frequencies, which are related more closely to actual observables than canonical action and angle variables. The results are readily adapted to numerous experimental scenarios. Moreover, the thesis has demonstrated that there is no need for quantum-mechanical perturbation theory when the experiment is well within the classical limit.

For first-order frequency-shifts, the perturbative formalism comes down to identifying the terms that are in phase with the zeroth-order motion of the particle. Consequently, analyzing the frequency spectrum of products and powers of oscillatory terms has been a vital ingredient. For cylindrically-symmetric imperfections of the electric and magnetic field, it has been shown in Section 4.1 that there is a general pattern behind those naturally-resonant terms. Identifying this pattern has allowed to calculate the first-order frequency-shifts caused by these imperfections consistently in an all-encompassing manner, rather than individually for a particular imperfection of this type as was customary in the literature. The general treatment has yielded generating expressions for the associated frequency-shifts, which foster the link between the separate formulas in the literature and allow for more comprehensive statements concerning cancellations, for instance. Compared with the equally general treatment [99] via Hamiltonian perturbation theory, the use of binomial coefficients in the generating expressions for the shifts due to magnetic imperfections has proven to handle some special cases more conveniently, thereby yielding more compact expressions. For cylindrically-symmetric electrostatic imperfections, agreement with Reference [99] was found. The disagreement for cylindrically-symmetric magnetic imperfections was not to be resolved because the frequency-shifts given there lack more than just the perturbation parameter in their prefactor. Nevertheless, it is encouraging that a general treatment is possible, and this thesis provides a cross-check for future calculations with other methods.

The consistent treatment of cylindrically-symmetric imperfections was enabled by their parametrization in cylindrical coordinates in Section 2.2. Near the center of the empty trap, both the electric and the magnetic field result from scalar potentials that fulfill the Laplace equation. Even though cylindrical coordinates are the natural choice for imperfections of that symmetry, general expressions for polynomial solutions of the Laplace equation are rare in the literature, which typically relies on a solution with a Legendre polynomial in spherical coordinates. However, analyzing the multipole components of the trapping fields described by these polynomial solutions is a prerequisite for perturbation theory, which takes the homogeneous magnetic field and the electrostatic quadrupole potential as its starting point. When no recipe for the conversion of coordinates in these solutions is given, the general parametrization in cylindrical coordinates remains elusive, detracting from the possibility of

treating the frequency-shifts consistently. This thesis has shown how to derive polynomial solutions from a power series ansatz. Knowledge about Legendre polynomials was only required to match the prefactor of the solutions with those in the literature. Moreover, the result serves as an encouraging example that simple first principles can prevail against highbrow mathematics with its special functions. Due to the ubiquity of the Laplace equation in physics, the approach has been extended to solutions with discrete rotational symmetry featuring associated Legendre polynomials in Section A.3 in the appendix. In fact, parametrizing the radial magnetic field without an associated Legendre polynomial has greatly reduced the appeal of modeling the impact of the radial modes on the axial mode via their magnetic moment. With a polynomial parametrization in cylindrical coordinates, the radial magnetic field is no longer more complicated than the axial magnetic field from a mathematical point of view, and it is ready for use in the equations of motion.

Along the same lines of making results more comprehensible with less theoretical background, relativistic frequency-shifts have been derived perturbatively in Section 4.2 from the relativistic equations of motion rather than via a quantum-mechanical operator formalism, the standard treatment in the literature. The results agree in the limit of high quantum-numbers when quantization becomes unobservable and the particle is still only mildly relativistic. Prior treatments based on equations of motion have often relied on the auxiliary concept of relativistic mass-increase, which gives decent estimates in all cases, yet does not always reproduce the exact result. Like the treatment with operators, the perturbative result here is exact to first order.

Despite the focus on first-order frequency-shifts, the method of classical perturbation theory is neither limited to this order, nor to anharmonic frequency-shifts. Second-order effects have been considered for the one-dimensional anharmonic oscillator, again by spotting the pattern for generating naturally-resonant terms. No equally general result has been found in the literature. However, there is agreement with the specific expressions of Reference [59]. Because the corrections to the trajectory had to be calculated, it became clear that perturbation theory grows more tedious order by order for a single imperfection, not to mention the cross-terms different imperfections produce in concert. With the one-dimensional case already being so complicated, a general treatment of the Penning trap seems unfeasible, or at least very arduous, because solving the equations of motion is increasingly difficult in three dimensions. However, higher orders are interesting in order to estimate theoretical uncertainties and to determine the scope of the perturbative treatment. Moreover, the imperfections that are antisymmetric with respect to the axial coordinate ("odd terms") give rise to a frequency-shift only in second order. Rather than attempting an all-embracing treatment, it seems more reasonable to pick the imperfections that really matter in a particular experiment. The same point must be made for imperfections without cylindrical symmetry.

While odd imperfections of the electrostatic field were dismissed as being small thanks to the reflection symmetry when the trap is operated with symmetric voltages, the argument does not hold for the external magnetic field. Unlike the electrostatic potential, which has no net gradient at the particle's equilibrium position—a saddle point in the potential—such a gradient in the magnetic field cannot be ruled out. Therefore, it is worthwhile to use the classical formalism of perturbation theory in second order on this term specifically.

Not all known sources of frequency-shifts in a PENNING trap could be reconsidered, and no new shifts were discovered. The absence of such unpleasant surprises underlines how advanced (or narrow-minded) the theoretical description of the PENNING trap is. Apart from misalignment, which cancels in the invariance theorem, the interaction of the trapped particle with the detection system was ignored entirely. Even in a harmonic oscillator, there is a frequency-shift due to damping. The anharmonic oscillator adds a dependence on the particle's motional amplitudes, which were assumed to be constant throughout the thesis. Obviously, this is no longer the case when damping is present. Fortunately, the effect of damping in the axial mode is balanced by the axial drive at THe-Trap, and the basic assumptions of this thesis are not too far-fetched to render them unrealistic and the results irrelevant. Even without the damping brought about by the resistance of the detection system, the complex impedance, which becomes an issue when the resonant circuit is detuned from the particle's eigenfrequency, leads to static frequency-shifts. Prior treatments show that these static shifts are handled without advanced methods. When damping is slow, the formulas for the anharmonic shifts given here carry over by plugging in the particle's instantaneous amplitudes.

Second-order harmonic effects include the treatment of a slightly elliptic quadrupole potential and a small modulation of the ideal quadrupole potential. As a benchmark of the method, results from the literature were reproduced in both cases. The latter case is particularly interesting because it demonstrates that the classical perturbation method also handles periodic perturbations, albeit nonresonant ones, which do not turn the amplitudes into time-dependent quantities. Excitations of the particle remain a different story.

The thesis has stressed that all the frequency-shifts calculated for standard PENNING traps have to be adapted to the specific operation mode with locked axial-frequency at THe-Trap. The prescription for doing so has been given, thereby contributing to the understanding of axial lock and the experiment in general. The largest theoretical leap for the ongoing measurements at THe-Trap would be an improved model of the locked loop. So far, the driven ion is treated as a voltage-controlled oscillator with the detection system generating an error signal that indicates deviations from drive frequency [196]. While the error signal beyond the linear approximation has been included in simulations [70], the effect of anharmonicity on the axial mode beyond the frequency-shift has been ignored, even when the axial mode is not a harmonic oscillator with respect to its amplitude. With enhanced theoretical understanding, the feedback signal by the locked loop might serve as a much better diagnostic tool, possibly allowing to disentangle voltage and amplifier noise from loop-induced oscillations and actual ion dynamics, potentially triggered by anharmonic pulling or hysteresis.

As the locked loop is a much more dynamic feedback system, the time-dependence of the particle's amplitudes and frequencies upon continuous excitation will have to be considered for a complete description. Even without lock, this is far more challenging than deriving static frequency-shifts. For the axial mode, both damping and the axial drive have to be included. Additionally, the excitation drive for the radial modes is typically swept in frequency. A line-shape model beyond simple heuristics that allows to extract the initial radial frequency from a fit to the measured response of the locked loop would be the ultimate achievement in terms of theory. Despite the daunting task, the thesis shows that it is worth taking a fresh look at problems that were considered either solved or too disjointed to solve in a general manner.

A. Legendre polynomials

This chapter revisits the standard parametrization of solutions to the Laplace equation in the Penning-trap literature. To begin with, Section A.1 shows how the Legendre polynomials—solutions to the Legendre equation as their name suggests—turn into solutions to the Laplace equation in spherical coordinates. The remaining chapter then deals with the conversion of this solution to cylindrical coordinates.

Section A.2 attempts to answer the question why the conversion in Section 2.2.1 did not use a general explicit form of the Legendre polynomial P_η with its argument $\cos(\theta)$ and the factor r^η expressed in cylindrical coordinates. Instead, the coefficients of the polynomial in cylindrical coordinates were derived from a recursive relationship that resulted from demanding that the polynomial in ρ and z be a solution of the Laplace equation. We will examine the difficulties of a direct conversion here.

Section A.3 expands the methods of Sections 2.2.1 and A.2—a power series solution of the Laplace equation and the direct conversion, respectively—to associated Legendre polynomials P_η^m. This more general results also serves as a cross-check of the prior result for $m = 0$. In fact, Section A.2 may be skipped, since its specific result is covered by Section A.3.2. Even though the methods are almost identical, they are introduced best on a simpler case, however. The same also holds for the specific conversion in Section 2.2.1, which is a special case of Section A.3.1.

A.1. Legendre polynomials and the Laplace equation

For two integers η and m with $0 \leq m \leq \eta$, the associated Legendre differential equation [171]

$$\frac{\mathrm{d}}{\mathrm{d}\zeta}\left[\left(1-\zeta^2\right)\frac{\mathrm{d}f}{\mathrm{d}\zeta}\right] + \left[\eta(\eta+1) - \frac{m^2}{1-\zeta^2}\right] f = 0 \tag{A.1}$$

is solved by the function $f(\zeta) = P_\eta^m(\zeta)$, where P_η^m is an associated Legendre polynomial.[1] For $m > \eta$, the associated Legendre polynomials are the trivial solution $P_\eta^m(\zeta) = 0$. For $m = 0$, Equation (A.1) becomes the Legendre differential equation, and $P_\eta^0 \equiv P_\eta$ are the Legendre polynomials. We will turn to closed-form expressions for the P_η^0 later. In this section, they are not yet necessary, and Equation (A.1) is the relevant properties.

[1] Because of its link to the quantum number for orbital angular momentum when it comes to spherical harmonics [186], the parameter η is often called l in the literature. We will stick with our notation here. Despite our commitment for consistency, we stick with (the magnetic quantum number) m—the symbol used for the rest mass of the particle, too. Fortunately, the two do not appear in the same context.

In order to the unveil the link between the associated Legendre polynomials and the Laplace equation (2.57), we consider the Laplace operator [180]

$$\Delta = \frac{1}{r^2}\frac{\partial}{\partial r}\left(r^2\frac{\partial}{\partial r}\right) + \frac{1}{r^2\sin(\theta)}\frac{\partial}{\partial\theta}\left(\sin(\theta)\frac{\partial}{\partial\theta}\right) + \frac{1}{[r\sin(\theta)]^2}\frac{\partial^2}{\partial^2\phi^2} \tag{A.2}$$

in spherical coordinates. The azimuth angle is denoted by ϕ, both in spherical and cylindrical coordinates (see Figure 2.4). Since we have mainly dealt with cylindrically-symmetric solutions to the Laplace equation so far, the angle ϕ has received little attention. We like to recall its presence in order to keep the solution more general here.

When switching from the polar angle θ to $\cos(\theta)$ as the variable with

$$\frac{1}{\partial\theta} = \frac{\partial\cos(\theta)}{\partial\theta}\frac{1}{\partial\cos(\theta)} = -\sin(\theta)\frac{1}{\partial\cos(\theta)} \quad , \tag{A.3}$$

the Laplace operator takes the form

$$\Delta = \frac{1}{r^2}\frac{\partial}{\partial r}\left(r^2\frac{\partial}{\partial r}\right) + \frac{1}{r^2}\frac{\partial}{\partial\cos(\theta)}\left[[\sin(\theta)]^2\frac{\partial}{\partial\cos(\theta)}\right] + \frac{1}{[r\sin(\theta)]^2}\frac{\partial^2}{\partial\phi^2} \quad . \tag{A.4}$$

Since $\cos(\theta)$ is the variable now, the sine functions will have to be expressed in terms of the new variable as

$$[\sin(\theta)]^2 = 1 - [\cos(\theta)]^2 \quad . \tag{A.5}$$

Borrowing from the literature, the ansatz for a solution to the Laplace equation (2.57) takes the form

$$\tilde{\Phi}^m_\eta(r,\theta,\phi) = r^\eta P^m_\eta(\cos(\theta))\left[c^m_\eta\cos(m\phi) + s^m_\eta\sin(m\phi)\right] \quad , \tag{A.6}$$

where c^m_η and s^m_η are two arbitrary factors. The tilde on top of $\tilde{\Phi}^m_\eta$ serves as a reminder that we consider generic solutions to the Laplace equation, which may not have the unit of an electrostatic potential Φ. After all, the Laplace equation is a homogeneous one, and we are free to choose a global prefactor, or c^m_η and s^m_η accordingly, for the ansatz (A.6) to have the right dimension of the physical quantity that fulfills the Laplace equation.

We will now apply the Laplace operator (A.4) on the ansatz (A.6), abbreviating the new polar-angle variable as $\zeta = \cos(\theta)$. For clarity, we will show only the components that are affected by the operator. The components that act like a constant factor with respect to a particular part of the Laplace operator will not be shown.

The derivatives with respect to the distance r yield

$$\frac{1}{r^2}\frac{\partial}{\partial r}\left(r^2\frac{\partial}{\partial r}\right)r^\eta = \eta(\eta+1)r^{\eta-2} \quad . \tag{A.7}$$

The derivatives with respect to the azimuth angle ϕ give

$$\frac{r^\eta}{r^2(1-\zeta^2)}\frac{\partial^2}{\partial\phi^2}\left[c^m_\eta\cos(m\phi) + s^m_\eta\sin(m\phi)\right] = \frac{-m^2r^{\eta-2}}{(1-\zeta^2)}\left[c^m_\eta\cos(m\phi) + s^m_\eta\sin(m\phi)\right] \quad . \tag{A.8}$$

The associated LEGENDRE polynomial P_η^m is only affected by the derivative with respect to ζ. Rather than executing the derivatives in

$$\frac{1}{r^2}\frac{\partial}{\partial\zeta}\left[\left(1-\zeta^2\right)\frac{\partial}{\partial\zeta}\right]r^\eta P_\eta^m(\zeta) = r^{\eta-2}\frac{\partial}{\partial\zeta}\left[\left(1-\zeta^2\right)\frac{\partial P_\eta^m}{\partial\zeta}\right] \tag{A.9}$$

further, we combine the three results (A.7)–(A.9) to summarize the effect of the LAPLACE operator (A.4) on the ansatz (A.6) as

$$\begin{aligned}\Delta\,\tilde{\Phi}_\eta^m(r,\theta,\phi) = r^{\eta-2}&\left[c_\eta^m\cos(m\phi)+s_\eta^m\sin(m\phi)\right]\\ &\cdot\left\{\frac{\partial}{\partial\zeta}\left[\left(1-\zeta^2\right)\frac{\partial P_\eta^m}{\partial\zeta}\right]+\left[\eta(\eta+1)-\frac{m^2}{1-\zeta^2}\right]P_\eta^m\right\}=0\quad.\end{aligned} \tag{A.10}$$

Indeed, $\tilde{\Phi}_\eta^m$ solves the LAPLACE equation because the associated LEGENDRE polynomial P_η^m fulfills the associated LEGENDRE equation (A.1). Thus, we have constructed a solution to the LAPLACE equation from a solution to the associated LEGENDRE equation. The latter equation is also solved by the associated LEGENDRE function of the second kind [179], $Q_\eta^m(\zeta)$. Therefore, a solution to the LAPLACE equation could be constructed according to Equation (A.6) with the replacement $P_\eta^m \to Q_\eta^m$. However, the $Q_\eta^m(\zeta)$ diverge logarithmically for $\zeta = \pm 1$, which would mean that there is a singularity on the z-axis, since $\zeta = \cos(\theta)$. Such a singularity does not occur in an empty trap because it is related to a line of charge or current. Therefore, the additional solution is of little interest in the physical context here.

From solutions of the associated LEGENDRE equation (A.1), another solution with a different dependence on r may be constructed. Applying the differential operator with respect to r in the LAPLACE operator (A.4) on

$$\frac{1}{r^2}\frac{\partial}{\partial r}\left(r^2\frac{\partial}{\partial r}\right)r^{-(\eta+1)} = \eta(\eta+1)r^{-(\eta+3)} \tag{A.11}$$

reduces the exponent by 2, just like the factors of r^{-2} in front of the other differential operators do. Since the prefactor here is the same as in Equation (A.7), the ansatz (A.6) stays a solution of the LAPLACE equation upon the substitution $r^\eta \to r^{-(\eta+1)}$. Because of the negative exponent of r, such a solution diverges at the origin. From the physical point of view, the singularity might be related to a point-charge at the origin, which does not play a role for the potential inside an empty trap.

A.2. Direct conversion to cylindrical coordinates

In Section 2.2.1, the textbook solution (2.58) of the LAPLACE equation with cylindrical symmetry was converted from spherical coordinates to cylindrical coordinates (compare Equation (2.73)):

$$r^\eta P_\eta(\cos(\theta)) = \sum_{k=0}^{\lfloor\frac{\eta}{2}\rfloor}\frac{(-1)^k}{2^{2k}}\frac{\eta!}{(\eta-2k)!\,(k!)^2}\,z^{\eta-2k}\rho^{2k} \tag{A.12a}$$

$$= \sum_{k=0}^{\lfloor\frac{\eta}{2}\rfloor}\frac{(-1)^k}{2^{2k}}\binom{\eta}{k}\binom{\eta-k}{k}z^{\eta-2k}\rho^{2k}\quad. \tag{A.12b}$$

After expanding with $(\eta - k)!$, the coefficient $a_\eta(k)$ from Equation (2.71) has been rewritten here as a product of two binomial coefficients in the last step. As a reminder, the floor function for the upper limit of the sum is defined in Equation (2.60), and the binomial coefficient is introduced in (3.3).

Given that a general explicit expression of the Legendre polynomials for all η exists, the approach of determining a solution to the Laplace equation in cylindrical coordinates from scratch does not appear straightforward. Therefore, the straightforward conversion of coordinates is attempted here. From Rodrigues' formula

$$P_\eta(\zeta) = \frac{1}{2^\eta \eta!} \frac{\mathrm{d}^\eta}{\mathrm{d}\zeta^\eta} \left[\left(\zeta^2 - 1\right)^\eta \right] \quad , \tag{A.13}$$

the general explicit expression of the Legendre polynomials [181] follows as

$$P_\eta(\zeta) = \frac{1}{2^\eta} \sum_{j=0}^{\left\lfloor \frac{\eta}{2} \right\rfloor} (-1)^j \binom{\eta}{j} \binom{2\eta - 2j}{\eta} \zeta^{\eta - 2j} \quad . \tag{A.14}$$

Table A.1 shows the first few Legendre polynomials.

In $r^\eta P_\eta(\zeta)$ with the argument $\zeta = \cos(\theta)$, there will be terms of the kind

$$r^\eta [\cos(\theta)]^{\eta - 2j} = r^{2j} \left[r \cos(\theta) \right]^{\eta - 2j} = r^{2j} z^{\eta - 2j} \quad , \tag{A.15}$$

where we have absorbed the cosine terms in the axial coordinate $z = r\cos(\theta)$. The remaining spherical coordinate r is transformed into cylindrical coordinates with the help of binomial expansion:

$$r^{2j} = (r^2)^j = (\rho^2 + z^2)^j = \sum_{k=0}^{j} \binom{j}{k} \rho^{2k} z^{2(j-k)} \quad . \tag{A.16}$$

Combining Equations (A.15) and (A.16) yields

$$r^n [\cos(\theta)]^{\eta - 2j} = z^{\eta - 2j} r^{2j} = z^{\eta - 2k} \sum_{k=0}^{j} \binom{j}{k} \rho^{2k} z^{2(j-k)} = \sum_{k=0}^{j} \binom{j}{k} z^{\eta - 2k} \rho^{2k} \tag{A.17}$$

as the intermediate result to be merged with the general expression of the Legendre polynomial (A.14). The solution of the Laplace equation is then expressed in cylindrical coordinates as

$$r^\eta P_\eta(\cos(\theta)) = \sum_{j=0}^{\left\lfloor \frac{n}{2} \right\rfloor} \sum_{k=0}^{j} \frac{(-1)^j}{2^\eta} \binom{j}{k} \binom{\eta}{j} \binom{2\eta - 2j}{\eta} z^{\eta - 2k} \rho^{2k} \quad . \tag{A.18}$$

At this point, it has almost assumed the form of Equation (2.59), but the summation over j would have to be executed before the summation over k in order to extract the coefficient $a_n(k)$, which has yet to take its final form. Here, the upper limit of the sum over k still depends on j, making the coefficient $a_n(k)$ hard to evaluate.

Table A.1.: The first few Legendre polynomials. When η is even (odd), there are only even (odd) powers of the argument ζ. The coefficients are such that $P_\eta(1) = 1$ for all η.

η	$P_\eta(\zeta)$
0	1
1	ζ
2	$\frac{1}{2}\left(3\zeta^2 - 1\right)$
3	$\frac{1}{2}\left(5\zeta^3 - 3\zeta\right)$
4	$\frac{1}{8}\left(35\zeta^4 - 30\zeta^2 + 3\right)$
5	$\frac{1}{8}\left(63\zeta^5 - 70\zeta^3 + 15\zeta\right)$
6	$\frac{1}{16}\left(231\zeta^6 - 315\zeta^4 + 105\zeta^2 - 5\right)$
7	$\frac{1}{16}\left(429\zeta^7 - 693\zeta^5 + 315\zeta^3 - 35\zeta\right)$
8	$\frac{1}{128}\left(6435\zeta^8 - 12\,012\zeta^6 + 6930\zeta^4 - 1260\zeta^2 + 35\right)$
9	$\frac{1}{128}\left(12\,155\zeta^9 - 25\,740\zeta^7 + 18\,018\zeta^5 - 4620\zeta^3 + 315\zeta\right)$
10	$\frac{1}{256}\left(46\,189\zeta^{10} - 109\,395\zeta^8 + 90\,090\zeta^6 - 30\,030\zeta^4 + 3465\zeta^2 - 63\right)$

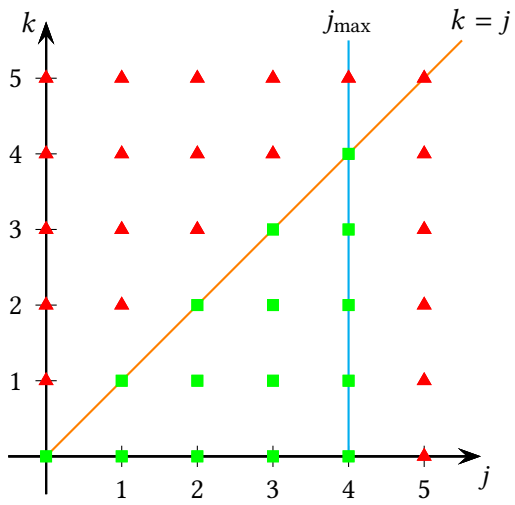

Figure A.1.: Illustrating the transformation of the summation limits summarized by Equation (A.19) in jk-parameter space. The green squares are part of the summation; the red triangles are not. The orange line is the boundary $k = j$; the blue line indicates the maximum value of j, with $j_{\max} = 4$ in the example shown. Summing over k from 0 to j—that is, along vertical lines—and then over j from 0 to $j_{\max}$ (along horizontal lines) is equivalent to summing over j from k to $j_{\max}$—that is, along horizontal lines—and then over k from 0 to $k_{\max} = j_{\max}$ (along vertical lines).

Figure A.1 shows how to change the order of summation with a suitable transformation of the limits, while the summation variables as such remain untouched. Expressed with a generic function $f(j,k)$ of the two summation variables, the recipe is

$$\sum_{j=0}^{j_{\max}} \sum_{k=0}^{j} f(j,k) = \sum_{k=0}^{j_{\max}} \sum_{j=k}^{j_{\max}} f(j,k) \quad . \tag{A.19}$$

The limits of the summation over k on the right-hand side no longer depend on the current value of j, and hence this sum can be executed last, after having summed over j. Applied to Equation (A.18), the result is

$$r^\eta P_\eta(\cos(\theta)) = \sum_{k=0}^{\lfloor \frac{\eta}{2} \rfloor} \sum_{j=k}^{\lfloor \frac{\eta}{2} \rfloor} \frac{(-1)^j}{2^\eta} \binom{j}{k} \binom{\eta}{j} \binom{2\eta - 2j}{\eta} z^{n-2k} \rho^{2k} \tag{A.20a}$$

$$= \sum_{k=0}^{\lfloor \frac{\eta}{2} \rfloor} \sum_{j=0}^{\lfloor \frac{\eta}{2} \rfloor - k} \frac{(-1)^{j+k}}{2^\eta} \binom{j+k}{k} \binom{\eta}{j+k} \binom{2\eta - 2k - 2j}{\eta} z^{n-2k} \rho^{2k} \quad . \tag{A.20b}$$

In the last step, we have shifted the summation variable according to $j \to j + k$ such that the sum over j starts at 0. The product of binomial coefficients is rearranged as

$$\binom{j+k}{k} \binom{\eta}{j+k} = \frac{(j+k)!}{j!\,k!} \frac{\eta!}{(j+k)!\,(\eta-k-j)!} = \frac{\eta!}{k!\,(\eta-k)!} \frac{(\eta-k)!}{(\eta-k-j)!\,j!} = \binom{\eta}{k} \binom{\eta-k}{j} \tag{A.21}$$

to give one binomial coefficient independent of j. Sorting the terms in Equation (A.20b) based on the summation variables then gives

$$r^\eta P_\eta(\cos(\theta)) = \frac{1}{2^\eta} \sum_{k=0}^{\lfloor \frac{\eta}{2} \rfloor} \binom{\eta}{k} (-1)^k \sum_{j=0}^{\lfloor \frac{\eta}{2} \rfloor - k} (-1)^j \binom{\eta-k}{j} \binom{2\eta - 2k - 2j}{\eta} z^{\eta-2k} \rho^{2k} \quad . \tag{A.22}$$

Unfortunately, it is not obvious how to execute the sum over j. At least, we know that the final result should look like Equation (A.12b), and we may conjecture that

$$\sum_{j=0}^{\lfloor \frac{\eta}{2} \rfloor - k} (-1)^j \binom{\eta-k}{j} \binom{2\eta - 2k - 2j}{\eta} = 2^{\eta-2k} \binom{\eta-k}{k} \tag{A.23}$$

is an identity.[2] It has to be if the calculation up to this point is correct. A rigorous proof using the properties of binomial coefficients would probably require advanced knowledge of hypergeometric functions. In any case, the straightforward conversion from spherical to cylindrical coordinates using the general explicit expression of the Legendre polynomial is not intuitive when it comes to determining the explicit form of the coefficient $a_\eta(k)$. Without prior knowledge of the final result, Equation (A.23) would certainly not occur very easily by staring madly at its left-hand side.[3]

[2] For $k = 0$, the left hand-side of Equation (A.23) closely resembles the general expression (A.14) of the Legendre polynomial (missing only the prefactor $2^{-\eta}$ and the argument $\zeta^{\eta-2j}$), and Equation (A.23) then reflects the property $P_\eta(1) = 1$.

[3] When evaluating the left-hand side numerically for the first few η as a function of k, sequence A133156 in the

A.3. Associated Legendre polynomials

This section generalizes Sections 2.2.1 and A.2 to associated Legendre polynomials.

A.3.1. Indirect conversion to cylindrical coordinates

Section A.1 showed that the ansatz (A.6)—$r^\eta P_\eta^m((\cos(\theta))$ times the trigonometric function $\cos(m\phi)$ or $\sin(m\phi)$—solves the Laplace equation (2.57). Similar to the case of $m = 0$ in Equation (2.59), we will now convert the more general ansatz (A.6) from spherical to cylindrical coordinates. This conversion affects r and $\cos(\theta)$; the azimuth angle ϕ remains unchanged. Based on the pattern of a few explicit conversions, we expect the polynomial in z and ρ to have the form

$$\tilde{\Phi}_\eta^m(\rho,\phi,z) = \sum_{k=0}^{\lfloor\frac{\eta-m}{2}\rfloor} a_\eta^m(k)\, z^{\eta-m-2k}\rho^{m+2k}\left[c_\eta^m\cos(m\phi) + s_\eta^m\sin(m\phi)\right] \quad , \tag{A.24}$$

where $a_\eta^m(k)$ is the coefficient that needs to be determined. Based on the general explicit expression (A.43) for the associated Legendre polynomial P_η^m, we will confirm this functional shape more rigorously in Section A.3.2.

Following the approach of Section 2.2.1, we apply the Laplace operator (2.63) in cylindrical coordinates to the ansatz (A.24). The equivalents of Equations (2.64) and (2.65) now become

$$\frac{1}{\rho}\frac{\partial}{\partial\rho}\left(\rho\frac{\partial}{\partial\rho}\right)\left[a_\eta^m(k+1)z^{\eta-m-2k-2}\rho^{m+2k+2}\right] = (m+2k+2)^2 a_\eta^m(k+1)z^{\eta-m-2k-2}\rho^{m+2k} \tag{A.25}$$

and

$$\frac{\partial^2}{\partial z^2}\left[a_\eta^m(k)\, z^{\eta-m-2k}\rho^{m+2k}\right] = (\eta-m-2k)(\eta-m-2k-1)a_\eta^m(k)\, z^{\eta-m-2k-2}\rho^{m+2k} \quad , \tag{A.26}$$

respectively. For space, we have suppressed the dependence on the azimuth angle ϕ because this part is unaffected by these two components of the Laplace operator. Although the coefficients $a_\eta^m(k+1)$ and $a_\eta^m(k)$ are not affected either, they are shown in order to emphasize which terms of the polynomial in z and ρ will have to cancel for the ansatz (A.24) to solve the Laplace equation.

In addition to Equations (A.25) and (A.26), there is the contribution

$$\frac{1}{\rho^2}\frac{\partial^2}{\partial\phi^2}\left[a_\eta^m(k+1)\, z^{\eta-m-2k-2}\rho^{m+2k+2}\cos(m\phi)\right] = -m^2 a_\eta^m(k+1)\, z^{\eta-m-2k-2}\rho^{m+2k}\cos(m\phi) \tag{A.27}$$

from the dependence on the azimuth angle ϕ. For space, we have shown only one of the two trigonometric functions. Similar to Equation (A.8), the result also holds with the substitution

On-Line Encyclopedia of Integer Sequences® (`https://oeis.org`) shows that the right-hand side gives the absolute value of the coefficient belonging to the term $x^{\eta-2k}$ in the Chebyshev polynomial $U_\eta(x)$ of the second kind. This connection might serve as a hint for a different proof.

$\cos(m\phi) \to \sin(m\phi)$. Because of the double derivative, the trigonometric function is preserved. Cosines do not turn into sines or vice versa. Taking into account that $\cos(m\phi)$ and $\sin(m\phi)$ are linearly independent, no cancellations between these terms occur. Instead, the two products with these trigonometric functions must solve the Laplace equation separately. This independence is also reflected by the fact that there is no specific link between the two prefactors c_η^m and s_η^m in Equations (A.6) and (A.24).

Combining Equations (A.25)—(A.27) for the full effect of the Laplace operator (2.63) on the terms that will have to cancel afterwards, we find

$$\left[(m+2k+2)^2 - m^2\right] a_\eta^m(k+1) + (\eta - m - 2k)(\eta - m - 2k - 1) a_\eta^m(k) = 0 \tag{A.28}$$

for the prefactor of the term $z^{\eta-m-2k-2}\rho^{m+2k}$. This prefactor has to vanish individually for all k in the polynomial for Equation (A.24) to solve the Laplace equation. With the simplification

$$(m+2k+2)^2 - m^2 = m^2 + 2m(2k+2) + (2k+2)^2 - m^2 = 4(k+1)(m+k+1) \quad , \tag{A.29}$$

we establish the recursive relation

$$a_\eta^m(k+1) = -\frac{(\eta - m - 2k)(\eta - m - 2k - 1)}{4(k+1)(m+k+1)} a_\eta^m(k) \tag{A.30}$$

between the adjacent coefficients $a_\eta^m(k+1)$ and $a_\eta^m(k)$. As a cross-check, we recover Equation (2.66) for $m = 0$. In analogy to Equation (2.67d), we will try to spot a pattern by repeating the recursion multiple times:

$$a_\eta^m(3) = \frac{-(\eta - m - 4)(\eta - m - 5)}{4 \cdot 3(m+3)} a_\eta^m(2) \tag{A.31a}$$

$$= \frac{-(\eta - m - 4)(\eta - m - 5)}{4 \cdot 3(m+3)} \frac{-(\eta - m - 2)(\eta - m - 3)}{4 \cdot 2(m+2)} a_\eta^m(1) \tag{A.31b}$$

$$= \frac{-(\eta - m - 4)(\eta - m - 5)}{4 \cdot 3(m+3)} \frac{-(\eta - m - 2)(\eta - m - 3)}{4 \cdot 2(m+2)} \frac{-(\eta - m)(\eta - m - 1)}{4 \cdot 1(m+1)} a_\eta^m(0) \tag{A.31c}$$

$$= \frac{(-1)^3}{4^3} \frac{(\eta - m)(\eta - m - 1)(\eta - m - 2)(\eta - m - 3)(\eta - m - 4)(\eta - m - 5)}{(3 \cdot 2 \cdot 1) \cdot (m+3)(m+2)(m+1)} a_\eta^m(0) \quad . \tag{A.31d}$$

In the last step, we have regrouped some terms to emphasize the pattern. The general expression becomes

$$a_\eta^m(k) = \frac{(-1)^k}{2^{2k}} \frac{(\eta - m)(\eta - m - 1) \cdots (\eta - m - 2k + 1)}{k!\,(m+k)(m+k-1) \cdots (m+1)} a_\eta^m(0) \tag{A.32a}$$

$$= \frac{(-1)^k}{2^{2k} k!} \frac{(\eta - m)!}{(\eta - m - 2k)!} \frac{m!}{(m+k)!} a_\eta^m(0) \quad , \tag{A.32b}$$

where we have expanded with $m!$ and $(\eta - m - 2k)!$ in the last step. Since m is a non-negative integer, there is no problem with the first expansion. The second expansion is also fine, because $\eta - m - 2k$ is non-negative within the limits of the sum in Equation (A.24). In fact, $\eta - m - 2k$ is

the exponent of z, and we do not consider solutions with singularities here, which means that the exponent must not be negative.

As a cross-check, we recover Equation (2.68b) from Equation (A.32b) for $m = 0$. Determining $a_\eta^m(0)$ is not a easy as in the case of $m = 0$, when we used the property $P_\eta(1) = 1$ for all η in Equation (2.70) in order to conclude that $a_\eta(0) = 1$. Assuming for the moment that $a_\eta^m(0) = 1$ and dividing Equation (A.6) by Equation (A.24) leads to the sequence A001498—coefficients of Bessel polynomials [175]—in the *On-Line Encyclopedia of Integer Sequences*® (`https://oeis.org`). We have ignored the sign of the ratio, which depends on the convention concerning the Condon–Shortley phase [177] of the associated Legendre polynomial. Including this factor of $(-1)^m$ here, the coefficient $a_\eta^m(0)$ is determined[4] as

$$a_\eta^m(0) = \frac{(-1)^m}{2^m} \frac{(\eta + m)!}{m!(\eta - m)!} \quad , \tag{A.33}$$

and Equation (A.32b) for the explicit expression of the coefficient becomes

$$a_\eta^m(k) = \frac{(-1)^{m+k}}{2^{m+2k}} \frac{(\eta + m)!}{k!(m + k)!(\eta - m - 2k)!} \quad . \tag{A.34}$$

This coefficient completes the ansatz (A.24). As a cross-check, Equation (2.71) is reproduced for $m = 0$. Additionally, using the recursion (A.30) with the explicit form of the coefficient $a_\eta^m(k)$ from Equation (A.34) as

$$a_\eta^m(k+1) = -\frac{(\eta - m - 2k)(\eta - m - 2k - 1)}{4(k + 1)(m + k + 1)} \frac{(-1)^{m+k}}{2^{m+2k}} \frac{(\eta + m)!}{k!(m + k)!(\eta - m - 2k)!} \tag{A.35a}$$

$$= \frac{(-1)^{m+k+1}}{2^{m+2k+2}} \frac{(\eta + m)!}{(k + 1)!(m + k + 1)!(\eta - m - 2k - 2)!} \tag{A.35b}$$

yields the explicit expression for $a_\eta^m(k + 1)$.

Finally, upon comparing Equations (A.6) and (A.24), the more general version of Equation (2.59) for the conversion from spherical to cylindrical coordinates is

$$r^\eta P_\eta^m(\cos(\theta)) = (-1)^m \frac{(\eta + m)!}{2^m} \sum_{k=0}^{\lfloor \frac{\eta - m}{2} \rfloor} \frac{(-1)^k}{2^{2k}} \frac{z^{\eta - m - 2k} \rho^{m+2k}}{k!(m + k)!(\eta - m - 2k)!} \tag{A.36a}$$

$$= \frac{(-1)^m}{2^m} \frac{(\eta + m)!}{\eta!} \sum_{k=0}^{\lfloor \frac{\eta - m}{2} \rfloor} \frac{(-1)^k}{2^{2k}} \binom{\eta}{k} \binom{\eta - k}{m + k} z^{\eta - m - 2k} \rho^{m+2k} \quad . \tag{A.36b}$$

If the Condon–Shortley phase [172] is not included in the associated Legendre polynomial P_η^m, the factor of $(-1)^m$ is to be omitted. For $m = 0$, Equations (A.36a) and (A.36b) reproduce Equations (A.12a) and (A.12b), respectively, for the conversion to cylindrical coordinates with a Legendre polynomial. To solve the Laplace equation (2.57) in the case of $m \neq 0$, Equation (A.36b) still has to multiplied with $\cos(m\phi)$ or $\sin(m\phi)$, which does not affect the

[4] Section A.3.3 confirms this conjecture rigorously.

conversion. Continuing to Cartesian coordinates via $x = \rho\cos(\phi)$ and $y = \rho\sin(\phi)$ is facilitated by the multiple-angle formulas [182]

$$\cos(m\phi) = \sum_{j=0}^{\lfloor \frac{m}{2} \rfloor} (-1)^j \binom{m}{2j} [\sin(\phi)]^{2j} [\cos(\phi)]^{m-2j} \quad , \tag{A.37}$$

$$\sin(m\phi) = \sum_{j=0}^{\lfloor \frac{m-1}{2} \rfloor} (-1)^j \binom{m}{2j+1} [\sin(\phi)]^{2j+1} [\cos(\phi)]^{m-2j-1} \quad , \tag{A.38}$$

and $\rho^2 = x^2 + y^2$.

A.3.2. Direct conversion to cylindrical coordinates

In this section, we attempt the direct conversion of the ansatz (A.6) with an associated Legendre polynomial P_η^m from spherical to cylindrical coordinates. This direct approach is conceptually identical to the conversion with the Legendre polynomial P_η in Section A.2, which should be reproduced for $m = 0$.

This time, the starting point is the general expression

$$P_\eta^m(\zeta) = (-1)^m \left(1 - \zeta^2\right)^{m/2} \frac{\mathrm{d}^m}{\mathrm{d}\zeta^m} P_\eta(\zeta) \tag{A.39}$$

for the associated Legendre polynomial [172]. The factor of $(-1)^m$ is the Condon–Shortley phase, which we have included here, because the computer algebra system Wolfram *Mathematica*® and the numerical computing environment Matlab, which are commonly used at the institute, use this definition.[5] The general explicit expression (A.14) for the Legendre polynomial $P_\eta(\zeta)$ makes it clear that terms of the kind

$$\frac{\mathrm{d}^m}{\mathrm{d}\zeta^m} \zeta^{\eta-2j} = (\eta-2j)(\eta-2j-1)\cdots(\eta-2j-m+1)\zeta^{\eta-2j-m} \tag{A.40}$$

will appear in the associated Legendre polynomial $P_\eta^m(\zeta)$. Since $\eta - 2j$ is a non-negative integer within the limits of the sum in Equation (A.14), the multiple derivatives yield zero after $\eta - 2j + 1$ operations, when zero appears as a prefactor. Thus, Equation (A.40) is simplified by distinguishing two cases:

$$\frac{\mathrm{d}^m}{\mathrm{d}\zeta^m} \zeta^{\eta-2j} = \begin{cases} 0 & \text{for } m > \eta - 2j \quad , \\ \frac{(\eta-2j)!}{(\eta-2j-m)!} \zeta^{\eta-2j-m} & \text{for } m \leq \eta - 2j \quad . \end{cases} \tag{A.41}$$

In the second case, Equation (A.40) has been expanded with $(n - 2j - m)!$, which is well-defined in this case. Since j is a non-negative integer, the derivative and hence the associated Legendre polynomial vanish for $m > \eta$, which motivates the restriction $0 \leq m \leq \eta$ imposed in Section A.1.

[5] This choice differs from Equation (2.83), taken from Reference [20], where we have tried to underline the difference by writing with two subscripts $P_{\eta m} = (-1)^m P_\eta^m$ as Reference [172] suggests.

Table A.2.: The first few associated Legendre polynomials $P_\eta^1(\zeta)$. When η is even (odd), the function is antisymmetric (symmetric) with respect to the argument ζ. For $m > \eta$, the associated Legendre polynomial P_η^m vanishes, which is the case for $\eta = 0$ here.

η	$P_\eta^1(\zeta)$
0	0
1	$-\sqrt{1-\zeta^2}$
2	$-3\zeta\sqrt{1-\zeta^2}$
3	$-\frac{3}{2}\sqrt{1-\zeta^2}\left(5\zeta^2-1\right)$
4	$-\frac{5}{2}\sqrt{1-\zeta^2}\left(7\zeta^3-3\zeta\right)$
5	$-\frac{15}{8}\sqrt{1-\zeta^2}\left(21\zeta^4-14\zeta^2+1\right)$
6	$-\frac{21}{8}\sqrt{1-\zeta^2}\left(33\zeta^5-30\zeta^3+5\zeta\right)$
7	$-\frac{7}{16}\sqrt{1-\zeta^2}\left(429\zeta^6-495\zeta^4+135\zeta^2-5\right)$
8	$-\frac{9}{16}\sqrt{1-\zeta^2}\left(715\zeta^7-1001\zeta^5+385\zeta^3-35\zeta\right)$
9	$-\frac{45}{128}\sqrt{1-\zeta^2}\left(2431\zeta^8-4004\zeta^6+2002\zeta^4-308\zeta^2+7\right)$
10	$-\frac{55}{128}\sqrt{1-\zeta^2}\left(4199\zeta^9-7956\zeta^7+4914\zeta^5-1092\zeta^3+63\zeta\right)$

Combining the binomial coefficients in the general explicit expression (A.14) for the Legendre polynomial P_η with the additional factors that result from the multiple derivatives yields

$$\binom{\eta}{j}\binom{2n-2j}{\eta}\frac{(\eta-2j)!}{(\eta-2j-m)!} = \frac{\eta!}{j!(\eta-j)!}\frac{(2\eta-2j)!}{\eta!(\eta-2j)!}\frac{(\eta-2j)!}{(\eta-2j-m)!} = \frac{(2\eta-2j)!}{j!(\eta-j)!(\eta-2j-m)!} \quad . \tag{A.42}$$

Since the only contributions by the derivatives (A.40) are for $2j \leq \eta - m$, the upper limit of the sum over j is reduced from $\lfloor \eta/2 \rfloor$ to $\lfloor (\eta-m)/2 \rfloor$. Overall, we have

$$P_\eta^m(\zeta) = \frac{(-1)^m}{2^\eta}\left(1-\zeta^2\right)^{m/2}\sum_{j=0}^{\left\lfloor\frac{\eta-m}{2}\right\rfloor}(-1)^j\frac{(2\eta-2j)!}{j!\,(\eta-j)!\,(\eta-2j-m)!}\zeta^{\eta-m-2j} \tag{A.43}$$

for the general explicit expression of the associated Legendre polynomial. Table A.2 shows the first few P_η^1, because these functions were mentioned by Equation (2.82) in the context of the standard parametrization of the radial magnetic field in the literature.

With the argument $\zeta = \cos(\theta)$, the term in front of the sum is rewritten as

$$\left[1-(\cos(\theta))^2\right]^{m/2} = \left[(\sin(\theta))^2\right]^{m/2} = |\sin(\theta)|^m \quad . \tag{A.44}$$

Moreover, in the range of $0 \leq \theta \leq \pi$, with θ being a spherical coordinate here, $\sin(\theta)$ does not take negative values—that is, $\sin(\theta) \geq 0$—and the absolute value can be dropped. Thus,

the associated Legendre polynomial contains products of $[\sin(\theta)]^m[\cos(\theta)]^{\eta-m-2j}$, which have to be arranged as $\rho = r\sin(\theta)$ and $z = r\cos(\theta)$ for the conversion to cylindrical coordinates. Ignoring the sum over j for the moment, such terms in $r^\eta P_\eta(\cos(\theta))$ take the form

$$r^\eta[\sin(\theta)]^m[\cos(\theta)]^{\eta-m-2j} = r^{\eta-m}[r\sin(\theta)]^m[\cos(\theta)]^{\eta-m-2j} = \rho^m[r\cos(\theta)]^{\eta-m-2j}r^{2j} \tag{A.45a}$$

$$= \rho^m z^{\eta-m-2j}r^{2j} = \rho^m z^{\eta-m-2j}\sum_{k=0}^{j}\binom{j}{k}\rho^{2k}z^{2(j-k)} \tag{A.45b}$$

$$= \sum_{k=0}^{j}\frac{j!}{k!(j-k)!}z^{\eta-m-2k}\rho^{m+2k} \quad . \tag{A.45c}$$

In the second-to-last step, we have used Equation (A.16) to express the factor r^{2j}, for which there was no corresponding trigonometric function, as a polynomial in z and ρ by means of binomial expansion. Combining Equation (A.45c) with the prefactors and the sum in the general explicit expression (A.43) of the associated Legendre polynomial $P_\eta^m(\cos(\theta))$ yields

$$r^\eta P_\eta^m(\cos(\theta)) = \frac{(-1)^m}{2^\eta}\sum_{j=0}^{\lfloor\frac{\eta-m}{2}\rfloor}\sum_{k=0}^{j}\frac{(-1)^j\,(2\eta-2j)!}{(\eta-j)!\,(\eta-2j-m)!}\frac{z^{\eta-m-2k}\rho^{m+2k}}{k!(j-k)!} \quad . \tag{A.46}$$

Like in Equation (A.18) with the Legendre polynomial P_η, the two sums do not yet have the right shape to identify the coefficient $a_\eta^m(k)$ in the way it is defined in Equation (A.24). We would like to be left with a sum over k, because this sum creates all the different exponents of the polynomial in z and ρ, while the sum over j should determine the coefficient $a_\eta^m(k)$. To this end, we apply the transformation of summation variables described by Equation (A.19) and shown in Figure A.1. Since the summation variables as such are not transformed, the major difference here is that the maximum value of j is $\lfloor(\eta-m)/2\rfloor$ rather than $\lfloor\eta/2\rfloor$. In close analogy to (A.20a) we have

$$r^\eta P_\eta^m(\cos(\theta)) = \frac{(-1)^m}{2^\eta}\sum_{k=0}^{\lfloor\frac{\eta-m}{2}\rfloor}\sum_{j=k}^{\lfloor\frac{\eta-m}{2}\rfloor}\frac{(-1)^j\,(2\eta-2j)!}{(\eta-j)!(\eta-2j-m)!}\frac{z^{\eta-m-2k}\rho^{m+2k}}{k!(j-k)!} \tag{A.47a}$$

$$= \frac{(-1)^m}{2^\eta}\sum_{k=0}^{\lfloor\frac{\eta-m}{2}\rfloor}\sum_{j=0}^{\lfloor\frac{\eta-m}{2}\rfloor-k}\frac{(-1)^{k+j}}{k!j!}\frac{(2\eta-2j-2k)!\,z^{\eta-m-2k}\rho^{m+2k}}{(\eta-j-k)!(\eta-2j-2k-m)!} \quad . \tag{A.47b}$$

In the last step, we sent the summation variable $j \to j+k$, in order to shift the lower limit of the sum over j to 0. By expanding with $(\eta+m)!$ and $(\eta-k)!$, the latter being well-defined because $k \le \lfloor(\eta-m)/2\rfloor$ also means $k \le \eta$, the factorials are rewritten as

$$\frac{1}{(\eta-j-k)!j!}\frac{(2\eta-2j-2k)!}{(\eta-2j-2k-m)!} = \frac{(\eta-k)!}{(\eta-j-k)!j!}\frac{(\eta+m)!}{(\eta-k)!}\frac{(2\eta-2j-2k)!}{(\eta-2j-2k-m)!(\eta+m)!} \tag{A.48a}$$

$$= \frac{(\eta+m)!}{(\eta-k)!}\binom{\eta-k}{j}\binom{2\eta-2k-2k}{\eta+k} \tag{A.48b}$$

with two binomial coefficients. A third binomial coefficient may be created with the factor of $k!$ in the denominator on the right-hand side of Equation (A.47b) and by expanding with $\eta!$. After rearranging the two sums as

$$r^\eta P_\eta^m(\cos(\theta)) = \frac{(-1)^m}{2^\eta}\frac{(\eta+m)!}{\eta!}\sum_{k=0}^{\lfloor\frac{\eta-m}{2}\rfloor}(-1)^k\binom{\eta}{k}z^{\eta-m-2k}\rho^{m+2k} \cdot \sum_{j=0}^{\lfloor\frac{\eta-m}{2}\rfloor-k}(-1)^j\binom{\eta-k}{j}\binom{2\eta-2k-2j}{\eta+m} \quad , \tag{A.49}$$

the coefficient $a_\eta^m(k)$ from Equation (A.24) is clearly identified. Comparing with its explicit form (A.34) or Equation (A.36b) for the conversion to cylindrical coordinates, the sum over j must give

$$\sum_{j=0}^{\lfloor\frac{\eta-m}{2}\rfloor-k}(-1)^j\binom{\eta-k}{j}\binom{2\eta-2k-2j}{\eta+m} = 2^{\eta-m-2k}\binom{\eta-k}{m+k} \quad . \tag{A.50}$$

Since $\eta - m - 2k = (\eta - k) - (m + k)$, the right-hand side is described entirely by the two variables $\eta - k$ and $m + k$, which complicates the search for its mathematical provenance. As a cross-check, setting $m = 0$ reproduces Equation (A.23), which resulted from the direct conversion of $r^\eta P_\eta(\cos(\theta))$ to cylindrical coordinates. As with Equation (A.23), the more general identity (A.50) would be hard to spot without the direct comparison of Equations (A.36b) and (A.49). Therefore, the indirect conversion in Section A.3.1 helps tremendously.

Specific comparison

Reference [92] offers a partial check of the conversion (A.36a) to cylindrical coordinates and the explicit expression (A.43) for the associated Legendre polynomial, because it shows a general expression for

$$p_{2n,2m}(r,\theta) = \frac{r^{2(n+m)}P^{2n}_{2(n+m)}(\cos(\theta))}{\rho_\mathrm{r}^{2(n+m)}P^{2n}_{2(n+m)}(0)} \tag{A.51}$$

in its Equation (76), where n and m are two non-negative integers. We have adjusted the expression, Equation (75), to our notation here, using r for the distance from the origin, rather than as the cylindrical radial coordinate called ρ in this thesis. The normalization factor ρ_r, called r_0 in Reference [92], is the distance from the origin to the ring electrode, see Figure 2.1.

From the explicit expression (A.43) for the associated Legendre polynomial, it is clear that the only contribution in $P_\eta^m(0)$ originates from the constant term ζ^0, which means that $2j = \eta - m$ is the only relevant value of the summation variable j. This also means that $\eta - m$ must be even, which is the case in Equation (A.51). After the particular replacements $m \to 2n$ and $\eta \to 2(n+m)$ in P_η^m, the specific value of the associated Legendre polynomial in the denominator becomes

$$P^{2m}_{2(n+m)}(0) = \frac{(-1)^m}{2^{2(n+m)}}\frac{[2(2n+m)]!}{m!\,(2n+m)!} \quad . \tag{A.52}$$

Applying the conversion (A.36a) to cylindrical coordinates (with j instead of k as the summation variable) on the numerator of Equation (A.51) yields

$$r^{2(n+m)} P^{2n}_{2(n+m)}(\cos(\theta)) = (-1)^{2n} \frac{[2(2n+m)]!}{2^{2n}} \sum_{j=0}^{m} \frac{(-1)^j}{2^{2j}} \frac{z^{2m-2j} \rho^{2n+2j}}{j!\,(2n+j)!\,(2m-2j)!} \tag{A.53}$$

$$= \frac{[2(2n+m)]!}{2^{2n}} \rho^{2n} \sum_{j=0}^{m} \frac{(-1)^{m-j}}{2^{2(m-j)}} \frac{z^{2j} \rho^{2(m-j)}}{(m-j)!\,(2n+m-j)!\,(2j)!} \quad . \tag{A.54}$$

Since n is an integer, $2n$ is even, and hence $(-1)^{2n} = 1$. In the last step, we have also shifted the summation variable according to $j \to m - j$, in order to end up with the same exponents of z and ρ as Reference [92].

With Equations (A.52) and (A.54), Equation (A.51) is rewritten as

$$p_{2n,2m}(\rho, z) = m!\,(2n+m)! \frac{\rho^{2n}}{\rho_{\mathrm{r}}^{2(n+m)}} \sum_{j=0}^{m} (-1)^j 2^{2j} \frac{z^{2j} \rho^{2(m-j)}}{(m-j)!\,(2n+m-j)!\,(2j)!} \tag{A.55}$$

$$= \frac{\rho^{2n}}{\rho_{\mathrm{r}}^{2(n+m)}} \sum_{j=0}^{m} (-2)^j \frac{m!\,(2n+m)!}{(2j)!\,(m-j)!\,(2n+m-j)!} \rho^{2(m-j)} \left(2z^2\right)^j \quad . \tag{A.56}$$

After some rearrangements in the last step, the expression closely resembles Equation (77) in Reference [92]. The corresponding coefficient $c_{n,m,j}$ from Equation (78) contains a double factorial, which for integers is defined as

$$(2j)!! = 2j \cdot (2j-2) \cdot (2j-4) \cdots 6 \cdot 4 \cdot 2 \qquad \text{for even arguments and} \tag{A.57a}$$

$$(2j-1)!! = (2j-1) \cdot (2j-3) \cdot (2j-5) \cdots 5 \cdot 3 \cdot 1 \qquad \text{for odd arguments.} \tag{A.57b}$$

In this definition, the arguments are chosen such that their parity is obvious for an integer j. With the two identities $j! = 2^{-j}(2j)!!$ and $(2j)!!\,(2j-1)!! = (2j)!$, the relevant coefficient $c_{n,m,j}$ is transformed according to

$$c_{n,m,j} = \frac{(-1)^j}{(2j-1)!!} \binom{m}{j} \frac{(2n+m)!}{(2n+m-j)!} = \frac{(-1)^j}{(2j-1)!!} \frac{m!}{j!\,(m-j)!} \frac{(2n+m)!}{(2n+m-j)!} \tag{A.58a}$$

$$= (-2)^j \frac{m!\,(2n+m)!}{(2j)!\,(m-j)!\,(2n+m-j)!} \quad , \tag{A.58b}$$

and it agrees with the coefficient inside the sum of Equation (A.56). Thus, the partial cross-check is fully successful.

A.3.3. Alternative route to matching the solutions

When converting $r^\eta P_\eta(\cos(\theta))$ from spherical to cylindrical coordinates in Section A.3.1, a specific value of the associated Legendre polynomial $P^m_\eta(\cos(\theta))$ has to be known, in order to determine the global prefactor, which the recursive relation (A.30) does not fix. At that point, no explicit form or special value of $P^m_\eta(\cos(\theta))$ was used, owing to a lack of availability. Instead, the value of the coefficient $a^m_\eta(0)$ was conjectured by observing a trend in the ratio of the two

solutions (A.6) and (A.24) to the Laplace equation. The two solutions had the same spatial dependence by design, but they differed by the factor (A.33) with a nontrivial dependence on η and m for $m \neq 0$, in which case the factor was known to be unity, see Equation (2.70). Now, the direct conversion in Section A.3.2 provides the tools to determine $a_\eta^m(0)$ rigorously.

Equation (A.47b) shows that there is only one value of j, namely $j = 0$, that contributes for the maximum value of k, which is

$$k_{\max} = \left\lfloor \frac{\eta - m}{2} \right\rfloor = \begin{cases} \frac{\eta-m}{2} & \text{for } \eta - m \text{ even,} \\ \frac{\eta-m-1}{2} & \text{for } \eta - m \text{ odd.} \end{cases} \tag{A.59}$$

Thus, the sum over j reduces to a single term, which yields the coefficient

$$a_\eta^m(k_{\max}) = \frac{(-1)^{m+k_{\max}}}{2^\eta} \frac{(2\eta - 2k_{\max})!}{k_{\max}!\,(\eta - k_{\max})!\,(\eta - m - k_{\max})!} \tag{A.60}$$

of the polynomial (A.24) in z and ρ. Solving the recursive relation (A.32b) for $a_\eta^m(0)$ links the coefficient $a_\eta^m(k_{\max})$ to the desired one according to

$$a_\eta^m(0) = (-1)^k 2^{2k} k! \frac{(\eta - m - 2k)!}{(\eta - m)!} \frac{(m + k)!}{m!} a_\eta^m(k) \tag{A.61a}$$

$$= \frac{(-1)^m}{2^{\eta - 2k_{\max}}} \frac{(2\eta - 2k_{\max})!}{m!\,(\eta - m)!} \frac{(m + k_{\max})!}{(\eta - k_{\max})!} \quad . \tag{A.61b}$$

The first line is a general one; in the second step, we have plugged in the specific coefficient (A.60), additionally using $(-1)^{2k_{\max}} = 1$ for the integer $k_{\max}$. If $\eta - m$ is even, then $m + k_{\max} = \eta - k_{\max}$, and Equation (A.61b) simplifies to

$$a_\eta^m(0) = \frac{(-1)^m}{2^m} \frac{(\eta + m)!}{m!\,(\eta - m)!} \quad . \tag{A.62}$$

If $\eta - m$ is odd, the last fraction in Equation (A.61b) requires a little more scrutiny. However, the final result

$$a_\eta^m(0) = \frac{(-1)^m}{2^{m+1}} \frac{(\eta + m + 1)!}{m!\,(\eta - m)!} \frac{\left(\frac{\eta+m-1}{2}\right)!}{\left(\frac{\eta+m+1}{2}\right)!} = \frac{(-1)^m}{2^{m+1}} \frac{(\eta + m + 1)!}{m!\,(\eta - m)!} \frac{2}{\eta + m + 1} \tag{A.63a}$$

$$= \frac{(-1)^m}{2^m} \frac{(\eta + m)!}{m!\,(\eta - m)!} \tag{A.63b}$$

is the same as in the first case. Consequently, Equations (A.62) and (A.63b) confirm the conjecture of Equation (A.33).

B. Laplace equation: Polynomial solutions from Bessel functions

Chapter A discusses the standard solution of the Laplace equation in spherical coordinates, and it converts the solution, which involves a Legendre polynomial, into cylindrical coordinates. In this way, a polynomial solution in the radial coordinate ρ and the axial coordinate z is obtained. In the context of cylindrical traps, Section 2.2.1 mentions Bessel functions as a way of expressing the electrostatic potential in cylindrical coordinates right away, thereby avoiding the conversion of coordinates. This chapter shows that the polynomial solutions of the Laplace equation are readily deduced from these general expressions with Bessel functions. In fact, this derivation is the most direct way if one is equipped with a textbook solution of the Laplace equation and a handbook of mathematical functions.[1]

B.1. Solutions with cylindrical symmetry

In cylindrical coordinates, cylindrically-symmetric solutions to the Laplace equation (2.57), which do not diverge on the whole z-axis, are given by

$$\tilde{\Phi}^{\mathrm{s}}_{\kappa}(\rho, z) = I_0(\kappa\rho)\cos(\kappa z) \qquad \text{and} \qquad \tilde{\Phi}^{\mathrm{a}}_{\kappa}(\rho, z) = I_0(\kappa\rho)\sin(\kappa z) \quad , \tag{B.1}$$

where I_0 is a modified Bessel function of the first kind. The modified Bessel function of the second kind, Y_0, also produces solutions, but the function is excluded here because of its singularity [185] at $\rho = 0$. The tilde indicates that general solutions to the Laplace equation rather electrostatic potentials with the correct unit are considered here. Since the Laplace equation is a homogeneous linear differential equation, we are free to include prefactors and add individual solutions. The overall solution is a sum over different values of the parameter κ, a real number with the dimension of inverse length, which is constrained by the boundary conditions on the electrodes [13], typically by setting the potential to zero at some distance $\pm z_{\mathrm{e}}$, where the endcaps are. However, the exact value of κ is of no importance here. The superscripts "s" and "a" distinguish between solutions that are symmetric and antisymmetric, respectively, with respect to the axial coordinate z.

[1] I wonder why this occurred to me only shortly before the deadline and after completing Section 2.2.1 and Chapter A. However, this chapter does not supersede these previous derivations, which prove how far one may get based on elementary math skills without an elaborate knowledge of special functions. Moreover, we had to match the prefactor of the polynomial solutions, in order to complete the conversion of the standard parametrization with Legendre polynomials from spherical to cylindrical coordinates. This chapter will not provide an easier answer for this global prefactor, because it depends on the properties of the Legendre polynomials, whose relations to Bessel functions we will not discuss here.

We will now expand the solutions (B.1) about the origin, that is, $\rho = 0$ and $z = 0$. The modified Bessel function of the first kind is given by [184]

$$I_0(\kappa\rho) = \sum_{k=0}^{\infty} \frac{(\kappa\rho)^{2k}}{2^{2k}\,(k!)^2} \quad ; \tag{B.2}$$

the series expansions of the trigonometric functions are

$$\cos(\kappa z) = \sum_{k=0}^{\infty} (-1)^k \frac{(\kappa z)^{2k}}{(2k)!} \qquad \text{and} \qquad \sin(\kappa z) = \sum_{k=0}^{\infty} (-1)^k \frac{(\kappa z)^{2k+1}}{(2k+1)!} \quad . \tag{B.3}$$

The form of these expansion as infinite series makes it clear why the solutions (B.1) are non-polynomial. Using the Cauchy product

$$\left(\sum_{k=0}^{\infty} \alpha_k\right)\left(\sum_{k=0}^{\infty} \beta_k\right) = \sum_{j=0}^{\infty} \sum_{k=0}^{j} \alpha_k \beta_{j-k} \quad , \tag{B.4}$$

which shown here for two generic sequences, whose elements are α_k and β_k, we obtain

$$\tilde{\Phi}_\kappa^{\mathrm{s}} = \sum_{j=0}^{\infty} \kappa^{2j} \sum_{k=0}^{j} \frac{(-1)^{j-k} \rho^{2k} z^{2j-2k}}{2^{2k}(k!)^2\,(2j-2k)!} \quad \text{and} \quad \tilde{\Phi}_\kappa^{\mathrm{a}} = \sum_{j=0}^{\infty} \kappa^{2j+1} \sum_{k=0}^{j} \frac{(-1)^{j-k} \rho^{2k} z^{2j-2k+1}}{2^{2k}(k!)^2\,(2j-2k+1)!} \tag{B.5}$$

for the solutions (B.1) to the Laplace equation. For space, we have suppressed the variables ρ and z in the argument of $\tilde{\Phi}_\kappa$ Since the Laplace equation has to be fulfilled for arbitrary values of the parameter κ, the sums over k have to be solutions on their own for all values of the other summation variable j. Therefore, all the prefactors that depend on j only play no role for the polynomial solutions to the Laplace equation, and we will ignore the terms κ^{2k} and $(-1)^j$. Of course, we must not drop $2j$ in the exponent of the variable z.

Apart from the upper limit j, the sums over k in Equation (B.5) depend on $2j$ and $2j+1$. The former is always even; the latter is always odd. Thus, we can rewrite the sums over k in terms of a single integer parameter η, where $\eta = 2j$ in the first case and $\eta = 2j+1$ in the second. In the first case, the upper limit of the sum over k is $\eta/2$; in the second case, it is $(\eta-1)/2$. Since $\eta/2 = \lfloor \eta/2 \rfloor$ for η even and $(\eta-1)/2 = \lfloor \eta/2 \rfloor$ for η odd according to the definition (2.60) of the floor function for integer arguments, both cases for the upper limit are handled by the choice $\lfloor \eta/2 \rfloor$. Because $2k$ is even for an integer k, we rewrite the sign-changing factor as $(-1)^{-k} = 1 \cdot (-1)^{-k} = (-1)^{2k}(-1)^{-k} = (-1)^k$.

Finally, the sums over k, which are polynomial solutions to the Laplace equation—their upper limit being finite—take the form

$$\Delta \sum_{k=0}^{\lfloor \eta/2 \rfloor} \frac{(-1)^k \rho^{2k} z^{\eta-2k}}{2^{2k}(k!)^2(\eta-2k)!} = 0 \quad , \tag{B.6}$$

where we have explicitly shown the impact of applying the Laplace operator (2.63), in order to emphasize that the sum is a harmonic function. Up to a global factor of $\eta!$, the sum is identical

to the polynomial solution (2.73) with its coefficient (2.71). Here, including a factor of $\eta!$ ensures that the coefficient of z^η is unity, which matches a property of the solution (2.59) with Legendre polynomials, see Equation (2.70).

In addition to the solutions (B.1), the functions

$$\tilde{\Psi}^{\mathrm{s}}_{\kappa}(\rho, z) = J_0(\kappa\rho)\cosh(\kappa z) \qquad \text{and} \qquad \tilde{\Psi}^{\mathrm{a}}_{\kappa}(\rho, z) = J_0(\kappa\rho)\sinh(\kappa z) \tag{B.7}$$

also solve the Laplace equation. In fact, the two solutions (B.1) and (B.7) are linked by the three relations $J_0(\mathrm{i}\kappa\rho) = I_0(\kappa\rho)$, $\cosh(\mathrm{i}\kappa z) = \cos(\kappa z)$ and $\sinh(\mathrm{i}\kappa z) = \mathrm{i}\sin(\kappa z)$ for imaginary arguments. Because the Bessel function of the first kind, J_0, has zeros, the parametrization here is useful for a cylindrical trap with a grounded ring electrode and the endcaps at some potential [5]. With the source-free and finite potential of an empty trap in mind, the solutions with the Bessel function of the second kind, K_0, are not shown because of the singularity [174] for $\rho = 0$.

With the nonsingular solutions (B.7), the same polynomial solutions as before—possibly up to a global prefactor—follow with the series expansions

$$J_0(\kappa\rho) = \sum_{k=0}^{\infty} (-1)^k \frac{(\kappa\rho)^{2k}}{2^{2k}\,(k!)^2} \tag{B.8}$$

for the Bessel function of the first kind [173], and the hyperbolic functions

$$\cosh(\kappa z) = \sum_{k=0}^{\infty} \frac{(\kappa z)^{2k}}{(2k)!} \qquad \text{and} \qquad \sinh(\kappa z) = \sum_{k=0}^{\infty} \frac{(\kappa z)^{2k+1}}{(2k+1)!} \quad . \tag{B.9}$$

Since the polynomial solutions are supposed to represent fundamental solutions of the Laplace equation, thereby constituting a set of basis functions, they have to be unique, barring their prefactor.[2] The only difference concerns how the fundamental solutions are combined in order to reproduce specific boundary conditions. In the series (B.5), the sum over j composes special functions from the fundamental polynomial solutions.

B.2. Solutions beyond cylindrical symmetry

The cylindrically-symmetric solutions (B.1) to the Laplace equation are special cases of the general solutions

$$\tilde{\Phi}^{\mathrm{s}}_{\kappa m}(\rho, \phi, z) = I_m(\kappa\rho)\cos(\kappa z) f(\phi) \qquad \text{and} \qquad \tilde{\Phi}^{\mathrm{a}}_{\kappa m}(\rho, \phi, z) = I_m(\kappa\rho)\sin(\kappa z) f(\phi) \tag{B.10}$$

in cylindrical coordinates for $m = 0$. Here, there is the additional function

$$f(\phi) = c_{\kappa m}\cos(m\phi) + s_{\kappa m}\sin(m\phi) \tag{B.11}$$

[2] Since the basis functions are classified uniquely based on their degree, we brush aside a different set of basis functions, composed by superimposing the polynomial solutions of different degrees, as an unnecessary complication.

of the angle variable ϕ, where $c_{\kappa m}$ and $s_{\kappa m}$ are two coefficients. We have suppressed the superscripts "s" and "a" for convenience, even though the coefficients may be chosen independently for solutions that are symmetric and antisymmetric, respectively, in the axial coordinate z. The structure of $f(\phi)$ is the same as in the ansatz (A.6) with associated Legendre polynomials. Since the angle variable ϕ points to the same spot after a full turn of 2π, the periodicity $f(\phi + 2\pi) = f(\phi)$ require that m be an integer. Without loss of generality, we take m to be non-negative.[3]

For a comparison with the associated Legendre polynomials of Section A.3, we are interested in the dependence of the solution (B.10) on the radial displacement ρ and the axial coordinate z. With the series expansion [184], valid for non-negative integers m,

$$I_m(\kappa\rho) = \sum_{k=0}^{\infty} \frac{(\kappa\rho)^{2k+m}}{2^{2k+m}\, k!\, (m+k)!} \tag{B.12}$$

for the modified Bessel function of the first kind, the series (B.3) for the trigonometric functions, and the Cauchy product (B.4), the components without a dependence on the azimuth angle ϕ in the solutions (B.10) to the Laplace equation are written as the infinite series

$$I_m(\kappa\rho)\cos(\kappa z) = \sum_{j=0}^{\infty} \frac{\kappa^{2j+m}}{2^m} \sum_{k=0}^{j} \frac{(-1)^{j-k}\rho^{2k+m} z^{2j-2k}}{2^{2k}\, k!\, (m+k)!\, (2j-2k)!} \quad , \tag{B.13}$$

$$I_m(\kappa\rho)\sin(\kappa z) = \sum_{j=0}^{\infty} \frac{\kappa^{2j+m+1}}{2^m} \sum_{k=0}^{j} \frac{(-1)^{j-k}\rho^{2k+m} z^{2j-2k+1}}{2^{2k}\, k!\, (m+k)!\, (2j-2k+1)!} \quad . \tag{B.14}$$

The polynomial component of the solution is now read off with the same reasoning as in Section B.1. Since the result after applying the Laplace operator has to be independent of the parameter κ, the sums over k have to be individual solutions when multiplied with $f(\phi)$ from Equation (B.11). The sums over k in Equations (B.13) and (B.14) depend on $2j$ and $2j+1$, respectively, apart from their upper limit j and the factor of $(-1)^j$. The latter is safely ignored as a prefactor; the upper limit requires some attention. Because $2j$, which is always even, and $2j+1$, which is always odd, eventually run through all non-negative integers, we condense the two possibilities in one parameter n. With the definition (2.60) of the floor function for integer arguments, the upper limit is summarized as $\lfloor n/2 \rfloor$ for both cases, and the sums over k take the common form

$$\sum_{k=0}^{\lfloor n/2 \rfloor} \frac{(-1)^k \rho^{2k+m} z^{n-2k}}{2^{2k} k!\, (m+k)!\, (n-2k)!} = \sum_{k=0}^{\lfloor \frac{\eta-m}{2} \rfloor} \frac{(-1)^k \rho^{2k+m} z^{\eta-m-2k}}{2^{2k} k!\, (m+k)!\, (\eta-m-2k)!} \quad . \tag{B.15}$$

In the last step, we have defined $n = \eta - m$, where $0 \leq m \leq \eta$, in order to close in on Equation (A.36b), which gives the polynomial in ρ and z by converting $r^\eta P_\eta^m(\cos(\theta))$ with the

[3] The sign of m does not matter in the even function $\cos(m\phi)$, and the change of sign in the odd function $\sin(m\phi)$ is absorbed in the prefactor $s_{\kappa m}$. Moreover, the modified Bessel functions of the first kind, I_m, do not depend on the sign of m because the modified Bessel differential equation does not [183]. The second fundamental solution to this second-order differential equation is not hidden in the sign of m; it manifests itself in the modified Bessel functions of the second kind, Y_m.

associated Legendre polynomial P_η^m from spherical to cylindrical coordinates. Up to a global factor, which does not matter for the solution to a homogeneous linear differential equation, the result is identical.

The solution (B.7) without singularities is extended beyond cylindrical symmetry by including the azimuth angle ϕ via the function $f(\phi)$ from Equation (B.11) as

$$\tilde{\Psi}^{\mathrm{s}}_{\kappa m}(\rho,\phi,z) = J_m(\kappa\rho)\cosh(\kappa z) f(\phi) \quad \text{and} \quad \tilde{\Psi}^{\mathrm{a}}_{\kappa m}(\rho,\phi,z) = J_m(\kappa\rho)\sinh(\kappa z) f(\phi) \quad . \tag{B.16}$$

With the expansion for the Bessel function of the first kind [173]

$$J_m(\kappa\rho) = \sum_{k=0}^{\infty} (-1)^k \frac{(\kappa\rho)^{2k+m}}{2^{2k+m}\, k!\, (m+k)!} \tag{B.17}$$

and the hyperbolic functions (B.9), the Cauchy product (B.4) yields the polynomial (B.15) in ρ and z again. Because they solve a homogeneous linear differential equation, the fundamental polynomial solutions, of which all solutions to the Laplace equation are composed, are defined up to a prefactor only.

C. Trigonometric identities

C.1. Powers of cosine

A crucial part of the calculation is to expand the powers of a trigonometric function into a sum of simple trigonometric functions in order to decompose the original function into its individual frequency components. The two relevant identities are introduced without proof as Equations (3.2) and (3.5) in Section 3.1. Although they can be found in the literature under the name of trigonometric power(-reduction) formulas [188], we will derive them here. Because they are an integral part of the thesis, we want to demonstrate that there is nothing arcane about them.

The essential step of deriving a general formula for powers of cosine is to recall that the cosine function can be expressed by exponential functions as

$$\cos(\chi) = \frac{1}{2}\left(\mathrm{e}^{\mathrm{i}\chi} + \mathrm{e}^{-\mathrm{i}\chi}\right) \quad . \tag{C.1}$$

Therefore, calculating the powers of cosine can be reduced to calculating the powers of exponential functions.

Even powers

We use binomial expansion to establish that

$$[\cos(\chi)]^{2n} = \left[\frac{1}{2}\left(\mathrm{e}^{\mathrm{i}\chi} + \mathrm{e}^{-\mathrm{i}\chi}\right)\right]^{2n} \tag{C.2a}$$

$$= \frac{1}{2^{2n}} \sum_{k=0}^{2n} \binom{2n}{k} \left[\mathrm{e}^{\mathrm{i}\chi}\right]^{k} \left(\mathrm{e}^{-\mathrm{i}\chi}\right)^{2n-k} \tag{C.2b}$$

$$= \frac{1}{2^{2n}} \sum_{k=0}^{2n} \binom{2n}{k} \left[\mathrm{e}^{\mathrm{i}\chi}\right]^{k} \left(\mathrm{e}^{\mathrm{i}\chi}\right)^{-2n+k} \tag{C.2c}$$

$$= \frac{1}{2^{2n}} \sum_{k=0}^{2n} \binom{2n}{k} \left[\mathrm{e}^{\mathrm{i}\chi}\right]^{2(k-n)} \tag{C.2d}$$

$$= \frac{1}{2^{2n}} \sum_{j=-n}^{n} \binom{2n}{j+n} \left[\mathrm{e}^{2\mathrm{i}\chi}\right]^{j} \quad . \tag{C.2e}$$

We substituted $j = k - n$ in the final step. The binomial coefficient is defined in Equation (3.3). By decomposing the whole sum into individual sums for $j < 0, j = 0, j > 0$ and by letting $j \to -j$

in the first sum, we obtain

$$[\cos(\chi)]^{2n} = \frac{1}{2^{2n}} \sum_{j=-n}^{n} \binom{2n}{j+n} \left[\mathrm{e}^{2\mathrm{i}\chi}\right]^{j} \tag{C.3a}$$

$$= \frac{1}{2^{2n}} \left\{ \sum_{j=-n}^{-1} \binom{2n}{j+n} \left[\mathrm{e}^{2\mathrm{i}\chi}\right]^{j} + \binom{2n}{n} + \sum_{j=1}^{n} \binom{2n}{j+n} \left[\mathrm{e}^{2\mathrm{i}\chi}\right]^{j} \right\} \tag{C.3b}$$

$$= \frac{1}{2^{2n}} \left\{ \sum_{j=1}^{n} \binom{2n}{n-j} \left[\mathrm{e}^{2\mathrm{i}\chi}\right]^{-j} + \binom{2n}{n} + \sum_{j=1}^{n} \binom{2n}{j+n} \left[\mathrm{e}^{2\mathrm{i}\chi}\right]^{j} \right\} \tag{C.3c}$$

$$= \frac{1}{2^{2n}} \left\{ \binom{2n}{n} + \sum_{j=1}^{n} \binom{2n}{n-j} \left[\mathrm{e}^{2\mathrm{i}j\chi} + \mathrm{e}^{-2\mathrm{i}j\chi}\right] \right\} \tag{C.3d}$$

$$= \frac{1}{2^{2n}} \left\{ \binom{2n}{n} + 2 \sum_{j=1}^{n} \binom{2n}{n-j} \cos(2j\chi) \right\} \quad . \tag{C.3e}$$

We made use of the identity (3.4)

$$\binom{2n}{n-j} = \binom{2n}{2n-(n-j)} = \binom{2n}{n+j} \tag{C.4}$$

for binomial coefficients.

Odd powers

The starting point is the same as for even powers:

$$[\cos(\chi)]^{2n+1} = \left[\frac{1}{2}\left(\mathrm{e}^{\mathrm{i}\chi} + \mathrm{e}^{-\mathrm{i}\chi}\right)\right]^{2n+1} \tag{C.5a}$$

$$= \frac{1}{2^{2n+1}} \sum_{k=0}^{2n} \binom{2n+1}{k} \left(\mathrm{e}^{\mathrm{i}\chi}\right)^{k} \left[\mathrm{e}^{-\mathrm{i}\chi}\right]^{2n+1-k} \tag{C.5b}$$

$$= \frac{1}{2^{2n+1}} \sum_{k=0}^{2n} \binom{2n+1}{k} \left[\mathrm{e}^{\mathrm{i}\chi}\right]^{k} \left(\mathrm{e}^{\mathrm{i}\chi}\right)^{-2n-1+k} \tag{C.5c}$$

$$= \frac{1}{2^{2n+1}} \sum_{k=0}^{2n} \binom{2n+1}{k} \left[\mathrm{e}^{\mathrm{i}\chi}\right]^{2(k-n)-1} \tag{C.5d}$$

$$= \frac{1}{2^{2n+1}} \left\{ \sum_{k=0}^{n} \binom{2n+1}{k} \left[\mathrm{e}^{\mathrm{i}\chi}\right]^{2(k-n)-1} + \sum_{k=n+1}^{2n+1} \binom{2n+1}{k} \left[\mathrm{e}^{\mathrm{i}\chi}\right]^{2(k-n)-1} \right\} \quad . \tag{C.5e}$$

Having decomposed the sum, we now substitute $j = k - n$ in the first part, and $j = k - n - 1$ in the second:

$$[\cos(\chi)]^{2n+1} = \frac{1}{2^{2n+1}} \left\{ \sum_{k=0}^{n} \binom{2n+1}{k} \left[e^{i\chi}\right]^{2(k-n)-1} + \sum_{k=n+1}^{2n+1} \binom{2n+1}{k} \left[e^{i\chi}\right]^{2(k-n)-1} \right\} \tag{C.6a}$$

$$= \frac{1}{2^{2n+1}} \left\{ \sum_{j=-n}^{0} \binom{2n+1}{j+n} \left[e^{i\chi}\right]^{2j-1} + \sum_{j=0}^{n} \binom{2n+1}{j+n+1} \left[e^{i\chi}\right]^{2j+1} \right\} \tag{C.6b}$$

$$= \frac{1}{2^{2n+1}} \left\{ \sum_{j=0}^{n} \binom{2n+1}{n-j} \left[e^{i\chi}\right]^{-(2j+1)} + \sum_{j=0}^{n} \binom{2n+1}{j+n+1} \left[e^{i\chi}\right]^{2j+1} \right\} \tag{C.6c}$$

$$= \frac{1}{2^{2n+1}} \sum_{j=0}^{n} \binom{2n+1}{n-j} \left[e^{-i(2j+1)\chi} + e^{i(2j+1)\chi}\right] \tag{C.6d}$$

$$= \frac{1}{2^{2n}} \sum_{j=0}^{n} \binom{2n+1}{n-j} \cos\left[(2j+1)\chi\right] \tag{C.6e}$$

We substituted $j \to -j$ in the first sum and used the identity (3.4)

$$\binom{2n+1}{n-j} = \binom{2n}{2n+1-(n-j)} = \binom{2n+1}{n+j+1} \tag{C.7}$$

for binomial coefficients.

C.2. Multiplication or mixing

The angle-sum and angle-difference identities

$$\cos(\alpha \pm \beta) = \cos(\alpha)\cos(\beta) \mp \sin(\alpha)\sin(\beta) \quad , \tag{C.8}$$

$$\sin(\alpha \pm \beta) = \sin(\alpha)\cos(\beta) \pm \sin(\beta)\cos(\alpha) \tag{C.9}$$

are linked with the product-to-sum identities

$$\cos(\alpha)\cos(\beta) = \frac{\cos(\alpha-\beta) + \cos(\alpha+\beta)}{2} \quad , \tag{C.10}$$

$$\sin(\alpha)\cos(\beta) = \frac{\sin(\alpha-\beta) + \sin(\alpha+\beta)}{2} \quad , \tag{C.11}$$

$$\sin(\alpha)\sin(\beta) = \frac{\cos(\alpha-\beta) - \cos(\alpha+\beta)}{2} \quad . \tag{C.12}$$

The latter are frequently used in the thesis to identify resonant terms when two oscillatory terms are multiplied, see the general prescriptions of Equations (4.39), (4.40), (4.126), and (4.128), for example.

The identity (C.10) may also be used to verify Equations (C.3e) and (C.6e) for the frequency components in powers of cosine without expressing cosine via exponential functions as in

Equation (C.1). Even though the new approach looks like a combinatorial one instead, it closely resembles the rearrangements after binomial expansion in Section C.1. In fact, the combinatorial meaning of binomial coefficients will play a key role.

Written as multiple products, there are $2n$ factors of $\cos(\chi)$ in $[\cos(\chi)]^{2n}$. According to Equation (C.10), every multiplication with $\cos(\chi)$ results in two terms: The prefactor of χ in the argument of the trigonometric function either increases or decreases by one. We will refer to the former as mixing up and to the latter as mixing down. In this sense, we write the multiplication of the constant term as $\cos(0)\cos(\chi) = \frac{1}{2}[\cos(\chi) + \cos(-\chi)]$. Apart from possibly changing the prefactor of χ, every multiplication reduces the amplitude of the resulting terms by a factor of two, and hence the overall prefactor 2^{2n} in the denominator of Equation (C.3e). Since every multiplication with $\cos(\chi)$ changes the parity of the prefactor of χ in the resulting terms, there will be not change after the even amount of $2n$ multiplications. Consequently, the prefactor $2j$ of χ in Equation (C.3e) is always even. There are no odd multiples of χ on the right-hand side. We will now examine the terms with even multiples of χ, including the zero dependence on χ, also known as the constant term.

How many possibilities are there to produce a constant term via the $2n$ multiplications in $[\cos(\chi)]^{2n}$? We have to mix up as many times as down—that is, n times. There are $\binom{2n}{n}$ combinations. Remember to interpret the binomial coefficient $\binom{n}{k}$ as "n choose k"—the number of possibilities to select k elements out of n, disregarding the order of the draw. Here, we select when to mix up (or down) in the $2n$ multiplications.[1]

How many possibilities are there to produce a term $\cos(2j\chi)$? We have to mix up $n + j$ times and down $n - j$ times, for which there are $\binom{2n}{n+j} = \binom{2n}{n-j}$ possibilities. Since cosine is an even function—that is, $\cos(\chi) = \cos(-\chi)$—the term $\cos(-2j\chi)$ contributes the same oscillatory term, too. It is produced by mixing up $n - j$ times and down $n + j$ times, which essentially doubles the possibilities of obtaining $\cos(2j\chi)$, where j is positive. Alternately, we could allow for negative j. In any case, we have reproduced the prefactor of $\cos(2j\chi)$ in Equation (C.3e).

The same combinatorial strategy also works for the odd powers of cosine with $2n + 1$ factors of $\cos(\chi)$ in $[\cos(\chi)]^{2n+1}$. Because each multiplication with $\cos(\chi)$ changes the parity of the prefactor of χ, there are no even multiplies of χ for the odd amount of $2n + 1$ multiplications. Therefore, all multiples of the argument χ are odd. A term $\cos[(2j + 1)\chi]$ is produced by mixing up $n + 1 + j$ times and mixing down $n - j$ times. There are $\binom{2n+1}{n+1+j} = \binom{2n+1}{n-j}$ possibilities to do so. For the total number, the terms $\cos[-(2j + 1)\chi]$, which result from mixing up $n - j$ times and down $n + j + 1$ times, have to be counted, too. Overall, there are twice as many possibilities. The additional factor of 2 combines with the 2^{2n+1} in the denominator from the $2n + 1$ multiplications to form the correct prefactor in Equation (C.6e), and the binomial coefficient fits, too.

[1] Since we mix either up or down with no other alternative, opting against one operation is equivalent to choosing the other. This is the meaning of Equation (3.4) in the combinatorial sense.

D. Definition of secularity

In this chapter, we review proper definitions of secularity. The equation numbers are assigned in this chapter; they are not from the original references. In contrast, the emphasis *in italics* is not mine; it is from the original references.

The following quote is from Reference [4]:

> "In general, secular terms always appear whenever the inhomogeneous term is itself a solution of the associated homogeneous *constant-coefficient* differential equation. A secular term always grows more rapidly than the corresponding solution of the homogeneous equation by at least a factor of t."

Note that this definition does not necessarily imply that secular terms diverge for $t \to \infty$ as the following example from Reference [4] illustrates.

> "The solution to the differential equation
>
> $$\ddot{y} - y = \mathrm{e}^{-t} \tag{D.1}$$
>
> has a secular term because e^{-t} satisfies the associated homogeneous equation. The general solution is
>
> $$y(t) = A\mathrm{e}^{-t} + B\mathrm{e}^{t} - \frac{1}{2}t\mathrm{e}^{-t} \quad . \tag{D.2}$$
>
> The particular solution $-\frac{1}{2}t\mathrm{e}^{-t}$ is secular relative to the homogeneous solution $A\mathrm{e}^{-t}$; we must regard the term $-\frac{1}{2}t\mathrm{e}^{-t}$ as secular even though it is negligible compared with the homogeneous solution $B\mathrm{e}^{t}$."

With respect to nearly periodic problems, Henri Poincaré offers a less mathematical but more pictorial definition in the introduction of his 1892 book[1] "Les méthodes nouvelles de la mécanique céleste."

> « Ces méthodes, qui consistent à développer les coordonnées des astres suivant les puissances des masses, ont en effet un caractère commun qui s'oppose à leur emploi pour le calcul des éphémérides à longue échéance. Les séries obtenues contiennent des termes dits *séculaires*, où le temps sort des signes sinus et cosinus, et il en résulte que leur convergence pourrait devenir douteuse si l'on donnait à ce temps t une grande valeur.

[1] https://archive.org/details/lesmthodesnouv001poin

> La présence de ces termes séculaires ne tient pas à la nature du problème, mais seulement à la méthode employée. Il est facile de se rendre compte, en effet, que si la véritable expression d'une coordonnée contient un terme en
>
> $$\sin(\alpha m t)\,, \tag{D.3}$$
>
> α étant une constante et m l'une des masses, on trouvera, quand on voudra développer suivant les puissances de m, des termes séculaires
>
> $$\alpha m t - \frac{\alpha^3 m^3 t^3}{6} + \cdots \tag{D.4}$$
>
> et la présence de ces termes donnerait une idée très fausse de la véritable forme de la fonction étudiée. »

I offer my own loose translation (not taken from an English version of the book, which I failed to procure).

> These methods of developing the coordinates of the celestial bodies as powers of the masses have a common feature which precludes their use for the calculation of ephemerides on long time-scales. The series obtained contain so-called *secular terms*, where the time leaves the sine and cosine symbols. As a result the convergence of the series becomes doubtful if the time t is given a large value.
>
> The presence of these secular terms is not related to the nature of the problem, but only to the method used. It is actually easy to note that if the real expression for a coordinate contains a term like
>
> $$\sin(\alpha m t)\,, \tag{D.5}$$
>
> α being a constant and m one of the masses, one will find secular terms
>
> $$\alpha m t - \frac{\alpha^3 m^3 t^3}{6} + \cdots \tag{D.6}$$
>
> when developing in powers of the masses. The presence of these terms would give a very wrong idea of the true shape of the function studied.

The introduction is also interesting from a physical point of view. Poincaré considers the comparison of observations and calculations as a test of Newton's law of gravitation.

> « Le but final de la Mécanique céleste est de résoudre cette grande question de savoir si la loi de Newton explique à elle seule tous les phénomènes astronomiques ; le seul moyen d'y parvenir est de faire des observations aussi précises que possible et de les comparer ensuite aux résultats du calcul. Ce calcul ne peut être qu'approximatif et il ne servirait à rien, d'ailleurs, de calculer plus de décimales que les observations n'en peuvent faire connaître. Il est donc inutile de demander au calcul plus de précision qu'aux observations ; mais on de doit pas non plus lui demander moins. Aussi l'approximation dont nous pouvons nous contenter aujourd'hui

> sera-t-elle insuffisante dans quelques siècles. Et, en effet, en admettant même, ce qui est très improbable, que les instruments de mesure ne se perfectionnent plus, l'accumulation seule des observations pendant plusieurs siècles nous fera connaître avec plus de précision les coefficients des diverses inégalités. »

Here is my loose translation:

> The final goal of celestial mechanics is to resolve that great question whether Newton's law alone explains all astronomical phenomena; the only way to do so is to make observations as precise as possible, and then compare them with the results of the calculation. This calculation can only be approximate, and calculating more digits than the observations can yield would therefore amount to nothing. It would hence be useless to demand more precision from the calculation than from the observations, but one must not demand less. Also, the approximation we can content ourselves with today will perhaps be insufficient in some centuries. Even conceding that measurement instruments might not improve, which is very unlikely, the mere accumulation of observations for several centuries will make known to us the coefficients of various inequalities with more precision.

Indeed, one of the astronomical problems of Poincaré's time—the perihelion precession of Mercury—is solved by general relativity rather than by a hypothetical planet ("Vulcan") that obeys Newton's law of gravity [41].

E. Explicit expressions for frequency-shifts

This chapter lists explicit first-order frequency-shifts for cylindrically-symmetric imperfections, thereby facilitating a comparison with the extensive compilation [128]. Table E.1 shows which general expressions are evaluated. Even though they are shown separately here to minimize clutter, the first-order frequency-shifts for multiple imperfections add linearly (to first-order). The axial (angular) frequency ω_z in the ideal trap is given by Equation (2.17); the unperturbed radial frequencies $\omega_\pm$ are defined in Equation (2.23). In the ideal trap, the sideband cyclotron-frequency (2.25) is equal to the free-space cyclotron-frequency ω_c of Equation (2.18). Equation (3.87) establishes the convention for the sign of a shift $\Delta\omega_i$ to these frequencies.

In cylindrical coordinates, the electrostatic potential Φ_{2n} is parametrized according to Equation (2.73), with the quadrupole potential Φ_2 of Equation (2.2) in the ideal trap. The axial and radial magnetic field are given by Equations (2.78) and (2.80), respectively. The magnetic field $\vec{B}_0$ of Equation (2.1) in the ideal trap follows for $\eta = 0$.

Table E.1.: Links to the general expression for the first-order frequency-shifts by electrostatic imperfections (represented by C_{2n}) and magnetostatic imperfections (represented by B_{2n}). Shifts to the radial frequencies under axial lock, as opposed to the normal free-running mode, are indicated by the inverted hat as in $\Delta\check{\omega}_\pm$. These shifts are related via Equation (4.152c). The shift to the sideband cyclotron-frequency is given only once as $\Delta\omega_c$, because it is the same in both modes of operation.

	C_{2n}	B_{2n}
$\Delta\omega_z$	Equation (4.36)	Equation (4.75)
$\Delta\omega_\pm$	Equation (4.50)	Equation (4.87)
$\Delta\check{\omega}_\pm$	Equation (4.159)	Equation (4.160)
$\Delta\omega_c$	Equation (4.55)	Equation (4.89)

E.1. Electrostatic imperfections

C_4

$$\Phi_4 = C_4 \frac{V_0}{2d^4}\left(z^4 - 3z^2\rho^2 + \frac{3}{8}\rho^4\right) \tag{E.1}$$

$$\frac{\Delta\omega_z}{\omega_z} = \frac{C_4}{C_2}\frac{3}{4d^2}\left(\hat{z}^2 - 2\hat{\rho}_+^2 - 2\hat{\rho}_-^2\right) \tag{E.2}$$

$$\Delta\omega_\pm = \mp\frac{C_4}{C_2}\frac{3}{2d^2}\frac{\omega_+\omega_-}{\omega_+ - \omega_-}\left(2\hat{z}^2 - \hat{\rho}_\pm^2 - 2\hat{\rho}_\mp^2\right) \tag{E.3}$$

$$\Delta\check{\omega}_\pm = \mp\frac{C_4}{C_2}\frac{3}{2d^2}\frac{\omega_+\omega_-}{\omega_+ - \omega_-}\left(\hat{z}^2 + \hat{\rho}_\pm^2\right) \tag{E.4}$$

$$\Delta\omega_\mathrm{c} = -\frac{C_4}{C_2}\frac{3}{2d^2}\frac{\omega_+\omega_-}{\omega_+ - \omega_-}\left(\hat{\rho}_+^2 - \hat{\rho}_-^2\right) \tag{E.5}$$

C_6

$$\Phi_6 = C_6\frac{V_0}{2d^6}\left(z^6 - \frac{15}{2}z^4\rho^2 + \frac{45}{8}z^2\rho^4 - \frac{5}{16}\rho^6\right) \tag{E.6}$$

$$\frac{\Delta\omega_z}{\omega_z} = \frac{C_6}{C_2}\frac{15}{16d^4}\left(\hat{z}^4 + 3\hat{\rho}_+^4 + 3\hat{\rho}_-^4 - 6\hat{\rho}_+^2\hat{z}^2 - 6\hat{\rho}_-^2\hat{z}^2 + 12\hat{\rho}_+^2\hat{\rho}_-^2\right) \tag{E.7}$$

$$\Delta\omega_\pm = \mp\frac{C_6}{C_2}\frac{15}{8d^4}\frac{\omega_+\omega_-}{\omega_+ - \omega_-}\left(3\hat{z}^4 + \hat{\rho}_\pm^4 + 3\hat{\rho}_\mp^4 - 6\hat{\rho}_\pm^2\hat{z}^2 - 12\hat{\rho}_\mp^2\hat{z}^2 + 6\hat{\rho}_+^2\hat{\rho}_-^2\right) \tag{E.8}$$

$$\Delta\check{\omega}_\pm = \mp\frac{C_6}{C_2}\frac{15}{4d^4}\frac{\omega_+\omega_-}{\omega_+ - \omega_-}\left(\hat{z}^4 - \hat{\rho}_\pm^4 - 3\hat{z}^2\hat{\rho}_\mp^2 - 3\hat{\rho}_+^2\hat{\rho}_-^2\right) \tag{E.9}$$

$$\Delta\omega_\mathrm{c} = \frac{C_6}{C_2}\frac{15}{4d^4}\frac{\omega_+\omega_-}{\omega_+ - \omega_-}\left(\hat{\rho}_+^2 - \hat{\rho}_-^2\right)\left(-3\hat{z}^2 + \hat{\rho}_+^2 + \hat{\rho}_-^2\right) \tag{E.10}$$

C_8

$$\Phi_8 = C_8\frac{V_0}{2d^8}\left(z^8 - 14z^6\rho^2 + \frac{105}{4}z^4\rho^4 - \frac{35}{4}z^2\rho^6 + \frac{35}{128}\rho^8\right) \tag{E.11}$$

$$\begin{aligned}\frac{\Delta\omega_z}{\omega_z} = \frac{C_8}{C_2}\frac{35}{32d^6}\big(&\hat{z}^6 - 4\hat{\rho}_+^6 - 4\hat{\rho}_-^6 + 18\hat{\rho}_+^4\hat{z}^2 + 18\hat{\rho}_-^4\hat{z}^2 \\ &- 36\hat{\rho}_+^4\hat{\rho}_-^2 - 36\hat{\rho}_+^2\hat{\rho}_-^4 + 72\hat{\rho}_+^2\hat{\rho}_-^2\hat{z}^2 - 12\hat{\rho}_+^2\hat{z}^4 - 12\hat{\rho}_-^2\hat{z}^4\big)\end{aligned} \tag{E.12}$$

$$\begin{aligned}\Delta\omega_\pm = \mp\frac{C_8}{C_2}\frac{35}{16d^6}\frac{\omega_+\omega_-}{\omega_+ - \omega_-}\big(&4\hat{z}^6 - \hat{\rho}_\pm^6 - 4\hat{\rho}_\mp^6 + 12\hat{\rho}_\pm^4\hat{z}^2 + 36\hat{\rho}_\mp^4\hat{z}^2 \\ &- 12\hat{\rho}_\pm^4\hat{\rho}_\mp^2 - 18\hat{\rho}_\pm^2\hat{\rho}_\mp^4 - 18\hat{\rho}_\pm^2\hat{z}^4 - 36\hat{\rho}_\mp^2\hat{z}^4 + 72\hat{\rho}_+^2\hat{\rho}_-^2\hat{z}^2\big)\end{aligned} \tag{E.13}$$

$$\Delta\check{\omega}_\pm = \mp\frac{C_8}{C_2}\frac{105}{16d^6}\frac{\omega_+\omega_-}{\omega_+ - \omega_-}\left(\hat{z}^6 + \hat{\rho}_\pm^6 + 8\hat{\rho}_\pm^4\hat{\rho}_\mp^2 + 6\hat{\rho}_\mp^4\hat{\rho}_\pm^2 - 2\hat{\rho}_\pm^4\hat{z}^2 + 6\hat{\rho}_\mp^4\hat{z}^2 - 2\hat{\rho}_\pm^2\hat{z}^4 - 8\hat{\rho}_\mp^2\hat{z}^4\right) \tag{E.14}$$

$$\Delta\omega_\mathrm{c} = -\frac{C_8}{C_2}\frac{105}{16d^6}\frac{\omega_+\omega_-}{\omega_+ - \omega_-}\left(\hat{\rho}_+^2 - \hat{\rho}_-^2\right)\left(6\hat{z}^4 + \hat{\rho}_+^4 + \hat{\rho}_-^4 - 8\hat{\rho}_+^2\hat{z}^2 - 8\hat{\rho}_-^2\hat{z}^2 + 3\hat{\rho}_+^2\hat{\rho}_-^2\right) \tag{E.15}$$

E.2. Magnetostatic imperfections

B_2

$$\vec{B}_2 = B_2\left[\left(z^2 - \frac{1}{2}\rho^2\right)\vec{e}_z + (-z\rho)\,\vec{e}_\rho\right] \tag{E.16}$$

$$\frac{\Delta\omega_z}{\omega_z} = \frac{B_2}{4B_0}\frac{\omega_+ + \omega_-}{\omega_+\omega_-}\left(\hat{\rho}_-^2\omega_- + \hat{\rho}_+^2\omega_+\right) \tag{E.17}$$

$$\frac{\Delta\omega_+}{\omega_+} = \frac{B_2}{2B_0}\frac{\omega_+ + \omega_-}{\omega_+ - \omega_-}\left[\hat{z}^2 - \hat{\rho}_+^2 - \hat{\rho}_-^2\left(1 + \frac{\omega_-}{\omega_+}\right)\right] \tag{E.18}$$

$$\frac{\Delta\omega_-}{\omega_-} = -\frac{B_2}{2B_0}\frac{\omega_+ + \omega_-}{\omega_+ - \omega_-}\left[\hat{z}^2 - \hat{\rho}_+^2\left(\frac{\omega_+}{\omega_-} + 1\right) - \hat{\rho}_-^2\right] \tag{E.19}$$

$$\frac{\Delta\check{\omega}_\pm}{\omega_\pm} = \pm\frac{B_2}{2B_0}\frac{\omega_+ + \omega_-}{\omega_+ - \omega_-}\left(\hat{z}^2 - \hat{\rho}_\mp^2\right) \tag{E.20}$$

$$\frac{\Delta\omega_\mathrm{c}}{\omega_\mathrm{c}} = \frac{B_2}{2B_0}\left[\hat{z}^2 - \hat{\rho}_-^2\frac{\omega_+}{\omega_+ - \omega_-} + \hat{\rho}_+^2\frac{\omega_-}{\omega_+ - \omega_-}\right] \tag{E.21}$$

B_4

$$\vec{B}_4 = B_4\left[\left(z^4 - 3z^2\rho^2 + \frac{3}{8}\rho^4\right)\vec{e}_z + \left(-2z^3\rho + \frac{3}{2}z\rho^3\right)\vec{e}_\rho\right] \tag{E.22}$$

$$\frac{\Delta\omega_z}{\omega_z} = \frac{3B_4}{8B_0}\frac{\omega_+ + \omega_-}{\omega_+\omega_-}\left[\omega_-\left(-\hat{\rho}_-^4 + \hat{\rho}_-^2\hat{z}^2 - 2\hat{\rho}_+^2\hat{\rho}_-^2\right) + \omega_+\left(-\hat{\rho}_+^4 + \hat{\rho}_+^2\hat{z}^2 - 2\hat{\rho}_+^2\hat{\rho}_-^2\right)\right] \tag{E.23}$$

$$\begin{aligned}\frac{\Delta\omega_+}{\omega_+} = \frac{3B_4}{8B_0}\frac{\omega_+ + \omega_-}{\omega_+ - \omega_-}\Bigg[&\hat{z}^4 + \hat{\rho}_+^4 + \hat{\rho}_-^4\left(1 + 2\frac{\omega_-}{\omega_+}\right) - 4\hat{\rho}_+^2\hat{z}^2 \\ &- 4\hat{\rho}_-^2\hat{z}^2\left(1 + \frac{\omega_-}{\omega_+}\right) + 4\hat{\rho}_+^2\hat{\rho}_-^2\left(1 + \frac{\omega_-}{2\omega_+}\right)\Bigg]\end{aligned} \tag{E.24}$$

$$\frac{\Delta\check{\omega}_+}{\omega_+} = \frac{3B_4}{8B_0}\frac{\omega_+ + \omega_-}{\omega_+ - \omega_-}\left[\hat{z}^4 - \hat{\rho}_+^4 + \hat{\rho}_-^4 - 2\hat{\rho}_+^2\hat{z}^2 - 2\hat{\rho}_-^2\hat{z}^2\left(2 + \frac{\omega_-}{\omega_+}\right) - 2\frac{\omega_-}{\omega_+}\hat{\rho}_+^2\hat{\rho}_-^2\right] \tag{E.25}$$

$$\begin{aligned}\frac{\Delta\omega_-}{\omega_-} = -\frac{3B_4}{8B_0}\frac{\omega_+ + \omega_-}{\omega_+ - \omega_-}\Bigg[&\hat{\rho}_+^4\left(2\frac{\omega_+}{\omega_-} + 1\right) + 2\hat{\rho}_+^2\hat{\rho}_-^2\left(\frac{\omega_+}{\omega_-} + 2\right) \\ &- 4\hat{\rho}_+^2\hat{z}^2\left(\frac{\omega_+}{\omega_-} + 1\right) + \hat{z}^4 + \hat{\rho}_-^4 - 4\hat{\rho}_-^2\hat{z}^2\Bigg]\end{aligned} \tag{E.26}$$

$$\frac{\Delta\check{\omega}_-}{\omega_-} = -\frac{3B_4}{8B_0}\frac{\omega_+ + \omega_-}{\omega_+ - \omega_-}\left[\hat{z}^4 + \hat{\rho}_+^4 - \hat{\rho}_-^4 - 2\hat{\rho}_+^2\hat{z}^2\left(\frac{\omega_+}{\omega_-} + 2\right) - 2\hat{\rho}_-^2\hat{z}^2 - 2\frac{\omega_+}{\omega_-}\hat{\rho}_+^2\hat{\rho}_-^2\right] \tag{E.27}$$

$$\frac{\Delta\omega_\mathrm{c}}{\omega_\mathrm{c}} = \frac{3B_4}{8B_0}\left[\hat{z}^4 + 2\hat{\rho}_+^2\hat{\rho}_-^2 + \frac{\omega_\mathrm{c}\left(-\hat{\rho}_+^4 + \hat{\rho}_-^4\right) + 4\hat{z}^2\left(\hat{\rho}_+^2\omega_- - \hat{\rho}_-^2\omega_+\right)}{\omega_+ - \omega_-}\right] \tag{E.28}$$

F. Magnetic moment: impact on axial mode

This chapter reviews the model of describing the effect of the radial modes on the axial motion in a nonuniform magnetic field via their average magnetic moment. We mentioned the model in Section 4.1.3 in the context of axial frequency-shifts caused by magnetic imperfections. Here, we will discuss one successful and very simple case, which has probably promoted the model because it is so intuitive. However, we have to warn of its general limitations.

The key ingredient of the model is the averaged orbital magnetic moment of the ion in the PENNING trap. Starting from the energy $\mathcal{E}_{\mathrm{mag}} = -\vec{\mu} \cdot \vec{B}$ of a magnetic moment $\vec{\mu}$ in a magnetic field $\vec{B}$, the average magnetic energy of the orbiting ion in the trap is defined as

$$\overline{\mathcal{E}_{\mathrm{mag}}} = -\left\langle \vec{\mu} \right\rangle_0 \cdot \vec{B} = -\left\langle \mu_z \right\rangle_0 \cdot B^{(z)} \quad . \tag{F.1}$$

The radial components (2.39a) and (2.39b) of the orbital magnetic moment generally do not possess a constant component; the axial component (2.39c) does and it is given by Equation (2.40). Note that this time-averaging is not equal to selecting the constant component of the energy:

$$\overline{\mathcal{E}_{\mathrm{mag}}} \neq \left\langle \mathcal{E}_{\mathrm{mag}} \right\rangle_0 = -\left\langle \vec{\mu} \cdot \vec{B} \right\rangle_0 \quad . \tag{F.2}$$

In the latter case, correlations between the magnetic moment of the ion and the magnetic field the ion sees along its trajectory would be taken into account. Of course, the magnetic field in Equation (F.1) has to be evaluated the ion's position, whose time-dependence has been neglected so far. Instead, the ion's coordinates have been treated as general coordinates, even though the solutions (2.30)–(2.32) for trajectory in the ideal Penning trap have been used to calculate the average magnetic moment.

Part of the reason for treating the magnetic field independent of the ion's motion is probably related to the fact that the magnetic moment of the modified cyclotron-motion is an adiabatic invariant [23, 112]. Moreover, ignoring the implicit time-dependence of the magnetic field due to the ion's motion is fine for the ideal PENNING trap with its constant magnetic field. Additionally, the radial components of the magnetic moment do not matter because there is no radial magnetic field. However, it remains to be seen whether the additional forces by higher-order terms in the magnetic field are reproduced correctly.

Because the ion seeks to minimize its total energy, the magnetic energy (F.1) leads to an additional force

$$F_\mu^{(z)} = -\frac{\partial \overline{\mathcal{E}_{\mathrm{mag}}}}{\partial z} = \langle \mu_z \rangle_0 \, \frac{\partial B^{(z)}}{\partial z} \tag{F.3}$$

in the axial direction. With the additional acceleration $\ddot{z}_\mu = F_\mu^{(z)}/m$, the axial equation of motion (2.16) becomes

$$\ddot{z} + \omega_z^2 z - \frac{\langle \mu_z \rangle_0}{m} \frac{\partial B^{(z)}}{\partial z} = 0 \quad . \tag{F.4}$$

For a magnetic field with cylindrical symmetry, the axial magnetic field is given by a sum over $B_\eta^{(z)}$ from Equation (2.78). Assuming that each of these terms is small, they are treated separately to first order in perturbation theory. There is no contribution for $\eta = 0$ because this component of the magnet field has no spatial dependence and hence the derivative vanishes. Thus, we did not miss out on an effect in the ideal PENNING trap. In fact, the model of describing the impact of the radial modes on the axial mode via their magnetic moment should somehow follow from the force (2.13) in the equations of motion, since we deal with a pointlike particle without internal degrees of freedom.

Before attempting a general comparison of Equation (F.4) with the exact axial equation of motion (4.61), we pick the famous example of $\eta = 2$, which leads to the equation of motion

$$\ddot{z} + \omega_z^2 z - \frac{\langle \mu_z \rangle_0}{m} 2B_2 z = 0 \tag{F.5}$$

for a harmonic oscillator. See Table 2.1 or Equation (E.16) for the explicit form of $B_2^{(z)}$. With the average magnetic moment (2.40) and the free-space cyclotron-frequency (2.18), the frequency-changing term becomes

$$-\frac{\langle \mu_z \rangle_0}{m} 2B_2 = B_2 \frac{q}{m} \left(\omega_+ \hat{\rho}_+^2 + \omega_- \hat{\rho}_-^2 \right) = \frac{B_2}{B_0} \omega_\mathrm{c} \left(\omega_+ \hat{\rho}_+^2 + \omega_- \hat{\rho}_-^2 \right) \quad . \tag{F.6}$$

Because the oscillator is still harmonic, the new frequency is simply read off as

$$\omega_z \sqrt{1 + \frac{B_2}{B_0} \frac{\omega_\mathrm{c}}{\omega_z^2} \left(\omega_+ \hat{\rho}_+^2 + \omega_- \hat{\rho}_-^2 \right)} \approx \omega_z \left[1 + \frac{B_2}{2B_0} \frac{\omega_\mathrm{c}}{\omega_z^2} \left(\omega_+ \hat{\rho}_+^2 + \omega_- \hat{\rho}_-^2 \right) + \dots \right] \quad , \tag{F.7}$$

where we have approximated the square root as usual for a small change of ω_z. After applying Equation (2.26) in order express the axial frequency squared as a product of the radial frequencies, the axial frequency-shift is given by

$$\frac{\Delta \omega_z}{\omega_z} = \frac{B_2}{4B_0} \frac{\omega_+ + \omega_-}{\omega_+ \omega_-} \left(\omega_+ \hat{\rho}_+^2 + \omega_- \hat{\rho}_-^2 \right) \quad , \tag{F.8}$$

and the result agrees with Equation (E.17), which was derived via first-order perturbation theory.

There is a second case rather basic case. For $\eta = 1$, the additional term in the axial equation of motion (F.4) is constant, see Table 2.1. This term $-B_1 \langle \mu_z \rangle_0 / m$ shifts the axial equilibrium position by $B_1 \langle \mu_z \rangle_0 / (m\omega_z^2)$ without giving rise to an axial frequency-shift of first order, see Section 3.2. However, the radial frequencies will change because the ion now orbits in a different magnetic field, the magnetic gradient B_1 ensuring that the magnetic field is no longer homogeneous. Because the change of the magnetic field seen by the ion is proportional to B_1 like the shift of the equilibrium position, this frequency-shift is of second order overall. Therefore, we have no exact perturbative result here[1] to compare with the estimate via the magnetic moment [167].

[1] Elsewhere, there is Reference [123].

In the other cases, the axial equation of motion (F.4) describes an anharmonic oscillator, and the axial frequency-shift will most likely have to be determined with perturbation theory again. Rather than doing so, we will examine whether agreement with the first-order result (4.75) is to be expected.

With the free-space cyclotron-frequency (2.18) and the radial magnetic field (2.80), the axial equation of motion (4.61) is indeed written as

$$\ddot{z} + \omega_z^2 z + \frac{2\mu_z}{m}\frac{B_\eta^{(\rho)}}{\rho} = 0 \tag{F.9}$$

in terms[2] of the magnetic moment (2.38). However, the magnetic moment μ_z is still a time-dependent quantity here. No averaging has taken place.

A comparison of the axial equations of motion (F.4) and (F.9) requires a link between the radial magnetic field and the derivative of the axial magnetic field with respect to the axial coordinate. Such a link is for instance established via the divergence [176]

$$\vec{\nabla}\cdot\vec{B} = \frac{1}{\rho}\frac{\partial}{\partial\rho}\left(\rho B^{(\rho)}\right) + \frac{1}{\rho}\frac{B^{(\phi)}}{\partial\phi} + \frac{\partial B^{(z)}}{\partial z} \tag{F.10}$$

of the vector field

$$\vec{B} = B^{(\rho)}\vec{e}_\rho + B^{(\phi)}\vec{e}_\phi + B^{(z)}\vec{e}_z \tag{F.11}$$

in cylindrical coordinates. The $\vec{e}_i$ are the unit vectors in this coordinate system, and the $B^{(i)}$ describe the components of the vector field.

The divergence of a magnetic field vanishes ($\vec{\nabla}\cdot\vec{B} = 0$), because there are no sources. Since we deal with a magnetic field of cylindrical symmetry, $B^{(\phi)} = 0$. Overall we have

$$\frac{\partial B^{(z)}}{\partial z} = -\frac{1}{\rho}\frac{\partial}{\partial\rho}\left(\rho B^{(\rho)}\right) = -\frac{\partial B^{(\rho)}}{\partial\rho} - \frac{B^{(\rho)}}{\rho} \tag{F.12}$$

for the relation between the axial and the radial component. This relation does not transfer Equation (F.4) into (F.9), even when the difference between the average magnetic moment $\langle\mu_z\rangle_0$ and the time-dependent magnetic moment μ_z is ignored. Apart from a factor of 2, there is the derivative of the radial magnetic field (2.80). If it were equal to the second term on the right-hand side of Equation (F.12), most of the discrepancy would be resolved. However, comparing

$$\frac{\partial B_\eta^{(\rho)}}{\partial\rho} = B_\eta \sum_{k=1}^{\left\lfloor\frac{\eta+1}{2}\right\rfloor} (2k-1)\tilde{a}_\eta(k)\, z^{\eta-2k+1}\,\rho^{2k-2} \tag{F.13}$$

and

$$\frac{B_\eta^{(\rho)}}{\rho} = B_\eta \sum_{k=1}^{\left\lfloor\frac{\eta+1}{2}\right\rfloor} \tilde{a}_\eta(k)\, z^{\eta-2k+1}\,\rho^{2k-2} \tag{F.14}$$

[2] There is no such equivalent for the radial equations of motion (4.59) because $B_\eta^{(z)}/z \neq B_\eta^{(y)}/y$ and $B_\eta^{(z)}/z \neq B_\eta^{(x)}/x$, compare Equations (2.78) and (4.60). Thus, there is no common magnetic field to factor out that would leave behind the product of velocities and coordinates of magnetic moment (2.38).

shows that only the terms for $k = 1$ are equal. These are the terms without a dependence on ρ in Equations (F.13) and (F.14), the exponent of ρ being 0. Given the polynomial form of the radial magnetic field (2.80), we should have guessed so because the two operations

$$\frac{\partial}{\partial\rho}\rho^n = n\rho^{n-1} \qquad \text{and} \qquad \frac{\rho^n}{\rho} = \rho^{n-1} \tag{F.15}$$

are equal only for $n = 1$, if ρ is not assigned the special value of 0 afterwards.[3] Consequently, the relations we had hoped for to reconcile the axial equations of motion (F.4) and (F.9) hold generally only for vanishing radial displacement:

$$\left.\frac{\partial B_\eta^{(\rho)}}{\partial\rho}\right|_{\rho=0} = \left.\frac{B_\eta^{(\rho)}}{\rho}\right|_{\rho=0} \qquad \text{and} \qquad \left.\frac{\partial B_\eta^{(z)}}{\partial z}\right|_{\rho=0} = -2\left.\frac{B_\eta^{(\rho)}}{\rho}\right|_{\rho=0} . \tag{F.16}$$

The cases of $\eta = 1$ and $\eta = 2$ are an exception[4] because $B_\eta^{(\rho)} \propto \rho$, see Table 2.1.

$B_\eta^{(\rho)}/\rho$ not depending on ρ helps average the axial component (2.39c) of the magnetic moment in Equation (F.9) to $\langle\mu_z\rangle_0$, despite the presence of oscillatory terms in the magnetic field due to the ion's motion. The oscillatory component[5] of the magnetic moment μ_z at the difference frequency $\omega_+ - \omega_-$ is irrelevant then, because there is no component it could mix with in order to produce naturally-resonant terms at the frequencies of the radial modes. Unfortunately, demanding $\rho = 0$ in the other cases leaves us with a conceptual problem: there is no magnetic moment of the radial modes if their amplitudes are zero. Concerning the lack of an axial first-order frequency-shift (4.78) for vanishing radial displacement, we noted that there is no cylindrically-symmetric radial magnetic field on the z-axial for reasons of that symmetry. Equation (F.4) would probably get the frequency-shift by the term without dependence on ρ right. It should be the same as the frequency-shift caused by the term term without dependence on ρ in Equation (F.9). However, all other result obtained from the model of magnetic moment via Equation (F.4) would be dubious.[6]

Unless for the special cases in which the model is known to work for a good reason, it is more prudent to rely on the actual axial equation of motion (4.61) or (F.9), just like Section 4.1.3 does. Thanks to Equation (2.80), the radial magnetic field is ready for use.[7]

[3] The division by ρ requires the particular value of 0 not be assigned beforehand. Of course, the derivative must always use ρ as a general variable.

[4] There is also the trivial case of $\eta = 0$ with constant $B_0^{(z)} = B_0$ and vanishing $B_0^{(\rho)} = 0$.

[5] We ignore the difference from the perturbed frequencies $\tilde{\omega}_\pm$ here because we do not actually plan to implement perturbation theory here. The statement holds with the replacement $\omega_\pm \to \tilde{\omega}_\pm$.

[6] The approach of neglecting all other terms might be justifiable if the axial amplitude is much larger than the amplitudes of the radial modes because the term with the smallest exponent of ρ has the largest exponent of z.

[7] I believe that the mathematical trouble of the standard representation (2.82) with an *associated* Legendre polynomial is largely responsible for the fact that the radial component of the magnetic field is almost never written down explicitly, not even for the first few η. The model of Equation (F.4) with the magnetic moment is so appealing because it uses the axial magnetic field, which has the same spatial dependence as the electrostatic potential, compare Equations (2.73) and (2.78). To be fair, part of the model originates from the semiclassical description of an intrinsic magnetic moment carried by the stored particle, for which the axial magnetic field provides the quantization axis for the projection.

Bibliography

[1] W. A. Anderson. Electrical current shims for correcting magnetic fields. *Review of Scientific Instruments*, 32(3):241–250, 1961. doi: 10.1063/1.1717338. URL http://scitation.aip.org/content/aip/journal/rsi/32/3/10.1063/1.1717338. (Cited on page 43.)

[2] D. J. Bate, K. Dholakia, R. C. Thompson, and D. C. Wilson. Ion oscillation frequencies in a combined trap. *Journal of Modern Optics*, 39(2):305–316, 1992. doi: 10.1080/09500349214550301. URL http://www.tandfonline.com/doi/abs/10.1080/09500349214550301. (Cited on page 155.)

[3] E. C. Beaty. Calculated electrostatic properties of ion traps. *Physical Review A*, 33(6): 3645–3656, 1986. doi: 10.1103/PhysRevA.33.3645. URL http://link.aps.org/doi/10.1103/PhysRevA.33.3645. (Cited on pages 32 and 35.)

[4] C. M. Bender and S. A. Orszag. *Advanced Mathematical Methods for Scientists and Engineers: Asymptotic Methods and Perturbation Theory*. McGraw-Hill, New York, 1978. (Cited on pages 44, 52 and 195.)

[5] M.-N. Benilan and C. Audoin. Confinement d'ions par un champ électrique de radio-fréquence dans une cage cylindrique. *International Journal of Mass Spectrometry and Ion Physics*, 11(5):421–432, 1973. doi: 10.1016/0020-7381(73)80071-3. URL http://www.sciencedirect.com/science/article/pii/0020738173800713. (Cited on pages 35 and 187.)

[6] T. Bergeman, G. Erez, and H. J. Metcalf. Magnetostatic trapping fields for neutral atoms. *Physical Review A*, 35(4):1535–1546, 1987. doi: 10.1103/PhysRevA.35.1535. URL http://link.aps.org/doi/10.1103/PhysRevA.35.1535. (Cited on pages 41 and 97.)

[7] I. Bergström, C. Carlberg, T. Fritioff, G. Douysset, J. Schönfelder, and R. Schuch. SMILETRAP—A Penning trap facility for precision mass measurements using highly charged ions. *Nuclear Instruments and Methods in Physics Research Section A: Accelerators, Spectrometers, Detectors and Associated Equipment*, 487(3):618–651, 2002. doi: 10.1016/S0168-9002(01)02178-7. URL http://www.sciencedirect.com/science/article/pii/S0168900201021787. (Cited on page 125.)

[8] J. K. Bhattacharjee, D. Dutta, and A. Sarkar. Approximation techniques for non linear oscillators. *ArXiv e-prints*, arXiv:0904.1793, April 2009. URL http://arxiv.org/abs/0904.1793. (Cited on page 53.)

[9] K. Blaum. High-accuracy mass spectrometry with stored ions. *Physics Reports*, 425(1): 1–78, 2006. doi: 10.1016/j.physrep.2005.10.011. URL http://www.sciencedirect.com/science/article/pii/S0370157305004643. (Cited on page 11.)

[10] K. Blaum, Yu. N. Novikov, and G. Werth. Penning traps as a versatile tool for precise experiments in fundamental physics. *Contemporary Physics*, 51(2):149–175, 2010. doi: 10.1080/00107510903387652. URL http://www.tandfonline.com/doi/abs/10.1080/00107510903387652. (Cited on page 11.)

[11] I. A. Boldin and E. N. Nikolaev. Fourier transform ion cyclotron resonance cell with dynamic harmonization of the electric field in the whole volume by shaping of the excitation and detection electrode assembly. *Rapid Communications in Mass Spectrometry*, 25(1):122–126, 2011. doi: 10.1002/rcm.4838. URL http://onlinelibrary.wiley.com/doi/10.1002/rcm.4838/abstract. (Cited on page 30.)

[12] G. Bollen, R. B. Moore, G. Savard, and H. Stolzenberg. The accuracy of heavy-ion mass measurements using time of flight-ion cyclotron resonance in a Penning trap. *Journal of Applied Physics*, 68(9):4355–4374, 1990. doi: 10.1063/1.346185. URL http://scitation.aip.org/content/aip/journal/jap/68/9/10.1063/1.346185. (Cited on pages 32, 88, 92, 94, 95, 96 and 113.)

[13] R. F. Bonner, J. E. Fulford, R. E. March, and G. F. Hamilton. The cylindrical ion trap. Part I. General introduction. *International Journal of Mass Spectrometry and Ion Physics*, 24 (3):255–269, 1977. doi: 10.1016/0020-7381(77)80034-X. URL http://www.sciencedirect.com/science/article/pii/002073817780034X. (Cited on pages 35 and 185.)

[14] A. S. Borodkin. Electron motion in combined homogeneous magnetic and hyperbolic electric field. *Soviet Physics – Technical Physics*, 21(5):621–623, 1976. (Cited on page 85.)

[15] A. S. Borodkin. Electron motion in canted hyperbolic electric field and a homogeneous magnetic field. *Soviet Physics – Technical Physics*, 23(5):520–522, 1978. (Cited on page 85.)

[16] M. Breitenfeldt, S. Baruah, K. Blaum, A. Herlert, M. Kretzschmar, F. Martinez, G. Marx, L. Schweikhard, and N. Walsh. The elliptical Penning trap: Experimental investigations and simulations. *International Journal of Mass Spectrometry*, 275(1–3):34–44, 2008. doi: 10.1016/j.ijms.2008.05.008. URL http://www.sciencedirect.com/science/article/pii/S1387380608001838. (Cited on page 90.)

[17] M. Brodeur, T. Brunner, C. Champagne, S. Ettenauer, M. Smith, A. Lapierre, R. Ringle, V. L. Ryjkov, G. Audi, P. Delheij, D. Lunney, and J. Dilling. New mass measurement of ^{6}Li and ppb-level systematic studies of the Penning trap mass spectrometer TITAN. *Physical Review C*, 80(4):044318, 2009. doi: 10.1103/PhysRevC.80.044318. URL http://link.aps.org/doi/10.1103/PhysRevC.80.044318. (Cited on page 125.)

[18] M. Brodeur, V. L. Ryjkov, T. Brunner, S. Ettenauer, A. T. Gallant, V. V. Simon, M. J. Smith, A. Lapierre, R. Ringle, P. Delheij, M. Good, D. Lunney, and J. Dilling. Verifying the accuracy of the TITAN Penning-trap mass spectrometer. *International Journal of Mass Spectrometry*, 310:20–31, 2012. doi: 10.1016/j.ijms.2011.11.002. URL http://www.sciencedirect.com/science/article/pii/S1387380611004568. (Cited on pages 96 and 113.)

[19] L. S. Brown and G. Gabrielse. Precision spectroscopy of a charged particle in an imperfect Penning trap. *Physical Review A*, 25(4):2423–2425, 1982. doi: 10.1103/PhysRevA.25.2423. URL http://link.aps.org/doi/10.1103/PhysRevA.25.2423. (Cited on pages 21, 88 and 89.)

[20] L. S. Brown and G. Gabrielse. Geonium theory: Physics of a single electron or ion in a Penning trap. *Reviews of Modern Physics*, 58(1):233–311, 1986. doi: 10.1103/RevModPhys.58.233. URL http://link.aps.org/doi/10.1103/RevModPhys.58.233. (Cited on pages 26, 40, 91, 92, 94, 125, 126, 135, 157, 161 and 178.)

[21] L. S. Brown, G. Gabrielse, K. Helmerson, and J. Tan. Cyclotron motion in a microwave cavity: Lifetime and frequency shifts. *Physical Review A*, 32(6):3204–3218, 1985. doi: 10.1103/PhysRevA.32.3204. URL http://link.aps.org/doi/10.1103/PhysRevA.32.3204. (Cited on pages 126 and 145.)

[22] S. Brunner, T. Engel, A. Schmitt, and G. Werth. Helium and deuterium mass ratios in a room temperature Penning trap. *AIP Conference Proceedings*, 457(1):125–129, 1999. doi: 10.1063/1.57451. URL http://scitation.aip.org/content/aip/proceeding/aipcp/10.1063/1.57451. (Cited on pages 94, 113 and 124.)

[23] J. Byrne. 5.—Adiabatic motion in a charged particle trap. *Proceedings of the Royal Society of Edinburgh. Section A. Mathematical and Physical Sciences*, 70:47–61, 1972. doi: 10.1017/S008045410000889X. URL http://journals.cambridge.org/abstract_S008045410000889X. (Cited on pages 27 and 203.)

[24] J. Byrne and P. S. Farago. On the production of polarized electron beams by spin exchange collisions. *Proceedings of the Physical Society*, 86(4):801–815, 1965. doi: 10.1088/0370-1328/86/4/317. URL http://stacks.iop.org/0370-1328/86/i=4/a=317. (Cited on page 19.)

[25] O. Chun-Sing, G. F. Gärtner, and H. A. Schuessler. Field imperfection induced frequency shifts in a Penning trap. *Applied Physics Letters*, 41(1):33–35, 1982. doi: 10.1063/1.93312. URL http://scitation.aip.org/content/aip/journal/apl/41/1/10.1063/1.93312. (Cited on pages 32 and 139.)

[26] D. A. Church. Collision measurements and excited-level lifetime measurements on ions stored in Paul, Penning and Kingdon ion traps. *Physics Reports*, 228(5–6):253–358, 1993. doi: 10.1016/0370-1573(93)90030-H. URL http://www.sciencedirect.com/science/article/pii/037015739390030H. (Cited on page 33.)

[27] M. B. Comisarow. Cubic trapped-ion cell for ion cyclotron resonance. *International Journal of Mass Spectrometry and Ion Physics*, 37(2):251–257, 1981. doi: 10.1016/0020-7381(81)80013-7. URL http://www.sciencedirect.com/science/article/pii/0020738181800137. (Cited on page 18.)

[28] H. G. Dehmelt. Radiofrequency spectroscopy of stored ions I: Storage. In D. R. Bates and I. Estermann, editors, *Advances in Atomic and Molecular Physics*, volume 3, pages 53–72. Academic Press, 1968. doi: 10.1016/S0065-2199(08)60170-0. URL http://www.sciencedirect.com/science/article/pii/S0065219908601700. (Cited on page 11.)

[29] H. G. Dehmelt. Entropy reduction by motional sideband excitation. *Nature*, 262:777, 1976. doi: 10.1038/262777a0. URL http://www.nature.com/nature/journal/v262/n5571/abs/262777a0.html. (Cited on page 92.)

[30] H. G. Dehmelt. Continuous Stern–Gerlach effect: Principle and idealized apparatus. *Proceedings of the National Academy of Sciences*, 83(8):2291–2294, 1986. URL http://www.pnas.org/content/83/8/2291. (Cited on pages 11 and 43.)

[31] H. G. Dehmelt. Experiments with an isolated subatomic particle at rest. *Review of Modern Physics*, 62(3):525–530, 1990. doi: 10.1103/RevModPhys.62.525. URL http://link.aps.org/doi/10.1103/RevModPhys.62.525. (Cited on page 11.)

[32] H. G. Dehmelt and F. L. Walls. "Bolometric" technique for the rf spectroscopy of stored ions. *Physical Review Letters*, 21(3):127–131, 1968. doi: 10.1103/PhysRevLett.21.127. URL http://link.aps.org/doi/10.1103/PhysRevLett.21.127. (Cited on page 92.)

[33] K. Dholakia, G. Zs. K. Horvath, D. M. Segal, and R. C. Thompson. Photon correlation measurement of ion oscillation frequencies in a combined trap. *Journal of Modern Optics*, 39(11):2179–2185, 1992. doi: 10.1080/09500349214552201. URL www.tandfonline.com/doi/abs/10.1080/09500349214552201. (Cited on page 155.)

[34] C. Diehl. *First mass measurements with the MPIK/UW-PTMS*. PhD thesis, Ruprecht-Karls-Universität Heidelberg, 2011. URL http://www.ub.uni-heidelberg.de/archiv/12038. (Cited on page 12.)

[35] C. Diehl, K. Blaum, M. Höcker, J. Ketter, D. B. Pinegar, S. Streubel, and R. S. Van Dyck, Jr. Progress with the MPIK/UW-PTMS in Heidelberg. *Hyperfine Interactions*, 199(1–3):291–300, 2011. doi: 10.1007/s10751-011-0324-6. URL http://link.springer.com/article/10.1007/s10751-011-0324-6. (Cited on page 12.)

[36] J. DiSciacca, M. Marshall, K. Marable, and G. Gabrielse. Resolving an individual one-proton spin flip to determine a proton spin state. *Physical Review Letters*, 110(14):140406, 2013. doi: 10.1103/PhysRevLett.110.140406. URL http://link.aps.org/doi/10.1103/PhysRevLett.110.140406. (Cited on pages 11 and 92.)

[37] J. DiSciacca, M. Marshall, K. Marable, G. Gabrielse, S. Ettenauer, E. Tardiff, R. Kalra, D. Fitzakerley, M. George, E. Hessels, C. Storry, M. Weel, D. Grzonka, W. Oelert, and T. Sefzick. One-particle measurement of the antiproton magnetic moment. *Physical Review Letters*, 110(13):130801, 2013. doi: 10.1103/PhysRevLett.110.130801. URL http://link.aps.org/doi/10.1103/PhysRevLett.110.130801. (Cited on page 11.)

[38] DLMF. NIST Digital Library of Mathematical Functions, Release 1.0.9 of 2014-08-29. URL http://dlmf.nist.gov/. Online companion to [113]. (Cited on pages 155 and 218.)

[39] R. A. Douglas, J. Zabritski, and R. G. Herb. Orbitron vacuum pump. *Review of Scientific Instruments*, 36(1):1–6, 1965. doi: 10.1063/1.1719315. URL http://scitation.aip.org/content/aip/journal/rsi/36/1/10.1063/1.1719315. (Cited on page 33.)

[40] G. Drexlin, V. Hannen, S. Mertens, and C. Weinheimer. Current direct neutrino mass measurements. *Review of Scientific Instruments*, page Article ID 293986, 2013. doi: 10.1155/2013/293986. URL http://www.hindawi.com/journals/ahep/2013/293986/. (Cited on page 12.)

[41] A. Einstein. Erklärung der Perihelbewegung des Merkur aus der allgemeinen Relativitätstheorie. *Sitzungsbericht der preußischen Akademie der Wissenschaft*, 47(2):831–839, 1915. URL https://archive.org/details/sitzungsberichte1915deut. (Cited on page 197.)

[42] S. Eliseev, K. Blaum, M. Block, C. Droese, M. Goncharov, E. Minaya Ramirez, D. A. Nesterenko, Yu. N. Novikov, and L. Schweikhard. Phase-imaging ion-cyclotron-resonance measurements for short-lived nuclides. *Physical Review Letters*, 110(8):082501, 2013. doi: 10.1103/PhysRevLett.110.082501. URL http://link.aps.org/doi/10.1103/PhysRevLett.110.082501. (Cited on page 114.)

[43] S. Eliseev, K. Blaum, M. Block, A. Dörr, C. Droese, T. Eronen, M. Goncharov, M. Höcker, J. Ketter, E. Minaya Ramirez, D. A. Nesterenko, Yu. N. Novikov, and L. Schweikhard. A phase-imaging technique for cyclotron-frequency measurements. *Applied Physics B*, 114 (1–2):107–128, 2014. doi: 10.1007/s00340-013-5621-0. URL http://link.springer.com/article/10.1007/s00340-013-5621-0. (Cited on pages 20 and 114.)

[44] D. L. Farnham. *A Determination of the Proton/Electron Mass Ratio and the Electron's Atomic Mass via Penning Trap Mass Spectroscopy*. PhD thesis, University of Washington, Seattle, 1995. URL http://search.proquest.com/docview/304244811. (Cited on pages 94, 125, 135 and 140.)

[45] E. Fischer. Die dreidimensionale Stabilisierung von Ladungsträgern in einem Vierpolfeld. *Zeitschrift für Physik*, 156(1):1–26, 1959. doi: 10.1007/BF01332512. URL http://link.springer.com/10.1007/BF01332512. (Cited on page 154.)

[46] T. J. Francl, E. K. Fukuda, and R. T. McIver, Jr. A diffusion model for nonreactive ion loss in pulsed ion cyclotron resonance experiments. *International Journal of Mass Spectrometry and Ion Physics*, 50(1–2):151–167, 1983. doi: 10.1016/0020-7381(83)80006-0. URL http://www.sciencedirect.com/science/article/pii/0020738183800060. (Cited on pages 89 and 152.)

[47] G. Gabrielse. Relaxation calculation of the electrostatic properties of compensated Penning traps with hyperbolic electrodes. *Physical Review A*, 27(5):2277–2290, 1983. doi: 10.1103/PhysRevA.27.2277. URL http://link.aps.org/doi/10.1103/PhysRevA.27.2277. (Cited on pages 18 and 93.)

[48] G. Gabrielse. Detection, damping, and translating the center of the axial oscillation of a charged particle in a Penning trap with hyperbolic electrodes. *Physical Review A*, 29(2): 462–469, 1984. doi: 10.1103/PhysRevA.29.462. URL http://link.aps.org/doi/10.1103/PhysRevA.29.462. (Cited on pages 33 and 109.)

[49] G. Gabrielse. Relativistic mass increase at slow speeds. *American Journal of Physics*, 63(6): 568–569, 1995. doi: 10.1119/1.17870. URL http://link.aip.org/link/?AJP/63/568/1. (Cited on page 135.)

[50] G. Gabrielse. The true cyclotron frequency for particles and ions in a Penning trap. *International Journal of Mass Spectrometry*, 279(2–3):107–112, 2009. doi: 10.1016/j.ijms.2008.10.015. URL http://www.sciencedirect.com/science/article/pii/S1387380608004247. (Cited on pages 11, 20, 88 and 89.)

[51] G. Gabrielse and F. C. Mackintosh. Cylindrical Penning traps with orthogonalized anharmonicity compensation. *International Journal of Mass Spectrometry and Ion Processes*, 57(1):1–17, 1984. doi: 10.1016/0168-1176(84)85061-2. URL http://www.sciencedirect.com/science/article/pii/0168117684850612. (Cited on pages 18, 33, 35 and 109.)

[52] G. Gabrielse, H. Dehmelt, and W. Kells. Observation of a relativistic, bistable hysteresis in the cyclotron motion of a single electron. *Physical Review Letters*, 54(6):537–539, 1985. doi: 10.1103/PhysRevLett.54.537. URL http://link.aps.org/doi/10.1103/PhysRevLett.54.537. (Cited on page 125.)

[53] G. Gabrielse, L. Haarsma, and S. L. Rolston. Open-endcap Penning traps for high precision experiments. *International Journal of Mass Spectrometry and Ion Processes*, 88(2–3):319–332, 1989. doi: 10.1016/0168-1176(89)85027-X. URL http://www.sciencedirect.com/science/article/pii/016811768985027X. (Cited on pages 18, 33, 35 and 109.)

[54] G. Gabrielse, L. Haarsma, and S. L. Rolston. Errata: Open-endcap Penning traps for high precision experiments. *International Journal of Mass Spectrometry and Ion Processes*, 93(1):121, 1989. doi: 10.1016/0168-1176(89)83080-0. URL http://www.sciencedirect.com/science/article/pii/0168117689830800. (Cited on page 18.)

[55] G. Gabrielse, D. Phillips, W. Quint, H. Kalinowsky, G. Rouleau, and W. Jhe. Special relativity and the single antiproton: Fortyfold improved comparison of $\overline{p}$ and p charge-to-mass ratios. *Physical Review Letters*, 74(18):3544–3547, 1995. doi: 10.1103/PhysRevLett.74.3544. URL http://link.aps.org/doi/10.1103/PhysRevLett.74.3544. (Cited on page 125.)

[56] A. V. Gaponov and M. A. Miller. Potential wells for charged particles in a high-frequency electromagnetic field. *Journal of Experimental and Theoretical Physics*, 34:168–169, 1958. (Cited on page 163.)

[57] Ch. Gerz, D. Wilsdorf, and G. Werth. A high precision Penning trap mass spectrometer. *Nuclear Instruments and Methods in Physics Research Section B: Beam Interactions with Materials and Atoms*, 47(4):453–461, 1990. doi: 10.1016/0168-583X(90)90626-6. URL http://www.sciencedirect.com/science/article/pii/0168583X90906266. (Cited on page 94.)

[58] K. J. Gillig, B. K. Bluhm, and D. H. Russell. Ion motion in a Fourier transform ion cyclotron resonance wire ion guide cell. *International Journal of Mass Spectrometry and Ion Processes*, 157–158:129–147, 1996. doi: 10.1016/S0168-1176(96)04465-5. URL

http://www.sciencedirect.com/science/article/pii/S0168117696044655. (Cited on page 33.)

[59] J. Goldman and G. Gabrielse. Optimized planar Penning traps for quantum-information studies. *Physical Review A*, 81(5):052335, 2010. doi: 10.1103/PhysRevA.81.052335. URL http://link.aps.org/doi/10.1103/PhysRevA.81.052335. (Cited on pages 18, 60, 65, 69, 71, 74 and 166.)

[60] G. Gräff and E. Klempt. Messung der Zyklotronfrequenz im Vierpolkäfig. *Zeitschrift für Naturforschung*, 22a:1960–1962, 1967. URL http://zfn.mpdl.mpg.de/data/Reihe_A/22/ZNA-1967-22a-1960.pdf. (Cited on page 29.)

[61] G. Gräff, E. Klempt, and G. Werth. Method for measuring the anomalous magnetic moment of free electrons. *Zeitschrift für Physik*, 222(3):201–207, 1969. doi: 10.1007/BF01392119. URL http://link.springer.com/article/10.1007/BF01392119. (Cited on page 125.)

[62] G. Gräff, H. Kalinowsky, and J. Traut. A direct determination of the proton electron mass ratio. *Zeitschrift für Physik A*, 297(1):35–39, 1980. doi: 10.1007/BF01414243. URL http://link.springer.com/article/10.1007/BF01414243. (Cited on pages 20, 28 and 114.)

[63] S. Guan and A. G. Marshall. Ion traps for Fourier transform ion cyclotron resonance mass spectrometry: principles and design of geometric and electric configurations. *International Journal of Mass Spectrometry and Ion Processes*, 146–147:261–296, 1995. doi: 10.1016/0168-1176(95)04190-V. URL http://www.sciencedirect.com/science/article/pii/016811769504190V. (Cited on page 18.)

[64] S. Guan, M. V. Gorshkov, G. M. Alber, and A. G. Marshall. Resonant excitation of relativistic-ion cyclotron orbital motion. *Physical Review A*, 47(4):2730–2737, 1993. doi: 10.1103/PhysRevA.47.2730. URL http://link.aps.org/doi/10.1103/PhysRevA.47.2730. (Cited on page 125.)

[65] N. Guise, J. DiSciacca, and G. Gabrielse. Self-excitation and feedback cooling of an isolated proton. *Physical Review Letters*, 104(14):143001, 2010. doi: 10.1103/PhysRevLett.104.143001. URL http://link.aps.org/doi/10.1103/PhysRevLett.104.143001. (Cited on page 92.)

[66] L. Guo-Zhong. A quantum particle in a combined trap. *Zeitschrift für Physik D – Atoms, Molecules and Clusters*, 10(4):451–456, 1988. doi: 10.1007/BF01425763. URL http://dx.doi.org/10.1007/BF01425763. (Cited on page 154.)

[67] D. Hanneke, S. Fogwell Hoogerheide, and G. Gabrielse. Cavity control of a single-electron quantum cyclotron: Measuring the electron magnetic moment. *Physical Review A*, 83(5):052122, 2011. doi: 10.1103/PhysRevA.83.052122. URL http://link.aps.org/doi/10.1103/PhysRevA.83.052122. (Cited on pages 11, 126 and 145.)

[68] E. R. Harrison. Epicyclic orbits of charged particles. *American Journal of Physics*, 27(5):314–317, 1959. doi: 10.1119/1.1934843. URL http://scitation.aip.org/content/aapt/journal/ajp/27/5/10.1119/1.1934843. (Cited on page 22.)

[69] H. Hartmann, K.-M. Chung, G. Baykut, and K.-P. Wanczek. Dependence of ion cyclotron frequency on electric field inhomogeneity. *The Journal of Chemical Physics*, 78(1):424–431, 1983. doi: 10.1063/1.444520. URL http://link.aip.org/link/?JCP/78/424/1. (Cited on page 95.)

[70] N. Hehn. *Simulation des axialen Detektionssystems von THe-Trap*. Bachelor thesis, Ruprecht-Karls-Universität Heidelberg, 2011. URL http://hdl.handle.net/11858/00-001M-0000-0010-19D9-5. (Cited on page 167.)

[71] N. Hermanspahn, H. Häffner, H.-J. Kluge, W. Quint, S. Stahl, J. Verdú, and G. Werth. Observation of the continuous Stern–Gerlach effect on an electron bound in an atomic ion. *Physical Review Letters*, 84(3):427–430, 2000. doi: 10.1103/PhysRevLett.84.427. URL http://link.aps.org/doi/10.1103/PhysRevLett.84.427. (Cited on page 11.)

[72] G. Zs. K. Horvath, J.-L. Hernandez-Pozos, K. Dholakia, J. Rink, D. M. Segal, and R. C. Thompson. Ion dynamics in perturbed quadrupole ion traps. *Physical Review A*, 57(3):1944–1956, 1998. doi: 10.1103/PhysRevA.57.1944. URL http://link.aps.org/doi/10.1103/PhysRevA.57.1944. (Cited on pages 43, 89 and 155.)

[73] Q. Hu, R. J. Noll, H. Li, A. Makarov, M. Hardman, and R. Graham Cooks. The Orbitrap: a new mass spectrometer. *Journal of Mass Spectrometry*, 40(4):430–443, 2005. doi: 10.1002/jms.856. URL http://onlinelibrary.wiley.com/doi/10.1002/jms.856/abstract. (Cited on page 33.)

[74] Y. Huang, G.-Z. Li, S. Guan, and A. G. Marshall. A combined linear ion trap for mass spectrometry. *Journal of the American Society for Mass Spectrometry*, 8(9):962–969, 1997. doi: 10.1016/S1044-0305(97)82945-5. URL http://www.sciencedirect.com/science/article/pii/S1044030597829455. (Cited on pages 155 and 164.)

[75] K. Hübner, H. Klein, Ch. Lichtenberg, G. Marx, and G. Werth. Instabilities of ion confinement in a Penning trap. *EPL (Europhysics Letters)*, 37(7):459, 1997. doi: 10.1209/epl/i1997-00172-5. URL http://stacks.iop.org/0295-5075/37/i=7/a=459. (Cited on page 85.)

[76] R. L. Hunter, M. G. Sherman, and R. T. McIver, Jr. An elongated trapped-ion cell for ion cyclotron resonance mass spectrometry with a superconducting magnet. *International Journal of Mass Spectrometry and Ion Physics*, 50(3):259–276, 1983. doi: 10.1016/0020-7381(83)87004-1. URL http://www.sciencedirect.com/science/article/pii/0020738183870041. (Cited on page 18.)

[77] W. M. Itano and D. J. Wineland. Laser cooling of ions stored in harmonic and Penning traps. *Physical Review A*, 25(1):35–54, 1982. doi: 10.1103/PhysRevA.25.35. URL http://link.aps.org/doi/10.1103/PhysRevA.25.35. (Cited on page 92.)

[78] W. M. Itano, J. C. Bergquist, J. J. Bollinger, and D. J. Wineland. Cooling methods in ion traps. *Physica Scripta*, 1995(T59):106, 1995. doi: 10.1088/0031-8949/1995/T59/013. URL http://stacks.iop.org/1402-4896/1995/i=T59/a=013. (Cited on page 92.)

[79] J. D. Jackson. *Classical electrodynamics*. Wiley, New York, 1962. (Cited on page 35.)

[80] A. E. Kaplan. Hysteresis in cyclotron resonance based on weak relativistic-mass effects of the electron. *Physical Review Letters*, 48(3):138–141, 1982. doi: 10.1103/PhysRevLett.48.138. URL http://link.aps.org/doi/10.1103/PhysRevLett.48.138. (Cited on page 125.)

[81] J. Ketter. Verbesserungen der Ionennachweissysteme des Präzisions-Penningfallen-Massenspektrometers TRIGA-TRAP. Diplomarbeit, Johannes Gutenberg-Universität Mainz, 2009. URL http://hdl.handle.net/11858/00-001M-0000-0011-767C-C. (Cited on page 23.)

[82] J. Ketter. C_n and B_n: Calculating the first-order frequency shifts caused by cylindrically-symmetric electrostatic and magnetic imperfections of a Penning trap, 2013. Internal Report. (Cited on pages 43, 75, 79, 84 and 91.)

[83] J. Ketter, T. Eronen, M. Höcker, M. Schuh, S. Streubel, and K. Blaum. Classical calculation of relativistic frequency-shifts in an ideal Penning trap. *International Journal of Mass Spectrometry*, 361:34–40, 2014. doi: 10.1016/j.ijms.2014.01.028. URL http://www.sciencedirect.com/science/article/pii/S1387380614000426. Preprint arXiv:1310.4463. (Cited on pages 13, 91 and 130.)

[84] J. Ketter, T. Eronen, M. Höcker, S. Streubel, and K. Blaum. First-order perturbative calculation of the frequency-shifts caused by static cylindrically-symmetric electric and magnetic imperfections of a Penning trap. *International Journal of Mass Spectrometry*, 358:1–16, 2014. doi: 10.1016/j.ijms.2013.10.005. URL http://www.sciencedirect.com/science/article/pii/S1387380613003722. Preprint arXiv:1305.4861. (Cited on pages 13, 43, 75, 79 and 91.)

[85] K. H. Kingdon. A method for the neutralization of electron space charge by positive ionization at very low gas pressures. *Physical Review*, 21(4):408–418, 1923. doi: 10.1103/PhysRev.21.408. URL http://link.aps.org/doi/10.1103/PhysRev.21.408. (Cited on page 33.)

[86] R. D. Knight. Storage of ions from laser-produced plasmas. *Applied Physics Letters*, 38 (4):221–223, 1981. doi: 10.1063/1.92315. URL http://scitation.aip.org/content/aip/journal/apl/38/4/10.1063/1.92315. (Cited on page 33.)

[87] M. König, G. Bollen, H.-J. Kluge, T. Otto, and J. Szerypo. Quadrupole excitation of stored ion motion at the true cyclotron frequency. *International Journal of Mass Spectrometry and Ion Processes*, 142(1–2):95–116, 1995. doi: 10.1016/0168-1176(95)04146-C. URL http://www.sciencedirect.com/science/article/pii/016811769504146C. (Cited on pages 20 and 114.)

[88] Ch. Kraus, B. Bornschein, L. Bornschein, J. Bonn, B. Flatt, A. Kovalik, B. Ostrick, E. W. Otten, J. P. Schall, Th. Thümmler, and Ch. Weinheimer. Final results from phase II of the Mainz neutrino mass search in tritium β decay. *The European Physical Journal C – Particles and Fields*, 40(4):447–468, 2005. doi: 10.1140/epjc/s2005-02139-7. URL http://link.springer.com/10.1140/epjc/s2005-02139-7. (Cited on page 12.)

[89] M. Kretzschmar. A theory of anharmonic perturbations in a Penning trap. *Zeitschrift für Naturforschung. Teil A: Astrophysik, Physik und physikalische Chemie*, 45a(8):965–978, 1990. URL http://zfn.mpdl.mpg.de/data/Reihe_A/45/ZNA-1990-45a-0965.pdf. (Cited on pages 85, 94 and 95.)

[90] M. Kretzschmar. Single particle motion in a Penning trap: description in the classical canonical formalism. *Physica Scripta*, 46(6):544, 1992. doi: 10.1088/0031-8949/46/6/011. URL http://stacks.iop.org/1402-4896/46/i=6/a=011. (Cited on pages 18, 94, 95, 154, 157 and 161.)

[91] M. Kretzschmar. The Ramsey method in high-precision mass spectrometry with Penning traps: Theoretical foundations. *International Journal of Mass Spectrometry*, 264(2–3): 122–145, 2007. doi: 10.1016/j.ijms.2007.04.002. URL http://www.sciencedirect.com/science/article/pii/S1387380607001649. (Cited on page 114.)

[92] M. Kretzschmar. Theory of the elliptical Penning trap. *International Journal of Mass Spectrometry*, 275(1):21–33, 2008. doi: 10.1016/j.ijms.2008.05.009. URL http://www.sciencedirect.com/science/article/pii/S1387380608001759. (Cited on pages 85, 86, 88, 89, 90, 152, 181 and 182.)

[93] M. Kretzschmar. Model calculation of amplitudes for FT-ICR ion detection in a cylindrical Penning trap. *Applied Physics B – Laser and Optics*, 107(4):1007–1017, 2012. doi: 10.1007/s00340-012-4905-0. URL http://link.springer.com/article/10.1007/s00340-012-4905-0. (Cited on page 43.)

[94] M. Kretzschmar. Theoretical investigations of different excitation modes for Penning trap mass spectrometry. *International Journal of Mass Spectrometry*, 349–350:227–239, 2013. doi: 10.1016/j.ijms.2013.03.023. URL http://www.sciencedirect.com/science/article/pii/S1387380613001383. (Cited on page 28.)

[95] M. Lara and J. P. Salas. Dynamics of a single ion in a perturbed Penning trap: Octupolar perturbation. *Chaos: An Interdisciplinary Journal of Nonlinear Science*, 14(3):763–773, 2004. doi: 10.1063/1.1775331. URL http://link.aip.org/link/?CHA/14/763/1. (Cited on page 43.)

[96] F. H. Laukien. The effects of residual spatial magnetic field gradients on Fourier transform ion cyclotron resonance spectra. *International Journal of Mass Spectrometry and Ion Processes*, 73(1–2):81–107, 1986. doi: 10.1016/0168-1176(86)80012-X. URL http://www.sciencedirect.com/science/article/pii/016811768680012X. (Cited on pages 95 and 119.)

[97] G.-z. Li. Combined trap and related experiments. *Communications in Theoretical Physics*, 12 (4):355, 1989. doi: 10.1088/0253-6102/12/4/355. URL http://stacks.iop.org/0253-6102/12/i=4/a=355. (Cited on page 154.)

[98] F. G. Major and H. G. Dehmelt. Exchange-collision technique for the rf spectroscopy of stored ions. *Physical Review*, 170(1):91–107, 1968. doi: 10.1103/PhysRev.170.91. URL http://link.aps.org/doi/10.1103/PhysRev.170.91. (Cited on page 154.)

[99] F. G. Major, V. N. Gheorghe, and G. Werth. *Charged Particle Traps*. Springer, Berlin Heidelberg, 2005. doi: 10.1007/b137836. URL http://link.springer.com/book/10.1007/b137836. (Cited on pages 32, 35, 37, 41, 85, 97, 108, 112, 113, 119, 123, 124, 125 and 165.)

[100] A. Makarov. Electrostatic axially harmonic orbital trapping: A high-performance technique of mass analysis. *Analytical Chemistry*, 72(6):1156–1162, 2000. doi: 10.1021/ac991131p. URL http://pubs.acs.org/doi/abs/10.1021/ac991131p. (Cited on page 33.)

[101] D. W. Mitchell. Theory of trapped ion motion in the non-quadrupolar electrostatic potential of a cubic ion cyclotron resonance cell. *International Journal of Mass Spectrometry and Ion Processes*, 142(1–2):1–22, 1995. doi: 10.1016/0168-1176(94)04090-T. URL http://www.sciencedirect.com/science/article/pii/016811769404090T. (Cited on page 95.)

[102] D. W. Mitchell, A. L. Rockwood, and R. D. Smith. Frequency shifts and modulation effects due to solenoidal magnetic fild inhomogeneities in ion cyclotron mass spectrometry. *International Journal of Mass Spectrometry and Ion Processes*, 141(2):101–116, 1995. doi: 10.1016/0168-1176(94)04106-H. URL http://www.sciencedirect.com/science/article/pii/016811769404106H. (Cited on page 95.)

[103] F. L. Moore, L. S. Brown, D. L. Farnham, S. Jeon, P. B. Schwinberg, and R. S. Van Dyck, Jr. Cyclotron resonance with 10^{-11} resolution: Anharmonic detection and beating a coherent drive with the noise. *Physical Review A*, 46(5):2653–2667, 1992. doi: 10.1103/PhysRevA.46.2653. URL http://link.aps.org/doi/10.1103/PhysRevA.46.2653. (Cited on pages 12 and 43.)

[104] A. Mooser, H. Kracke, K. Blaum, S. A. Bräuninger, K. Franke, C. Leiteritz, W. Quint, C. C. Rodegheri, S. Ulmer, and J. Walz. Resolution of single spin flips of a single proton. *Physical Review Letters*, 110(14):140405, 2013. doi: 10.1103/PhysRevLett.110.140405. URL http://link.aps.org/doi/10.1103/PhysRevLett.110.140405. (Cited on pages 11 and 92.)

[105] A. Mooser, S. Ulmer, K. Blaum, K. Franke, H. Kracke, C. Leiteritz, W. Quint, C. C. Rodegheri, C. Smorra, and J. Walz. Direct high-precision measurement of the magnetic moment of the proton. *Nature*, 509(7502):596–599, 2014. doi: 10.1038/nature13388. URL http://www.nature.com/nature/journal/v509/n7502/full/nature13388.html. (Cited on pages 11 and 92.)

[106] W. G. Mourad, T. Pauly, and R. G. Herb. Orbitron ionization gauge. *Review of Scientific Instruments*, 35(6):661–665, 1964. doi: 10.1063/1.1746679. URL http://scitation.aip.org/content/aip/journal/rsi/35/6/10.1063/1.1746679. (Cited on page 33.)

[107] E. G. Myers. The most precise atomic mass measurements in Penning traps. *International Journal of Mass Spectrometry*, 349-350:107–122, 2013. doi: 10.1016/j.ijms.2013.03.018. URL http://www.sciencedirect.com/science/article/pii/S1387380613001097. (Cited on pages 11, 30, 97 and 125.)

[108] Sz. Nagy, T. Fritioff, M. Björkhage, I. Bergström, and R. Schuch. On the Q-value of the tritium β-decay. *EPL (Europhysics Letters)*, 74(3):404, 2006. doi: 10.1209/epl/i2005-10559-2. URL http://stacks.iop.org/0295-5075/74/i=3/a=404. (Cited on page 12.)

[109] T. Nakamura, S. Ohtani, M. Wada, K. Okada, I. Katayama, and H. A. Schuessler. Ion dynamics and oscillation frequencies in a linear combined trap. *Journal of Applied Physics*, 89(5):2922–2931, 2001. doi: 10.1063/1.1345514. URL http://scitation.aip.org/content/aip/journal/jap/89/5/10.1063/1.1345514. (Cited on pages 155 and 164.)

[110] Y. I. Neronov. Use of an isolated electron to maintain the unit of voltage. *Measurement Techniques*, 31(12):1185–1188, 1988. doi: 10.1007/BF00862618. URL http://link.springer.com/article/10.1007/BF00862618. (Cited on page 138.)

[111] E. N. Nikolaev, I. A. Boldin, R. Jertz, and G. Baykut. Initial experimental characterization of a new ultra-high resolution FTICR cell with dynamic harmonization. *Journal of The American Society for Mass Spectrometry*, 22(7):1125–1133, 2011. doi: 10.1007/s13361-011-0125-9. URL http://link.springer.com/article/10.1007/s13361-011-0125-9. (Cited on page 30.)

[112] T. G. Northrop. Adiabatic charged-particle motion. *Reviews of Geophysics*, 1(3):283–304, 1963. doi: 10.1029/RG001i003p00283. URL http://onlinelibrary.wiley.com/doi/10.1029/RG001i003p00283/abstract. (Cited on pages 27 and 203.)

[113] F. W. J. Olver, D. W. Lozier, R. F. Boisvert, and C. W. Clark, editors. *NIST Handbook of Mathematical Functions*. Cambridge University Press, New York, NY, 2010. Print companion to [38]. (Cited on pages 155 and 210.)

[114] E. W. Otten and C. Weinheimer. Neutrino mass limit from tritium β decay. *Reports on Progress in Physics*, 71(8):086201, 2008. doi: 10.1088/0034-4885/71/8/086201. URL http://stacks.iop.org/0034-4885/71/i=8/a=086201. (Cited on page 12.)

[115] P. Paasche, C. Angelescu, S. Ananthamurthy, D. Biswas, T. Valenzuela, and G. Werth. Instabilities of an electron cloud in a Penning trap. *The European Physical Journal D – Atomic, Molecular, Optical and Plasma Physics*, 22(2):183–188, 2003. doi: 10.1140/epjd/e2002-00239-3. URL http://link.springer.com/article/10.1140/epjd/e2002-00239-3. (Cited on page 85.)

[116] F. L. Palmer. Excitation of spin flips in geonium at small cyclotron quantum numbers: Transition rates and frequency shifts. *Physical Review A*, 47(4):2610–2615, 1993. doi: 10.1103/PhysRevA.47.2610. URL http://link.aps.org/doi/10.1103/PhysRevA.47.2610. (Cited on pages 154, 157 and 161.)

[117] W. Paul. Electromagnetic traps for charged and neutral particles. *Review of Modern Physics*, 62(3):531–540, 1990. doi: 10.1103/RevModPhys.62.531. URL http://link.aps.org/doi/10.1103/RevModPhys.62.531. (Cited on page 11.)

[118] S. Peil and G. Gabrielse. Observing the quantum limit of an electron cyclotron: QND measurements of quantum jumps between fock states. *Physical Review Letters*, 83(7):1287–1290, 1999. doi: 10.1103/PhysRevLett.83.1287. URL http://link.aps.org/doi/10.1103/PhysRevLett.83.1287. (Cited on page 92.)

[119] F. M. Penning. Die Glimmentladung bei niedrigem Druck zwischen koaxialen Zylindern in einem axialen Magnetfeld. *Physica*, 3(9):873–894, 1936. doi: 10.1016/S0031-8914(36)80313-9. URL http://www.sciencedirect.com/science/article/pii/S0031891436803139. (Cited on page 11.)

[120] F. M. Penning. Ein neues Manometer für niedrige Gasdrücke, insbesondere zwischen 10^{-3} und 10^{-5} mm. *Physica*, 4(2):71–75, 1937. doi: 10.1016/S0031-8914(37)80123-8. URL http://www.sciencedirect.com/science/article/pii/S0031891437801238. (Cited on page 11.)

[121] R. H. Perry, R. G. Cooks, and R. J. Noll. Orbitrap mass spectrometry: Instrumentation, ion motion and applications. *Mass Spectrometry Reviews*, 27(6):661–699, 2008. doi: 10.1002/mas.20186. URL http://onlinelibrary.wiley.com/doi/10.1002/mas.20186/abstract. (Cited on page 33.)

[122] J. R. Pierce. *Theory and Design of Electron Beams*. D. Van Nostrand Company, Inc., Princeton, New Jersey, 1949. (Cited on page 16.)

[123] J. Pinder and J. Verdú. A planar Penning trap with tunable dimensionality of the trapping potential. *International Journal of Mass Spectrometry*, 356(0):49–59, 2013. doi: 10.1016/j.ijms.2013.10.003. URL http://www.sciencedirect.com/science/article/pii/S1387380613003709. (Cited on pages 90 and 204.)

[124] D. B. Pinegar. *Tools for a Precise Tritium to Helium-3 Mass Comparison*. PhD thesis, University of Washington, Seattle, 2007. URL http://search.proquest.com/docview/304796368/abstract. (Cited on page 146.)

[125] D. B. Pinegar, S. L. Zafonte, and R. S. Van Dyck, Jr. The UW-PTMS. *Hyperfine Interactions*, 174(1–3):47–53, 2007. doi: 10.1007/s10751-007-9563-y. URL http://link.springer.com/10.1007/s10751-007-9563-y. (Cited on page 12.)

[126] H. Poritsky and R. P. Jerrard. An integrable case of electron motion in electric and magnetic field. *Journal of Applied Physics*, 23(8):928–930, 1952. doi: 10.1063/1.1702332. URL http://scitation.aip.org/content/aip/journal/jap/23/8/10.1063/1.1702332. (Cited on page 86.)

[127] J. V. Porto. Series solution for the image charge fields in arbitrary cylindrically symmetric Penning traps. *Physical Review A*, 64(2):023403, 2001. doi: 10.1103/PhysRevA.64.023403. URL http://link.aps.org/doi/10.1103/PhysRevA.64.023403. (Cited on pages 32, 146, 147 and 151.)

[128] S. Rainville. *A Two-Ion Balance for High Precision Mass Spectrometry*. PhD thesis, Massachusetts Institute of Technology, Dept. of Physics, 2003. URL http://hdl.handle.net/1721.1/16934. (Cited on pages 74, 95, 96, 97, 98 and 199.)

[129] N. Ramsey. Experiments with separated oscillatory fields and hydrogen masers. *Review of Modern Physics*, 62(3):541–552, 1990. doi: 10.1103/RevModPhys.62.541. URL http://link.aps.org/doi/10.1103/RevModPhys.62.541. (Cited on page 11.)

[130] M. Redshaw, J. McDaniel, W. Shi, and E. G. Myers. Mass ratio of two ions in a Penning trap by alternating between the trap center and a large cyclotron orbit. *International Journal of Mass Spectrometry*, 251(2–3):125–130, 2006. doi: 10.1016/j.ijms.2006.01.015. URL http://www.sciencedirect.com/science/article/pii/S1387380606000492. (Cited on page 125.)

[131] D. L. Rempel, E. B. Ledford, S. K. Huang, and M. L. Gross. Parametric mode operation of a hyperbolic Penning trap for Fourier transform mass spectrometry. *Analytical Chemistry*, 59(20):2527–2532, 1987. doi: 10.1021/ac00147a018. URL http://pubs.acs.org/doi/abs/10.1021/ac00147a018. (Cited on page 159.)

[132] K. Ringhofer. "Classical" treatment of $(g-2)$-resonance experiments. *Acta Physica Austriaca*, 39:193–197, 1974. (Cited on page 125.)

[133] M. E. Rose. Magnetic field corrections in the cyclotron. *Physical Review*, 53(9):715–719, 1938. doi: 10.1103/PhysRev.53.715. URL http://link.aps.org/doi/10.1103/PhysRev.53.715. (Cited on page 43.)

[134] C. Roux. *High-resolution mass spectrometry: The trap design and detection system of PENTATRAP and new Q-values for neutrino studies*. PhD thesis, Ruprecht-Karls-Universität Heidelberg, 2012. URL http://www.ub.uni-heidelberg.de/archiv/14006. (Cited on pages 35 and 36.)

[135] C. Roux, C. Böhm, A. Dörr, S. Eliseev, S. George, M. Goncharov, Yu. N. Novikov, J. Repp, S. Sturm, S. Ulmer, and K. Blaum. The trap design of PENTATRAP. *Applied Physics B – Laser and Optics*, 107(4):997–1005, 2012. doi: 10.1007/s00340-011-4825-4. URL http://link.springer.com/article/10.1007/s00340-011-4825-4. (Cited on page 35.)

[136] C. Roux, K. Blaum, M. Block, C. Droese, S. Eliseev, M. Goncharov, F. Herfurth, E. M. Ramirez, D. A. Nesterenko, Y. N. Novikov, and L. Schweikhard. Data analysis of q-value measurements for double-electron capture with SHIPTRAP. *The European Physical Journal D – Atomic, Molecular, Optical and Plasma Physics*, 67(7):1–9, 2013. doi: 10.1140/epjd/e2013-40110-x. URL http://link.springer.com/article/10.1140/epjd/e2013-40110-x. (Cited on page 96.)

[137] G. Savard, St. Becker, G. Bollen, H.-J. Kluge, R. Moore, Th. Otto, L. Schweikhard, H. Stolzenberg, and U. Wiess. A new cooling technique for heavy ions in a Penning trap. *Physics Letters A*, 158(5):247–252, 1991. doi: 10.1016/0375-9601(91)91008-2. URL http://www.sciencedirect.com/science/article/pii/0375960191910082. (Cited on page 92.)

[138] D. Schuch, K.-M. Chung, and H. Hartmann. Effect of magnetic field inhomogeneity on exact mass determination in ICR spectrometry. *International Journal of Mass Spectrometry and Ion Processes*, 56(2):109–121, 1984. doi: 10.1016/0168-1176(84)85036-3. URL http://www.sciencedirect.com/science/article/pii/0168117684850363. (Cited on page 95.)

[139] H. A. Schuessler, E. N. Fortson, and H. G. Dehmelt. Hyperfine structure of the ground state of $^3He^+$ by the ion-storage exchange-collision technique. *Physical Review*, 187 (1):5–38, 1969. doi: 10.1103/PhysRev.187.5. URL http://link.aps.org/doi/10.1103/PhysRev.187.5. (Cited on page 154.)

[140] M. Schuh. *Simulations of the electrostatic and magnetic field properties and tests of the Penning-ion source at THe-Trap*. Master thesis, Ruprecht-Karls-Universität Heidelberg, 2014. URL http://hdl.handle.net/11858/00-001M-0000-0024-46A3-7. (Cited on page 147.)

[141] L. Schweikhard, M. Lindinger, and H.-J. Kluge. Parametric-mode-excitation/dipole-mode-detection Fourier-transform-ion-cyclotron-resonance spectrometry. *Review of Scientific Instruments*, 61(3):1055–1058, 1990. doi: 10.1063/1.1141475. URL http://scitation.aip.org/content/aip/journal/rsi/61/3/10.1063/1.1141475. (Cited on page 159.)

[142] L. Schweikhard, J. Ziegler, H. Bopp, and K. Lützenkirchen. The trapping condition and a new instability of the ion motion in the ion cyclotron resonance trap. *International Journal of Mass Spectrometry and Ion Processes*, 141(1):77–90, 1995. doi: 10.1016/0168-1176(94)04092-L. URL http://www.sciencedirect.com/science/article/pii/016811769404092L. (Cited on page 85.)

[143] P. B. Schwinberg, R. S. Van Dyck, Jr., and H. G. Dehmelt. New comparison of the positron and electron g factors. *Physical Review Letters*, 47(24):1679–1682, 1981. doi: 10.1103/PhysRevLett.47.1679. URL http://link.aps.org/doi/10.1103/PhysRevLett.47.1679. (Cited on page 11.)

[144] T. E. Sharp, J. R. Eyler, and E. Li. Trapped-ion motion in ion cyclotron resonance spectroscopy. *International Journal of Mass Spectrometry and Ion Physics*, 9(5):421–439, 1972. doi: 10.1016/0020-7381(72)80027-5. URL http://www.sciencedirect.com/science/article/pii/0020738172800275. (Cited on page 18.)

[145] M. Smith, M. Brodeur, T. Brunner, S. Ettenauer, A. Lapierre, R. Ringle, V. L. Ryjkov, F. Ames, P. Bricault, G. W. F. Drake, P. Delheij, D. Lunney, F. Sarazin, and J. Dilling. First Penning-trap mass measurement of the exotic halo nucleus ^{11}Li. *Physical Review Letters*, 101(20):202501, 2008. doi: 10.1103/PhysRevLett.101.202501. URL http://link.aps.org/doi/10.1103/PhysRevLett.101.202501. (Cited on page 20.)

[146] A. A. Sokolov and Yu. G. Pavlenko. Induced and spontaneous emission in crossed fields. *Optics and Spectroscopy*, 12(1):3–8, 1967. (Cited on page 29.)

[147] S. Stahl, F. Galve, J. Alonso, S. Djekic, W. Quint, T. Valenzuela, J. Verdú, M. Vogel, and G. Werth. A planar Penning trap. *The European Physical Journal D – Atomic, Molecular, Optical and Plasma Physics*, 32(1):139–146, 2005. doi: 10.1140/epjd/e2004-00179-x. URL http://link.springer.com/article/10.1140/epjd/e2004-00179-x. (Cited on page 18.)

[148] S. Streubel. *Kontrolle der Umwelteinflüsse auf THe-Trap am Beispiel der Bestimmung des Massenverhältnisses von Kohlenstoff-12 zu Sauerstoff-16*. PhD thesis, Ruprecht-Karls-Universität Heidelberg, 2014. URL http://www.ub.uni-heidelberg.de/archiv/16870. (Cited on page 12.)

[149] S. Streubel, T. Eronen, M. Höcker, J. Ketter, M. Schuh, R. S. Dyck, Jr., and K. Blaum. Toward a more accurate Q value measurement of tritium: status of THe-Trap. *Applied Physics B – Laser and Optics*, 114(1–2):137–145, 2014. doi: 10.1007/s00340-013-5669-x. URL http://link.springer.com/article/10.1007/s00340-013-5669-x. (Cited on page 12.)

[150] S. Sturm. *The g-factor of the electron bound in $^{28}Si^{13+}$: the most stringent test of bound-state quantum electrodynamics*. PhD thesis, Johannes Gutenberg-Universität Mainz, 2012. URL http://ubm.opus.hbz-nrw.de/volltexte/2012/3108/. (Cited on pages 30 and 119.)

[151] S. Sturm, A. Wagner, B. Schabinger, and K. Blaum. Phase-sensitive cyclotron frequency measurements at ultralow energies. *Physical Review Letters*, 107(14):143003, 2011. doi: 10.1103/PhysRevLett.107.143003. URL http://link.aps.org/doi/10.1103/PhysRevLett.107.143003. (Cited on pages 92 and 125.)

[152] S. Sturm, A. Wagner, M. Kretzschmar, W. Quint, G. Werth, and K. Blaum. g-factor measurement of hydrogenlike $^{28}Si^{13+}$ as a challenge to QED calculations. *Physical Review A*, 87(3):030501, 2013. doi: 10.1103/PhysRevA.87.030501. URL http://link.aps.org/doi/10.1103/PhysRevA.87.030501. (Cited on pages 32, 146 and 152.)

[153] S. Sturm, F. Köhler, J. Zatorski, A. Wagner, Z. Harman, G. Werth, W. Quint, C. H. Keitel, and K. Blaum. High-precision measurement of the atomic mass of the electron. *Nature*, 506 (7489):467–470, 2014. doi: 10.1038/nature13026. URL http://www.nature.com/nature/journal/v506/n7489/full/nature13026.html. (Cited on page 11.)

[154] V. L. Talrose and E. N. Nikolaev. Superaccurate mass determination by mass spectrometry of ion cyclotron resonance. *Advances in Mass Spectrometry*, A10:343–357, 1985. (Cited on page 126.)

[155] J. K. Thompson. *Two-ion control and polarization forces for precise mass comparisons*. PhD thesis, Massachusetts Institute of Technology, Dept. of Physics, 2003. URL http://hdl.handle.net/1721.1/17011. (Cited on pages 74, 95 and 97.)

[156] J. K. Thompson, S. Rainville, and D. E. Pritchard. Cyclotron frequency shifts arising from polarization forces. *Nature*, 430(6995):58–61, 2004. doi: 10.1038/nature02682. URL http://www.nature.com/nature/journal/v430/n6995/full/nature02682.html. (Cited on page 93.)

[157] M. D. Tinkle and S. E. Barlow. Image charge forces inside conducting boundaries. *Journal of Applied Physics*, 90(3):1612–1624, 2001. doi: 10.1063/1.1383016. URL http://scitation.aip.org/content/aip/journal/jap/90/3/10.1063/1.1383016. (Cited on pages 32, 146 and 147.)

[158] R. S. Van Dyck, Jr., D. J. Wineland, P. A. Ekstrom, and H. G. Dehmelt. High mass resolution with a new variable anharmonicity Penning trap. *Applied Physics Letters*, 28(8):446–448, 1976. doi: 10.1063/1.88793. URL http://link.aip.org/link/?APL/28/446/1. (Cited on pages 43 and 93.)

[159] R. S. Van Dyck, Jr., F. L. Moore, D. L. Farnham, and P. B. Schwinberg. Variable magnetic bottle for precision geonium experiments. *Review of Scientific Instruments*, 57(4):593–597, 1986. doi: 10.1063/1.1138875. URL http://link.aip.org/link/?RSI/57/593/1. (Cited on page 43.)

[160] R. S. Van Dyck, Jr., P. B. Schwinberg, and H. G. Dehmelt. Electron magnetic moment from geonium spectra: Early experiments and background concepts. *Physical Review D*, 34(3):722–736, 1986. doi: 10.1103/PhysRevD.34.722. URL http://link.aps.org/doi/10.1103/PhysRevD.34.722. (Cited on pages 11, 88 and 92.)

[161] R. S. Van Dyck, Jr., P. B. Schwinberg, and H. G. Dehmelt. New high-precision comparison of electron and positron g factors. *Physical Review Letters*, 59(1):26–29, 1987. doi: 10.1103/PhysRevLett.59.26. URL http://link.aps.org/doi/10.1103/PhysRevLett.59.26. (Cited on page 11.)

[162] R. S. Van Dyck, Jr., F. L. Moore, D. L. Farnham, and P. B. Schwinberg. Number dependency in the compensated Penning trap. *Physical Review A*, 40(11):6308–6313, 1989. doi: 10.1103/PhysRevA.40.6308. URL http://link.aps.org/doi/10.1103/PhysRevA.40.6308. (Cited on pages 32, 146, 147 and 151.)

[163] R. S. Van Dyck, Jr., D. L. Farnham, S. L. Zafonte, and P. B. Schwinberg. Ultrastable superconducting magnet system for a Penning trap mass spectrometer. *Review of Scientific Instruments*, 70(3):1665–1671, 1999. doi: 10.1063/1.1149649. URL http://link.aip.org/link/?RSI/70/1665/1. (Cited on page 20.)

[164] R. S. Van Dyck, Jr., S. L. Zafonte, and P. B. Schwinberg. Ultra-precise mass measurements using the UW-PTMS. *Hyperfine Interactions*, 132(1–4):163–175, 2001. doi: 10.1023/A:1011914310458. URL http://link.springer.com/article/10.1023/A:1011914310458. (Cited on page 154.)

[165] R. S. Van Dyck, Jr., D. B. Pinegar, S. Van Liew, and S. L. Zafonte. The UW-PTMS: Systematic studies, measurement progress, and future improvements. *International Journal of Mass Spectrometry*, 251(2–3):231–242, 2006. doi: 10.1016/j.ijms.2006.01.038. URL http://www.sciencedirect.com/science/article/pii/S1387380606000650. (Cited on page 12.)

[166] J. Verdú. Theory of the coplanar-waveguide Penning trap. *New Journal of Physics*, 13(11):113029, 2011. doi: 10.1088/1367-2630/13/11/113029. URL http://stacks.iop.org/1367-2630/13/i=11/a=113029. (Cited on page 18.)

[167] J. L. Verdú Galiana. *Ultrapräzise Messung des elektronischen g-Faktors in wasserstoffähnlichem Sauerstoff*. PhD thesis, Johannes Gutenberg-Universität Mainz, 2003. (Cited on page 204.)

[168] M. Vogel, W. Quint, and W. Nörtershäuser. Trapped ion oscillation frequencies as sensors for spectroscopy. *Sensors*, 10(3):2169–2187, 2010. doi: 10.3390/s100302169. URL http://www.mdpi.com/1424-8220/10/3/2169. (Cited on page 94.)

[169] A. Wagner, S. Sturm, F. Köhler, D. Glazov, A. Volotka, G. Plunien, W. Quint, G. Werth, V. Shabaev, and K. Blaum. g factor of lithiumlike silicon $^{28}Si^{11+}$. *Physical Review Letters*, 110(3):033003, 2013. doi: 10.1103/PhysRevLett.110.033003. URL http://link.aps.org/doi/10.1103/PhysRevLett.110.033003. (Cited on page 11.)

[170] Y. Wang and J. Franzen. The non-linear ion trap. Part 3. Multipole components in three types of practical ion trap. *International Journal of Mass Spectrometry and Ion Processes*, 132 (3):155–172, 1994. doi: 10.1016/0168-1176(93)03939-J. URL http://www.sciencedirect.com/science/article/pii/016811769303939J. (Cited on page 32.)

[171] E. W. Weisstein. Associated Legendre differential equation. From *MathWorld* — A Wolfram Web Resource, 2014. URL http://mathworld.wolfram.com/AssociatedLegendreDifferentialEquation.html. (Cited on page 169.)

[172] E. W. Weisstein. Associated Legendre polynomial. From *MathWorld* — A Wolfram Web Resource, 2014. URL http://mathworld.wolfram.com/AssociatedLegendrePolynomial.html. (Cited on pages 40, 177 and 178.)

[173] E. W. Weisstein. Bessel function of the first kind. From *MathWorld* — A Wolfram Web Resource, 2014. URL http://mathworld.wolfram.com/BesselFunctionoftheFirstKind.html. (Cited on pages 187 and 189.)

[174] E. W. Weisstein. Bessel function of the second kind. From *MathWorld* — A Wolfram Web Resource, 2014. URL http://mathworld.wolfram.com/BesselFunctionoftheSecondKind.html. (Cited on page 187.)

[175] E. W. Weisstein. Bessel polynomial. From *MathWorld* — A Wolfram Web Resource, 2014. URL http://mathworld.wolfram.com/BesselPolynomial.html. (Cited on page 177.)

[176] E. W. Weisstein. Cylindrical coordinates. From *MathWorld* — A Wolfram Web Resource, 2014. URL http://mathworld.wolfram.com/CylindricalCoordinates.html. (Cited on page 205.)

[177] E. W. Weisstein. Condon–Shortley phase. From *MathWorld* — A Wolfram Web Resource, 2014. URL http://mathworld.wolfram.com/Condon-ShortleyPhase.html. (Cited on pages 40 and 177.)

[178] E. W. Weisstein. Chu–Vandermonde identity. From *MathWorld* — A Wolfram Web Resource, 2014. URL http://mathworld.wolfram.com/Chu-VandermondeIdentity.html. (Cited on page 101.)

[179] E. W. Weisstein. Legendre function of the second kind. From *MathWorld* — A Wolfram Web Resource, 2014. URL http://mathworld.wolfram.com/LegendreFunctionoftheSecondKind.html. (Cited on page 171.)

[180] E. W. Weisstein. Laplacian. From *MathWorld* — A Wolfram Web Resource, 2014. URL http://mathworld.wolfram.com/Laplacian.html. (Cited on pages 35 and 170.)

[181] E. W. Weisstein. Legendre polynomial. From *MathWorld* — A Wolfram Web Resource, 2014. URL http://mathworld.wolfram.com/LegendrePolynomial.html. (Cited on page 172.)

[182] E. W. Weisstein. Multiple-angle formulas. From *MathWorld* — A Wolfram Web Resource, 2014. URL http://mathworld.wolfram.com/Multiple-AngleFormulas.html. (Cited on page 178.)

[183] E. W. Weisstein. Modified Bessel differential equation. From *MathWorld* — A Wolfram Web Resource, 2014. URL http://mathworld.wolfram.com/ModifiedBesselDifferentialEquation.html. (Cited on page 188.)

[184] E. W. Weisstein. Modified Bessel function of the first kind. From *MathWorld* — A Wolfram Web Resource, 2014. URL http://mathworld.wolfram.com/ModifiedBesselFunctionoftheFirstKind.html. (Cited on pages 186 and 188.)

[185] E. W. Weisstein. Modified Bessel function of the second kind. From *MathWorld* — A Wolfram Web Resource, 2014. URL http://mathworld.wolfram.com/ModifiedBesselFunctionoftheSecondKind.html. (Cited on page 185.)

[186] E. W. Weisstein. Spherical harmonic. From *MathWorld* — A Wolfram Web Resource, 2014. URL http://mathworld.wolfram.com/SphericalHarmonic.html. (Cited on page 169.)

[187] E. W. Weisstein. Solid harmonic. From *MathWorld* — A Wolfram Web Resource, 2014. URL http://mathworld.wolfram.com/SolidHarmonic.html. (Cited on page 35.)

[188] E. W. Weisstein. Trigonometric power formulas. From *MathWorld* — A Wolfram Web Resource, 2014. URL http://mathworld.wolfram.com/TrigonometricPowerFormulas.html. (Cited on page 191.)

[189] E. W. Weisstein. Zonal harmonic. From *MathWorld* — A Wolfram Web Resource, 2014. URL http://mathworld.wolfram.com/ZonalHarmonic.html. (Cited on page 35.)

[190] D. Wineland, P. Ekstrom, and H. Dehmelt. Monoelectron oscillator. *Physical Review Letters*, 31(21):1279–1282, 1973. doi: 10.1103/PhysRevLett.31.1279. URL http://link.aps.org/doi/10.1103/PhysRevLett.31.1279. (Cited on page 154.)

[191] D. J. Wineland and H. G. Dehmelt. Principles of the stored ion calorimeter. *Journal of Applied Physics*, 46(2):919–930, 1975. doi: 10.1063/1.321602. URL http://scitation.aip.org/content/aip/journal/jap/46/2/10.1063/1.321602. (Cited on page 146.)

[192] D. J. Wineland, R. E. Drullinger, and F. L. Walls. Radiation-pressure cooling of bound resonant absorbers. *Physical Review Letters*, 40(25):1639–1642, 1978. doi: 10.1103/PhysRevLett.40.1639. URL http://link.aps.org/doi/10.1103/PhysRevLett.40.1639. (Cited on page 92.)

[193] D. J. Wineland, W. M. Itano, J. C. Bergquist, and R. G. Hulet. Laser-cooling limits and single-ion spectroscopy. *Physical Review A*, 36(5):2220–2232, 1987. doi: 10.1103/PhysRevA.36.2220. URL http://link.aps.org/doi/10.1103/PhysRevA.36.2220. (Cited on page 92.)

[194] D. F. A. Winters, M. Vogel, D. M. Segal, and R. C. Thompson. Electronic detection of charged particle effects in a Penning trap. *Journal of Physics B: Atomic, Molecular and Optical Physics*, 39(14):3131, 2006. doi: 10.1088/0953-4075/39/14/019. URL http://stacks.iop.org/0953-4075/39/i=14/a=019. (Cited on page 146.)

[195] J. Yu, M. Desaintfuscien, and F. Plumelle. Ion density limitation in a Penning trap due to the combined effect of asymmetry and space charge. *Applied Physics B – Laser and Optics*, 48(1):51–54, 1989. doi: 10.1007/BF00694417. URL http://link.springer.com/article/10.1007/BF00694417. (Cited on page 85.)

[196] S. L. Zafonte. *A Determination of the Mass of the Deuteron*. PhD thesis, University of Washington, Seattle, 2012. URL http://hdl.handle.net/1773/20247. (Cited on page 167.)

Acknowledgments

Since I became so tired of writing towards the end of the thesis, I contemplated skipping this part, which was the last to be completed. However, I do not wish to imply that I am fed up with the people I worked with, and I realized that these acknowledgments are an integral part of citing my sources. Okay, full disclosure, you are all so great:[1]

- First and foremost, I would like to thank my supervisor *Prof. Dr. Klaus Blaum* for his tremendous confidence in my work and his constant encouragement to keep it up. Thanks for being so open-minded and letting the thesis evolve as it happened. Thanks for letting me travel to three international conferences with a train station nearby and the Spring Meetings of the German Physical Society. However, I will be scratching my long beard about the unconventional deployment as Santa Claus on the Christmas party of the division.

- I thank *Prof. Dr. Manfred Lindner* for agreeing to be the second referee of the thesis.

- Thanks to the whole crew at THe-Trap. I acknowledge earlier contributions by *David Pinegar*—I am shocked it ended like this—and by *Christoph Diehl*—thanks for the time during diploma studies in Mainz—as well as by bachelor and diploma students. Good luck to the new PhD students.

  Thanks to *Tommi Eronen* from Finland for making German winters look less dark and less depressing. His Linux skills, probably second only to the other Finnish Linux guy, have greatly facilitated remote access to the institute, and I have enjoyed the comfort of keeping this thesis synchronized with an SVN repository. He kept me amused with "Biolan musta multa kanankakka" commercials. Unfortunately, the only Finnish that stuck was "saksanpaimenkoira" and "kultainennoutaja," which will not get me anywhere. I had to look up "tajunnanräjäyttäjä," you mind exploder, because all these vowels keep me confused.

  Thanks to MATLAB magician *Martin Höcker* for the fresh FSU perspective and his enthusiasm about implementing novelties.

  Sebastian Streubel continues to work his magic on the magnet and the stabilization system.

  Thanks to *Marc Schuh* for his simulations of the electric potential and the image-charge field, which sparked part of the discussion in this thesis.

  Thanks to *Robert S. van Dyck, Jr.,* for sharing his colossal knowledge of and his almost lifelong experience with the UW-PTMS via email.

[1] Variation of *Sports Song* from "Weird Al" Yankovic's 2014 album *Mandatory Fun.*

- An experiment with tritium requires safety measures, which might involve a lot of red tape. Thanks to Radiation Safety Officers *Ralf Lackner* and *Dr. Jochen Schreiner* for the smooth pragmatic cooperation and for always finding a safe practical solution without shutting down the entire experiment. Special thanks to *Ralf Lackner* for documenting the experiment on camera and photographs, which refreshes everybody's memories later.

- Thanks to the Mainz proton g-factor team.

  In the acknowledgments of my diploma thesis, I forgot to thank *Crícia de Carvalho Rodegheri* for her introduction to soldering. I only mentioned her introduction to Eagle PCB design software. This omission now comes back to haunt me years later when writing these acknowledgments. Let me set it right this time. Unfortunately, I succumbed to the *Ulmer* side, drowning components in a sea of solder. Solidified once, that blob never liquifies again before everything else has molten.

- Thanks to the Mainz Triga-Trap team for continuing the collaboration on that power supply. Hopefully, we will have something to show for it soon.

- Thanks to the Mainz bound-electron g-factor crew.

  Special thanks to *Sven Sturm* for always taking his time to share his amazing innate understanding of physics—always with a sincere desire to be helpful, never for showmanship or self-display. I guess when you have reached this level of mastery, there is nothing to gain from playing these cheap smug games. You would simply embarrass yourself instead. There is no more need to be vying for respect; you will be respected for who you are. Kudos.

- Thanks to the former Heidelberg Katrin FT-ICR members.

  Michael Heck was always in such joyful mood with a smile on his face, in spite of cheering for 1. FC Kaiserslautern.

- Thanks to the Piperade crew, or that French-speaking office, for showing that there are other languages than English.

  Special thanks to *Pauline Ascher* for checking my translation of Poincaré's definition of secularity.

- Thanks to the PentaTrap team for providing a second opinion on Penning traps. They had to go through many of the same difficulties, which seem to be somehow inherent in cold-bore magnets.

  Christine Böhm released a prototype of the StaReP voltage source for tests at THe-Trap, and *Mikhail Goncharov* did the initial LabView programming. Thanks to all the off-topic chat.

  I am indebted to *Sergey Eliseev* for some discussion which ended up with me as a co-author on one PI-ICR paper.

  Alexander Rischka approached me with an exercise on the Kapitza pendulum, and the ensuing literature search turned into the subsection on pseudopotentials.

Thanks to *Andreas Dörr* for all the sports-related discussion during lunch, proving that there is more than physics. How will I ever get over Swiss television being kicked from local cable?

Julia Repp pointed out the institute has an online subscription to international journals. Damn it, it should have read the email announcement more thoroughly. Back in those days, this still included *Kicker* sports magazine. I wonder why they canceled that subscription.

Thanks to *Christian Roux* for being genuine and for not wearing blinders. Conversations were entertaining and comforting. I will never figure out how to apply for a job though.

- I acknowledge support by the International Max Planck Research School for Precision Tests of Fundamental Symmetries (IMPRS-PTFS).

  Thanks to *Jörg Evers* and *José Ramón Crespo López-Urrutia* for reading my biannual progress reports. That should be over now.

  Thanks to the IMPRS-PTFS secretary, *Mrs. Schwartz*, for always extending the deadline handing in these reports—due to the co-advisors attending important conferences, of course.

  I thank the IMPRS-PTFS coordinator, *Werner Rodejohann*, for letting my contribute my fair share—name tags, officially—to the successful evaluation of the IMPRS-PTFS in July 2014, despite my pessimistic predictions for Germany's games in the pool stage of the 2012 European Championship.

- Thanks to the Heidelberg Graduate School of Fundamental Physics (HGSFP), in particular for the *Carl Bender* Lecture Series on Mathematical Physics. I enjoyed these lectures even though I grasped only a fraction, which was still enough to understand secularity and implement perturbation theory (two years after the actual lecture).

- The infrastructure at the institute is marvelous, and it works so reliably that it almost goes unnoticed. Although I will sometimes mention the whole department, I am fully aware that it is run by people.

  Thanks to the group secretary, *Mrs. Dücker*, for administrative support.

  Thanks to group technician *Ralph Zilly* for tools and for filling the magnet with liquid nitrogen. What happened to the power supply that was supposed to be adapted for 110V operation by a certified professional?

  Thanks to the *Netzwerkgruppe* and *Mr. Koeck* for software licenses, computer hardware and computing services.

  Thanks to *Mr. Jänner* for dedicated support on National Instruments products.

  Thanks to the numerous mechanical workshops for providing spare pieces and emergency repairs or modifications.

  Thanks to the *Elektronik* for stocking electronic components in the *Elektroniklager*, which does not even need a storekeeper.

Thanks to *Beschleunigerelektronik* for repairing old-style high-voltage power-supplies based on vacuum tubes. Typically, an electrolytic capacitor had dried out.

Thanks to the *Haustechnik* for putting up with my constant over-reporting of mice, dormice, faulty lamps, doors, windows, sinks . . . you name it. They respond so quickly—by taking action, that is.

Thanks to the librarian, *Mr. Vogt*, for procuring obscure articles and for identifying those who hog books.

Thanks to *Mr. Lorentz* for keeping the printers in shape and binding theses. His extensive supply of stationery in the *Lager* means that it is not for a lack of pens and paper that I fail to write down something meaningful. Do not let him know that I would love to take over his job.

Thanks to the *Einkauf* for the seamless integration into the electronic procurement when online shops would long be dead and buried if they used the SAP interface. Thanks to the *Pforte* for coping with the material consequence of a spending spree—the deliveries.

- Thanks to my parents and my siblings. No explanation needed.

So, you have reached the end of this list without reading *your name*? Sorry, I apologize for forgetting *your name* while being in a hurry to finish in time. Just because I failed to mention *your contribution* not does not mean I forgot about it entirely. As the example of *Crícia* shows, I will acknowledge it in some document years from now. Just be patient and stay tuned. Thank you.

Declaration of own work

Sworn Affidavit according to § 8 of the doctoral degree regulations of the Combined Faculty of Natural Sciences and Mathematics

This thesis entitled *"Theoretical treatment of miscellaneous frequency-shifts in Penning traps with classical perturbation theory"* I have submitted is my own work. I have only used the sources indicated and have not made unauthorized use of services of a third party. Where the work of others has been quoted or reproduced, the source is always given. I have not presented this thesis or parts thereof to a university as part of an examination or degree before.

I confirm that the declarations made above are correct. I am aware of the importance of a sworn affidavit and the criminal prosecution in case of a false or incomplete affidavit. I affirm that the above is the absolute truth to the best of my knowledge and that I have not concealed anything.

Heidelberg, January 7, 2015

Georg Jochen Ketter